The Role of Interferon in Semliki Forest Virus Encephalitis

Lucy Breakwell

2006

Submitted for the degree of Doctor of Philosophy

Contents

Chapter and Title		Page
	Declaration	ii
	Acknowledgements	iii
	List of Figures	iv
	List of Tables	vii
	Abbreviations	viii
	Abstract	xii
1	Introduction	1
2	Materials & Methods	47
3	Development of assays to quantify IFN	80
4	Does SFV4 infection induce IFN expression *in vitro* and in the brains of adult and neonatal mice?	101
5	Does Protein kinase R (PKR) have a role in IFN induction during SFV infection?	123
6	Differential dynamics of IFN induction by different strains of SFV	147
7	Final Discussion	173
	Reference List	181

Declaration

I declare that all the work included in this thesis is my own except where otherwise stated. No part of this work has been, or will be submitted for any other degree of professional qualification.

Lucy Breakwell

2006

Centre for Infectious Diseases
University of Edinburgh
Summerhall
Edinburgh
EH9 1QH

Acknowledgements

I would like to thank my supervisors **John Fazakerley** and **Bob Dalziel** for their encouragement, mentoring and careful scrutiny of the manuscript. Throughout my PhD, John was a source of inspiration and was always available to advise on day-to-day issues. He also provided me with many opportunities to interact with leading European SFV researchers and facilitated a three month collaboration with the Karolinska Institut. Thank you!

I would not have been able to accomplish this thesis without the other members of the Fazakerley laboratory who provided exceptional experimental advice and support. **Audrey Graham**, who provided a wealth of knowledge on immunostaining, which helped to set up my protocols, and who was an ever entertaining drinking companion at the European conferences; **Clive McKimmie**, who was the laboratory expert on quantitative PCR and who listened to my concerns with much patience; **Amanda Boyd**, who assisted with all of the animal work and **Cat Dixon**, **Rennos Fragkoudis**, and **Gerald Barry,** who have been a source of advice and reassurance.

I would also like to thank **Dawn Everington**, who came in at the last minute to help with statistical issues.

A big thank you to the members of the Liljeström laboratory, particularly **Gerald McInerney**, **Pia Dosenovic**, and **Åsa Hidmark,** who reinvigorated my interest in academic research and contributed to the final results chapter.

An especially big thank you to all the PhD students in the tower block, who have provided empathy and distraction, particularly **Kerra Templeton** and **Anna Cliffe,** who gave exceptional emotional support and were always available for a glass of wine! And finally, I would like to thank my housemate **Hannah Raine**, who has pretty much fed me for the last two years and my **parents** whose unwavering belief in my abilities has gotten me to this point.

List of Figures

Chapter 1

1A Induction of NF-κB.....13

1B Iinduction of IRF-3.....14

1C The IFN-β Enhanceosome.....17

1D Type I IFN Jak-STAT signalling.....20

1E SFV genome.....41

Chapter 2

2A Graphical representation of the absorbance values of IFN standard and test samples after incubation with WST-1 reagent for 3 hours.....61

2B Agilent RNA 6000 Nano assay chip.....68

Chapter 3

3A Quality and quantity assessment of RNA.....83

3B The specificity and sensitivity of the primers.....87

3C β-actin and GAPDH down regulation during SFV4 infection of mouse embryo fibroblasts.....89

3D The range of data from the qPCR assay.....92

3E The range of the serial dilutions and 50 % end points produced from laboratory standard IFN run in two experiments.....94

3F Comparison of serial dilutions (i) and (ii) and median 50 % cell death end point values (iii) of the 3 plates assessed per experiment.....95

3G Assessment of intra plate variation of two-fold serial dilutions of laboratory standard IFN.....96

3H Distribution of 50 % end points.....97

Chapter 4

4A Production of IFN-β transcripts in mouse L-cells following an SFV4 infection.105

4B IFN-β transcripts do not increase with increasing levels of virus RNA.....105

4C Production of functional IFN by a mouse fibroblast cell line (L-929).....106
4D Production of IFN-β transcripts in mouse brains following SFV4 infection.....109
4E Levels of IFN-β transcripts increase with increasing levels of virus RNA.....110
4F Production of IFN-β transcripts in neonatal mouse brains following SFV4 infection.....112
4G Neonatal and adult mouse brains produce functional IFN.....113
4H Mouse survival (days) after SFV L10 inoculation and treatment with Multiferon.....116

Chapter 5

5A Genetic confirmation of $PKR^{o/o}$ or wild type mouse strains and MEFs.....127
5B Functional IFN in the brains of SFV4 infected (ic) wild type and $PKR^{o/o}$ mice at 24 hours.....128
5C IFN-β and IFN-α transcripts in wt and $PKR^{o/o}$ mouse brains after SFV4 infection.....130
5D Levels of IFN-β transcripts correlated with levels of SFV RNA.....132
5E Levels of IFN-α transcripts correlated with levels of SFV RNA.....132
5F Functional IFN and infectious virus levels in 129 wt and $PKR^{o/o}$ mice infected with SFV4.....133
5G IFN-β transcripts in wt and $PKR^{o/o}$ MEFs after SFV4 infection.....134
5H Experiment II: IFN-β transcripts in wt and $PKR^{o/o}$ MEFs after SFV4 infection.....136
5I IFN-α transcripts in wt and $PKR^{o/o}$ MEFs after SFV4 infection.....137
5J β-actin transcripts in wt and $PKR^{o/o}$ MEFs after SFV4 infection.....139
5K MEF percentage survival after SFV4 infection.....140
5L Functional IFN in wt and $PKR^{o/o}$ cells after SFV4 infection.....141

Chapter 6

6A Localisation of naP2 during an SFV4 or SFV4nsP2RDR infection.....151
6B Growth curves of SFV4 and SFV4nsp2RDR in BHK cells and MEFs.....152
6C IFN-β transcript induction by SFV4, SFV4nsP2RDR and SFV A7(74).....154

6D β-actin and GAPDH transcript levels in PBS, SFV4, SFV4nsP2RDR and SFV A7(74) infected cell cultures.....156
6E Reduction of cellular transcripts in SFV infected cells.....158
6F Functional IFN induced by SFV4 and SFV4nsP2RDR in L-929 cells.....159
6G Functional IFN induced by SFV4 or SFV4nsP2RDR infected MEFs over 24 hours.....160
6H Cellular translation shut-off in SFV4 and SFV4nsP2RDR infected MEFs.....162
6I Nuclear translocation of NF-κB and IRF-3 in SFV infected MEFs.....164
6J IFN-β promoter bound NF-κB during an SFV4 or SFV4nsP2RDR infection.....167

List of Tables

Chapter 1

1A Different subtypes of type I IFN.....7

1B Virus inverse interference of the IFN response.....34

Chapter 2

2A Cytopathic Effect plate design.....55

2B CPERA plate design.....62

2C Swedish IFN Bioassay plate set up.....63

2D Primer sequence and annealing conditions.....65

Chapter 3

3A SFV4 transcripts quantified from the same RNA sample.....90

3B IFN-β transcripts quantified from the same RNA sample.....91

3C 50 % cell death end point values for laboratory standard IFN run on 6 plates.....97

Chapter 4

4A Multiferon treatment regime.....115

Chapter 5

5A A comparison of virus and IFN levels between wt and $PKR^{o/o}$ mouse brains.....133

Abbreviations

ADAR-1	Adenosine deaminase
ADV	Adenovirus
ANOVA	Analysis of Variance
AP-1	Activator protein
APCs	Antigen presenting cells
ARRE2	Antigen receptor response element
ATF-2	Activating transcription factor
BHK-21	Baby hamster kidney cells
BME	Beta mercaptoethanol
BSA	Bovine serum albumin
BVDV	Bovine viral diarrhoea virus
CARD	Caspase recruitment domain
CBP	CREB binding protein
CDKs	Cyclin dependent kinases
CIITA	Class II transactivator
CKI	Cyclin kinase inhibitors
CNS	Central nervous system
CPE	Cytopathic effect
CPERA	Cytopathic effect reduction assay
CPV	Cytopathic vacuole
CREB	c-AMP response element binding protein
DCs	Dendritic cells
DDB1	UV damaged DNA binding protein
DISC	Death inducing signalling complex
DMEM	Dulbecco's modified Eagles medium
dNTP	Deoxy nucleotide triphosphate
(c)DNA	(Copy) deoxyribonucleic acid
dsRBM	Double stranded RNA binding motifs
dsRNA	Double stranded ribonucleic acid
DTT	Dithiothreitol
EBER	Epstein Barr virus encoded RNA
EBV	Epstein Barr virus
EDTA	Ethylenediaminetetraacetic acid
EEE	Eastern equine encephalitis
eGFP	Enhanced green fluorescent protein
EGTA	Ethyleneglycol-bis(B-aminoethyl)-N,N,N,N'tetraacetic acid
eIF	Elongation initiation factor
EMCV	Encephalomyocarditis virus
EMSA	Electromobility shift assay

FADD	Fas associated death domain
FCS	Foetal calf serum
FLIP	FLICE inhibitory proteins
FMDV	Foot and mouth disease virus
GAPDH	Glyceraldehyde-3-phosphate dehydrogenase
GAS	IFN-G activated sequence
GMEM	Glasgow's modified essential medium
HAV	Hepatitis A virus
HCMV	Human cytomegalovirus
HCV	Hepatitis C virus
HEPES	N'-[2-hydroxyethyl]piperazine-N'-[2-ethanesulphonic acid]
HIV	Human immunodeficiency virus
HMGI(Y)	High mobility group I (Y) proteins
HPIV2	Human parainfluenza virus 2
HRP	Horse radish peroxidase
Hsp	Heat shock protein
HSV-1	Herpes simplex virus
HTLV	Human T-cell leukaemia virus type 1
IAP	Inhibitors of apoptosis proteins
ICAD	Inhibitors of caspase activated DNase
IFN	Interferon
IFNAR	Interferon alpha receptor
IFNGR	Interferon gamma recepter
Ig	Immunoglobulin
IKK	Inhibitory kappa kinase
IL	Interleukin
IPS	IFN-beta promoter stimulator protein
IRAK	IL-1 receptor associated kinase
IRF	IFN regulatory factor
IRS IFN	International reference standard IFN
ISGF3	IFN stimulated gene factor 3
ISGs	IFN stimulated gene
ISRE	IFN stimulated response element
IU	International units
IκB	Inhibitory kappa B
JNK	c-Jun N-terminal kinase
KSHV	Kaposi's sarcoma herpes virus
LB	Luria broth
LMCV	Lymphocytic choriomeningitis virus
LPS	Lipopolysaccharide
Mal	MyD88 adaptor like protein
MAP	Mitogen activated protein

MAPK	Mitogen activated protein kinase
MCMV	Murine CMV
mda-5	Melanoma differentiation associated factor 5
MEFs	Mouse embryo fibroblasts
MHC	Major histocompatibility complex
MIP	Macrophage inflammatory protein
MKK	Mitogen activated protein kinase kinase
moi	Multiplicity of infection
MTOR	Mammalian target of rapamycin
MyD88	Myeloid differentiation factor 88
NBCS	Newborn calf serum
NDV	Newcastle disease virus
NFAT	Nuclear factor of activated T cells
NF-κB	Nuclear factor kappa B
NK cells	Natural killer cells
NO	Nitric oxide
NOS	Nitric oxide synthase
NP	Nucleoprotein
nsP	Non-structural protein
2' – 5' OAS	Oligoadenylate synthase
P/S	Penicillin and streptomycin
PACT	PKR activator
PAMPs	Pathogen associated molecular patterns
PBSA	Phosphate buffered saline albumin
(q)PCR	(quantitative) Polymerase chain reaction
PDGF	Platelet derived growth factor
PFU	Plaque forming unit
PI3K	Phosphotidylinositol-3-kinase
PIAS	Protein inhibitors of activated STATs
PKR	Protein kinase R
PML	Promyelocytic leukaemia protein
PMSF	Phenylmethylsulphyl fluoride
pRb	Retinoblastoma protein
PRD	Postive regulatory domain
RHD	REL homology domain
RIG-I	Retinoic acid inducible gene
RIP-1	Receptor interacting protein
RLI	RNase L inhibitor
(m)RNA	(messenger) ribonucleic acid
RNAPol II	RNA polymerse II
RNase L	Endoribonuclease L
RRV	Ross river virus

RSV	Respiratory syncitial virus
RT-PCR	Reverse transcription PCR
SCID	Severe combined immunodeficient
SDS-PAGE	Sodium dodecyl sulphate - polyacrylamide gel electrophoresis
SFV	Semliki forest virus
SOCS	Suppressors of cytokine signalling
sPBS	Sterile phosphate buffered saline
STAT	Signal transducers and activators of transcription
SV	Sindbis virus
SV5	Simian virus 5
TAK-1	Transforming growth factor beta activating kinase 1
TANK	TRAF family member associated NF-kappa B activator
TBE	Tris borate EDTA
TBK-1	TANK binding kinase 1
$TCID_{50}$	Tissue culture infecious dose 50
Th cells	T helper cells
THOV	Thogoto virus
TIR	Toll/IL-1 receptor
TLR	Toll-like receptor
TNF	Tumour necrosis factor
TNFR	TNF receptor
TRAF6	TNFR associated factor 6
TRAM	TRIF related adaptor molecule
TRIF	TNFR associated IFN-beta inducing factor
VA RNA	Virus associated RNA
VEE	Venezuelan equine encephalitis virus
VHS	Virus host shut-off inducer
VSV	Vesicular stomatitis virus
VV	Vaccinia virus
WEE	Western equine encephalitis virus
WT	Wild type

Abstract

The type I interferon (IFN) system is a potent anti-viral innate immune response. It is primed by IFN-β and IFN-α_4, which are the immediately expressed IFNs following detection of virus infection. IFN-β establishes the anti-viral immune response within the infected cell, augments further IFN production through the induced expression of IRF-7, a transcription factor for other IFN-αs, and promotes the adaptive immune response. Induction of IFN-β requires the activation of multiple transcription factors, including NF-κB; some of these are maintained in an inactive state within the cytoplasm of the resting cell. PKR is an IFN-induced, dsRNA-activated kinase capable of phosphorylating and activating the IκK, which ultimately releases NF-κB enabling its nuclear translocation. Within the nucleus NF-κB associates with IRF-3 and AP-1 on the IFN-β promoter to induce IFN-β expression. Delineation of the pathways that result in IFN-β expression has revealed viral proteins which target components of these signalling networks. To date no anti-IFN mechanisms have been observed for Semliki Forest virus (SFV), an alphavirus of the *Togaviridae*. The SFV genome is 11 kb in length and encodes two open reading frames; the non-structural proteins (nsP 1-4), which encode the replicase complex and the structural proteins. Studies with Sindbis virus, a closely related alphavirus have suggested that nsP2 may play a role in IFN suppression. Previous studies with SFV nsP2 observed that 50 % of nsP2 was translocated to the nucleus. When nsP2 nuclear translocation is prevented, the infection has reduced neuropathology.

This thesis explores the importance of IFN in SFV encephalitis. A quantitative PCR assay for IFN-β and IFN-α transcripts and a quantitative IFN bioassay were developed to determine differences in IFN expression under different infection conditions. Mouse models and primary cell lines were used to establish the importance of PKR for IFN-β expression during SFV infection and to determine whether SFV nsP2 has a role in modulating IFN responses. In the absence of PKR, at early times post-infection, cultured cells reproducibly produced significantly lower levels of IFN-β transcripts. Reduced levels of functional IFN were also demonstrated

by bioassay. Previous data has shown that PKR is not required for IFN-β induction. The sensitivity of the qPCR assay has allowed the demonstration that PKR, although not critical for IFN induction, is involved in IFN-β induction and is particularly important at early time points post-infection.

SFV-nsP2 has been postulated to be involved in IFN interference. Comparing SFV4 to SFV4-nsP2-RDR (a mutant virus with a single amino acid change within the nuclear localisation signal of nsP2, which prevents its translocation into the nucleus) demonstrated that relative to the number of infected cells, the SFV4nsP2-RDR mutant induced over ten-fold more IFN-β transcripts than the wildtype SFV4 strain; this upregulation was specific to IFN-β. The IFN bioassay results supported this data; SFV4-nsP2-RDR induced higher functional IFN levels in comparison to wt SFV4. Both viruses grew to similar titres and at similar rates. In the mutant and wt infections both NF-κB and IRF-3 translocated into the nucleus; however, preliminary EMSA data has suggested that the amount of NF-κB bound to the IFN-β promoter is reduced during a wt infection. This suggests a possible mechanism for the differential IFN expression and represents the first IFN evasion mechanism described for Semliki Forest virus.

Chapter 1: Introduction

Contents

Introduction 3
The anti-viral immune response 4
Innate Immunity 4
Adaptive Immunity 4
T cell responses 4
B cell responses 5
The Role of IFNs in Innate Immunity 6
Type I IFNs 6
Type II IFN 8
The roles of type I IFN 9
Induction of IFN-β 10
IFN induction pathways 10
The Toll-like Receptors 10
TLR activation of transcription factors required for IFN-β expression 11
MyD88 dependent NF-κB activation 11
TRIF dependent NF-κB activation 11
MyD88 dependent IRF activation 12
TRIF dependent IRF-3 activation 12
Cytoplasmic-localised receptor activation of transcription factors required for IFN-β gene expression 15
Activation of ATF-2/c-Jun 16
IFN-β Enhanceosome 16
The role of IRFs 17
IFN signalling 18
Alternative IFN signalling pathways 21
Augmentation of IFN signalling 22
Control of STAT signalling 22
IFN Stimulated Genes 23

Formation of the anti-viral state....23
Protein Kinase R (PKR)....23
2'-5'OAS and RNase L....24
ADAR-1....25
MxA....25
Other IFN induced genes....26
Modulation of cell proliferation and immune responses by IFNs....26
Inverse Interference....27
DNA viruses....28
Herpesviruses....28
Poxviruses....29
Double stranded RNA viruses....30
Negative stranded RNA viruses....30
Paramyxoviruses....30
Positive stranded RNA viruses....32
Flaviviruses....32
Picornaviruses....33
Tumour Necrosis Factor and cell death pathways are other targets of viral antagonism....35
Semliki Forest virus....37
Alphavirus Family....37
SFV Pathogenesis....38
Age-dependent Virulence....39
SFV Replication....40
Roles of the Non-Structural Proteins....41
NsP1....41
NsP2....41
NsP3 and nsP4....42
The Involvement of the Immune Response....43
Semliki Forest Virus and Interferons....43
Aims & Hypotheses....45

Introduction

This thesis focuses on the interaction of Semliki Forest virus (SFV) with the interferon (IFN) response. The aim of this chapter is to review the IFN response and the plethora of IFN evasion mechanisms currently described for viruses. Further evidence is provided to support the complexity of pathogen-host interactions by reviewing another cytokine, tumour necrosis factor (TNF) and several virus TNF evasion mechanisms. Despite the wealth of information available on virus interactions with the IFN response, little is known about this with regard to alphaviruses, which are in many other ways amongst the most studied of viruses. The second section of this chapter reviews the virulence and pathogenicity of SFV; an alphavirus used as a model to study virus encephalitis. Determining alphavirus interactions with the IFN system is important, it adds to knowledge on this important model system and since many alphaviruses can cause encephalitis, in the absence of vaccines, IFN has been proposed as a potential therapy.

The anti-viral immune response

Innate Immunity

Immunity is critical for host survival against infection; the vertebrate immune system has evolved two major systems to combat disease. These are classified as the innate and adaptive immune responses. The innate immune response is the primary non-specific response to an invading pathogen. Host cell receptors encoded within the germline detect pathogen associated molecular patterns. With respect to RNA virus infections, a replication intermediate, dsRNA, is detected by several receptors including Toll like receptor – 3 (TLR-3), retinoic acid inducible gene –I (RIG-I), melanoma differentiation associated factor 5 (mda-5) and PKR (Matsumoto et al., 2002; Yoneyama et al., 2004; Andrejeva et al., 2004; Clemens et al., 1993). These induce the IFN response, a component of innate immunity. Other components of innate immunity are also involved in anti-viral immune responses and include natural killer (NK) cells, complement, phagocytes, chemokines and various cytokines including interferon (IFN). NK cells induce death of virally infected cells through non-specific receptor interactions; for example, poor expression of MHC I molecules acts as a positive signal for NK cell induced cell death (this is important as many viruses downregulate expression of MHC I molecules to avoid detection by cytotoxic T cells, Plougastel et al., 2006). Complement and phagocytes play a role in anti-viral immunity alongside antibodies and IFNs induce the expression of thousands of genes involved in anti-viral responses, immuno-modulation and regulation of cell proliferation (Samuel, 2001).

Adaptive Immunity

T cell responses

In addition to direct anti-pathogen effects the innate immune response induces and skews the adaptive immune response. Antigen-presenting cells (APCs), dendritic cells (DCs) and macrophages express pathogen epitopes on major histocompatibility complex II (MHC II) molecules which are presented to CD4+ T helper cells (Th). Further stimulation of T cells by APCs is required for complete activation of T cells.

Co-stimulation can be in the form of additional adhesion molecule interactions and/or cytokine signalling. Specific cytokine dominance surrounding maturing CD4+ Th cells can influence the type of Th cell response. Initially activated T cells, T_0 cells, release interleukin (IL) – 2, IL – 4 and IFN-γ. IFN-γ inhibits the proliferation of Th 2 cells. Th2 cells favour B cell activation and antibody production. On the other hand IL – 10, a Th 2 cell cytokine, inhibits IFN-γ and IL-2 secretion and so inhibits Th 1 responses. The Th1 response promotes CD8+ cytotoxic T cell activation and hence is a key component in anti-viral immunity. Th 1 cells secrete IFN-γ, IL – 2 and TNF-β; these contribute to both macrophage and T cell activation. CD8+ T cells detect antigen presented on MHC I molecules. MHC I molecules are expressed on the surface of all nucleated cells with the exception of neurones where expression can be induced by IFN-γ (Rottenberg and Kristensson, 2002). This subclass of T cells requires a stronger co-stimulation signal than the Th cells. DCs are the only cells capable of activating CD8+ T cells alone, all other APCs must be associated with a Th 1 cell so that a secondary signal (IL – 2) can be sent from the Th 1 cell to activate the CD8+ T cell. The active CD8+ T cell then traverses the body until it comes into contact with a cell expressing peptide bound MHC I molecules, where the peptide is specific for the activated T cell, upon which it secretes mediators (perforin and granzymes) of target cell death.

B cell responses

Antibodies function primarily against extracellular pathogens. Extracellular virions can be neutralised and opsonised by specific antibodies. In addition, enveloped viruses express viral antigens on the surface of the plasma membrane of the cells they infect and these can be targeted by antibodies for complement mediated destruction. Th 1 cells secrete IL – 3 which induces B cell class switching. B cells primarily secrete immunoglobulin (Ig) M. Upon IL – 3 exposure the antibody secreted is changed to IgG_1 or IgG_3. Antibody binds and neutralises the virus by preventing host cell interactions and hence infection. Ig mediated uptake of virus by phagocytes via Fc receptor interactions or via complement receptors is referred to as opsonisation. Antibody activation of complement on the cell surface ultimately results in perforating the lipid envelope inducing death by osmotic dysregulation.

The Role of IFNs in Innate Immunity

The anti-viral immune response is initially dominated by IFNs; these are the first cytokines secreted in response to cellular infection with virus. They act in an autocrine and paracrine manner by inducing expression of anti-viral proteins within the infected cell and by inducing an anti-viral state within neighbouring non-infected cells. Isaacs and Lindenmann (1957) first discovered the anti-viral activity of IFNs, since then several other roles for IFN have been elucidated, including control of cell proliferation and modulation of the immune response (Tanaka et al., 1998; Biron et al., 1999). IFNs, which are only found in vertebrates (Oritani and Kanakura, 2005), are sub-divided into type I IFNs, consisting of the IFN-αs, IFN-β, IFN-ω, -τ, -κ, -δ and -ε; type II IFNs, IFN-γ the immune IFN and a novel subgroup of IFNs partially related to IFN-α, IFN-λ.

Type I IFNs

Type I IFNs all converge upon the IFN-α/β receptor (IFNAR), which is expressed on the plasma membrane of all cells examined, to induce signalling and gene expression (Brierley and Fish, 2002). IFN-α is encoded on human chromosome 9; 14 genes encode the different IFN-α subtypes although only 13 functional proteins are expressed as ifna13 encodes the same protein as ifna1 (Oritani and Kanakura, 2005; Bekisz et al., 2004; Foster and Finter, 1998). The mature IFN-α proteins share between 75 % and 99 % homology (Bekisz et al., 2004). IFN-β and IFN-ω are also encoded on human chromosome 9, but share less homology with IFN-α, 30 % and 75 %, respectively (Bekisz et al., 2004) and are only encoded by a single gene locus (Roberts et al., 1998). IFN-α is predominantly associated with leukocytes; plasmacytoid dendritic cells produce approximately 10^3 times greater amounts of IFN-α than other blood cells (Siegal et al., 1999). IFN-β is historically the fibroblast IFN, but can be produced by most cells. Of the more recently discovered IFNs, IFN-τ, -δ and –ξ are not expressed in humans. IFN- τ is a 172 amino acid polypeptide and is only expressed by ruminant ungulate species during pregnancy; the trophoblast secretes IFN- τ to facilitate implantation (Martal et al., 1998). Despite its absence in humans, this IFN still functions on human cells (Martal et al., 1998). IFN-δ is a 149

amino acid glycopeptide only expressed in porcine trophoblasts. Unlike IFN- τ, IFN-δ is species specific and does not function on human cells (Lefevre et al., 1998). IFN–ξ, otherwise known as limitin, has homology to IFN-α, -β and –ω and is only expressed in mice. However, in contrast to other IFNs it does not influence proliferation of myeloid or erythroid progenitors (Kawamoto et al., 2003).
To date two other human type I IFNs have been discovered, IFN-κ and IFN-ε. IFN-κ is expressed in human keratinocytes (LaFleur et al., 2001) and IFN-ε is thought to have a reproductive function in placental mammals (Bekisz et al., 2004).
Another type of IFN, the IFN-λ family, possesses anti-viral activities and shares homology with IFN-α. However, IFN- λ interacts with an alternative receptor, a class II receptor composed of IFN λ receptor 1 and IL – 10 receptor 2 which may define this as a new class of IFNs. Despite associating with a different cellular receptor, IFN-λ induces the same signalling components (ISGF3) as the IFNAR (Kotenko et al., 2003). IFN- λ (1 – 3) are also termed IL – 28A, IL – 28B and IL – 29 (Bekisz et al., 2004). All of the type I IFNs are summarised in table 1A.

Type	Details	Associated Cell Type	Species	Receptor	Function
IFN-α	14 subtypes	Leukocytes	Human	IFNAR	Induction of antiviral state
IFN-β		Fibroblasts (most cells)	Human	IFNAR	Induction of antiviral state
IFN-ω			Human	IFNAR	Induction of antiviral state
IFN-δ		Trophoblasts	Pig	IFNAR	Facilitates implantation
IFN-ε			Placental mammals	IFNAR	Involved in reproduction
IFN-λ	IL-28A, IL-28B, IL-29		Human	IFNλ receptor 1 plus IL-10 receptor 2	Induction of antiviral state
IFN-ζ	(Limitin)		Mouse		Induction of antiviral state
IFN-τ		Trophoblast	Ruminant (ungulate)	IFNAR	Facilitates implantation
IFN-κ		Keratinocytes	Human		Unknown

Table 1A: Different subtypes of type I IFN
All of the currently known type I IFN subtypes are listed. The table indicates the cells and species with which they are associated, the receptor they bind and their major functional role.

Type II IFN

The second class of IFNs, IFN-γ is produced by NK cells, CD4 Th1 cells and CD8 cytotoxic suppressor cells. It is not induced directly by virus infection, but by mitogens or antigens presented on MHC class I and II molecules (Samuel, 2001). IFN- γ has only a single gene locus and unlike the type I IFNs, IFN-γ mRNA contains both exons and introns (Rottenberg and Kristensson, 2002). IFN-γ, once expressed associates with the IFN- γ receptor (IFNGR). This receptor is composed of two subunits IFNGR 1 and IFNGR 2, which form a heterotetramer. IFNGR 1 is ubiquitously expressed, although CNS expression of the IFNGR is restricted to specific locations within the brain, the olfactory bulb, piriform and entorhinal cortex, midline thalamus and the medial hypothalamic structures (Rottenberg and Kristensson, 2002; Robertson et al., 2000). Expression of the IFNGR 2 subunit is regulated by specific cytokines. Ligand attachment to the IFNGR activates signalling cascades which induce the expression of a two wave response. Bound IFNGR activates Jak 1 and Jak 2, receptor associated tyrosine kinases, to phosphorylate signal transducer and activator of transcription (STAT) -1, resulting in STAT 1 dimerisation and nuclear translocation. Within the nucleus the STAT 1 homodimer associates with IFN- γ activated sequences (GAS). These sequences are present within the promoters of specific genes and induce their transcription. Two such genes are the transcription factors IRF-1 and class II transactivator (CIITA). These mediate the second wave of signalling and induce the expression of MHC I and II molecules, upregulate the IP-10 chemokine and activate a plethora of anti-viral mechanisms although with reduced kinetics in comparison to the type I IFNs (Bach et al., 1997; Farrar and Schreiber, 1993). The pathway described above is the most researched signalling pathway of the IFNGR; however, other signalling pathways exist, including the mitogen activated protein kinase pathway (Sakatsume et al., 1998). Many of the components of the IFN- γ induced anti-viral response are also induced by the type I IFNs and are described further in the following sections; these include Mx A, RNase L, PKR and 2' – 5' OAS (Arnheiter and Haller, 1983; Castelli et al., 1997; Clemens and Elia, 1997). In addition to these proteins, IFN- γ induces the expression of nitric oxide synthase (NOS) in macrophages (Marletta, 1993a; 1993b; Chesler and Reiss, 2002). NOS produces nitric oxide (NO) by converting L-arginine into L-citrulline (Marletta, 1994). NO and its reactive products are effective anti-viral molecules, NO

nitrosylates viral proteins specifically cysteine and tyrosine residues resulting in structural misfolding of the protein and functional impairment (Colasanti et al., 1999).

The roles of type I IFN

Type I IFN is composed of 12 functional IFN-α proteins, IFN-β and IFN-ω all of which converge onto the same IFNAR. This raises the question as to why there are so many subtypes. There are several possible explanations:

1) Different subtypes of IFNs induce differential gene expression.
2) Different IFNs are induced by different pathogens.
3) Different IFNs are expressed at different times during an infection.

It is possible that different IFNs induce a different array of gene expression as differential requirements by type I IFNs for downstream signalling components have been observed. All type I IFNs require the Janus N-terminal kinase (JNK), Tyk-2, a component of the Jak/STAT signalling pathway; however, IFN-β can induce signalling in the absence of Tyk-2 (Pellegrini and Schindler, 1993). In fact, IFN-β can induce the expression of additional genes not induced by other IFNs, for example the hypoxia-inducible factor 1 gene (Rani et al., 1996).

Different IFNs are induced by different pathogens. IFN expression is promoted by transcription factors, IFN regulatory factors (IRFs). Different IRFs induce different subsets of IFN. The fact that different IFNs are induced by different regulatory factors suggests that different IRFs may be activated by different pathogens. For example, IRF-5 stimulates synthesis of a specific set of IFN-αs, distinct from those targeted by IRF-7 and is only activated by certain viruses e.g. Newcastle disease virus (NDV) (Barnes et al., 2001).

Different IFNs are expressed at different times during an infection. In response to a viral infection host cells initially produce IFN-β and IFN-α_4. These IFNs induce expression of IRF-7, which induces the expression of other IFN-α genes (Marie et al., 1998). IRF-7 is only activated if virus is still detected within the cell. This enables the cell to control the expansion of IFN expression and primes cells adjacent to infected cells for a rapid response.

Induction of IFN-β

IFN induction pathways

A variety of different cellular receptors, including TLRs, PKR, RIG-I and mda-5, enable the cell to detect virus at multiple stages of infection (Yoneyama et al., 2004; Clemens et al., 1993; Andrejeva et al., 2004). Pathogen bound receptors activate signalling cascades, which ultimately activate NF-κB, IRF-3 and AP-1, the transcription factors required for IFN-β gene expression.

The Toll-like receptors

Toll was first discovered in drosophila in association with embryogenesis (reviewed in Takeda et al., 2005). However, adult drosophila lacking Toll mutants were observed to be more susceptible to fungal infections than wild type adults. It was determined that the cell surface expressed Toll interacted with 'spaetzle' and that this interaction induced the production of an antifungal protein drosomycin (Brennan and Anderson, 2004). The sequence homology of Toll with the intracellular component of the IL-1R led to the discovery of 11 mammalian Toll-like receptors (TLR), each of which detects particular pathogen associated molecular patterns (PAMPs). For example, TLR-2 binds bacterial lipopeptides (Hirschfeld et al., 2000); TLR-3 binds dsRNA (Matsumoto et al., 2002); TLR-4 associates with lipopolysaccharide (LPS) (Poltorak et al., 1998), TLR-5 interacts with bacterial flagellin (Mizel and Snipes, 2002), TLR-7 detects ssRNA (Heil et al., 2004) and TLR-9 detects unmethylated CpG motifs expressed on DNA viruses (Lund et al., 2003). TLR-3, -7 and –9 are localised to endosomal compartments and are well placed to monitor neighbouring infected or dead cells (Honda et al., 2005). Other TLRs are cell surface expressed and have greater association with bacterial, fungal and parasitic infections. In addition to their role in anti-bacterial immune responses, TLR-2 and TLR-4 can also detect virus. For example, TLR-2 binds the haemagglutinin protein of measles virus (Bieback et al., 2002) and TLR-4 binds the fusion protein of respiratory syncitial virus (RSV) (Kurt-Jones et al., 2000). This suggests that TLRs are less specific than first thought as multiple pathogens can interact with and activate the same receptor.

TLR activation of transcription factors required for IFN-β expression

All of the TLRs, with the exception of TLR-3 signal through myeloid differentiation factor 88 (MyD88) to activate NF-κB (Medzhitov et al., 1998). TLR-3 associates with TNFR-associated IFN-β inducing protein (TRIF) to activate NF-κB and IRF-3 (Yamamoto et al., 2003), see figures 1A and 1B .

MyD88 dependent NF-κB activation (Figure 1A)

Ligand bound TLRs recruit MyD88 directly (Medzhitov et al., 1998) or interact with MyD88 through MyD88 adaptor-like protein (Mal) e.g. TLR-2 and TLR-4 (Mansell et al., 2004; Fitzgerald et al., 2001). MyD88 associates with IL-1R associated kinase family members (IRAK) 1 – 4 (Martin and Wesche, 2002); interactions between IRAK-1 and MyD88 induce hyperphosphorylation of IRAK-1 (Li et al., 2002). The hyperphosphorylated form of IRAK-1 is released and associates with a ubiquitin kinase (Deng et al., 2000), TNFR associated protein 6 (TRAF6) (Burns et al., 2000). TRAF6 activates the transforming growth factor β activating kinase – 1 (TAK-1) (Ninomija-Tsuji et al., 1999), which phosphorylates the downstream kinases IKKα and IKKβ (Yi and Krieg, 1998). NF-κB is held within the cytoplasm by the inhibitory κB complex (IκB). Phosphorylation of the IκBα subunit targets the subunit for ubiquitin-dependent, 26 S proteosome-mediated degradation releasing active NF-κB dimers for nuclear entry (Figure 1A) (Li et al., 1995; Scherer et al., 1995).

TRIF dependent NF-κB activation (Figure 1A)

TLR-3 directly associates with and activates TRIF to induce IFN-β gene expression; TLR-4 can also induce IFN expression, although at a reduced rate (Doyle et al., 2003) by indirect activation of TRIF through the TRIF related adaptor molecule (TRAM) (Oshiumi et al., 2003). For TLR-3 activation of NF-κB, a protein complex including TRAF-6, TBK-1 and a poly-ubiquitinated form of RIP-1 are recruited to TLR-3 (Figure 1A) (Cusson-Hermance et al., 2005). The necessity of TRAF6 has been questioned and could be cell type dependent (Sato et al., 2003; Gohda et al., 2004; Meylan et al., 2004). This complex ultimately activates IKKα and IKKβ, which phosphorylate IκB to release NF-κB as described before.

MyD88 dependent IRF activation

Plasmacytoid dendritic cells (pDCs) detect virus through TLR-7 and TLR-9 (Heil et al., 2004; Lund et al., 2003), which signal through MyD88. pDCs are capable of inducing massive amounts of IFN-α. It is thought that MyD88 interacts with the high pDC basal levels of IRF-7, IRAK-4 and TRAF-6 (Izaguirre et al., 2003; Uematsu et al., 2005; Honda et al., 2004). These interactions result in IRF-7 activation through the ubiquitin ligase activity of TRAF-6 (Honda et al., 2004) and induce high IFN-α expression. In addition, IRF-5 was recently associated with TLR-7 induction of IFN gene expression in pDCs (Schoenemeyer et al., 2005).

TRIF dependent IRF-3 activation (Figure 1B)

TRIF activates TRAF-family member associated NF-κB activator kinase (TANK) – binding kinase – 1 (TBK-1) and IKKε, either of which can induce IRF-3 phosphorylation and activation (Fitzgerald et al., 2003; Sharma et al., 2003). TRIF interactions with TBK-1 and IKKε are facilitated by TANK family protein NAK-associated protein 1 (NAP1) (Figure 1B) (Sasai et al., 2005). TBK-1 is thought to be the predominant kinase, as it is constitutively expressed in many cell types whereas IKKε has a restricted expression (Perry et al., 2004). Mice or primary cell cultures lacking TBK-1 are severely impaired in their ability to induce IFN and IFN stimulated gene expression or activate IRF-3, whereas $IKK\varepsilon^{-/-}$ cell lines express normal IRF-3 activation in response to dsRNA or LPS (McWhirter et al., 2004; Hemmi et al., 2004). Complete IRF-3 activation also requires the phosphatidylinosital 3 - OH kinase (PI3K). Ligand bound TLR-3 recruits PI3K, which activates the downstream kinase Akt, which further phosphorylates IRF-3. Akt phosphorylation of IRF-3 promotes c-AMP response element binding protein (CREB) – binding protein (CBP) co-activator interactions (Figure 1B, Sarkar et al., 2004).

IRF-3 encodes nuclear import and export signals, which enable it to move freely between the nucleus and cytoplasm. Phosphorylation of the IRF-3 C-terminus prevents nuclear export and enables dimerization and activation (Nguyen et al., 1997; Taniguchi et al., 2001). Upon activation IRF-3 recruits p300 and CBP (Suhara et al., 2002). Both of these possess an intrinsic histone acetyltransferase activity, which ultimately makes the promoter site more accessible to transcription factors.

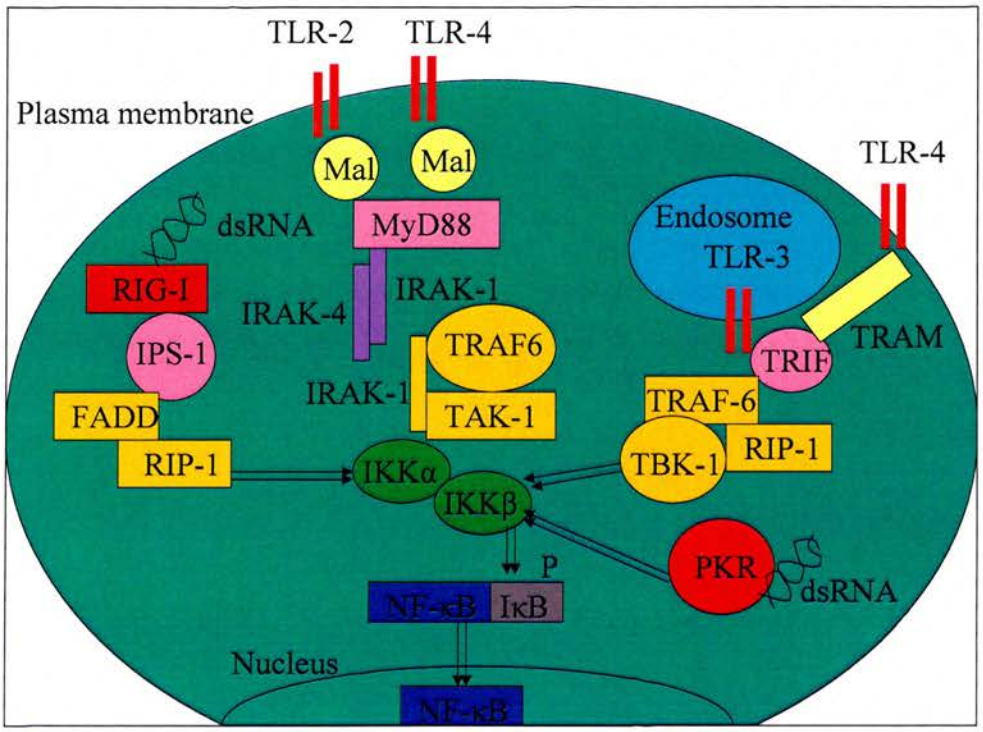

Figure 1A: Induction of NF-κB

Virus infection can be sensed at multiple levels; by both plasma membrane receptors and intracellular cytoplasmic receptors (red). Receptors are associated with adaptor proteins (pink), which link the receptors to downstream signalling complexes (orange). Some receptors require additional proteins (yellow), which enable them to associate with the adaptor protein. MyD88 signalling requires additional proteins, IRAK-1 and IRAK-4 (purple). All of the signalling complexes converge on the inhibitory kappa kinase (IKK, green); this kinase phosphorylates IκB (grey) targeting it for poly-ubquitination and proteosome degradation. Free NF-κB (blue) can then enter the nucleus where it associates with gene promoters, e.g. IFN-β promoter.

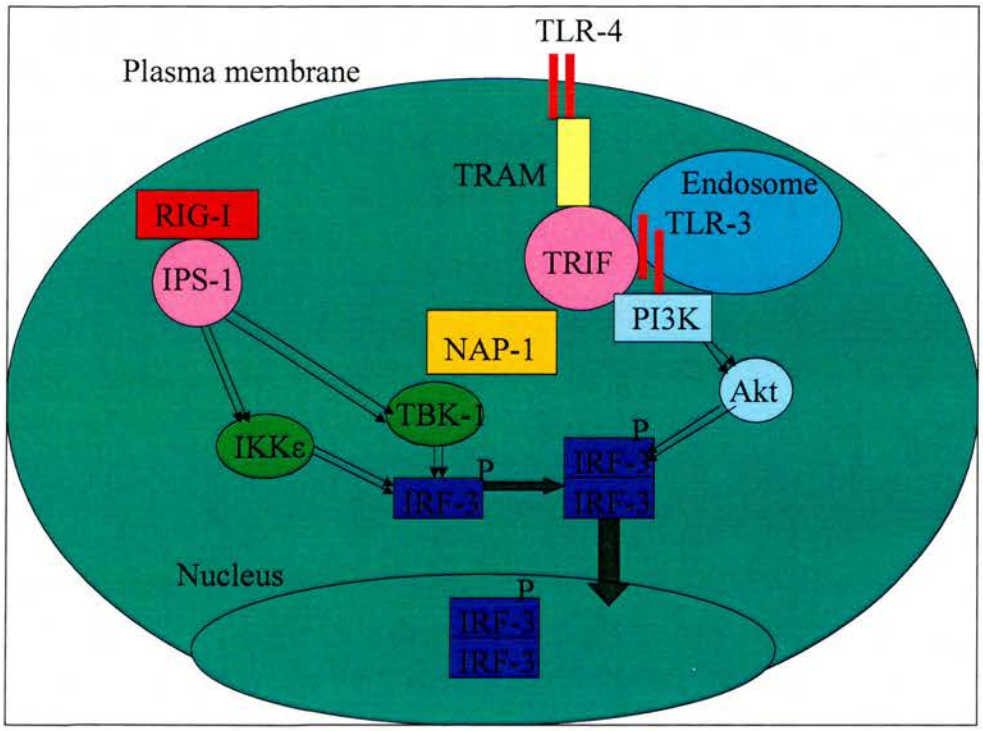

Figure 1B: Induction of IRF-3

Virus infection can be sensed at multiple levels by both plasma membrane receptors and intracellular cytoplasmic receptors (red). Receptors are associated with adaptor proteins (pink), which link the receptors to downstream signalling complexes (orange). Some pathways do not show downstream signalling complexes as these have yet to be elucidated. TLR-4 requires an additional protein (yellow), which enables it to associate with TRIF. In addition to TRIF induction of IRF-3, TLR-3 recruits PI3K, which activates the downstream kinase Akt (pale blue). These kinases are required for complete phosphorylation of IRF-3. All of the signalling pathways converge on TANK-binding kinase 1 (TBK-1) or Inhibitory kappa kinase ε (IKKε) (green); these kinases phosphorylate IRF-3 (blue). Phosphorylation of IRF-3 results in homodimer formation and activation; active IRF-3 enters the nucleus to associate with promoters containing specific domains e.g. IFN-β promoter.

Cytoplasmic-localised receptor activation of transcription factors required for IFN-β gene expression

PKR, RIG-I and mda-5 proteins are dsRNA receptors localised to the cytoplasm and are ideally situated to ascertain virus infection within the cell (Clemens et al., 1993; Andrejeva et al., 2004). All three receptors activate NF-κB. RIG-I and mda-5 can also activate IRF-3. Activation of both NF-κB and IRF-3 is required for IFN-β gene expression.

PKR is an IFN-induced dsRNA activated serine/threonine kinase (Clemens et al., 1993). dsRNA associates with the PKR dsRNA binding motifs (dsRBM) located in the N-terminal region. This association induces a conformational change resulting in PKR autophosphorylation and activation. Binding to dsRNA also facilitates homodimer formation. PKR activation of NF-κB is associated with PKR:IKKβ interactions, through a mechanism independent of PKR kinase activities. There is much evidence showing the importance of PKR in NF-κB activation; dominant negative forms of PKR, 2-aminopurine (a PKR inhibitor) and PKR deletions, all prevent NF-κB activation following IRF-1, TNF-α, IFN-γ and dsRNA treatment (Kirchhoff et al., 1999; Cheshire et al., 1999; Deb et al., 2001; Kumar et al., 1997).

RIG-I (retinoic acid inducible gene I) and mda-5 (melanoma differentiation associated gene 5) are members of the 'helicard' family, which possess an RNA-binding helicase domain and 2 caspase recruitment domains (CARDs) (Yoneyama et al., 2004). The importance of RIG-I for IFN expression was demonstrated by Kato et al., (2005); RIG-I$^{-/-}$ cells infected with vesicular stomatitis virus (VSV) have severely impaired IFN-β responses compared to wt cells. To induce IFN-β gene expression, dsRNA interacts with the helicase domain causing a signalling cascade to be induced by the CARD domain. RIG-I recruits IFN-β promoter stimulator protein (IPS) -1 (Kawai et al., 2005), which associates with Fas-associated death domain (FADD) and RIP-1 activating IKKα/β and ultimately NF-κB (Figure 1A) (Kawai et al., 2005). RIG-I also activates IRF-3 via TBK-1 or IKKε (Figure 1B). IPS-1 is localised to the outer membrane of the mitochondria (Seth et al., 2005); the importance of this localisation is demonstrated by HCV NS3-4a protease, which cleaves IPS-1 disrupting RIG-I signalling. The position of the NS3-4a cleavage site causes IPS-1 to detach from the

mitochondrial membrane resulting in its dysfunction (Foy et al., 2005; Meylan et al., 2005).

Activation of ATF-2/c-Jun

Several other transcription factors are required to complete the IFN-β enhanceosome, ATF-2 and c-Jun (Thanos and Maniatis, 1995). These transcription factors are also activated in response to dsRNA; dsRNA induces the stress activated mitogen activated kinase (MAP) pathway (Servant et al., 2002; Chu et al., 1999; Iordanov et al., 2000). This consists of p38 MAPKs and c-jun N-terminal kinases (JNK); MEK 3 and 6 are the upstream kinases of p38 MAPKs and MEK 4 and 7 are the upstream kinases of JNK. P38 MAPK and JNK then phosphorylate and activate latent cytoplasmic ATF-2 and c-jun respectively. These transcription factors associate to form the heterodimer AP-1, which translocates into the nucleus and associates with the IFN-β promoter.

IFN-β Enhanceosome

IFN-β expression requires multiple transcription factors, NF-κB, IRF-3, ATF-2 and c-Jun, to associate with specific positive regulatory domains (PRD) of the IFN-β promoter (Figure 1C). The promoter region is located between 105 and 55 bp upstream of the transcriptional start site. Figure 1C indicates the layout of the PRDs within the promoter. The NF-κB p50 and p65 heterodimer binds to PRD II; the ATF-2 and c-Jun heterodimer associates with PRD IV, and PRD III and PRD I bind to interferon regulatory factors (IRF), -3 and -7 (Maniatis et al., 1998; Berkowitz et al., 2002; Panne et al., 2004). NF-κB transcription factors are part of the Rel family; five distinct subunits have been isolated from mammals, NF-κB1 (p50/p105), NF-κB2 (p52/p100), p65 (Rel A), Rel B and c-Rel (Chen et al., 1999). A highly conserved region is found within all of these transcription factors termed the Rel homology domain (RHD); this has been implicated in DNA binding, subunit dimerization and interactions with the IκB proteins (Baldwin Jr, 1996). ATF-2 and c-Jun are basic region leucine zipper proteins (bZIP); which include a DNA binding region and a dimerization domain (Ellenberger et al., 1992). The IRF family encodes 10 mammalian IRFs (Nguyen et al., 1997; Taniguchi et al., 2001). Each contains a conserved DNA binding domain within the N-terminus, which recognises the IFN

stimulated response element (ISRE, 5' – AANNGAAA – 3'). A further two architectural proteins are required to complete the formation of the enhanceosome to enable IFN-β expression, the high mobility group I (Y) proteins (HMG I (Y)). These are situated, one on each of PRD II and PRD IV in association with NF-κB and ATF-2/c-Jun respectively (Yie et al., 1999).

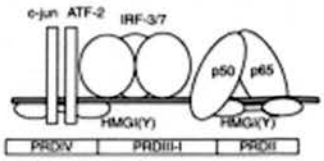

Figure 1C: The IFN-β Enhanceosome
(Taken from Falvo et al., 2000)
The NF-κB subunits, p50 and p65, bind to PRDII in association with HMGI(Y) molecules; the IRFs either IRF-3 or IRF-7 interact with PRDIII and PRDI and the components of AP-1 (c-jun and ATF-2) are located at PRDIV with HMGI(Y) molecules on the IFN-β promoter. Together these transcription factors represent the IFN-β enhanceosome.

The role of IRFs

IRFs, including IRF-3, IRF-5, IRF-7 and IRF-9, induce IFN and ISGs; they contain a DNA binding domain at the N-terminus and an IRF-association domain at the C-terminus to enable dimerisation (Lohoff and Mak, 2005). In addition to IFN-β and IFN-α_4 expression (Schafer et al., 1998), IRF-3 is implicated in direct activation of RANTES specifically after paramyxovirus infection (Lin et al., 1999), and induction of IL-15 and ISG56 (Grandvaux et al., 2002). IRF-7 is induced following IFN-β expression and augments the IFN-α response (Marie et al., 1998). TLR-3, -4, -5, -7 and –9 can activate IRF-5, which is constitutively expressed in B cells and DCs. It induces pro-inflammatory genes and several ISGs (Takaoka et al., 2005; reviewed in Moynagh, 2005). Interestingly, IRF-5 activation is virus specific; NDV, VSV and HSV-1 infections all activate IRF-5-dependent gene expression whereas Sendai virus does not (Barnes et al., 2001; 2004). IRF-9 is a component of the IFN stimulated gene factor 3 (ISGF3), a complex induced following activation of the type I IFNAR, which promotes the expression of genes containing ISREs within their promoters. Of the other IRFs, IRF-1 plays a key role in type II IFN induced gene expression. IRF-1 was the original IRF to be described; it is constitutively expressed at low levels in most cell types (Lohoff and Mak, 2005). IFN-γ expressed by NK cells activates the IFN- γ receptor on APCs and induces IRF-1 in a STAT-1 dependent signalling

cascade (Elser et al., 2002; Coccia et al., 2000). IRF-1 promotes the expression of IL-12p35 and IL-12p40 subunits, which induce IFN- γ expression and plays a key role in skewing the T helper cell response to a Th1 response (Galon et al., 1999; Elser et al., 2002; Lohoff et al., 1997). Within T helper cells, IRF-1 associates with three separate binding sites of the IL-4 promoter to repress its expression; IL-4 is essential for driving the Th2 response (Elser et al., 2002). IRF-1 also induces iNOS expression, upregulates the IL-12β2 receptor subunit and induces caspase-1 expression to cleave preIL-18 into IL-18, another cytokine that stimulates IFN- γ production (Kamijo et al., 1994; Fantuzzi et al., 2001). IRF-4 function appears to antagonise IRF-1 function and its expression is restricted to lymphocytes and macrophages (Eisbenbeis et al., 1995). IRF-4 promotes Th 2 cell responses; $Irf4^{-/-}$ T cells are impaired in their ability to differentiate into Th 2 cells and IRF-4 binds to the IL-4 promoter to induce transcription (Lohoff et al, 2002; Hu et al., 2002).

IFN signalling

Primary IFN expression, IFN-β and IFN-α_4, signals through the type I IFN receptor, IFNAR on the infected cell as well as on uninfected cells in the vicinity of the infected cell, priming their anti-viral state. The importance of the IFNAR is demonstrated in many mouse experiments; mice encoding IFNAR mutants are more susceptible to lethal viral infections (Muller et al., 1994; Van den Broek et al., 1995; Hwang et al., 1995; Garcia-Sastre et al., 1998; Grieder and Vogel, 1999; Knipe et al, 2001). The IFNAR is composed of two subunits IFNAR1 and IFNAR2 (reviewed in Mogensen et al., 1999). The intracellular components of the subunits are attached to tyrosine kinases. IFNAR1 is associated with Tyk2 and IFNAR2 is associated with Jak1 (Colamonici et al., 1994; Novick et al., 1994). IFN attachment to the receptor induces conformational changes resulting in dimerisation of the receptor subunits; this causes autophosphorylation and activation of the associated tyrosine kinases (Novick et al., 1994). Tyk2 is responsible for the phosphorylation of the IFNAR subunits, creating new docking sites for the STATs (reviewed in Goodbourn et al., 2000). STAT-2 is initially associated with IFNAR2. Following Tyk2 phosphorylation of the IFNAR, STAT-2 docks with IFNAR1 and recruits STAT-1 (reviewed in Samuel, 2001). STAT-1: STAT-2 heterodimers translocate to the nucleus and associate with IRF-9 forming the ISGF3 (Veals et al., 1992; Goodbourn et al., 2000). This complex

interacts with the cis acting IFN stimulated response element (ISRE) contained within many ISG promoters (Figure 1D). Despite the importance of the classical Jak – STAT pathway, several STATs are activated by type I IFNs, STAT-1, -2, -3, and –5 (Darnell et al., 1994); STAT-4 and –6 activation by IFN-α is restricted to endothelial cells and cells of lymphoid origin (Torpey et al., 2004; Matikainen et al., 1999). All of these STAT types can be phosphorylated, resulting in activation and dimerisation; many of the homo- or heterodimers formed can also activate gene transcription (Darnell, 1997). The ISGF3 is the only complex known to bind to ISREs and stimulate transcription; however many ISGs contain other binding sites within their promoters, IRF binding sites and IFN-γ activated sequences (GAS), the later of which different STAT dimers can bind to and initiate gene transcription (Darnell, 1997).

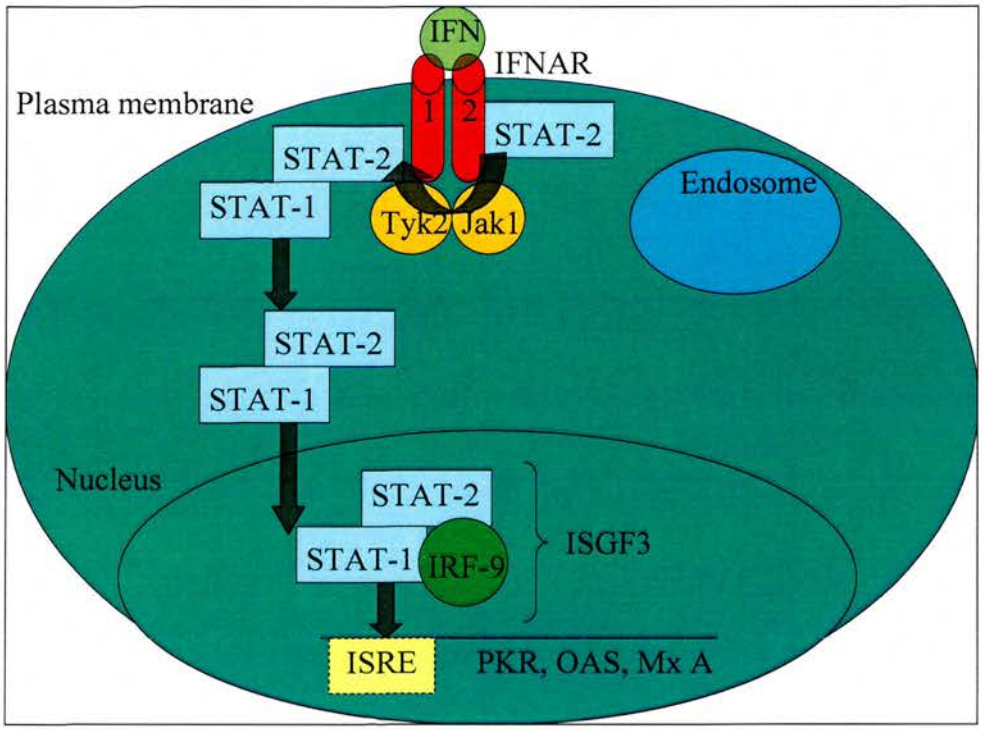

Figure 1D: Type I IFN Jak-STAT signalling
IFN binding to the IFNAR causes conformational changes, which result in dimerisation of the receptor subunits. This induces autophosphorylation and activation of the associated janus kinases (Tyk2, Jak1). STAT-2 is initially docked with IFNAR2. Following Tyk2 phosphorylation STAT-2 docks with IFNAR1. Here it recruits STAT-1, these form a heterodimer and translocate to the nucleus. Within the nucleus the STAT heterodimer associates with IRF-9 forming the IFN-stimulated gene factor 3 (ISGF3). ISGF3 associates with IFN-stimulated response elements (ISREs) found in the promoters of IFN stimulated genes such as PKR, OAS and Mx A.

Alternative IFN signalling pathways

Recent advances have been made in discovering alternative signalling pathways induced by IFNs to activate ISGs; these include CRK proteins, p38 MAPK and PI3K. The CRK proteins are homologues of the viral CRK, an oncogene encoded by avian sarcoma virus, which transforms cells and induces tumours in newborn chicks (Mayer et al., 1988). CRK proteins interact with tyrosine kinases and guanine nucleotide exchange factors, e.g C3G (Ahmad et al., 1997; Feller, 2001). C3G is a guanine nucleotide exchange factor for RAP1, a GTPase that responds to hormones and cytokines to induce cell proliferation and differentiation (Bos et al., 2001). It is postulated that RAP-1 functions to control growth in an IFN dependent manner, the effect is determined by stimulant and cell type (Hattori et al., 2003). Another observed CRK IFN signalling interaction was the association of CRKL with STAT-5. These complexes translocate to the nucleus and bind to GAS elements (Fish et al., 1999). It is possible that CRKL functions as a nuclear adaptor for STAT-5, as this complex is essential for GAS promoter induction (Grumbach et al., 2001).

P38 MAPK signalling is essential for the induction of anti-proliferation effects. It is important in both ISRE and GAS element dependent gene induction as inhibition of p38 MAPK blocks IFN-α dependent genes controlled by ISRE elements and p38 MAPK is required for GAS dependent type I IFN gene transcription (Li et al., 2004; Uddin et al., 2000). However, its exact role in gene expression has yet to be elucidated, as it is not required for STAT phosphorylation or ISGF3 formation (Uddin et al., 1999). A specific role for p38 MAPK in anti-viral immunity has been demonstrated as IFN-α induced anti-viral responses were suppressed following p38 inhibition during VSV and EMCV infections (Mayer et al., 2001).

PI3K is activated by type I IFNs through the insulin receptor substrate pathway (Uddin et al., 1995; 1997). It induces Akt, a kinase linked to promotion of survival or apoptosis pathways. The pathway that is promoted is dependent upon the cell type (Vivanco et al., 2002). PI3K is also involved in the regulation of IFN-β dependent phosphorylation of the p65 subunit of NF-κB (Rani et al., 2002) and regulation of IFN inducible activation of mammalian target of rapamycin (MTOR), which induces initiation of mRNA translation (Lekmine et al., 2003).

Augmentation of IFN signalling

IRF-7 gene expression is induced following IFN-β expression. IRF-7 is a regulatory factor involved in the positive feedback loop for the induction of further IFN-α subsets. It is maintained within the cytoplasm and activated by TBK-1 and IKKε, the same kinases responsible for IRF-3 activation (Fitzgerald et al., 2003). After activation, IRF-7 translocates to the nucleus where it interacts with promoters of the delayed early IFN-α genes, IFN-$\alpha_{2, -5, -6}$ and $_{-8}$ inducing their expression. This produces a concentrated and varied IFN response (Marie et al., 1998). Differential IFN induction provides an innate control of the IFN response, preventing exponential expression of pro-inflammatory and anti-viral genes.

Control of STAT signalling

In addition to the IRF control of IFN expression many other proteins play a role in suppression of the Jak-STAT signalling pathway e.g. SOCS, PIAS proteins and SHP-1 proteins. Suppressors of cytokine signalling (SOCS) have 8 members and each contain a central SH2 domain. SOCS are induced by several cytokines e.g. IFN-γ and function by binding the kinase domain of Jaks suppressing their activation (Yasukawa et al., 1999). SHP-1 is a cytoplasmic tyrosine phosphatase; it contains two SH2 domains and directly interacts with Jak kinases catalysing their dephosphorylation (David et al., 1995). To enable SHP-1 activation, SHP-1 is recruited to SH2 binding sites on cytokine receptors where it is phosphorylated by JAKs and activated inducing its phosphatase function (reviewed in Tonks et al., 2001). PIAS (protein inhibitors of activated STAT) directly interact with activated STAT proteins in response to IFNs or IL-6 to prevent DNA binding (Shuai, 1999; Liao et al., 2000). There are five mammalian members, PIAS-1 – 5; PIAS-1 associates with STAT-1 to inhibit DNA binding (Liu et al., 1998; Gross et al., 2001).

IFN Stimulated Genes

The IFN response induces the expression of hundreds of genes that contribute to formation of the anti-viral state, modulation of cell proliferation and induction of the adaptive immune response.

Formation of the anti-viral state

Protein Kinase R (PKR)

PKR is highly effective against viral replication. It is constitutively expressed in most cells and maintained in an inactive form in the cytoplasm (Meurs et al., 1990). Its expression is enhanced by IFN through the ISRE (Kuhen and Samuel, 1997). dsRNA binding to PKR enables homodimer formation and PKR activation (Katze et al., 1991). The length of the dsRNA determines PKR: RNA complex stability; 80 bp is the optimum (Manche et al., 1992). Large quantities of RNA suppress the activity of PKR as saturation of the dsRBMs prevents dimer formation and PKR activation (reviewed in Samuel, 2001). In addition to dsRNA, PKR activity is controlled by the PKR activator (PACT), the PKR inhibitor ($p58^{IPK}$) and heat shock proteins (Hsp), (Patel et al., 2000; Tang et al., 1999; Melville et al., 1997). For example, Hsp 40 binds to $p58^{IPK}$, suppressing its inhibitory role and Hsp70 has been shown to possess both PKR stimulatory and inhibitory activities (Melville et al., 1997; 1999).

Active PKR induces complete host cell protein synthesis shutdown by phosphorylating the serine 51 residue of the eukaryotic translation initiation factor 2α (eIF-2α) (Meurs et al., 1992). eIF-2α in association with GTP is required for the recruitment and attachment of Met-tRNA to the 40S ribosomal subunit. Further association of this complex with mRNA and other translation factors results in the hydrolysis of GTP to GDP. In order for translation initiation to continue, the eIF-2α bound GDP must be recycled to GTP through the guanine nucleotide exchange factor (eIF-2B). However, once phosphorylated eIF-2α binds strongly to eIF-2B preventing its release and the recycling of GDP to GTP, ultimately halting translation initiation and viral replication (Ramaiah et al., 1994; reviewed in Goodbourn et al., 2000).

Other roles for PKR include cell growth control (Zamanian-Daryoush et al., 1999) and tumour suppression (Donze et al., 1995); for example, PKR phosphorylation of 90 kDa NFAT protein and PKR induction of apoptosis. Nuclear factors of activated T cells (NFAT) proteins are essential for early T cell gene induction e.g. IL-2, which stimulates T-cell proliferation. NF90 binds dsRNA and is phosphorylated in a dsRNA dependent manner by PKR; this promotes nuclear translocation and dimerisation with NF45. In the nucleus this heterodimer associates with the antigen receptor response element 2 (ARRE2) found with the IL-2 promoter to induce transcription (Langland et al., 1999). The involvement of PKR in the induction of apoptosis is shown by the over expression of wild-type PKR, which results in the induction of apoptosis in the presence of dsRNA (Lee et al., 1997). PKR has also been shown to upregulate Fas gene expression, which is directly linked to an apoptosis inducing pathway via the Fas associated death domain (FADD) (Balachandran et al., 1998). An important link between cell proliferation and induced cell death is PKR activation of NF-κB, which was described previously. Other transcription factors influenced by PKR, which are pertinent to the IFN response include STAT-1, IRF-1 and p53 (Williams, 1999).

2'-5'OAS and RNase L

The OAS/RNase-L antiviral response is especially successful in inhibiting replication of viruses in the *Picornaviridae, Poxviridae* and *Reoviridae* families (reviewed in Samuel, 2001). 2'-5' Oligoadenylate synthase (OAS) polymerises ATP forming various sizes of 2'-5'oligoadenylates (2'-5'A) (Kerr and Brown, 1978). Three forms of human OAS have been isolated, *OAS1, 2* and *3*, however examination of the mouse genome indicates three individual Oas genes with 8 isoforms of *Oas 1* (Mashimo et al., 2003). The relevance of multiple murine isoforms is still not understood. The *Oas1b* isoform has been linked to innate resistance to West Nile virus in mice (Mashimo et al., 2002), suggesting that the different isoforms provide protection against different types of RNA viruses. The different forms of OAS (1, 2 and 3) have been localised to different sub-cellular organelles with different requirements for RNA concentration and optimal reaction conditions (Rebouillat and Hovanessian, 1999). 2'-5'A, the product of OAS, binds to the duplicated phosphate binding motif in the N-terminal domain of the latent endoribonuclease, RNase-L (Hassel et al., 1993). This enables dimer formation (Dong and Silverman, 1995), which activates

RNase-L to cleave the 3'side of –UpXp- sequences of both cellular and viral ssRNAs catalysing their degradation (Floyd-Smith et al., 1981). RNase-L has been shown to degrade 28S ribosomal RNA and so is another protein leading to translation inhibition (Iordanov et al., 2000). It is also involved in the induction of apoptosis, as RNase-$L^{-/-}$ mice show defects in apoptosis following viral infection (Li et al., 2004). Li et al., (2004) determined that chemical inactivation of the c-Jun N-terminal kinase (JNK) prevented apoptosis by 2'-5' A, suggesting that RNase L and JNK function within the same signalling pathway to promote apoptosis.

ADAR-1

ADAR-1 is an RNA specific adenosine deaminase expressed ubiquitously in the nuclei of higher eukaryotes (Bass, 2002). It alters adenosine to inosine through deamination in both viral RNAs and cellular pre-mRNAs (Polson et al., 1991; Bass, 1997). The resulting inosine, which is read by transcription machinery as guanine (Alberts et al., 1994), causes dsRNA helix instability due to incorrect base pairings. Two forms of editing can occur, site specific editing and promiscuous editing. Site specific editing induces mis-sense codons in favourable secondary structures and is commonly observed in mRNAs important to the nervous system (Kallman et al., 2003; Wong et al., 2001). Promiscuous editing results in hyper-editing creating an unstable RNA duplex. Cellular mRNA that is hyper-edited is retained within the nucleus (Bass and Weintraub, 1988; Kumar and Carmichael, 1997; Zhang and Carmichael, 2001; Dong et al., 1993; Kameoka et al., 2004). Hyper-edited mRNAs interact with a protein complex containing vigilin, resulting in the formation of heterochromatin to cause gene silencing (Wang et al., 2005). The hyper-editing of viral RNA may enable the host cell to remove the virus dsRNA in conjunction with a cytoplasmic endonuclease that cleaves specific hyper-edited dsRNA species (Scadden and Smith, 2001). In addition to decreasing the stability of viral replication complexes, hyper-editing could induce mutations into the virus genome. Interestingly, hepatitis delta virus is hyper-edited in vitro and this is required for virion formation but not replication (Polson et al., 1996; Casey, 2002).

MxA

MxA belongs to a family of GTPases which are members of the dynamin family (reviewed in Haller and Kochs, 2002). The IFN-induced MxA protein sequesters

nucleocapsid structures through its C-terminus. This class of antiviral proteins are particularly effective against negative sense RNA viruses. During bunyavirus infection MxA prevents nucleocapsid translocation to the Golgi apparatus, the intracellular site of viral assembly. MxA also prevents Thogoto virus nucleocapsid nuclear translocation, the nucleus is the replication site of this orthomyxovirus (Kochs et al., 2002; Kochs and Haller, 1999).

Other IFN induced genes

PKR, RNase L and MxA are important in the formation of the anti-viral state and yet mice triply deficient for each of these proteins can still induce an antiviral effect against EMCV (Zhou et al., 1999). Many other IFN induced antiviral genes have been elucidated and include:

(i) ISG-20, a 3'-5' exonuclease specific for RNA viruses (Espert et al., 2003);

(ii) ISG-15, a ubiquitin-like protein with antiviral activity against Sindbis virus. ISG-15 prevented lethal Sindbis virus infection and reduced viral replication although did not control virus spread (Lenschow et al., 2005).

(iii) Viperin, an IFN-α and $-\gamma$ induced protein with anti-viral activities against human cytomegalovirus and hepatitis C virus (Chin and Cresswell, 2001; Helbig et al., 2005).

(iv) promyelocytic leukaemia protein (PML) expression is enhanced by IFN-α/β (Chelbi-Alix et al., 1998); it accumulates in nuclear bodies and in the nucleoplasm in association with chromatin. PML deficiency increases the susceptibility of cells to virus infections and over expression of PML inhibits replication of VSV, LMCV, influenza virus and human foamy virus (Regad and Chelbi-Alix, 2001). PML is essential for IFN induced apoptosis, it is thought that nuclear bodies, whose structural integrity is maintained by PML, act as platforms for p53 regulation (Moller and Schmitz, 2003). The specific mechanism of PML antiviral properties is not yet understood, but many viral infections demonstrate disrupted nuclear bodies and re-localisation of PML.

Modulation of cell proliferation and immune responses by IFNs

In addition to induction of the anti-viral state, IFNs can suppress cell proliferation and induce the adaptive immune response. IFN modulation of cell growth ranges from

apoptosis induction, for example through PKR and RNase L, to induction of G1 arrest and pauses at other phases of the cell cycle (Roos et al., 1984). Progression of the cell cycle is determined by cyclin-dependent activation of cyclin-dependent protein kinases (CDKs). These phosphorylate multiple proteins including the retinoblastoma tumour suppressor protein (pRb). Phosphorylation of pRb results in release of E2F transcription factors which induce expression of genes essential for progression into the S phase of the cell cycle (Weinberg, 1995; Muller, 1995). All stages of the cell cycle are potential targets for the IFN response. For example, IFN increases the expression level of CKI p21, a cyclin-dependent kinase inhibitor, IFN-α inhibits IL-3 induced cyclin expression and prevents pRb dependent transcription factor activation by maintaining pRb in a hypophosphorylated state. These effects are accompanied by high level PKR activation linking translational suppression to cell cycle arrest (Prietzsch et al., 2002). Signalling pathways also contribute to cell proliferation inhibition; CRK proteins link the type I IFN receptor to C3G/Rap1 growth inhibition pathway (Ahmad et al., 1997) and Vav contributes to p38 MAPK inhibitory responses through interactions with Rac for which it functions as a guanine nucleotide exchange factor (Crespo et al., 1996).

Type I IFNs link the adaptive and innate immune responses. They increase the efficiency of the transitional phase by augmenting the levels of MHC class I molecules and the availability of MHC I antigens (Boehm et al., 1997; Guidotti and Chisari, 2001). They regulate the expression of Th1 cytokines through IRF-1, e.g. IL-12, IL-18, IL-15 and IFN-γ (Biron, 2001). They increase the expression of chemokines, RANTES, a T cell chemokine, and MIP-1α, the macrophage inflammatory protein (Cremer et al., 2002; Zang et al., 2001). They can also enhance NK cell cytotoxicity by increasing perforin expression (Biron et al., 1998) and influence DC maturation (Luft et al., 1998).

Inverse Interference

Given their potent anti-viral activities viruses from many virus families have evolved mechanisms to antagonise the IFN response. Viruses have developed proteins and

nucleic acids to interfere with and disrupt all stages of this response, from the initial induction of IFN to effector protein expression and activation (reviewed in Garcia-Sastre, 2002; Samuel, 2001; Goodbourn et al., 2000).

DNA viruses

Herpesviruses

The herpes family induces IFN through a variety of pathways and encodes genes to control the induced IFN response (reviewed in Mossman and Ashkar, 2005). For example, Herpes simplex type 1 (HSV-1) induces IFN through TLR-2 and TLR-9. TLR-2 is activated by viral glycopeptides expressed on the surface of the virion (Kurt-Jones et al., 2004). TLR-9 is located in the endosome and is activated by unmethylated CpG motifs in the HSV-1 genome (Krug et al., 2004). The ICP0 protein expressed by HSV-1 inhibits the activation of IRF-3 and IRF-7 by functioning as an E3 ubiquitin ligase (Boutell et al, 2005; Lin et al., 2004). However, it also induces the activation of NF-κB by targeting the IκBα subunit for polyubiquitination (Diao et al, 2005). Several herpes viruses contain NF-κB binding sites within some of their gene promoters and require this cellular transcription factor to promote their own replication. For example, human cytomegalovirus (HCMV) contains 4 NF-κB binding sites in its major immediate early promoter and so requires NF-κB activation in the absence of IFN activation (Meier and Pruessner, 2000; Sambucetti et al., 1989). In addition to ICP0 inhibition of IRFs, the HCMV p65 structural protein affects the DNA binding capability of NF-κB, IRF-1 and IRF-3 (Browne and Shenk, 2003; Abate et al., 2004) and Kaposi's sarcoma herpes virus (KSHV) encodes several viral homologues of IRFs, which suppress the IFN response through interactions with cellular IRFs and partners of cellular IRFs (Cunningham et al., 2003). For example, KSHV vIRF-1 binds to the transcription enhancers p300 and CBP and so prevents their histone acetylase function suppressing transcription (Burysek et al., 1999; Lin et al., 2001; Seo et al., 2000) and KSHV vIRF-4 interacts with IRF-7 inhibiting its phosphorylation and nuclear accumulation (Zhu et al., 2002).

Following IFN expression, viruses of the herpesviridae can also interfere with IFNAR signalling and expression of ISGs. For example, the HSV-1 expressed VHS protein is

a viral inducer of host cell translation shut-off. VHS is an endoribonuclease, which degrades cellular transcripts in fibroblasts (Lin et al., 2004). VHS mediated transcript degradation would prevent IRF-7 expression and hence the second wave of IFN-α expression and augmentation of the IFN response (Smiley, 2004). HSV-1 also prevents the phosphorylation of Jak-1, Tyk-2 and STAT-1 and -2 by increasing the expression of the suppressor of cytokine signalling (SOCS) – 3 (Yokota et al., 2001; 2004). In addition to HSV-1 interference of IFNAR signalling, HCMV causes the degradation of JAK-1 and IRF-9, a component of ISGF-3 (Miller et al., 1998; 1999) and murine CMV (MCMV) pM27 protein binds STAT-2 targeting it for ubiquitination and proteosome degradation (Zimmermann et al., 2005). Herpes viruses encode proteins that mop up viral dsRNA and so prevent the activation of many anti-viral proteins; for example the HCMV genome encodes two ORFs, TRS1 and IRS1, whose proteins bind and sequester dsRNA (Child et al., 2002). PKR is antagonised by the HSV-1 ICP34.5 protein, which recruits cellular phosphatase 1 and this complex dephosphorylates eIF-2α thereby counteracting PKR activity (He et al., 1997). Another HSV-1 protein, Us11 directly binds to PKR and prevents autophosphorylation and activation (Cassady et al., 1998; 2002). KSHV vIRF also inhibits PKR; vIRF-2 binds PKR and prevents autophosphoryation and vIRF-3 represses activation of caspase 3 and so prevents PKR triggered apoptosis (Burysek and Pitha, 2001; Esteban et al., 2003).

Poxviruses

Vaccinia virus (VV) targets the IFN response at multiple stages. Firstly, at the initial TLR signalling cascade, A46R contains a TIR domain and targets MyD88, Mal, TRIF and TRAM, and A52R associates with IRAK2 and TRAF6 blocking NF-κB activation by TLR-3 (Stack et al., 2005; Bowie et al., 2000; Harte et al., 2003). Secondly, at the induction of IFN stimulated genes, B18R encodes a soluble cytokine receptor for IFN-α/β, which acts as a decoy for these cytokines (Alcami et al., 2000). This contains 3 Ig domains that bind to type I IFN with high affinity. Thirdly the virus targets ISGs, E3L protein binds dsRNA to prevent PKR activation and K3L competitively binds PKR and blocks phosphorylation of eIF-2α (Davis et al., 1993; Xiang et al, 2002).

Further virus specific targeting of PKR by DNA viruses is observed in adenoviruses; virus associated RNAs (VA RNAs) act as competitive substrates for PKR preventing PKR activation and dimerisation (Mathews and Shenk, 1991). Epstein Barr virus encodes RNAs, EBERs, which show homology to VA RNAs and can functionally substitute for VA RNAs (Elia et al., 1996).

Double stranded RNA viruses

Reoviruses cause gastroenteritis and myocarditis (reviewed in Clarke et al., 2005). The reovirus σ3 protein, which forms the outer capsid binds dsRNA in a sequence independent manner and prevents PKR activation *in vitro* (Denzler and Jacobs, 1994; Huismans and Joklik, 1976; Schiff et al., 1988; Imani and Jacobs, 1988).

Negative stranded RNA viruses

Paramyxoviruses

The paramyxoviruses have non-segmented negative-stranded RNA genomes; they include the Rubula-, Henipah- and morbilivirus genera. Many paromyxoviruses including Simian virus 5 (SV5), human parainfluenza virus 2, Sendai virus, mumps virus and Hendra virus inhibit mda-5, a dsRNA binding protein (Andrejeva et al., 2004). Insertion of several guanine nucleotides into the phosphoprotein (P) ORF during transcription results in expression of the alternate V protein (Thomas et al., 1988). The paromyxovirus V protein is also an inhibitor of IFN responses. V proteins expressed by the Rubulavirus genus induce poly-ubiquitination of specific STAT proteins (Parisien et al., 2001; Ulane et al., 2002). For example, Simian virus 5 (SV5) targets STAT-1, human parainfluenza virus 2 is specific for STAT-2 and mumps virus targets both STAT-1 and STAT-3 (Parisien et al., 2001; Ulane et al., 2003). During *Rubulavirus* infection, a specific protein complex is formed consisting of V protein, STATs, DDB1 (UV- damaged DNA binding protein) and the Cullin family of SCF ubiquitin ligases which results in poly-ubiquitination and ultimately degradation of STAT (Ulane et al., 2002; 2003). STAT-3 degradation by mumps virus prevents IL-6 induced signalling and alongside STAT-1 degradation is thought to enable the virus to control a broader range of cytokine signalling in response to

viral infection (Ulane et al, 2003; Levy and Lee, 2002). The V proteins of Henipaviruses suppress STAT activity without inducing protein degradation. They sequester STAT-1 and STAT-2 in high molecular weight cytoplasmic complexes and are capable of nuclear shuttling enabling the viruses to relocalise nuclear STAT proteins to the cytoplasm (Rodriguez et al., 2002; 2003). The V protein of measles virus shares little (20 %) homology with the previously mentioned V proteins and blocks IFN signalling by preventing nuclear import of STAT-1 and STAT-2 (Palosaari et al., 2003). Similar to the V proteins expressed by the Henipahviruses, measles virus also sequesters STAT proteins in cytoplasmic bodies in association with the measles virus nucleocapsid protein (Palosaari et al., 2003; Bohn et al., 1990).
In addition to blocking/disrupting IFNAR signalling, other paramyxoviruses affect type I IFN expression. For example, the NS1 and NS2 proteins of respiratory sycytial virus (RSV) prevent phosphorylation and activation of IRF-3 (Bossert et al., 2003; Spann et al., 2004). Measles virus and RSV specifically target TLR-dependent IFN-α production in plasmacytoid dendritic cells (Schlender et al., 2005). The effectiveness of targeting DCs is demonstrated by the general immunosuppression induced by measles virus during an *in vivo* infection (Moss et al., 2004; Schneider-Schaulies et al., 2003).

Many other negative strand RNA viruses interfere with IFN induction. Rabies virus phosphoprotein targets TBK-1 phosphorylation of IRF-3 and prevents STAT-1 nuclear accumulation (Brzozka et al., 2005; Vidy et al., 2005); Ebola virus VP35 protein prevents IRF-3 phosphorylation (Basler et al., 2003) and Thogoto virus (THOV) ML protein interacts with IRF-3 but does not affect its phosphorylation. The ML protein interferes with IRF-3 dimerisation and CBP recruitment within the nucleus (Jennings et al., 2005). To prevent ISG expression, VSV and Rift Valley fever virus encode the M protein and the NSs protein respectively to induce global cellular transcription inhibition (Ahmed et al., 2003; Le May et al., 2004). VSV M protein targets the transcription factor IID (TFIID) and reduces the efficiency of nuclear-cytoplasmic transport of mRNAs (Yuan et al., 1998; Her et al., 1997). Rift Valley fever virus NSs protein interacts with components, specifically the p44 subunit, of the transcription factor IIH (Le May et al., 2004) to prevent RNA polymerase II function thereby inhibiting host mRNA synthesis including IFN

transcripts. Bunyamwera virus NSs also shows IFN-α/β suppression (Weber et al., 2002) and interacts with RNA polymerase II (RNAPol II). Disruption of RNAPol II phosphorylation patterns inhibits mRNA elongation and 3'-end processing (Thomas et al., 2004). The NS1 protein of influenza virus has been attributed many roles in host cell modulation; it was the first IFN antagonist identified. Its capacity to bind dsRNA prevents cellular detection of viral replication through RIG-I and TLR-3 and sequestration of dsRNA removes its ability to activate ISGs such as PKR, ADAR and OAS (Garcia-Sastre et al., 1998; Garcia-Sastre, 2004). Influenza A virus also induces the expression of a natural cellular inhibitor of PKR, $p58^{IPK}$ (Lee et al., 1990).

Positive stranded RNA viruses

Flaviviruses

Hepatitis C virus (HCV) is a positive-sense, single-stranded RNA virus. HCV NS3/4A protease interrupts IFN-β induction through cleavage of TRIF, the adaptor protein for TLR-3 and –4, and IPS-1 the adaptor protein for RIG-I (Foy et al., 2005; Li et al., 2005; Ferreon et al., 2005). IFNAR signalling is also disrupted by HCV. HCV replication suppresses STAT-1 activity by increasing the levels of protein phosphatase 2A and SOCS-3 (Heim et al., 1999; Duong et al., 2004; Bode et al., 2003). The HCV NS5A protein reduces ISG induction by promoting IL-8 expression, an IFN antagonist (Khabar et al., 1997; Geiss et al., 2003). In addition, NS5A and HCV E2 affect PKR activity. NS5A or E2 binding to PKR prevents its catalytic activity thereby repressing host translation shut-off (Taylor et al., 1999; Noguchi et al., 2001; Gimenez-Barcons et al., 2005). HCV infection also results in reduced expression of ISG56 and antagonism of the OAS/RNase L pathway (Sumpter et al., 2004; Taguchi et al., 2004). Some HCV genomes appear to have evolved to have few RNase L cleavage sites in their genome (Han et al., 2004).

Bovine viral diarrhoea virus (BVDV) has two pathological types, cytopathic (cp) and non-cytopathic (ncp) (Hoff and Donis, 1997). Infection of pregnant cows within the first 120 days of pregnancy with the non-cytopathic strain results in persistently infected calves (Brownlie et al., 1989). To establish a persistent infection, ncp BVDV interferes with the immune system and does not induce an IFN response (Adler et al., 1997; Charleston et al., 2001). During an ncp BVDV infection IRF-3 translocates to

the nucleus but does not associate with DNA. If co-infected with an IFN inducing virus, IRF-3 activity can not be rescued, suggesting that ncp BVDV IFN inhibition is mediated by disrupting the IRF-3 IFN-β promoter binding (Baigent et al., 2002).

Picornaviruses

Picornaviruses are small positive-sense RNA viruses, they include, foot and mouth disease virus (FMDV), hepatits A virus (HAV) and poliovirus (Ruekert, 1996). The L proteinase encoded by picornaviruses is responsible for viral polyprotein cleavage, but has also been implicated in host translation initiation factor eIF-4G cleavage (Strebel and Beck, 1986; Devaney et al., 1988; Guarne et al., 1998; Medina et al., 1993). eIF-4G cleavage prevents cap-dependent mRNA translation, ultimately inducing host cell shut-off, including shut-off of IFN mRNA (Chinsangaram et al., 1999; Grubman and Chinsangaram, 2000). HAV inhibits IFN-β expression through interactions with the IFN-β enhanceosome (Brack et al., 2002). It is believed that this facilitates HAV persistent infection. More recently, poliovirus has been shown to cleave the p65-RelA subunit of NF-κB. Initial infection induces NF-κB and IFN expression however, at later stages the poliovirus 3C protease cleaves the NF-κB p65 subunit. This effect has also been observed in other picornaviruses including, ECHO-1 virus and rhinovirus 14 (Neznanov et al., 2005). In addition to affecting IFN induction, poliovirus initiates the degradation of PKR (Black et al., 1993).

To date no inverse interference mechanisms have been elucidated for the Togaviridae. However, recent observations suggest that these viruses do encode mechanisms to suppress IFN expression. Sindbis virus non-structural protein 2 (nsP2) was mutated at a conserved amino acid, proline^{726}, and infections with this mutant virus induced significantly larger amounts of type I IFN compared to another mutant virus which replicated at a comparable rate (Frolova et al., 2002). Interestingly, SV is also innately resistant to PKR induced translational shut off (Ventoso et al., 2006). Ross River virus (RRV) causes cytokine dysregulation in infected macrophages, including IFN-β (Way et al., 2002).

	Target Protein	Virus Protein	Virus	Function
IFN-β Induction	IRF-3, IRF-7	ICP0	HSV-1	E3 ubquitin ligase
	NF-κB, IRF-1, IRF-3	P65	HCMV	Affects DNA binding
	P300, CBP	vIRF-1	KSHV	Sequestration
	IRF-7	vIRF-4	KSHV	Prevents phosphorylation and nuclear accumulation
	MyD88, Mal, TRIF, TRAM	A46R	VV	Binds through TIR domain
	IRAK, TRAF-6	A52R	VV	Blocks NF-κB activation
	RIG-I, TLR-3	NS1	Influ V	Binds dsRNA and prevents activation
	mda-5	?	SV5	Inhibits signalling
	IRF-3	NS1, NS2	RSV	Prevent phosphorylation and activation
	TBK-1	P	Rabies	Prevents IRF-3 phosphorylation
	IRF-3	VP35	Ebola	Prevents IRF-3 phosphorylation
	IRF-3	ML	THOV	Prevents dimerisation and CBP recruitment
	TRIF, IPS-1	NS3/4A	HCV	Cleaves adaptor proteins
	IRF-3	?	NcpBVD V	Prevents IRF-3 DNA binding
	IFN-β enhanceosome	?	HAV	Prevents IFN-β expression
	NF-κB (p65)	3C	PolioV	Cleaves NF-κB preventing transcription
IFNAR Signalling	Jak-1, Tyk-2, STAT-1, STAT-2	VHS, UL13	HSV-1	Increases host SOC-3 to prevent phosphorylation
	Jak-1, IRF-9		HCMV	Induces degradation
	STAT-2	PM27	MCMV	Targets for ubquitination and degradation
	IFNAR	B18R	VV	Soluble IFNAR
	STAT-1, IRF-9	E1A	ADV	Prevents ISGF3 formation
	STAT-1	V	SV5	Degradation
	STAT-2	V	HPIV2	Degradation
	STAT-1, STAT-3	V	Mumps	Degradation
	STAT-1, STAT-2	V	Henipa	Cytoplasmic sequestration
	STAT-1	?	HCV	Induces cellular phosphatase 2A
	STAT-1	Core	HCV	Induces cellular SOC-3
Anti-Viral Proteins	PKR, RNase L, ADAR	TRS1, IRS1	HCMV	Binds dsRNA and prevents activation
	EIF-2α	ICP34.5	HSV-1	Recruits cellular phosphatase 1 to dephosphorylate eIF-2α
	PKR, RNase L, ADAR	Us11	HSV-1	Directly binds, preventing activation
	PKR, RNase L, ADAR	VIRF-2	KSHV	Directly binds, preventing activation
	PKR, RNase L, ADAR	E3L	VV	Binds dsRNA and prevents activation
	PKR	K3L	VV	Prevents eIF-2α phosphorylation
	PKR, RNase L, ADAR	VA RNA	ADV	Binds dsRNA and prevents activation
	PKR, RNase L, ADAR	EBER	EBV	Binds dsRNA and

				prevents activation
Anti-Viral Proteins	PKR, RNase L, ADAR	NS1	Influ V	Binds dsRNA and prevents activation
	PKR, RNase L, ADAR	Σ3	ReoV	Binds dsRNA and prevents activation
	PKR	P58IPK	Influ V	Induces cellular PKR inhibitor
	ISGs	NS5A	HCV	Promotes IL-8 expression
	PKR	NS5A/E2	HCV	Binds and prevents activation
	PKR	?	Polio V	Degradation
	RNase L	RLI	EMCV	Induces cellular inhibitor
Global Transcription Shut Off	TFIID	M	VSV	Reduces mRNA nuclear-cytoplasmic transport
	TFIIH (p44 subunit)	NSs	RVFV	Prevents RNAPol II function
	RNAPol II	NSs	BunV	Inhibits mRNA elongation
Global Translation Shut Off	ISGs	VHS	HSV-1	Endoribonuclease; degrades ISG mRNA transcripts
	EIF-4G	L	FMDV	Cleavage prevents cap-dependent translation

Table 1B: Virus inverse interference of the IFN response
Many viruses possess mechanisms to evade the IFN response; in the table are examples of how viruses evade IFN-β induction, IFNAR signalling and anti-viral proteins and how they induce host transcription or translation shut off to suppress expression of IFN.

Tumour Necrosis Factor and cell death pathways are other targets of viral antagonism

IFNs play a critical role in the immune response and hence are heavily targeted by viruses to suppress their induction and responses. However, they are not the only cytokine family targeted by viruses. The tumour necrosis factor (TNF) family of cytokines regulate cell death and survival; they are expressed by immune effector cells and associate with specific receptors, which are expressed on all cells tested to date (reviewed in Ware, 2005). Induction of apoptosis or promotion of cell survival is dependant upon downstream signalling from the receptor. TNF receptors (TNFR) possessing death domains, recruit adaptor proteins and pro-caspases to form death-inducing signalling complexes (DISC), which process downstream caspases into their active form, resulting in genome cleavage and destruction of cellular integrity. This is known as the extrinsic apoptosis pathway (Hofmann, 1999; Zimmermann et al., 2001). For example, Fas association with Fas ligand initiates the recruitment of the

adaptor protein, Fas associated death domain (FADD), which in turn recruits pro-caspase 8 or 10. Within the resulting DISC these upstream caspases are activated enabling them to process pro-caspase 3 into its active form. Caspase 3 then cleaves inhibitors of caspase activated DNase (ICAD), which results in the fragmentation of cellular DNA (reviewed in Benedict et al., 2002). Diversions from this pathway can occur; DISC based caspase 8 can also cleave BID into its active form, tBID, which recruits Bax. Bax oligomerisation and association with Bak in the mitochondrial membrane induces the release of cytochrome c, which also signals cell death (reviewed in Benedict et al., 2002). Survival pathways are induced through the recruitment of TRAF and other kinases, which ultimately activate NF-κB and AP-1, transcription factors that promote the expression of pro-inflammatory genes.

As in the IFN system, viruses interact at all levels of TNF signalling. Many viruses express TNF receptor (TNFR) decoys to prevent TNF association with and activation of cellular receptors. For example, the poxvirus Shope fibroma virus encodes a TNFR2 orthologue (Smith et al., 1990), another orthologue is found in the smallpox virus (Reading et al., 2002) and the T2 protein of myxoma virus binds TNF (Upton et al., 1991). Adenovirus E3-10.4K and E3-14.5K proteins downregulate death receptor expression on infected cells (Shisler et al., 1997). These proteins target death receptors to endocytic compartments within the cytoplasm (Tollefson et al., 1998). Reduction in the expression of death receptors protects infected cells from immune cell induced death through FasL, TNF or TRAIL release (Ashkenazi and Dixit, 1999). Interference with DISC signalling is a common feature of γ-herpesvirus infections. Equine herpesvirus-2, herpesvirus saimiri, KSHV and bovine herpesvirus-4, all express homologues of cellular FLICE (caspase 8) inhibitor proteins (FLIPs, Bertin et al., 1997; Thome and Tschopp, 2001). FLIPs contain death effector domains, which interact with death inducing adaptor proteins and prevent their activation. Inhibitors of apoptosis proteins (IAPS) are cellular proteins which control caspase activation (Deveraux and Reed, 1999); to date eight have been identified (Shi Y, 2002). Poxviruses encode proteins with similar functions to IAPs. CrmA modifies caspase 8 and inhibits caspase 1 preventing IL-1β processing (Tewari and Dixit, 1995). African swine fever virus encodes a homologue of IAP, vIAP (Neilan et al., 1993), which inhibits caspase 3 activation.

Viruses have also developed orthologues of anti-apoptotic proteins e.g. Bcl-2 and Bcl-x_L. These proteins prevent the loss of mitochondrial membrane integrity and hence inhibit the release of cytochrome c. Adenovirus encodes E1B-19K, which interacts with Bax inhibiting its oligomerisation (Sundararajan and White, 2001). EBV and KSHV encode BHRF1, BALF1 and KSbcl-2, respectively, which suppress the release of cytochrome c from the mitochondria (Henderson et al., 1993; Marshall et al., 1999; Sarid et al., 1997). Human T cell leukaemia virus type I (HTLV-1) and the HIV Nef protein interfere with Bcl-2 family member expression. HTLV Tax protein activates the Bcl-x_L promoter and inhibits Bax expression (Tsukahara et al., 1999); Nef induces the phosphorylation of pro-BAD suppressing apoptosis in T cells (Wolf et al., 2001).

Semliki Forest virus

Alphavirus Family

Semliki Forest virus (SFV) is an alphavirus of the Togaviridae. It is an enveloped single-stranded, positive sense RNA virus with a genome of approximately 11 kb in length. SFV is studied as a model for neurotropic virus infections and as an example of the alphavirus genus. Alphaviruses are arboviruses transmitted by mosquitoes (Weaver et al., 2000). Thirty seven alphaviruses are known to cause human disease; these can be classified into seven antigenically distinct viruses: Eastern equine encephalitis virus (EEE), Venezuelan equine encephalitis virus (VEE), Sindbis virus (SV), Semliki Forest virus (SFV), Barmah Forest virus, Middleburg virus and Ndumu virus. The alphavirus family is endemic across the Americas, Africa and Australia (reviewed in Tsai et al., 2002).

Alphavirus infections have a wide host range, however, horses are particularly susceptible to EEE, Western equine encephalitis (WEE), VEE, SF and Middleburg viruses. The clinical disease and pathology of infection varies for each virus, but most cause encephalitis and or arthralgia. The severity of infection is determined by many factors but age is an important one; neonates are much more susceptible to a morbid infection (reviewed in Fazakerley, 2002). In humans, EEE causes severe CNS infection often resulting in 70 % fatality in some human epidemics and has

caused fatal outbreaks amongst commercial fowl (Tsai et al., 2002). VEE can result in large human and equine epidemics with 100,000's of cases. In addition to encephalitis, VEE can induce spontaneous abortions with massive cerebral necrosis and cerebral calcification in the foetuses (Wenger, 1977). Chikungunya virus, distributed throughout Africa and South East Asia, induces severe symptoms consisting of chills, incapacitating joint pains, fever and rash (Moore et al., 1969; Nimmannitya et al., 1969). SFV is 'Category 2' pathogen in the UK and is studied as a model for alphavirus infection.

SFV is an arbovirus and is transmitted by mosquitoes, primarily *Aedes africanus* or *Aedes aegypti.* SFV is normally found in sub-Saharan Africa. Its natural host species is unknown but infections have been observed in horses, monkeys and man. The first strain of SFV termed L10 was isolated in Uganda (Smithburn and Haddow, 1944) and since then several other strains have been isolated or derived from these primary isolates including avirulent strains. The avirulent A7 strain was isolated in Mozambique (McIntosh et al., 1961).

SFV Pathogenesis

SFV strains can be divided into two groups, those that are virulent to both adult and neonatal mice (virulent strains) and those that are solely virulent in neonates (avirulent strains). Both types produce fulminant encephalitis in neonates, triggering apoptosis in neurones and resulting in death within a few days (Zlotnik et al., 1972; Gates et al., 1985; Fazakerley et al., 1993). In adult mice, virulent strain infections are much the same; although neuronal death is most likely by necrosis (Atkins et al., 1990; Fazakerley et al., 1993). Avirulent infections are confined to small foci surrounding cerebral blood vessels; the virus is unable to spread efficiently between neurones (Fazakerley et al., 1993). Microscopically infected cells contain 'viral core aggregates' but no virions are observed. Around 6 – 10 days post-infection the virus is cleared from the CNS, following which lesions appear in the myelin tracts similar to those seen in multiple schlerosis (Suckling et al., 1978). This demyelination is caused by $CD8^+$ T cells (Fazkerley and Webb, 1987), most probably initiating oligodendrocyte cell death. Experiments with severe combined immuno-deficient mice (SCID) and nude mice have shown no and reduced demyelination respectively,

indicating that these lesions are dependent upon the cellular immune system (Amor et al., 1996). In pregnant mice some avirulent strains, specifically the A7 ts22 mutant, show teratogenesis, inducing defects in the skeleton, skin and neural tube (Mabruk et al., 1989).

Age-dependent Virulence

A distinct feature of the avirulent infection is age-dependent virulence. Experiments have shown that up to 11 days of age neonates infected with an avirulent strain develop panencephalitis and die, after 12 days of age infection is avirulent (Oliver et al., 1997; Oliver and Fazakerley, 1998). This pathology is not thought to be associated with the adaptive immune system, as adult SCID mice display similar infection patterns to adult immunocompetent mice, with small foci of virus infection (Amor et al., 1996). However, it could be attributed to CNS development. Mice develop their CNS synaptic connections up until two weeks post-partum (reviewed by Fazakerley, 2001). During this period, synaptogenesis and neuronal differentiation involve a significant amount of smooth membrane vesicle production (reviewed by Fazakerley, 2001). The importance of smooth membrane synthesis for viral replication is demonstrated when A7(74) infected mice are pre-treated with aurothiolates (gold containing compounds). This results in widespread infection and high virus titres (Scallan and Fazakerley, 1999). These observations are not due to toxic effects of the aurothiolates. It is suggested that the aurothiolates alter neuronal physiology to increase smooth membrane proliferation and that this allows virus replication (Mehta et al., 1990). This implies that the avirulent strains of SFV hijack lipid vesicles to spread throughout the developing CNS, but upon brain maturation are confined to their initial foci of infection. An alternative explanation is that immature neurones are more susceptible to apoptosis than adult neurones and that increased cell death could facilitate virus spread. In the developing CNS, apoptosis is used to remove incorrect or weak synapses. As the brain matures, surviving neurones become more resistant to apoptosis. For example, SFV A7(74) infection of immature neurons of the suckling mouse brain results in death by apoptosis, whereas SFV A7(74) infection of the adult mouse brain results in a persistent infection (Allsopp et al., 1998; Allsopp and Fazakerley, 2000; Fazakerley, 2002). Additionally, the rostral migratory stream, which is an area of the brain where neurones are constantly being

replaced and differentiating, is the only area of the adult mouse brain to show apoptotic neurones upon infection with avirulent strains (Sammin et al., 1999).

SFV Replication

SFV entry into a cell is mediated by a yet unknown cellular receptor, although Sindbis virus entry is mediated via interactions with the laminin receptor (Tsai et al., 2002). During a virulent infection the enveloped virion enters the cell by endocytosis (reviewed in Kielian and Jungerwirth, 1990). Fusion of the envelope with the endosome membrane is dependent upon the acid pH altering the conformation of the spike protein (Wahlberg and Garoff, 1992). The E1 spike protein mediates fusion between the virus and the vesicle membrane resulting in nucleocapsid release into the cytoplasm. The acidic conditions of the vesicle also promote conformational changes in the capsid protein exposing ribosomal binding structures and uncoating of the viral RNA (Grimley et al., 1968; Grimley and Freidman, 1970). Viral replication is associated with cytopathic vacuoles (CPV) I and II (Kujala et al., 2001); these are developed from endosomes and lysosomes. CPV I are covered in viral protein complexes (sperules), containing the viral non-structural proteins and are the sites for viral replication. Virus maturation occurs on CPV II, these vacuoles then translocate to the plasma membrane for virion release (Pathak et al., 1976). Spikes protrude from the budding SFV virion envelope and are comprised of three E1-E2 heterodimers per spike. The C'terminal end of E2 associates with the capsid protein, which in turn is associated with viral RNA. The interactions between the capsid and E2 proteins drive virus budding and virion release (Suomalainen et al., 1992).

SFV is a single-stranded, positive-sense enveloped RNA virus. It has an 11 kb genome composed of two open-reading frames, the non-structural genes (nsP1, nsP2, nsP3, nsP4) and the structural genes (C, E2, E3, 6 kDa, E1; Figure 1E). The 5' non-structural proteins (nsP) are translated into a polyprotein (Takkinen et al., 1986), nsP1, 2, 3 and 4, which is processed by the viral protease nsP2. Together these proteins form the replicase complex which synthesizes full length negative strands to be used as templates for the production of more genomic and then sub-genomic transcripts. *Cis* cleavage at the nsP3:nsP4 junction enables minus strand synthesis, further *trans* cleavage at the nsP1:nsP2 junction allows both minus and positive strand synthesis and the final cleavage separating nsP2:nsP3

terminates minus strand synthesis and switches the replicase to synthesis of the subgenomic RNA (Lemm and Rice, 1993a; Lemm et al., 1993b; Shirako and Strauss, 1990; Shirako and Strauss, 1994).

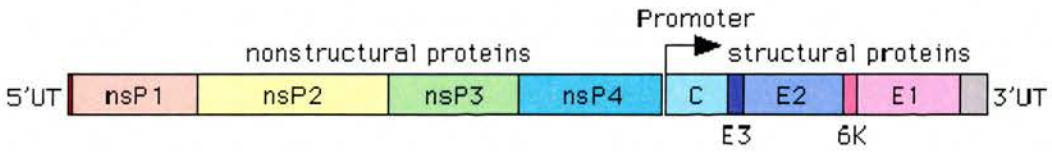

Figure 1E: SFV genome
The non-structural proteins (nsP), which form the replicase complex, are encoded at the 5' end of the genome. The structural proteins are encoded at the 3' end of the genome after a sub-genomic promoter.

Roles of the Non-Structural Proteins

NsP1

NsP1 is involved in the capping of viral RNAs, possesses methyl- and guanyl-transferase activity, aids initiation of negative strand RNA synthesis, and localises the replicase complex to cellular membranes (Ahola et al, 1997; Peranen and Kaariainen, 1991; Hahn et al., 1989). NsP1 plasma membrane attachment is essential for its capping activities (reviewed in Salonen et al., 2005). NsP1 attachment to membranes is mediated by an amphipathic helix and reinforced by palmitoylation (Laakkonen et al., 1996). Disruption of palmitoylation attenuates the virus. If the nsP1 threonine residue 538 of virulent SFV4 is changed to isoleucine as found in avirulent strains this attenuates the virus (Heise et al., 2003). The 538 residue forms part of the nsP1:nsP2 cleavage site, insertion of the isoleucine residue enhanced processing of the cleavage but reduced virulence.

NsP2

NsP2 possesses ATPase and GTPase activity (Rikkonen et al., 1994a) as well as RNA triphosphatase and RNA helicase activities (Gomez de Cedron et al., 1999). It is involved in terminating negative strand production and in controlling subgenomic RNA synthesis (Suopanki et al., 1998). It also cleaves the non-structural polyprotein through its papain-like protease domain (Merits et al., 2001) and contains a nuclear targeting sequence which induces nuclear translocation of approximately 50% of nsP2 (Rikkonen et al., 1992; Rikkonen et al., 1994b). An nsP2 mutant, SFV4nsP2-RDR where the central arginine residue of the nuclear translocation signal (RRR) is converted into an aspartic acid (D), revealed that this sequence was not essential for viral replication but was a determinant of

neurovirulence (Fazakerley et al., 2002; Rikkonen, 1996). *In vitro*, SFV4nsP2-RDR replicated comparably to SFV4 with reduced protein synthesis. *In vivo,* mice inoculated intracranially with SFV4nsP2-RDR survived whereas those infected with SFV4 virus died. SFV4 infected mice had higher brain virus titres than the mutant virus. To determine the role of the IFN response within this pathology, both viruses were inoculated into $IFNAR^{-/-}$ mice; all mice succumbed to infection regardless of the inoculating strain and produced similar virus titres (Fazakerley et al., 2002). This suggests several possibilities; firstly that *in vivo* SFV4nsP2-RDR does not replicate as well as SFV4 and that this slower replication allows time for control by the IFN response; secondly that SFV4 can suppress the IFN response, or is not susceptible to it, whereas the SFV4nsP2-RDR virus cannot suppress the response or is susceptible to it. Research with SV indicates that mutation of the nsP2 P_{726} residue, conserved throughout the alphaviruses, suppresses cytopathic effect and increases IFN production (Frolova et al., 2002). Similar observations were made *in vivo*, suggesting that nsP2 has a role in IFN suppression.

NsP3 and nsP4

NsP3 is a phosphoprotein involved in RNA synthesis (Peranen et al., 1988). Experiments comparing the virulence of chimeric viruses containing segments from virulent and avirulent strains, demonstrated that when virulent nsP3 and nsP4 proteins were expressed in an avirulent genetic background, high virus titres were observed in the brain and 95% of the mice died i.e. the virus was virulent. When only nsP3 was replaced, widespread infection was still observed throughout the cortex and cerebellum (Tuittila et al., 2000). The avirulent strain nsP3 protein possesses a 7 amino acid deletion at its C terminal end, which includes five hydrophobic amino acids. However, when the deletion was replaced (with the virulent strain sequence), the new virus was still unable to replicate efficiently and showed no clinical symptoms in infected mice. The avirulent nsP3 also has an opal stop codon at the 3'end. When the opal codon was altered to arginine, virulence was increased; 1/20 mice died and 5 were paralysed (Tuittila et al., 2000). However, several other neurovirulent alphaviruses possess an opal codon at the 3'end of nsp3 e.g. Ross River, Eastern and Western equine encephalitis, Sindbis and Middelburg viruses, questioning the importance of the opal codon in SFV virulence (Strauss et al., 1983). NsP4 is the viral RNA polymerase (Keranen & Kaarianen, 1979).

The Involvement of the Immune Response

Avirulent infections can be cleared from the blood of immunocompetent mice within three days and from the brain within 8 days (Fazakerley, 1993). IgM can be isolated from the blood within a few days and is followed by IgG2α and a slow accummulation of IgG1 (Fazakerley, 1993). By 4 days post-infection, plasma cells can be detected within the brain. Initial production of IgM neutralises virus but cannot completely clear the infection. A secondary wave of IgG2α is required for complete removal of infection (Amor et al., 1996). In support of this, infected μMT mice, which lack B cells, show continued cycling of viral RNA species over several months (unpublished data, Rennos Fragkoudis). However, T-cells play a critical role in SFV immune responses. T-cell deficient mice, *nu/nu* mice, clear infectious avirulent A7(74) virus from their blood but cannot completely clear it from the brain. The brain requires IgG antibodies to clear the virus infection. In the absence of CD4+ T-cells, B cell Ig class switching is not induced and so no neutralising IgG antibody is produced (Amor et al., 1996; Fazakerley and Webb, 1987). SCID mice, which lack all forms of adaptive immunity, are unable to clear A7(74) infection, but they survive for several weeks before succumbing to the infection (Amor et al., 1996). Passive transfer of SFV specific IgM or IgG prevents death but does not entirely remove the virus emphasizing the necessity of T-cells for complete viral clearance (Amor et al., 1996). The major cerebral infiltrating cells are CD8+ T-cells with a few B cells (Amor et al., 1996; Morris et al., 1997). Cytotoxic T-cells have been associated with primary demyelination (Mokhtarian et al., 2003). IFN-γ is released by T-cells and is associated with neuronal SFV immune responses. $IFNGR^{-/-}$ mice demonstrate higher levels of neuronal necrosis than wt mice; this is associated with increased viral antigens and high numbers of macrophage and B cells (Keogh et al., 2003). No difference is observed in the levels of demyelination between $IFNGR^{-/-}$ and WT mice. Following an i.p. infection, type I IFNs are released. Other cytokines such as IL-1α, -1β, -3, -6, -10 and TNF-α are also observed although their role has yet to be determined (Moris et al., 1997).

Semliki Forest Virus and Interferons

During an SFV infection, blood levels of IFN correspond to levels of viraemia (Bradish et al., 1975). When SFV-infected L-cells are treated with anti-IFN

antibodies, larger plaques develop than when cells are untreated. *In vivo*, treatment of mice with anti-IFN antibody increases brain virus titres and mortality (Fauconnier, 1969). In the CNS, SFV antigen expression is reduced when mice are treated with IFN-α/β (Morris et al., 1986). Several other experiments provide evidence for the protective effect of IFN against SFV. The protective effect of IFN, given prior to virus infection, is proportional to the amount of IFN given (Finter et al., 1966). Administration of a dose of IFN earlier than 48 hours prior to infection results in the loss of the protective effect. Also, endogenous IFN induces a greater protective effect than administered IFN, as mice previously infected with Newcastle Disease virus are protected against an SFV challenge to a greater degree than those treated with high doses of IFN (Finter et al., 1966). When IFN is administered 24 hours prior to infection with L10 SFV it delays death; however, when mice are treated with poly I:C 4 hours prior to L10 SFV infection, the infection is rendered avirulent (Bradish and Titmuss, 1981). Similar IFN concentrations from mixed samples of blood, muscle and spleen are induced by the virulent V13 strain and avirulent A7 strains (Smillie et al., 1973). Mice infected with A7 are protected against V13 challenge, 63 hours later (Smillie et al., 1973), and mice infected with A7(74) three hours prior to challenge with L10 are protected against panencephalitis (Oliver, 1997). Only small foci of brain infection are apparent, suggesting SFV A7(74) stimulates an antiviral response, most likely IFN, that can control the SFV L10 infection. The importance of the IFN response in containing an SFV infection is further demonstrated in $IFNAR^{-/-}$ mice, infection with all strains of SFV results in death within 2 days (Bradish et al., 1975; Muller et al., 1994; Fazakerley et al., 2002).

Aims & Hypotheses

The aim of this thesis is to further investigate the interactions between IFN and SFV. To date studies have demonstrated SFV sensitivity to IFN and the ability of SFV to induce IFN.

Questions to be addressed:

1) Does SFV4 induce IFN?

In vitro in cell cultures, the L10 and A7 strains of SFV are well-known inducers of type I IFN responses; however, the IFN response to the molecularly cloned SFV4 has not been studied.

2) Is the brain IFN system activated by SFV infection?

Recently, IFN-α mRNA transcripts have been detected in the brains of SFV4 infected adult mice (McKimmie et al., 2005). The dynamics of the IFN response and its relationship to the levels of virus have not been studied.

3) Do suckling mice induce differential levels of IFN in comparison to adult mice?

In mice up to the age of 12 days, SFV A7(74) causes severe infection; in adult mice the infection is avirulent (Fleming, 1977, Oliver et al., 1997). The pathology of the infected adult mouse brain demonstrates foci of SFV A7(74) infection, implying that the virus cannot spread between neurones. One explanation of this is that a host defence mechanism is controlling the infection in adult mice, but that this does not function or is impaired in suckling mice. This could be an impaired ability of immature (post-natal) CNS cells to produce or respond to IFN.

4) What is the role of PKR in the IFN response to an SFV4 infection?

Induction of IFN-β requires the activation of multiple transcription factors, including NF-κB. PKR is a cytoplasmic, dsRNA-activated kinase, which terminates host cell translation and promotes inflammation by activating NF-κB. PKR is not essential for IFN-β induction during several virus infections; however, the role of PKR in IFN-β induction during alphavirus infections has not been investigated.

5) Do virulent and avirulent strains induce different amounts of IFN?

There are several strains of SFV; these can be divided into two groups, those that cause panencephalitis in adult mice and those that present a restricted neuronal

infection. These differences in pathology could be attributed to differential induction of IFN.

5) Does SFV4 antagonise the IFN response?

Viruses from many families have developed mechanisms to antagonise the IFN system. Ross River virus antibody dependent enhanced infection of macrophages suppresses the expression of IFN-β and TNF-α by reducing nuclear NF-κB and other transcription factor complexes (Mahalingham and Lidbury, 2002). However, no area of the alphavirus genome has yet been identified as an antagonist of IFN expression. NsP2 mutants of Sindbis virus and SFV induce higher levels of IFN or induce less neuropathology and lower virus titres than wt virus, respectively (Frolova et al., 2002; Fazakerley et al., 2002). When the SFV nsP2 mutant is inoculated into $IFNAR^{-/-}$ mice, the pathology and virus titres are equivalent to those induced by wt virus. Possible explanations are that the nsP2 mutation affects replication and that the reduced level of replication enables the host immune system to control the infection or that wt virus can suppress the IFN response, or is not susceptible to it, whereas the mutant nsP2 virus cannot suppress the response or is susceptible to it.

Chapter 2: Materials & Methods

Contents

Cell lines, culture conditions & virus strains 49
Passaging adherent cell lines 49
Mouse Embryo Fibroblast (MEF) production 50
Infection of cells for functional IFN studies 50
Infection of cells for RNA extraction 51
Animal Experiments 51
Infection of mice 51
Perfusion 51
Brain Extraction 51
Virological Methods 52
Virus Sequencing 52
Reverse transcription PCR 52
High fidelity PCR 52
TOPO® Cloning 53
DNA Extraction 53
Purification of SFV 54
Plaque assay 54
Cytopathic effect assay 55
Immunocytochemistry 56
Detection of SFV nsP3 by NovaRED™ 56
Detection of SFV, IRF-3 and NF-κB by immunofluorescence 57
Cytopathic Effect Reduction Assay (CPERA) 58
Production of Laboratory IFN Standards 58
Determination of the quantity of International Reference Standard IFN required to achieve 50 % cell viability 58
Preparation of samples for CPERA 59
In vitro supernatants 58
In vivo - brain samples 59
CPERA 59
Swedish IFN bioassay 63

Polymerase Chain Reaction 64
Transcription Shut Down Analysis 65
Gel Preparation (25 ml total) 66
Quantitative real-time PCR 66
RNA Extraction 66
Tissue cultured cells 66
Brain samples 67
RNA quantification 68
Reverse transcription PCR 68
Preparation of Standards 69
Plasmid Cloning 69
Preparation of LB-Ampicillin plates 69
Transformation of DH5α cells 69
Purification of plasmid 69
Confirmation of purified plasmid 70
Preparation of samples for real-time PCR 71
Quantitative PCR 71
Protein Techniques 72
Western Blot 72
Gel preparation 72
Sample preparation 72
Sample preparation and transfer 73
Detection of transcription factors 73
Electromobility Shift Assay (EMSA) 74
Oligo design 74
Preparation of oligomers 75
Nuclear Extractions 75
Protein assay 76
Gel preparation (1) 76
Probe labelling 77
Gel preparation (2) 77
Translational shut-off experiment 78
Statistical Analysis 79

Cell lines, culture conditions & virus strains

BHK-21 cells were kindly provided by Deborah Allen (CID, Edinburgh); the cells were maintained in 10 % new born calf serum (NBCS, Invitrogen) Glasgows modified essential medium plus 10 % tryptose phosphate broth (Invitrogen), penicillin and streptomycin (P/S, final concentration 100 U/ml penicillin and 100 μg/ml streptomycin, Merck BDH) and L-Glutamine (2 mM, Merck BDH). L-929 cells were kindly provided by Deborah Allen (CID, Edinburgh) and cultured in 10 % foetal calf serum (FCS) Dulbecco's modified Eagles medium supplemented with P/S (100 U/ml / 100 μg/ml) plus L-Glutamine (2 mM). $PKR^{-/-}$ and WT 129/Sv/Ev mouse embryo fibroblasts (MEFs) were grown from 13.5 day old embryos; MEF preparation is described in detail below. MEFs were maintained in 10 % FCS DMEM plus P/S (100 U/ml / 100 μg/ml) plus L-Glutamine (2 mM). The virus strains, SFV4, L10, A7(74), SFV4nsP2RDR and SFV4nsP3Δ50 were kind gifts from Professor Leevi Kaariainen (University of Helsinki, Finland). The SFV vectors pSFV10b12A-NP and pSFV10RDRb12A-NP were kindly provided Pia Dosenovic (Karolinska Institutet, Sweden); the IFN-β plasmid pSFV4-ifnb was kindly provided by Kathrina Quinn (Trinity College Dublin, Ireland).

Passaging adherent cell lines

At confluence, the culture media was removed and the cells were washed with 0.02 % Versene. Five ml trypsin / EDTA (Invitrogen) was incubated with the cells for several minutes until they could be tapped free from the plastic. Trypsin was inactivated by the addition of 25 ml 10% FCS / NBCS media; this cell suspension was then centrifuged at 450 x g for 5 minutes to pellet the cells. The cell pellet was re-suspended in 2 ml 10% FCS / NBCS media. Ten μl of cell suspension was added to 90 μl trypan blue. This mixture was placed on a haemocytometer so that the mean number of cells per ml of cell suspension could be determined. The mean number of cells per square of the haemocytometer was ascertained and applied to the following calculation:

Mean number of cells per square x dilution factor (10) x total volume of a square (10^4) x final volume of cell suspension (2) = Mean number of cells per ml of cell suspension

Approximately 3 - 5 x 10^6 cells, cell type dependent, were seeded into a T175 flask in 30 ml medium to facilitate continued growth of the cell line.

Mouse Embryo Fibroblast (MEF) production

Mice were sacrificed by cervical dislocation after 13.5 days of pregnancy. The dead mice were sprayed with 70 % alcohol; two incisions were made at the base of the peritoneum and the cuts were extended rostrally along the flank of the animal. The exposed uterine horns were removed and washed in sPBS (150 mM; 2.5 mM KCl, 10 mM Na_2HPO_4, 1 mM KH_2PO_4 (pH 7.4)). Each embryo was released from its amniotic sack and transferred into a separate dish containing sPBS. Neuronal and hepatic tissues were removed by decapitation and extraction; the remaining embryonic tissue was cut using a scalpel blade in 1 ml trypsin/EDTA. A further 1 ml trypsin/EDTA was added to the tissue homogenate, which was then repeatedly triturated with a 1 ml pipette and incubated at 37°C for 10 minutes. Following the incubation, another 2 ml trypsin/EDTA was added and the homogenate re-triturated and re-incubated. The digested tissue was transferred to a universal tube and the supernatant was removed and placed in a separate universal tube, which was then topped up with media (10 % FCS DMEM plus P/S plus L-Glutamine). This was centrifuged at 450 x g for 5 minutes; the cell pellet was resuspended in 10 ml of media and spun again. Following the second wash the cell pellet was suspended in 10 ml of media and transferred to a T80 cell culture vessel to facilitate cell growth.

Infection of cells for functional IFN studies

Chamber slides were seeded with 2x10^5 of either L-929 cells or MEFs in 10 % FCS DMEM and incubated at 5 % CO_2 and 35°C for 24 hours. At 80-90 % confluence the growth media was removed and the cells were washed with sPBS. Each well was inoculated for 1 hour at room temperature with 400 µl of virus suspension. After 1 hour, the inoculum was removed, the monolayers washed twice with sPBS and then

covered with 1.5 ml of 0.5 % or 2 % FCS DMEM for L-929 cells or MEFs, respectively. The chamber slides were incubated at 5 % CO_2 and 35°C for 20 – 24 hours. Following incubation 700 µl of supernatant was collected for plaque assays and 700 µl was collected for the CPERA to determine the levels of infectious virus and functional IFN, respectively. Once the supernatant had been removed the monolayers were washed twice with sPBS and fixed prior to SFV nsP3 immunostaining.

Infection of cells for RNA extraction

T20 flasks were seeded with approximately $1x10^6$ MEFs or $1x10^6$ L-929 cells in 10 % FCS DMEM. For each time point or virus strain investigated T20 flasks were set up in triplicate. At confluence the culture media was removed and the monolayers were infected as described in 'Infection of cells for functional IFN studies'.

Animal Experiments

Infection of mice

All of the adult mice used in this thesis were aged 4 – 6 weeks; wild type 129/Sv/Ev mice and $PKR^{-/-}$ mice were inoculated intracranially with $5x10^3$ pfu in 0.2 µl PBSA or with PBSA alone, Balb/c mice were inoculated intraperitoneally with 1 x 10^3 pfu of SFV L10. Neonates, four days old (P4), derived from 129 mice were inoculated intranasally; 50 µl of $1x10^5$ pfu/ml SFV4 were placed on the nostrils and inspired.

Perfusion

Mice were deeply anaesthetised with halothane and the thorax opened to expose the heart. A butterfly needle attached to a 50 ml syringe filled with sPBS was inserted into the left ventricle and the sPBS was slowly perfused in. Maintenance of a pulse during the procedure is necessary to pump the sPBS throughout the body to remove all of the blood. The sPBS was continually passed through the heart until the skin (tail), eyes and lungs became pale.

Brain Extraction

Animals were killed by exposure to CO_2 according to the Home Office regulations; the animals were scalped and an incision made into the base of the skull. This incision was extended along the sides of the skull at the widest point up until the eye socket. The skull was carefully lifted away from the brain; the top of the spinal cord was cut and the hemispheres of the brain separated bilaterally down the midline and then each was removed and placed in RNALater or snap frozen on dry ice.

Virological Methods

Virus Sequencing

Reverse transcription PCR

Two μg RNA from an infected cell culture was made up to a total volume of 10.5 μl with RNase free water. One μl of 50 pM of the 3'SFV4nsP2RDR or 3'SFV4nsP3Δ50 primer and 1 μl 40 μM dNTP mix (Promega) was added to the RNA then incubated at 65°C for 5 minutes. Following the initial denaturing phase, the samples were cooled on ice for 5 minutes then incubated with 4 μl 5x buffer (Invitrogen), 2 μl 0.1 M DTT (Invitrogen) and 40 U RNaseIn (Promega) for 2 minutes at 42°C. Two hundred U of superscript II Murine Moloney leukaemia virus reverse transcriptase (Invitrogen) was added to the reaction mix and incubated for a further 58 minutes at 42°C. The reaction was completed with 15 minutes at 70°C.

High fidelity PCR

Platinum Pfx DNA polymerase (Invitrogen) was used to clone fragments spanning the SFV4nsP2RDR and SFV4nsP3Δ50 mutations for sequencing. Individual reactions were set up as described below for 50 μl final volume.

10 X Pfx amplification buffer	5 μl
10 mM dNTP mix	1.5 μl
50 mM $MgSO_4$	1 μl
Primer A (50 pM)	1 μl
Primer B (50 pM)	1 μl
Template DNA	2 μl

DNA Polymerase	1 U
dH_2O	38.1 µl

Tubes were briefly centrifuged and then the template DNA was denatured for 2 mins at 94°C. Samples can directly enter the amplification cycles as the polymerase is antibody bound, so does not require a 'hot start' for greater specificity. Samples were processed through thirty rounds of 94°C for 15 seconds, 55°C for 30 seconds and 68°C for 2 minutes. Followed by 10 minutes at 68°C for the final extension stage.

TOPO® Cloning

One µl of PCR product, 1 µl salt solution, 3 µl sterile water and 1 µl pCR®II-Blunt-TOPO® were added in the order described to set up the TOPO® cloning reaction (Invitrogen) and were incubated at room temperature for 7 minutes. Two µl of the TOPO® cloning reaction were added to a vial of chemically competent DH5α *E.coli* cells and incubated on ice for 20 minutes. The cells were exposed to 42°C for 30 seconds and then transferred to ice. Two hundred and fifty µl of SOC media (1x LB broth, 20 mM glucose, 20 mM $MgCl_2$) was added to the vial, which was shaken for 1 hour at 37°C. Following the incubation, 50 µl or 100 µl of the bacterial suspension were added to and spread across LB agar (1 x LB broth, 1.5 % (w/v) bacto-agar) plus kanamycin plates (50 mg/ml), which were incubated overnight at 37°C. The next morning three colonies were selected and transferred into 3 universals containing 5 ml Luria Bertani broth (1 % (w/v) tryptone, 0.5 % (w/v) yeast extract, 1 % (w/v) NaCl) plus kanamycin and shaken at 37°C for 8 hours. Mini-preps following the Qiagen mini-prep protocol were prepared for each culture and the extracted DNA was sequenced in the Biomedical Sciences Molecular Pathology Unit, University of Edinburgh.

DNA Extraction

DNA was extracted in accord with the Qiagen mini-prep protocol; briefly 5 ml of bacterial culture was spun at 360 x g for 5 minutes. The pellet was resuspended in 250 µl of buffer P1, 250 µl of buffer P2 was added to the suspension which was then gently inverted 4 – 6 times. To this, 350 µl of buffer N3 was added and the suspension was inverted 4 – 6 times immediately afterwards. This was centrifuged at maximum speed > 8000 x g for 10 minutes on a bench top centrifuge. Following the spin, the supernatant was spun through a Qiagen spin column for 1 minute at

maximum speed on a bench top centrifuge and the flow-through discarded. The column was washed with 750 µl of buffer PE and centrifuged as before. The flow-through was removed and the column spun for a further minute. The DNA was eluted with 50 µl of buffer EB (10 mM Tris.Cl, pH 8.5); the buffer was added for 1 minute and then the DNA was eluted by centrifugation.

Purification of SFV

Ten T175 flasks were seeded with BHK-21 cells, which were grown to confluence in 10 % GMEM. At confluence, the cells were infected at a moi 0.01 of virus in 2 ml media for 1 hour at room temperature. Following infection, the monolayers were incubated in 40 ml 10 % GMEM for 24 - 48 hours, until CPE was observed. The supernatants were collected and clarified by centrifugation at 7,000 rpm (Sorvall GSA rotor) for 20 minutes. To the supernatant, 23 g/L NaCl and 70 g/L PEG 8,000 were added, the suspension was continually stirred overnight at 4°C. After the overnight incubation, the suspension was centrifuged as before (7,000 rpm for 20 minutes) and the pellet was resuspended in 8 ml of low salt buffer (0.15 M NaCl, 10 mM Tris pH 7.4). Sucrose gradients were prepared in SW41 centrifugation tubes ranging from 20 % to 70 % in increments of 10 %; 4 ml of the virus suspension was placed on top of the gradients. The virus suspension was separated by overnight centrifugation at 35,000 rpm on an SW41 rotor. Two ml of material surrounding the virus band was removed and each of the bands from all of the tubes were pooled and diluted with low salt buffer. The purified virus was pelleted by centrifugation at 35,000 rpm on an SW41 rotor for 1 hour at 4°C and the pellets were resuspended in 200 µl low salt buffer.

Plaque assay

BHK cells were seeded at $4x10^5$ onto 6 well plates in 2 ml 10 % GMEM and incubated at 5 % CO_2 and 37°C until they reached 80 % confluence. At 80 % confluence, the growth media was removed, the cells washed with sPBS and infected with 400 µl of virus suspension. A series of ten-fold virus dilutions were prepared in sPBS, each dilution of virus was tested in duplicate. Infected cells were incubated for 1 hour at room temperature in a damp tissue culture box. Two ml of molten, approximately 45°C, 2 % FCS DMEM mixed at a 10:3 ratio with 4 % agar was added

to the cells and allowed to set. The plates were incubated for 48 hours at 5 % CO_2 and 37°C. After incubation, the cells were fixed with 2 ml 10 % neutral buffered formaldehyde solution for 3 hours; this was removed along with the agar plug and the cells were stained with 0.1 % Toludine blue for >1 hour. The stain was removed and the plaques counted, to calculate the pfu per ml the following calculation was applied:

Mean pfu per well x dilution factor x 2.5 = pfu/ml

Cytopathic effect assay

L-929 cells were seeded at $3x10^4$ cells per well in a 96 well plate in 0.1 ml 10 % FCS DMEM and incubated for 24 hours at 5 % CO_2 and 37°C. At confluence, the culture media was replaced with 100 µl 0.5 % FCS DMEM and a further 50 µl of virus solution from a specific 10-fold serial dilution step was added in quadruplicate (see Table 2A).

1	2	3	4	5	6
NEAT	NEAT	NEAT	NEAT	MEDIUM	MEDIUM
10^{-1}	10^{-1}	10^{-1}	10^{-1}	MEDIUM	MEDIUM
10^{-2}	10^{-2}	10^{-2}	10^{-2}	MEDIUM	MEDIUM
10^{-3}	10^{-3}	10^{-3}	10^{-3}	MEDIUM	MEDIUM
10^{-4}	10^{-4}	10^{-4}	10^{-4}	MEDIUM	MEDIUM
10^{-5}	10^{-5}	10^{-5}	10^{-5}	MEDIUM	MEDIUM
10^{-6}	10^{-6}	10^{-6}	10^{-6}	MEDIUM	MEDIUM
10^{-7}	10^{-7}	10^{-7}	10^{-7}	MEDIUM	MEDIUM

Table 2A: Cytopathic Effect plate design
Columns 1-4 contain quadruplicate repeats of virus dilutions and columns 5 and 6 were incubated with media for controls. If the virus needed to be diluted further for quantification the above set up was repeated across the remainder of the 96-well plate starting at dilution 10^{-8}.

Plates were incubated at 5 % CO_2 and 37°C, and checked after 24 hours for cytopathic effect. The $TCID_{50}$, the tissue culture infectious dose resulting in the death of 50 % of cells, was determined by the number of wells showing a cytopathic effect and calculated by the Karber method:

$$Log_{10}\ TCID_{50} / 50\ \mu l = L - d(s - 0.5)$$

Where L = log of the lowest dilution (-1)

d = difference between dilution steps

s = sum of proportion of positive wells

Immunocytochemistry

Detection of SFV nsP3 by NovaRED™

Monolayers were fixed for 20 minutes with 4 % paraformaldehyde and then washed with sPBS. Cells were treated with 0.1 % Triton-X100 for 5 minutes to permeate the lipid membrane and then washed with sPBS. This treatment was followed with a 30 minute CAS block (Zymed) incubation; the block was not washed off prior to addition of primary antibody. Excess block was drained off the slides. The primary antibody was a monoclonal rabbit anti-SFVnsP3 antibody supplied by T. Ahola (Institute of Biotechnology, University of Helsinki). Four hundred µl of a 1:3000 dilution of primary antibody in CAS block was incubated with the slides for 1.5 hours at room temperature on a rocking platform. After incubation the cells were washed three times for 5 minutes in PBS, again on the rocking platform. The secondary antibody was a biotinylated goat anti-rabbit IgG (Vector Laboratories). Four hundred µl of a 1:400 dilution of the secondary antibody in CAS block was incubated with the slides for 1 hour at room temperature on a rocking platform. The cells were washed as before. Addition of the Vectastain *Elite* ABC reagents following incubation with the secondary biotinylated antibody increased the sensitivity of the staining. The reagent consisted of a preformed avidin and biotinylated horseradish peroxidase macromolecular complex, which was prepared by the addition of 2 drops of reagent A and 2 drops of reagent B to 10 ml PBS; the solution was mixed following the addition of each reagent. This was allowed to stand at 4°C for 30 minutes prior to addition to the slides. On completion of the three 5 minute washes in PBS the Vectastain reagent was incubated with the slides at room temperature for 30 minutes and then washed as before. To visualise the immunostaining, a NovaRED™ chromogen was used (Vector Laboratories). NovaRED™ substrate was prepared immediately before use; 3 drops of Reagent 1 were added to 5 ml of distilled water and mixed, followed by 2 drops of Reagent 2, 2 drops of Reagent 3 and 2 drops of the Hydrogen Peroxide Solution. The solution was mixed after the addition of each reagent. NovaRED™ was added to the slides and incubated in the dark for approximately 5 minutes and

then rinsed immediately with water. Each of the slides was counter stained with Haematoxylin (Vector Laboratories) at 1/10 dilution until appropriately stained and then mounted in aqueous mounting media (Dakocytomation).

Detection of SFV, IRF-3 and NF-κB by immunofluorescence

Primary antibody dilutions

Mouse α-Spike E2-1	1 / 200	(T. Ahola, University of Helsinki)
Rabbit α-NF-κB p65	1 / 100	(Mauro D'Amato, Karolinska Institutet)
Goat α-IRF-3	1 / 200	(Santa Cruz Biotechnology)
Mouse α-Replicase	1 / 200	(T. Ahola, University of Helsinki)

Secondary antibodies

Donkey α-goat Cy 3	1 / 1000	(Jackson Immunoresearch)
Donkey α-mouse Cy 2	1 / 100	(Jackson Immunoresearch)
Donkey α-rabbit texas red	1 / 200	(Jackson Immunoresearch)
Goat α-rabbit FITC	1 / 450	(Jackson Immunoresearch)
HOERST	1 / 1000	(Molecular probes, Eugene, Oregon)

Cells were grown on coverslips, infected at moi of 1 and then fixed by washing in sPBS and then incubating in 4 % paraformaldehyde for 8 minutes at room temperature followed by ice-cold methanol for a further 8 minutes at - 20°C. The methanol was washed off with PBS prior to being blocked for 1 hour at room temperature with serum (2.5 ml horse sera, 100 µl NaN_3 (sodium azide, 10 % stock) and 47.5 ml PBS). The block was drained from the cells and the specific primary antibody added at the designated concentration diluted in the serum solution and incubated for 1.5 hours at room temperature in the dark. The primary antibody was removed by washing the cover slips 3 x with PBS; the secondary antibody was incubated on the cells for 1 hour in same blocking buffer. Excess secondary antibody was removed by washing the cells 3 x in PBS then once with pure water. The coverslips were mounted using vinol mounting media (Fukui et al., 1987). Excess mounting media was washed away and the slides were allowed to dry.

Cytopathic Effect Reduction Assay (CPERA)

Production of Laboratory IFN Standards

Three T-175 flasks were seeded with $2x10^6$ L-929 cells in 50 ml 10 % FCS DMEM and incubated at 5 % CO_2 and 37°C until 48 hours post confluence (approximately four days). The growth media was removed and the monolayers washed twice with 15 ml DMEM. The cells were infected with a moi 10 of either L10 SFV or A7(74) SFV diluted in 2 ml serum free DMEM and incubated with the virus for 1 hour at room temperature. The third flask was mock infected with serum free DMEM. After one hour the virus was removed and the cells were washed twice with 15 ml DMEM, then immediately covered with 50 ml protein free DMEM containing 1 mM phenylmethylsuphyl fluoride (PMSF, Sigma), a protease inhibitor, and incubated for approximately 24 hours at 37°C and 5 % CO_2 until cells exhibited a clear CPE. At this point, the culture fluid was harvested and centrifuged at 7,700 x g for 20 minutes at 4°C to remove any cellular debris. To inactivate infectious virus, the supernatant was left for 4 days at 4°C and pH 2. This was achieved by adding 1 M HCl to the culture fluid. After 4 days the fluid was neutralised with 1 M NaOH and stored at -70°C in the presence of 1-3 mg/ml BSA and 1 mM PMSF.

Determination of the quantity of IRS IFN required to achieve 50 % cell viability

A CPERA was performed for 5, two-fold dilution series of International Reference Standard (IRS) IFN murine IFN alpha/beta (GU02-901511 Braton Biotech Inc, NIAID). The average 50 % end point was determined. This is the amount of IFN required to maintain 50 % cell viability during an EMCV infection and was calculated to be 0.45 International Units (IU) IRS IFN.

Preparation of samples for CPERA

In vitro supernatants

Supernatants were centrifuged at 8000 x g in a bench top centrifuge, acidified to pH 2 with 1 M HCl and incubated at 4°C for 4 days. After incubation samples were neutralised to pH 7 with 1 M NaOH and stored at -70°C.

In vivo - brain samples

The average weight of an adult half brain is 0.3 g. A 1:10 (weight: volume) dilution was made by homogenising the brain in 2.7 ml sPBS and 1:1000 dilution of protease inhibitor cocktail (Sigma); the homogenate was passed through a 21 G needle 5 times to dissipate tissue clumps, then centrifuged at 8000 x g in a bench top centrifuge for 5 minutes; the supernatants were then collected and acidified as above.

CPERA

In a 96 well plate, $3x10^4$ L-929 cells were seeded per well in 0.1 ml 10 % FCS DMEM supplemented with 1 % L-glutamine. The plates were incubated overnight at 5 % CO_2 and 37°C until a confluent monolayer was formed. In a separate 96-well plate, a 2-fold dilution series of the IFN samples was prepared (See Table 2B). To each well, except wells A2 - A12, 0.1 ml 0.5 % FCS DMEM was added. To wells A2 and A6, 0.2 ml of 1:10 laboratory standard IFN: DMEM was added. Wells A3 – A5, A7 – A9 and A10 – A12 contained 0.2 ml of three different samples repeated in triplicate. A two-fold dilution series was then created down the test columns by transferring and mixing 0.1 ml from row A into row B; this was repeated down the plate. After tituration of row H, the extra 0.1 ml was discarded and the plates incubated at 5 % CO_2 and 37°C for 30 minutes to re-equilibrate the pH of the media.

The growth media from the cell plates was then removed and replaced with the prepared dilution series, and the plates were re-incubated for a further 24 hours at 5 % CO_2 and 37°C. After incubation, the IFN samples were removed and replaced with a challenge virus suspension. Encephalomyocarditis virus was added to the cells at 300 $TCID_{50}$ per 0.1 ml 0.5 % FCS DMEM. Column 1 (no IFN standard or test sample) served as cell and virus controls. Wells A1 – D1 received 0.1 ml 0.5 % FCS DMEM

and wells E1 – H1, 0.1 ml challenge virus suspension. The plates were incubated at 5 % CO_2 and 37°C until complete CPE was observed in the virus controls, usually after approximately 48 hours. When complete CPE was observed in the virus controls, the media was removed from all the wells and replaced with fresh 0.5 % FCS DMEM. Ten µl of WST-1 cell proliferation reagent (Roche) was then added to each well and the absorbance read immediately at 420 – 480 nm on a MRX microplate reader (Dynex Technologies). The plates were incubated in the dark at 5 % CO_2 and 37°C for three hours and then read again. Viable cells cleave the WST-1 tetrazolium salts to formazan through their mitochondrial dehydrogenases; the activity of these enzymes directly correlates to the number of metabolically active cells in the culture. The level of formazan is determined by measuring absorbance values upon addition of the WST-1 reagent and again 3 hours later. An advantage of this reagent is that hydrolysis of tetrazolium salts to formazan is not accompanied by high background readings which can be observed with traditional dyes.

To determine the amount of functional IFN within a test sample: Primarily a mean value for each of the dilutions of the two-fold dilution series was obtained for each sample, this data was graphically represented on a linear scatter graph, where the absorbance readings were plotted against the two-fold dilution series. A threshold was determined, the 50 % end point, which was equivalent to the half way value between the absorbance readings of the cell and virus controls. The point at which the test sample crossed the threshold was determined from the graph (Figure 2A). This was multiplied by its reciprocal dilution factor and 0.45 IU to determine the initial amount of IFN added to the CPERA; the amount of IFN per ml of supernatant or g of brain was then determined for each sample.

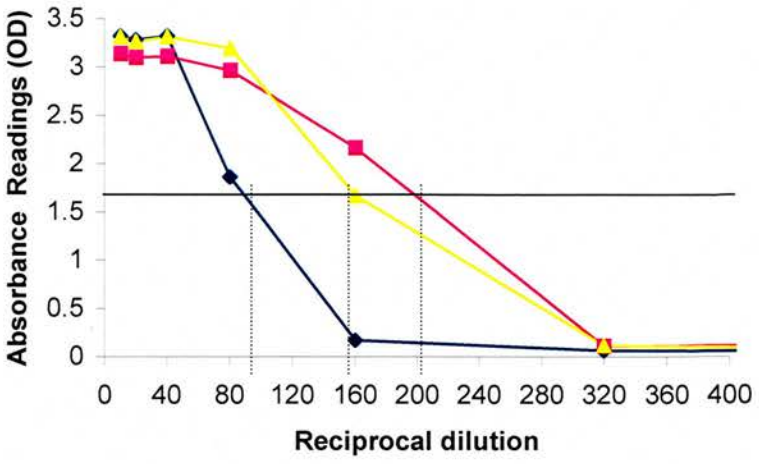

Figure 2A: Graphical representation of the absorbance values of IFN standard and test samples after incubation with WST-1 reagent for 3 hours.
Each point for each graph is equivalent to a dilution within the two fold dilution series, the blue line represents standard IFN and the pink and yellow lines represent two test samples. The black horizontal line is the 50 % end point threshold; the point at which each sample crosses the threshold is determined from the graph, as indicated by the dashed lines.

	1	2	3	4	5	6	7	8	9	10	11	12
A	VC	1:10	1:2	1:2	1:2	1:10	1:2	1:2	1:2	1:2	1:2	1:2
B	VC	1:20	1:4	1:4	1:4	1:20	1:4	1:4	1:4	1:4	1:4	1:4
C	VC	1:40	1:8	1:8	1:8	1:40	1:8	1:8	1:8	1:8	1:8	1:8
D	VC	1:80	1:16	1:16	1:16	1:80	1:16	1:16	1:16	1:16	1:16	1:16
E	CC	1:160	1:32	1:32	1:32	1:160	1:32	1:32	1:32	1:32	1:32	1:32
F	CC	1:320	1:64	1:64	1:64	1:320	1:64	1:64	1:64	1:64	1:64	1:64
G	CC	1:640	1:128	1:128	1:128	1:640	1:128	1:128	1:128	1:128	1:128	1:128
H	CC	1:1280	1:256	1:256	1:256	1:1280	1:256	1:256	1:256	1:256	1:256	1:256

Table 2B: CPERA plate design

VC and CC indicate virus and cell controls respectively, each sample was tested in triplicate repeats and the standards are laboratory prepared A7(74) SFV IFN. The ratios indicate two-fold dilution series.

Swedish IFN bioassay

(Miller and Anders, 2003)

L-929 cells were seeded at a density of 1.5 x 10^3 per well in a 96 well plate in 100 µl 10 % FCS DMEM and incubated for 24 hours at 5 % CO_2 and 37°C, until 90 % confluent. At 90 % confluence, the media was removed by shaking the plate upside down and replaced with 50 µl 10 % FCS DMEM. Samples were tested in duplicate and diluted across the plate in a two-fold dilution series. The first and last rows were excluded from the experiment and used as virus controls (Table 2C). Fifty µl of sample was added to the first well of each row, mixed and then transferred into the next well along the plate. This was repeated until the end of the row. An IFN standard was included on each plate, supplied by the NIH reference centre. The samples were incubated with the cells for 24 hours at 5 % CO_2 and 37°C.

		1	2	3	4	5	6	7	8	9	10	11	12
A		Virus Control											
B	Sample 1a	1	2	4	8	16	32	64	128	256	512	1024	2048
C	Sample 1b	1	2	4	8	16	32	64	128	256	512	1024	2048
D	Sample 2a	1	2	4	8	16	32	64	128	256	512	1024	2048
E	Sample 2b	1	2	4	8	16	32	64	128	256	512	1024	2048
F	Sample 3a	1	2	4	8	16	32	64	128	256	512	1024	2048
G	Sample 3b	1	2	4	8	16	32	64	128	256	512	1024	2048
H		Virus Control											

Table 2C: Swedish IFN bioassay plate set up
The top and bottom rows are left blank and used as virus controls to indicate 100 % cytopathic effect. The six rows in between are used to assay two-fold dilutions of each sample in duplicate. The numbers in the wells indicate the reciprocal dilution of the two-fold dilution series. Where standards were included on the plate, one of the samples was replaced with 100 IU IRS IFN (stock – 10,000 IU/ml).

Following the 24 hour incubation, the media was removed and replaced with the infectious challenge media. SFV4 was made up to a concentration of 1.5 x 10^4 pfu / 50 µl in infection media (MEM plus 0.2 % BSA, 2 mM glutamine, 20 mM Hepes). Fifty µl of infectious challenge media was added to each well and incubated for 1 hour at 5 % CO_2 and 37°C. The media was removed and replaced with 100 µl 10 % FCS DMEM and the plates were incubated for a further 48 hours until CPE was visible. When total CPE was observed in the virus controls, the media was removed

and 50 µl of 10 % MTT solution was added to each of the wells and incubated at 5 % CO_2 and 37°C for 4 hours.

10 % MTT solution: 5 mg/ml MTT (3-(4,5-dimethylthiazol-2-yl)-2,5-diphenylte-trazolium bromide) is dissolved in OPTImem (minus phenol red plus L-glutamine, 1 x NEAA, 2 % FCS, P/S).

After the incubation, the MTT solution was discarded and replaced with 100 µl 0.1 M HCl in anhydrous isopropanol to solubilise the crystals. The plate was left on a gyratory shaker for 1 hour and then read at 570 nm and normalised against the 630 nm reading.

Polymerase Chain Reaction

Different conditions had to be established for different sets of primers. Here a general description of the protocol used is given; specific conditions and primers are listed below (Table 2D).

An individual reaction was set up as below

10 x PCR buffer	5 µl
25 mM $MgCl_2$	3 µl
10 mM dNTPs	1 µl
Forward primer (50 pM)	1 µl
Reverse primer (50 pM)	1 µl
cDNA	2 µl
dH_2O	36.6 µl
Taq DNA polymerase	2.5 U

For each experiment a master mix was created for the total number of reactions, including buffer, $MgCl_2$, dNTPs, forward primer, reverse primer and dH_2O. Two µl cDNA was added separately to each PCR 200 µl tube followed by 47.6 µl of master mix. Each tube was incubated for 3 minutes at 94°C, after which 0.4 µl Taq polymerase was added. Samples were held at the annealing temperature, 62°C for 30 seconds and extended at 72°C for 2 minutes. After the initial reaction, samples were cycled through 30 –35 reactions of

94°C for 15 seconds

62°C for 30 seconds

72°C for 2 minutes

followed by 72°C for 10 minutes for the final extension phase. Products were examined on an agarose gel (the percentage of agarose used was dependent upon the PCR product size).

Primers	Sequence	Annealing temp	Product size (bp)
IFNβ	For 5' CACAGCCCTCTCCAT CAACT Rev 5' GCATCTTCTCCGTCATCTCC	62°C	152
SFV4 E1	For 5' CGCATCACCTTCTTTTGTG Rev 5' CCAGACCACCCGAGATTTT	62°C	173
PKR	For 5' CAAAGCAGGAGGCAAGAAAC Rev 5' GCTGACTGGGAAACACCATT	55°C	369
IFNα	For 5' AGGACAGGAAGGATTTTGGA Rev 5' GCTGCTGATGGAGGTCATT	62°C	186
β-actin	For 5' CGTTGACATCCGTAAAGACC Rev 5' CTGGAAGGTGGACAGTGAG	62°C	202
GAPDH	For 5' AACTCCCACTCTTCCACCTT Rev 5' GCCCCTCCTGTTATTATGG	62°C	269
NsP2RDR	For 5' AAGGCAGTAGGGTTGAGTGG Rev 5' GCTGGTAGTGGTGGATTCTG	55°C Platinum Pfx Pol conditions	231
NsP3Δ50	For 5' GGAGGCAAACGAACGGAT Rev 5' TTCCTAAACGCAGTCCTTGG	52°C Platinum Pfx Pol conditions	663
NsP3Δ50 Outer	For 5' GCTTTGTTACCTGTTGTAGC	N/A	N/A
NsP2RDR Outer	For 5' GGACCACCTTCCTACATA	N/A	N/A

Table 2D: Primer sequence and annealing conditions

Transcription Shut Down Analysis

MEFs were seeded at 5 x 10^5 cells per well in a 6 well plate; the cells were infected at a moi of 50 with SFV4 or SFV4nsP2RDR in 300 µl of media (MEM plus 0.2 % BSA, 2 mM glutamine, 20 mM Hepes). Virus was incubated on the cells for one hour and then replaced with 2 ml of culture media; the cells were incubated in culture media for 4.5 hours at 37°C and 5 % CO_2. After 4.5 hours 1 ml of media containing 1 µg/µl actinomycin D was added to specific wells. Following 30 minutes incubation with actinomycin D, radioactive carbon-14 uridine was added to all wells, diluted in either plain media or media containing actinomycin D (5 ml media plus 100 µl Uridine). At 8 hours post-infection, the media was removed, the cells washed in ice cold PBS and

250 µl of lysis buffer (containing guanidine thiocyanate and 2-mercaptoethanol, GenElute™ Mammalian Total RNA Miniprep Kit, Sigma-Aldrich) was added per well. The lysis buffer was prepared in accordance with the manufacturer's instructions (Sigma). The cells were incubated on ice in the lysis buffer for 1 – 2 minutes and the lysates were collected and stored at -70°C. RNA was extracted as described below and quantified by spectrometer.

To 1.8 µg RNA, 3 µl 10 x MOPS, 1.8 µl formaldehyde, 15 µl formamide, and 3 µl water were added. The samples were incubated at 55°C for 15 minutes and then 2 µl of Loading Buffer (Final concentrations: 95 % formamide, 0.025 % w/v bromophenol blue, 0.025 % w/v xylene cyanol blue, 5 mM EDTA pH 8.0 and 0.025 % w/v SDS) were added to each sample. For each test sample, 5 µl were loaded onto a formaldehyde agarose gel.

Gel Preparation (25 ml total)

0.35 g agarose
36.5 ml DEPC water
9 ml formaldehyde (37 %)
5 ml 10 x MOPS buffer - 0.1 M MOPS
40 mM NaAc
5 mM EDTA (pH 8)

The gel was run at 60V for 20 minutes then 70V for 2 hours until the blue dye reached the end of the gel. Following the run, the gel was placed in sodium salicylate for 30 minutes on a rocker and then dried. In a vacuum dryer, the gel was incubated for 1 hour without heat, then for another hour at 80°C. The dried gel was exposed to film.

Quantitative real-time PCR

RNA Extraction

Tissue cultured cells

Cells were incubated with virus for a specific time and collected for RNA extraction. Briefly, monolayers were washed with versene, trypsinised and neutralised with 25 ml

10 % FCS DMEM. The cells were centrifuged at 450 x g and the pellets were immediately snap frozen on dry ice and stored at -70°C until RNA could be extracted. RNA was extracted using the QIAGEN RNeasy Mini kit following the animal cells protocol. Six hundred µl buffer RLT with β-mercaptoethanol (10 µl β-mercaptoethanol per 1 ml buffer RLT) was added to the frozen cell pellet (< $1x10^7$ cells). The pellet was vortexed in the buffer until cells were evenly distributed; further membrane disruption was induced by passing the cells through a 21 gauge needle 5 times. Seventy % ethanol was added to the lysate at a 1:1 ratio and 700 µl of the suspension was placed in an RNeasy mini column. The column was centrifuged at 8000 x g in a microfuge for 15 seconds. All spins were carried out under these conditions unless otherwise stated. The cell suspension was repeatedly added to the same column in 700 µl aliquots until all of the lysate had been centrifuged. Three hundred and fifty µl of buffer RW1 was added to each tube and spun, following which the tubes were incubated at room temperature for 15 minutes with 80 µl RNase-free DNase (Qiagen). A further 350 µl buffer RW1 was added to the tubes which were then centrifuged; following this 500 µl buffer RPE (an ethanol solution) was added to the column to precipitate the RNA and the tubes spun again. A second 500 µl of buffer RPE was added to the tubes, which at this point were spun for 2 minutes. After discarding the flow-through the tubes were spun at top speed for another 3 minutes. Thirty µl RNase-free water was used to elute the RNA by centrifuging at 8000 x g for 1 minute. This final step was repeated using the first eluate to concentrate the RNA.

Brain samples

Following dissection, brain tissue for RNA analysis was stored in RNAlater (Sigma). Forty µg was removed and homogenised in 600 µl RLT buffer (Qiagen RNeasy kit) plus β-mercaptoethanol (β-ME 10 µl/ml buffer) using a mortar and pestle. The homogenate was then passed through a 20-gauge needle and syringe 10 times to further disrupt the lysate. Each lysate was then centrifuged for 3 minutes at maximum speed in a bench top centrifuge (> 8000 x g) and the supernatant transferred to a fresh tube. To this 1 volume (1400 µl) of 70 % ethanol was added and mixed immediately by pipetting. The sample was then processed to extract RNA following the protocol described above.

RNA quantification

RNA was quantified on the Agilent bioanalyser (Agilent technologies) using the RNA 6000 Nano assay. Figure 2B shows an example of an Agilent chip.

Figure 2B: Agilent RNA 6000 Nano assay chip
Wells numbered 1 – 12 are used to quantify test RNA samples; gel-dye mixture is inserted into all wells represented by **G** and the well represented by is used to quantify the test RNA samples through addition of an RNA ladder.

Briefly, 1 µl dye concentrate was added to a 65 µl aliquot of gel matrix and spun for 10 minutes at 13,000 x g. Nine µl of gel-dye mixture was added to the well marked , this was dispersed throughout the chip using a 'priming station' and 'plunger'. Another 2 aliquots of gel-dye mixture were then added to the wells marked . Five µl of marker solution was added to the ladder well and to all sample wells. Test samples and RNA ladder were held at 70°C for 2 minutes then placed immediately on ice. One µl of ladder was added to the ladder well and 1 µl of each sample was added to each test well. On completion, the chip was vortexed for 1 minute and read in the bioanalyser by the total eukaryotic nano RNA electrophoresis assay.
For more details on the technology and procedure visit:
http://www.chem.agilent.com/scripts/generic.asp?lPage=1565&indcol=N&prodcol=Y

Reverse transcription PCR

Two µg RNA from each sample was made up to a total volume of 10.5 µl with RNase free water. Five hundred ng of oligo dT(15) (Promega) and 1 µl of a 40 µM dNTP mix (Promega) was added to the RNA then incubated at 65°C for 5 minutes. Following the initial denaturing phase, the samples were cooled on ice for 5 minutes then incubated with 4 µl 5 x buffer (Invitrogen), 2 µl 0.1 M DTT (Invitrogen) and 40 U RnaseIn (Promega) for 2 minutes at 42°C. Two hundred U of superscript II Murine Moloney leukaemia virus reverse transcriptase (Invitrogen) was added to the reaction

mix and incubated for a further 58 minutes at 42°C. The reaction was completed with 15 minutes at 70°C.

Preparation of Standards

Plasmid Cloning

Two types of standard were used to normalise the qPCR assay and quantify mRNA transcripts. PCR products were used as standards to quantify IFN-α, β-actin and GAPDH and plasmids were used as standards to quantify SFV4 (pSFV-GEM1) and IFN-β (pSFV1-IFNb). Clive McKimmey kindly provided the PCR product standards; the plasmid standards were amplified in *E.coli* cells and then extracted and purified.

Preparation of LB-Ampicillin plates

Five hundred ml Luria broth and 7.5 g agar were heated in a microwave until clear. The suspension was allowed to cool and 1 ml (50 mg/ml) ampicillin was added before the plates were poured.

Transformation of DH5α cells

Five hundred pg of control plasmid, (pUC19) was added to 100 µl of competent cells (Life Technologies). To a further two aliquots of cells, 5 µl of water and 5 µl plasmid (1 µg/µl) was added. The cells were incubated on ice for 30 minutes, heat shocked for 45 seconds at 42°C then transferred to ice for a further 2 minutes. Nine hundred µl LB-AMP was added and the eppendorfs placed in universals, which were transferred to the 37°C shaker for 1 hr at 225 rpm. Fifty µl of the cell suspension was added to the LB-AMP plates and spread evenly across the surface. The plates were left for 5 minutes to absorb the solution, then incubated overnight at 37°C.

Purification of plasmid

Single colonies were selected from the plates and cultured overnight in 5 ml LB-AMP. One ml of broth was removed and spun at 360 x g for 5 minutes in a bench top centrifuge. One ml 50 % glycerol in dH_2O was added to the cell pellets, each sample was vortexed, placed on dry ice and finally transferred to -70°C for storage. The remaining 4 ml were processed through Qiagen miniprep columns to elute purified plasmid; the DNA was extracted as described previously.

Confirmation of purified plasmid

The pSFV1-ifnb plasmid was incubated at 37°C with bovine serum albumin (BSA), buffer 2 (New England Biolabs) and Spe I for approximately 1.5 hours. The reagents were added as indicated below.

pSFV1-ifnb	1 µg
BSA 10X (1 µg/µl)	5 µl
Buffer 2	5 µl
Spe I	10 U
dH_2O	29 µl

After incubation, the temperature was increased to 65°C for 20 minutes.

To linearise the SFV structural proteins plasmid, pGEM1-SFV, the plasmid was incubated as above with Sph I (5 U). This enzyme does not require BSA and so was incubated with 34 µl dH_2O.

The Spe I and Sph I digestions gave, as expected, a single band of the correct size. Both plasmids have the same SFV backbone and were also digested with Eco RI:

Eco RI buffer	2 µl
Eco RI	20 U
cDNA	1 µl
water	16 µl

Each reaction was incubated for 2 hours at 37°C and then run on a 1 % agarose gel to visualise the bands. Three bands were produced for each plasmid, but pSFV4-ifnb had larger band sizes due to the insert. Following confirmation, the standards were quantified on the spectrometer and the copy number determined from the calculation below:

Copies DNA / µl = $(6.023 \times 10^{23} \times \text{mass/µl}) / \text{molecular weight of DNA}$

6.023×10^{23} is Avogadro's number and is the number of molecules per mole; the molecular weight is determined by gene length (base pairs) x 660 Daltons (660 Daltons is the average molecular weight of a base pair).

Preparation of samples for real-time PCR

Following 1st strand cDNA synthesis samples were frozen at -20°C, thawed and diluted in filtered water to 1:100 and 1:10 to measure SFV E1 transcripts and cellular mRNA transcripts, respectively.

Quantitative PCR

A master mix was prepared for the total number of reactions. Each reaction consisted of:

Primer A (50 pM)	0.4 µl
Primer B (50pM)	0.4 µl
40 mM dNTPs	0.4 µl
10 x Buffer plus 2 mM $MgCl_2$	2 µl
25 mM $MgCl_2$	0.8 µl
RNase-free water	13.1 µl
1:20,000 SYBR Green (Biogene Ltd)	0.75 µl
Fast start Taq (Roche Applied Science)	5 U
cDNA/ plasmid DNA	2 µl

The master mix was vortexed and 17.9 µl aliquots were dispensed into 100 µl tubes. To each tube, 2 µl of cDNA or standard DNA was added in triplicate. The fast start taq was activated by 5 minutes at 94°C, the PCR was then cycled through 94°C for 20 seconds, 62°C for 20 seconds and 72°C for 20 seconds for 40 cycles on a RotorGene 3000 (Corbett Research). At the end of each cycle SYBR green associates with dsDNA and the PCR machine emitted fluorescence is recorded. A melt curve analysis is carried out at the end of the cycling reactions in accord with manufacturer's instructions; fluorescence is measured as the temperature is increased from 65°C to 94°C in increments of 0.3 degrees.

Protein Techniques

Western Blot

Gel preparation

1 - Running gel

The gel cassette was set up and filled with a 10 % SDS gel, prepared as described below,

Water	9.9 ml
30 % acrylamide/ bisacrylamide	8.3 ml
1.5 M TRIS (pH 8.8)	6.3 ml
10 % w/v SDS	0.25 ml
10 % w/v ammonium persulphate	0.25 ml
TEMED	0.01 ml

A 2 cm space was left at the top of the gel to add the stacking gel. Whilst the running gel was setting, 100 µl of isopropanol was placed on the top of each gel within the cassette to level the surface and the gel pack kept in humid conditions to avoid desiccation.

2 – Stacking gel

The isopropanol was drained and the gel pack thoroughly washed to remove all traces of the alcohol. The stacking gel was prepared as described below:

Water	6.8 ml
30 % acrylamide/ bisacrylamide	1.7 ml
1.0 M TRIS (pH 6.8)	1.25 ml
10 % w/v SDS	0.1 ml
10 % w/v ammonium persulphate	0.1 ml
TEMED	0.01 ml

Stacking gel was added to each individual gel within the cassette; when completed, combs were inserted into each layer and the excess gel was removed.

Sample preparation

The protein content of each sample was determined and 25 mg was added per well for both cytoplasmic and nuclear samples. The samples were mixed with the appropriate

volume of 4 x sample buffer ((200 mM Tris-HCL (pH8.8), 20% (v/v) glycerol, 5 mM EDTA, 0.02 % bromophenol blue) 70 % (v/v) of which was added to 20 % (v/v) SDS and 10 % 0.5 M DTT). The samples were heated to 95°C for five minutes then added to the gel. The first well contained protein ladder.

Sample preparation and transfer

A set gel was transferred to the running equipment, which was pre-filled with 1 x SDS running buffer and 20 µl of sample was loaded into each well. The samples were initially run at 60 V for 30 minutes through the stacking gel and then at 100 V until completion of the run. To visualize the separated proteins, the sample runs were transferred onto a membrane. Cold transfer buffer (3 g TRIS, 14.4 g Glycine in 800 ml water plus 200 ml cold methanol) was prepared prior to the transfer. The transfer cassette was layered as indicated below

Sponge
Filter paper
Gel
Imobillon membrane
Filter paper
Sponge

The membrane was pre-soaked in methanol for 5 seconds and then placed in transfer buffer for a further 5 minutes alongside the sponges and the filter paper. Gel transfer was carried out in a Boehringer box which was kept on ice and filled with an ice block to maintain a low temperature. The transfer was run in cold transfer buffer for 1.5 hours at 100 V.

Detection of transcription factors

An overnight incubation in TBS plus 0.1 % w/v Tween with skimmed milk powder (5 g/100 ml) at 4°C was used to block the membrane. To detect the transcription factors, the membrane was drained and placed in a 50 ml Falcon tube, protein side facing inwards, with 4 ml milk solution plus primary antibody. The primary antibody was incubated for 1.5 hours on a rocker, to ensure all of the membrane was exposed to the antibody.

Primary antibody concentrations

Rabbit α NF-κB	p65	(SDS Biosciences)	1 / 300
Rabbit α eIF-2α		(SDS Biosciences)	1 / 200
Mouse α nsP2 (two monoclonal antibodies 2C7 + 3B5)			1 / 500

(Kindly donated by Leevi Kaariainen, University of Helsinki, Finland)

After the primary antibody incubation, the membrane was washed in TBS plus 0.1 % Tween for 2 x 30 seconds, the excess liquid was drained off between each step, and then washed a further 2 x 10 minutes in the same buffer. The same procedure was followed for the secondary antibody which was bound to horseradish peroxidase except that the secondary antibody was diluted in 4 ml 3 % BSA.

Secondary antibody concentrations

Goat α rabbit HRP	(BD Biosciences)	1 / 5000
Goat α mouse HRP	(DAKO)	1 / 5000

The secondary antibody was incubated for 1 hour on a rocker and then washed as desccribed above. To detect any reaction the membrane was incubated with 2 ml of a 1:1 mix of western immunoblot reagents (ECC Western Blotting analysis system, Amersham Biosciences) for a minute. The membrane was drained completely and transferred protein side down to a piece of clingfilm to develop on film.

Electromobility Shift Assay (EMSA)

Oligo design

Sequences derived from the literature describing NF-κB and IRF-3 binding sites on the IFN-β promotor were used to develop probes for NF-κB and IRF-3. Each probe was 29 nucleotides long, had 5' overhangs and enveloped the specified binding site. It was necessary to include a G in the overhang so P^{32} could be incorporated into the probe in a cysteine nucleotide.

NF-κB

FOR: 5'	ACTGA AAGTGGGAAAT TCC TC TGAG	
REV:	T TCACCCT T TAAGGAGAC TC CGTC	5'

IRF-3

FOR: 5' AAATG ACAGAGGAAAACTGAAAGGG

REV: TGTCTCC T TT T GACT T TCCC TCTTG 5'

Preparation of oligomers

The oligomers were diluted to a final concentration of 100 pM/µl; 2.5 µl of each oligo was made up to 100 µl with 10 x Boehringer buffer H and purified water.

i.e.	oligo FOR	2.5 µl
	oligo REV	2.5 µl
	10 x buffer	10 µl
	water	85 µl

The solution was brought to the boil for 2 minutes and left to cool slowly overnight. The prepared oligos were stored at -20°C.

Nuclear Extractions

MEFs were seeded in 6 well plates at 4 x 10^5 cells per well in 10 % FCS DMEM until confluent. At confluence, the cells were washed with PBS and then infected at moi of 50 with either SFV4 or SFV4nsP2RDR. The wells were incubated for an hour at 37°C and rocked every 10 minutes. After an hour, virus was removed and the cells were washed and incubated in 600 µl 10 % FCS DMEM. A low volume was used so that the supernatant could be collected and tested in the bioassay. After 4, 5, 6 or 7 hours, 250 µl of supernatant was collected to test in the IFN bioassay. This was acidified with 40 µl 1M HCl. The cell monolayer was then trypsinised in a volume of 300 µl until the cells could be tapped free from the culturing wells and then treated with 1 ml 10 % FCS DMEM to inactivate the trypsin. The cell suspension was centrifuged (300 x g, 5 minutes) and the pellet collected in 1.5 ml eppendorfs. The pellet was washed twice in ice-cold PBS and centrifuged between each wash.

Two buffers were required for the extraction of nuclear proteins:

Buffer A	Buffer B
10 mM HEPES (pH 7.9)	10 mM HEPES (pH 7.9)
10 mM KCl	0.4 M NaCl
0.1 mM EDTA	1 mM EDTA
0.1 mM EGTA	1 mM EGTA

The following were added immediately before use:

Leupeptin 0.5 µg/ml (final)

Aprotinin 0.5 µg/ml (final)

DTT 1 mM (final)

PMSF 0.5 mM (final)

Cells were resuspended in 300 µl Buffer A and placed on ice for 15 minutes. Twenty µl of 10 % NP-40 was added to the cell suspension and vortexed for 10 seconds and then left on ice for 2 minutes. The suspension was centrifuged at 1,677 x g for 5 minutes at 4°C; the supernatant was removed and transferred to another eppendorf labeled cytoplasmic fragment. The cell pellet was washed in buffer A and centrifuged again. Eighty µl of Buffer B was added to the pellet and vortexed; this was left on ice for 60 minutes and intermittently vortexed. Following the hour incubation, the suspension was centrifuged at 11,337 x g for 5 minutes at 4 °C and the supernatant (nuclear fragment) aliquoted in 25 µl and stored at –70°C.

Protein assay

Both the cytoplasmic and nuclear fractions were assayed for protein content in the BIO-RAD DC protein assay (Bio-Rad Laboratories, US). Following the microplate protocol, 20 µl of reagent S was added to each ml of reagent A needed for the run (A'). A 2-fold dilution series was prepared of a BSA standard of 1.41 µg/µl in both buffer A and buffer B for the cytoplasmic and nuclear extractions respectively. Five µl from each of the dilution steps of the standards and 5 µl of each sample were added to a dry microtitre plate. To these 25 µl of reagent A' was added, followed by 200 µl reagent B. The wells were mixed and then transferred to another plate to avoid any bubbles generated from the mixing. The plates were left for 15 minutes then read at 750 nm.

Gel preparation (1)

The gels were poured the day before running:

40 % acrylamide	6.25 ml
5 x TBE	5 ml
Water	38.25 ml
10% APS	500 µl
TEMED	38 µl

The above were mixed together and then poured in between two glass plates.

Probe labelling

To an eppendorf the following were added:

10 x Klenow buffer	2 µl
dNTPs	1 µl
Oligo duplex	2 µl
Water to make volume to	20 µl
Alpha- 32P – dCTP	1 µl
Klenow fragment	1 µl

The reaction was incubated at room temperature for 30 minutes; then stopped by adding TE (10 mM Tris-HCl (pH 8.0), 1 mM EDTA) up to 50 µl. Oligos were purified through Amersham spin columns-G50. First the columns were spun at 800 x g for 1 minute to dry them, the labelling reaction was then added and the columns recentrifuged at 800 x g for 2 minutes. The eluted oligos were checked using a Geiger counter to verify counts per second (CPS), which were expected to be in the range of 200 – 300.

Gel Preparation (2)

The gel was set up with 0.5 x TBE (0.44 M Tris-borate, 0.44M Boric acid, 12 mM EDTA) and pre-run at 200 V, 4 °C for 30 minutes prior to addition of samples. During this period the samples were incubated with the hot oligos in the binding reaction described below.

Binding reaction:

3 µl purified oligo

5 µl sample = 1 µg

8 µl 2 x binding buffer

[2 x binding buffer: 50 µl polydI:dC (1µg/µl)
200 µl 4 x buffer
100 µl glycerol
50 µl water

4 x buffer	40 mM HEPES
	4 mM EDTA/ 4 mM EGTA]

This reaction was incubated at room temperature for 10 minutes and then loaded onto the gel. A total of 4.66 µg of nuclear protein was added to each well, at a concentration of 0.233 µg/µl. The running dye was in column 1 and the test samples were placed in the subsequent columns. None of the test samples were loaded with dye due to different refraction coefficients of glycerol and water and consequently could not be visualised. The samples were added at 4 °C and then run for approximately 2 hrs at 200 V. The position of the running dye was monitored and used to indicate the position of the test samples on the gel to determine when the gel run had completed. On completion of the run, the gel was removed and dried at 80°C for 1 hour, then put under film for several hours and exposed.

Translational shut-off experiment

BHK cells were seeded in 24-well plates at $1x10^5$ cells per well; at 90 % confluence the cells were infected at a moi of 10 with pSFV10b12A-NP or pSFV10RDRb12A-NP. At each of the following time-points post-infection 2, 2.5, 3, 3.5, 4, 4.5 and 5 hours, a well was starved of methionine and then incubated with ^{35}S labelled methionine as follows: Media was removed and the monolayers washed with PBS. 500 µl of starvation media (Methionine-free medium (MP Biomedicals), P/S, Hepes (Gibco) and L-Glutamine) was incubated with the cells for 10 minutes at 37°C. This was removed and replaced with 90 µl of pulse media (10 µl ^{35}S-methionine (Redivue L-^{35}S-methionine, >1000 Ci/mmol (#AG1094, Amersham Biosciences) per ml in starvation medium) for 10 minutes at 37°C. The pulse media was removed and the cells washed with PBS; to collect the cells, monolayers were incubated on ice with 300 µl lysis buffer (Tris-HCl (pH 7.6) containing 1 % NP-40, 150 mM NaCl, 2 mM EDTA (and protease inhibitors)) for 5 minutes. The lysate was collected and spun for 5 minutes at 6000 rpm at 4°C. The lysates were then analysed on an SDS-PAGE gel.

Statistical Analysis

All statistical analysis was carried out using Microsoft excel and Prism. Viral titre, qPCR and CPERA data were analysed with the non-parametric Mann-Whitney and Kruskal Wallis tests.

Chapter 3: Development of assays to quantify IFN

Contents

Objectives....81
Development of assays to quantify IFN....81
Quantitative (q) PCR....81
RNA Extraction....81
RNA Quantification....82
Quantification of cDNA by qPCR....83
Validation of qPCR....84
Specificity and Sensitivity of qPCR....84
Normalisation....88
Assessment of Variation....89
Cytopathic Effect Reduction Assay....92
Assessment of Variation....93
Discussion....98
Summary....100

Objectives

1) Develop a quantitative PCR assay to determine levels of viral RNA species and IFN-β and IFN-α transcripts in an infected sample.
2) Develop a quantitative bioassay to determine functional IFN levels in an infected sample.

Development of assays to quantify IFN

Quantitative PCR and the cytopathic effect reduction assay (CPERA) were developed as a means to establish levels of IFN gene expression and protein activities. Transcript copies of IFN-β and IFN-α were compared to copies of virus RNA to determine the amount of IFN gene transcription induced per unit of virus RNA. The CPERA quantified functional IFN by determining the dilution that induced an anti-viral state, determined by protection of L-929 cells from a set amount of cytopathic virus.

Quantitative (q) PCR

Transcript analysis of mRNA was a four step process; (i) RNA was extracted from infected cells or tissues, (ii) it was quantified and its quality assessed, (iii) the RNA was reverse transcribed into cDNA and (iv) the cDNA was quantified by qPCR.

RNA Extraction

Adherent cell monolayers were collected and immediately snap frozen on dry ice to reduce exposure to RNases. Each sample was initially handled individually to minimise RNase degradation. RNA was extracted from cell monolayers using the RNeasy kit (Qiagen) according to the manufacturer's instructions. Briefly, samples were triturated with RLT buffer containing β-mercaptoethanol to inactivate RNases. The homogenate was mixed with 70 % ethanol to precipitate nucleic acids and purified through a Qiagen mini column, where it was also DNase treated to remove contaminating DNA. The RNA was eluted from the column with RNase-free water and immediately frozen. Mouse brain samples were handled slightly differently due to the high lipid content of the brain. Only 40 mg of brain were used, to prevent

blockage of the spin column membrane. RNA was extracted from the brain using an RNA lipid kit (Qiagen). Briefly, the brain was homogenised in QIAzol lysis reagent and then mixed with chloroform. This suspension was centrifuged and the upper aqueous phase removed and mixed with 70 % ethanol to precipitate nucleic acids. Following precipitation, RNA purification and elution was carried out as described above.

RNA Quantification

The quality and quantity of RNA was assessed using Agilent technology. For qPCR, the quality of the RNA needs to be high. This microchip technology, RNA 6000 Nano assay, runs 12 samples of RNA against a quantified standard on a micro gel. The number of RNA bands in each sample is indicative of the quality of the RNA. An ideal sample produces two visible bands, representing the 18 S and 28 S ribosomal RNA species (Figure 3A (ii)); these comprise 95 % of the total RNA. Samples of poorer quality produce many bands. A completely degraded sample produces a smear down the gel. The Agilent software generates a graphical representation of the RNA species in each sample; the quantity of RNA is determined by integrating the area under the curve. A typical yield of RNA from cultured cells grown in a T20 flask, approximately $2 - 5 \times 10^6$ cells, is 30 μg. For each RNA sample to be analysed by qPCR, 2 or 5 μg RNA (tissue culture or brain samples, respectively) were reverse transcribed into cDNA using separate reactions with oligo-dT primers.

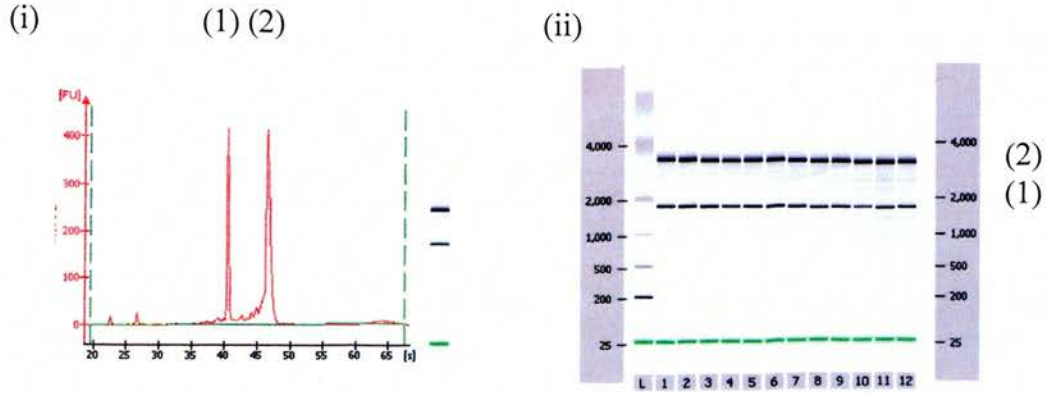

Figure 3A: Quality and quantity assessment of RNA.
RNA was extracted from tissues or cell monolayers, 1 µl of each sample was run on an Agilent microchip and compared to a pre-quantified RNA ladder. (**i**) A typical sample electrogram, the two major peaks represent the (1) 18 S and (2) 28 S ribosomal RNA species. The y-axis indicates the level of fluorescence and the x-axis the time in seconds. The amount of RNA present in a sample is calculated from the area under the curve. (**ii**) The gel bands give an indication of RNA degradation, the ladder bands are shown in the first column marked L. The numbered columns (1 – 12) are test samples; these all show two main bands, which are equivalent to the two peaks on the graph and represent the ribosomal RNA species. The numbers along the length of the gel indicate the size of the bands (bp).

Quantification of cDNA by qPCR

Two µl of a 1:100 dilution of each cDNA sample to be tested for SFV transcripts and 2 µl of a 1:10 dilution of each cDNA sample to be tested for IFN-β, IFN-α, β-actin and GAPDH transcripts were assayed as standard. Samples were diluted to reduce the concentration of the cDNA, which if too concentrated can inhibit the qPCR reaction. To allow quantification, a 10-fold serial dilution of a pre-quantified standard was run in each assay. Each dilution produces a sigmoid curve, where the fluorescence emitted from the dsDNA-bound SYBR green is plotted against PCR cycle number. As the PCR cycle number increases, the number of amplicons increases and so the emitted fluorescence is higher. After several PCR cycles, all dilutions of standard can be detected. A threshold is determined to create a standard curve; the point at which the dilutions cross the threshold gives their C_t values. Plotting the C_t against the logarithm of the copy number corresponding to that C_t should, using linear regression analysis, produce an R^2 value of 1. Using this standard curve, the C_t values of the test samples can be transformed into transcript copy numbers. Figure 3Bi (b) depicts a 10-fold serial dilution of standard; the line on the graph represents the threshold.

An important factor regarding quantification of cellular transcripts or viral RNA is the efficiency of the qPCR. In an optimal PCR reaction the number of amplicons would be expected to double after each elongation step in the PCR; this equates to 100 % efficiency. QPCR efficiency can be affected by several factors, including annealing temperature, primer specificity, primer dimer formation, NTP concentration and magnesium levels. Indications of efficiency are the gradient and regression co-efficient of the standard curve. Under ideal conditions the standard curve has an R^2 value of 0.98 and a gradient of –3.3 (Nolan, 2004). At the time when this work was carried out greater emphasis was given to the R^2 value. In all experiments presented in this thesis the R^2 value exceeded 0.98. Greater emphasis is now given to the gradient of the standard curve as a better indicator of efficiency. From analysis of the gradient, all of the experiments presented in this thesis have an efficiency of > 90 %, which is the minimal efficiency cut-off value recommended within the Laboratory of Clinical and Molecular Virology, University of Edinburgh. However, the IFN-β qPCR data experiments had an efficiency of >100 %, all of the efficiencies of these experiments are within 10 %. This increase in efficiency was not associated with the normal factors related to high efficiency e.g. non-specific products and primer dimer as demonstrated by the single phase melt curve.

Validation of qPCR

For a qPCR assay to be valid, it must be specific and sensitive. Quantitative PCR is particularly powerful as an assay as it is known to be quantitative over a large dynamic range and can differentiate between sub-types of the same gene e.g. IFN-α, with appropriate primers under optimal conditions.

Specificity and Sensitivity of qPCR

To determine the specificity and sensitivity of the qPCR, levels of five transcripts were investigated: SFV RNA species (genomic and sub-genomic), IFN-β, IFN-α, β-actin and GAPDH. To detect each transcript a set of PCR primers was developed. The specificity of the primer pair was determined by a melt curve and BLAST analysis and the sensitivity by analysis of a ten-fold serial dilution of a pre-quantified standard. The latter enabled limits of detection to be set for each gene transcript assayed and demonstrates the dynamic range for each primer pair (Figure 3B (b)).

DNA plasmids were used as standards for SFV and IFN-β transcript analysis and PCR products were used as standards for IFN-α, β-actin and GAPDH transcripts. The plasmids and PCR products were quantified by spectrometry. The primers used are listed in table 2D (Materials & Methods). The melt curves and the qPCR amplification curves generated by the serial dilutions are shown in figure 3B.

Each melt curve (Figure 3B (a)) for the five primers produced a single peak; this indicates that a PCR product of one size was produced from each primer pair. No peaks at lower temperatures were produced, demonstrating that primer dimer was not an issue for any of the sets of primers. During the design process for each set of primers, a BLAST analysis was performed. This tests the primer sequence against all known mouse gene sequences. None of the primers cross-matched with other mouse genes and so are assumed to be specific for the gene of interest. The range of sensitivity varied for each primer pair; for example SFV species could be quantified between 10^2 and 10^8 copies, the IFN-β primers were less sensitive and could quantify samples in the range of 10^3 and 10^6 copies. All of the standard curves generated were analysed with linear regression and produced an R^2 value of 0.99. No subsequent extrapolation of the curve was required to quantify any of the experiment samples.

(i) a

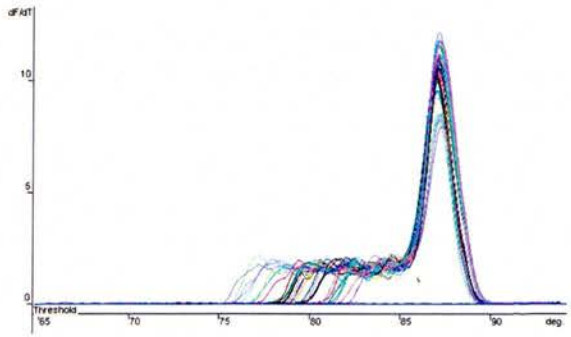

(i) b

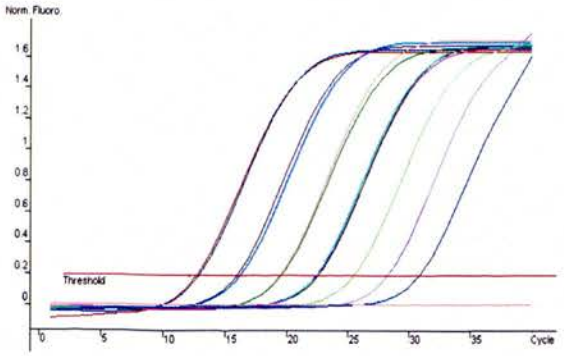

(ii) a

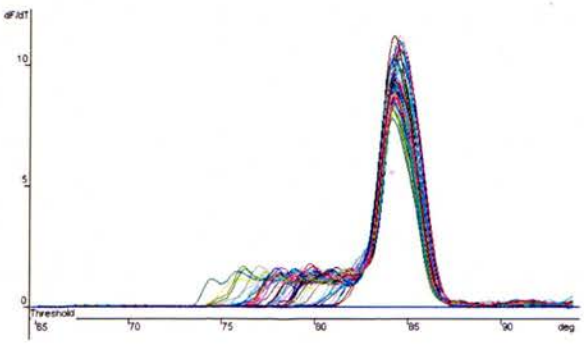

(ii) b

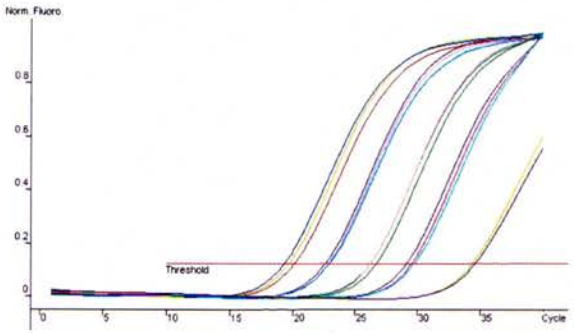

(iii) a

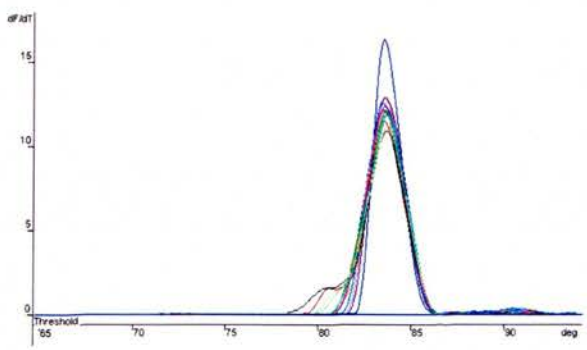

(iii) b

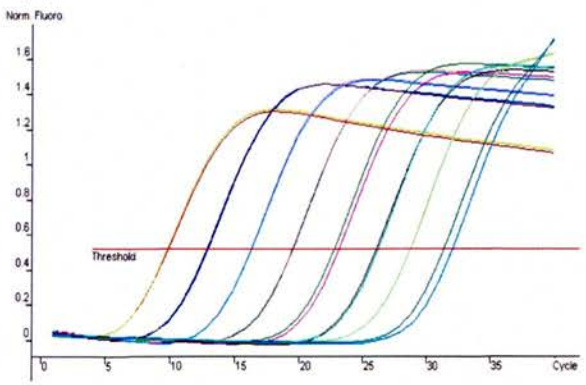

(iv) a

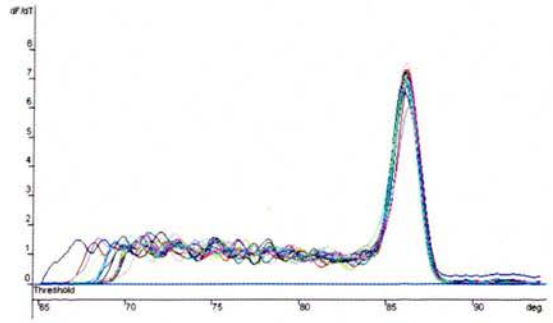

(iv) b

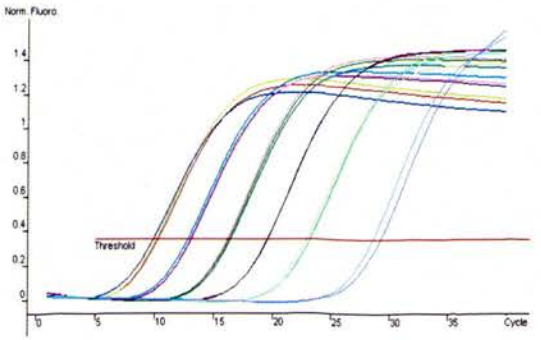

(v) a

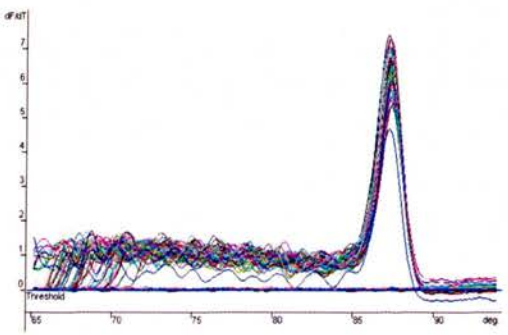

(v) b

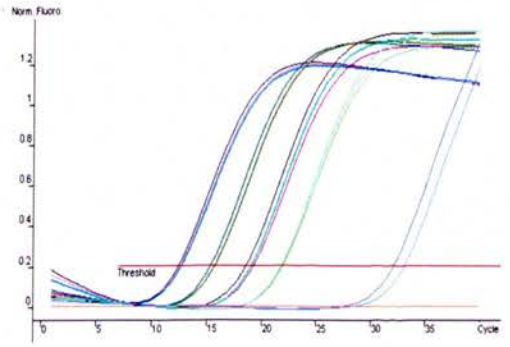

Figure 3B. The specificity and sensitivity of the primers

Ten-fold serial dilutions of pre-quantified standards for each gene of interest were assayed by qPCR. Melt curves were produced for each primer set; these demonstrated the range of product sizes generated by each primer pair. The 10-fold dilution series indicates the range of sensitivity of each qPCR. The y-axes are arbitrary fluorescence measurements; the x-axes represent degrees of temperature and cycle number for the melt curve and serial dilution respectively. (**i**) SFV E1 primers show the levels of viral genomic and sub-genomic species (a) melt curve, (b) 10-fold serial dilution of pSFV4 (pre-quantified standard can be detected from $10^2 - 10^8$ copies of virus RNA). (**ii**) IFN-β primers (a) melt curve, (b) 10-fold serial dilution of pSFV-IFNb (pre-quantified standard can be detected from $10^3 - 10^6$ copies of IFN-β transcript). (**iii**) IFN-α primers (a) melt curve, (b) 10-fold serial dilution of IFN-α PCR product (pre-quantified standard can be detected from $10^1 - 10^7$ copies of IFN-α transcript). (**iv**) β-actin primers (a) melt curve, (b) 10-fold serial dilution of β-actin PCR product (pre-quantified standard can be detected from $10^2 - 10^6$ copies of β-actin transcript). (**v**) GAPDH primers (a) melt curve, (b) 10-fold serial dilution of GAPDH PCR product (pre-quantified standard can be detected from $10^3 - 10^6$ copies of GAPDH transcript).

Normalisation

Standard practise when using qPCR would be to normalise to a housekeeping gene such as β-actin or GAPDH. This is based on the concept that these genes are expressed at the same level across the same cell type under the same conditions. However, this may not be the case in virally infected cells where infection often affects cellular transcription. To investigate the feasibility of normalisation using β-actin and GAPDH, transcript levels for these genes were determined over a 12-hour period (Figure 3C (i; ii). In two primary cell cultures, β-actin transcript levels at 8 and 12 hours post-infection were significantly reduced relative to mock-infected cells and infected cells at 4 hours post-infection ($p < 0.05$, Mann-Whitney). Each time point was significantly different to mock-infected cells ($p < 0.05$, Kruskall Wallis test). A significant decrease in GAPDH transcript levels was also observed between mock-infected cells and SFV4 infected cells sampled at 12 hours post-infection ($p < 0.05$, Mann-Whitney) (Figure 3C (iii)). These three sets of data indicate that housekeeping genes were affected during SFV infection precluding their use for normalisation. This was not unexpected as IFN induces anti-viral gene expression, including RNase-L and ADAR-1, which both induce degradation of cellular and viral transcripts (Samuel, 2001).

An alternative method for normalisation is to quantify the amount of ribosomal or total RNA. The majority of total RNA is ribosomal and should not vary with virus infection. This can be achieved by PCR assay using 18S rRNA primers or by direct quantification of the total RNA prior to qPCR. It was decided to quantify the total RNA using the Agilent mini gel system. Total RNA was quantified prior to qPCR and all transcripts assayed were normalised to 1 μg RNA.

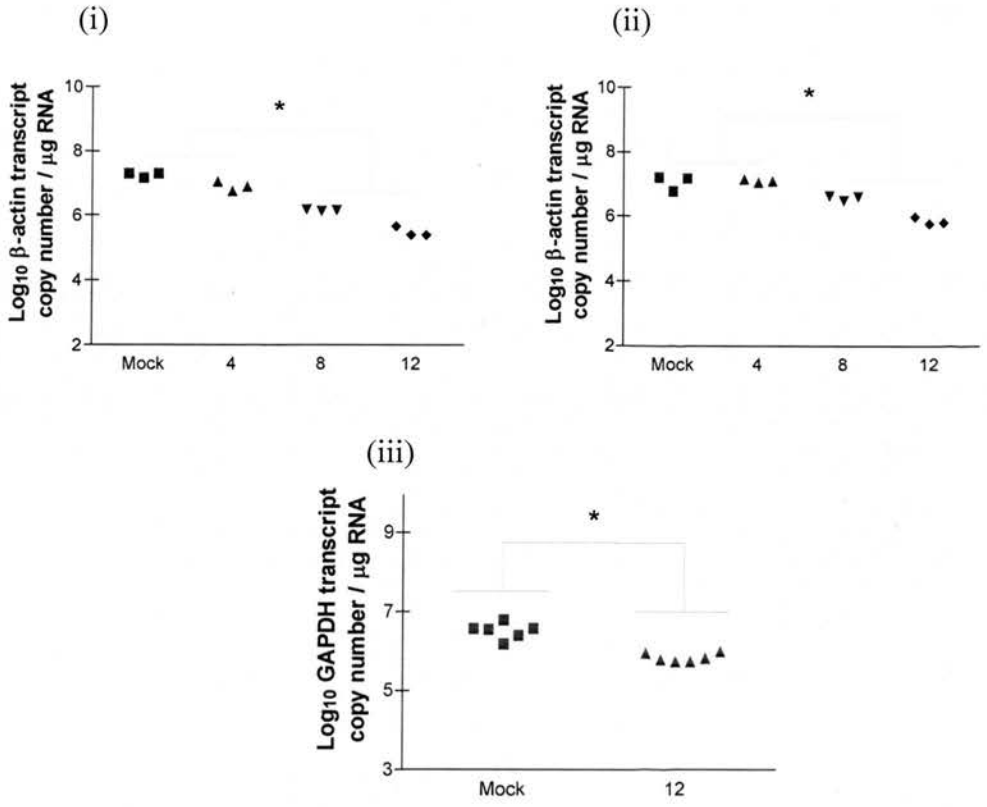

Figure 3C: β-actin and GAPDH down regulation during SFV infection of Mouse Embryo Fibroblasts.
Two cultures of primary cells (**i**) and (**ii**) were infected with a high moi SFV4; cell cultures were harvested at 4, 8 and 12 hours post-infection. The data was grouped as indicated to enable Mann-Whitney analysis and the two groups compared for levels of β-actin transcripts. (**iii**) Cells were infected with a high moi of SFV4 or mock infected with PBS, at 12 hours post-infection the cell cultures were harvested and assayed in triplicate for GAPDH transcripts by qPCR. Each point represents an individual cell culture, which was assayed in triplicate by qPCR; * indicates a significant difference ($p < 0.05$, Mann-Whitney). The x-axis crosses the y-axis at the limit of detection of the assay.

Assessment of Variation

Quantification of total RNA using the Agilent bioanalyser, does not directly quantify mRNA levels since quantification is based on the size of the peaks produced by the 18 S and 28 S ribosomal RNA species. It has been observed that the levels of mRNA within an RNA sample when normalised to total RNA can vary by up to 7 % (Solanas et al., 2001).

To investigate the variability of the qPCR in virus infected cells, two transcripts, SFV and IFN-β, were selected for detailed analysis. RNA isolated from SFV4 infected cells was quantified on the Agilent bioanalyser and 2 µg was added to each of five separate RT-PCR reactions. The cDNA generated from each reaction was quantified

in triplicate by qPCR and is presented in tables 3A and 3B. The number of viral copies or IFN-β transcripts per μg was calculated (second column), and used to determine the mean, standard deviation and from these the coefficient of variance (VAR) for each sample. The coefficient of variance demonstrates the percentage variation of the mean.

			Variation in qPCR					
Sample	SFV Transcripts	Copies / μg RNA	Mean	SD	VAR	Log 10	Mean	SD
SFV 1a	288,622,686	1.44E+11	1.11E+11	2.93E+10	0.26	11.16	11.03	0.108
b	188,680,818	9.43E+10				10.97		
c	185,887,618	9.29E+10				10.97		
SFV 2a	110,292,346	5.51E+10	6.81E+10	1.13E+10	0.17	10.74	10.83	0.076
b	151,987,220	7.60E+10				10.88		
c	146,424,534	7.32E+10				10.86		
SFV 3a	162,537,984	8.13E+10	8.42E+10	4.09E+09	0.05	10.91	10.93	0.021
b	177,753,679	8.89E+10				10.95		
c	164,980,326	8.25E+10				10.92		
SFV 4a	153,124,864	7.66E+10	6.12E+10	1.33E+10	0.22	10.88	10.78	0.090
b	109,472,927	5.47E+10				10.74		
c	104,682,688	5.23E+10				10.72		
SFV 5a	223,983,778	1.12E+11	1.10E+11	2.83E+09	0.03	11.05	11.04	0.011
b	223,983,778	1.12E+11				11.05		
c	214,182,853	1.07E+11				11.03		
		Mean	8.69E+10					
Variation in RT-PCR		SD	2.50E+10					
		VAR	0.27					

Table 3A: SFV transcripts quantified from the same RNA sample
The table demonstrates the amount of variation intrinsic to the SFV qPCR assay; one RNA sample was reversed transcribed in five separate reactions, the cDNA generated from each reaction was then quantified in triplicate by qPCR. The mean and standard deviation were calculated and from these the coefficient of variation (VAR) was determined. VAR is indicative of the percentage variation about the mean.

			Variation in qPCR					
Sample	IFN-β transcripts	Copies / μg RNA	Mean	SD	VAR	Log 10	Mean	SD
IFN 1a	37768	1888400	2028117	121891	0.06	6.28	6.31	0.027
b	41665	2083250				6.32		
c	42254	2112700				6.32		
IFN 2a	39948	1997400	2102350	169756	0.08	6.30	6.32	0.034
b	45964	2298200				6.36		
c	40229	2011450				6.30		
IFN 3a	29754	1487700	1494783	177931	0.12	6.17	6.17	0.052
b	33523	1676150				6.22		
c	26410	1320500				6.12		
IFN 4a	34477	1723850	1470700	351088	0.24	6.24	6.16	0.113
b	21398	1069900				6.03		
c	32367	1618350				6.21		
IFN 5a	25321	1266050	1340267	67116	0.05	6.10	6.13	0.022
b	27161	1358050				6.13		
c	27934	1396700				6.15		
		Mean	1687243					
Variation in RT-PCR		SD	366908.1					
		VAR	0.22					

Table 3B: IFN-β transcripts quantified from the same RNA sample
The table demonstrates the amount of variation intrinsic to the IFN-β qPCR assay; one RNA sample was reversed transcribed in five separate reactions, the cDNA generated from each reaction was quantified in triplicate by qPCR. The mean and standard deviation were calculated and from these the coefficient of variation (VAR) was determined. VAR is indicative of the percentage variation about the mean.

The complete qPCR assay consists of two main stages, RT-PCR and qPCR; it would be expected that most of the variation would be introduced at these stages. Tables 3A and 3B demonstrate this variation. Each of the triplicate repeats (SFV 1 – 5 (a, b, c) or IFN-β 1 – 5 (a, b, c)) indicates the variation in the final qPCR stage. The variation within the triplicate repeats never exceeds 2-fold. Considering the dynamic range of the assay (> 1,000,000) this 2-fold difference is inconsequential. However, differences of less than 2-fold need to be interpreted with caution. Given the large dynamic range of the assay, data of this type is often expressed logarithmically (Table 3A and 3B). Taking the mean of the triplicate repeats (Column 4) indicates the average viral RNA or IFN-β transcript copy per μg total RNA generated from each RT-PCR (SFV 1 – 5). Comparing these values demonstrates the variation within the RT-PCR stage. Again the difference between the means never exceeds 2-fold. The range of the triplicates and means is shown in figure 3D. Most biological systems

demonstrate a large variation with a normal distribution. Given the small sample size, no conclusion about the distribution of the data can be made, whereas the data would be expected to have a normal distribution this cannot be assumed and all the PCR results in this thesis have been analysed with a non-parametric test, Mann-Whitney ($p < 0.05$). Due to the requirements of this test some of the data has been grouped, where data has been grouped, this is indicated in the figures. Where Mann-Whitney was inappropriate data was compared with Kruskall Wallis analysis.

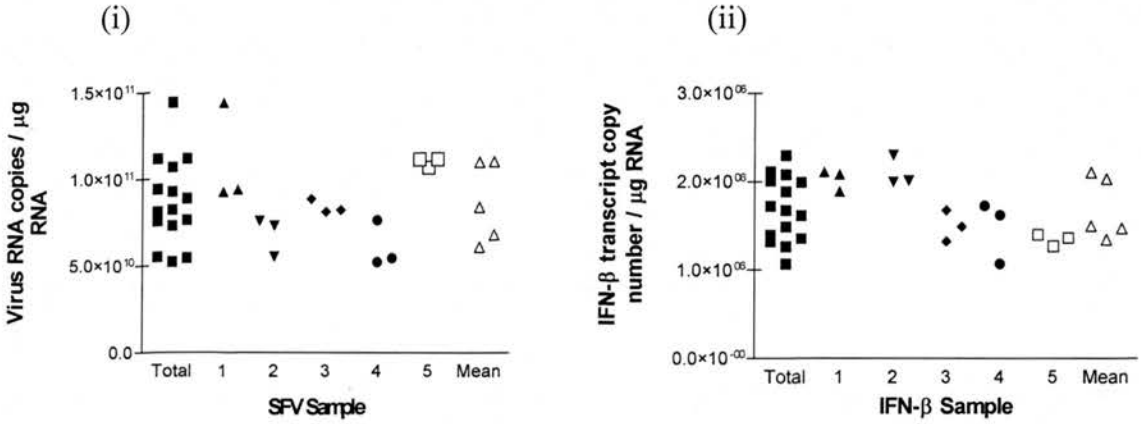

Figure 3D: The range of data from the qPCR assay.
RNA from a single infected cell culture was reverse transcribed into cDNA in five separate reactions (1 – 5); each of these cDNAs was quantified in triplicate by qPCR. The scatter plots indicate the range of the data for (**i**) SFV transcripts, (**ii**) IFN-β transcripts; the total range of data is indicated in the first column (Total), the three values for the samples labelled 1 – 5 represent the triplicate qPCR repeats of the cDNA from each RT-PCR. In the 'Mean' column, the points represent the mean values of viral RNA or IFN-β transcripts for each RT-PCR.

Cytopathic Effect Reduction Assay – Interferon Bioassay

The cytopathic effect reduction assay (CPERA) is a standard cell-based assay used to assess the total IFN content of a sample. Samples of supernatant taken from virus infected cells are incubated on a monolayer of L-929 mouse fibroblasts for 24 hours. Any IFN in the sample stimulates the L-929 cells anti-viral response so that upon subsequent virus challenge (with encephalomyocarditis virus, EMCV) the cells are protected from death. After virus challenge the viability of the cells is assessed (using the WST-1 cell viability reagent). For each sample, a two-fold dilution series was assayed. The amount of IFN was determined by comparison to a standard curve run

in the same assay. The standard curve was produced from a two-fold serial dilution of a laboratory standard. The amount of type I IFN in this laboratory standard was quantified using an International Reference Standard for murine total IFN (NIAID).

Assessment of Variation

To assess the level of variation within the CPERA three replicate plates, each containing 11 two-fold dilution series of the laboratory standard were assessed in each of two separate but identical experiments A and B (run on separate days). For each experiment, the reciprocal dilution of laboratory standard IFN correlating with 50 % cell death was determined for each of the 11 serial dilutions on each of the 3 plates. The inter-experiment, inter-plate and intra-plate variations were then determined. The variation in the absorbance readings of the serial dilutions generated from laboratory standard IFN from the two experiments is shown in figure 3E (i). The optical density:dilution curves generated in experiment A (blue) clearly localise differently to the optical density:dilution curves generated in experiment B (red). Box-whisker representation of the data demonstrates the difference between the ranges of values (Figure 3E (ii)). Using Mann-Whitney test the average 50 % cell death end point produced in the two experiments (run on different days) were significantly different with a p value of < 0.05. For many bioassays day to day variation is an important variable. To deal with this, assays are conventionally normalised by running a standard or a series on standards to create a standard curve on each assay. Laboratory standard IFN quantified by comparison to international reference standard IFN was used to normalise between experiments.

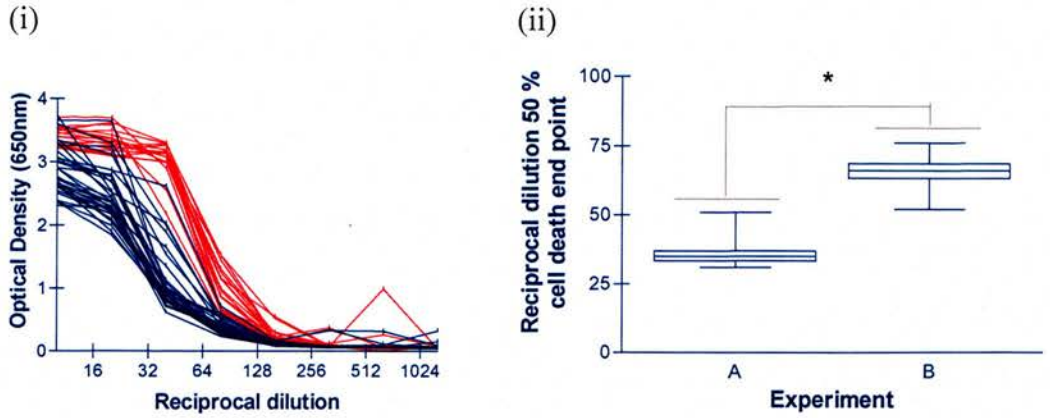

Figure 3E: The range of the serial dilutions and 50 % end points produced from laboratory standard IFN run in two experiments.
(**i**) Serial dilutions of laboratory standard run 33 times in two experiments, experiment A – blue, experiment B – red. (**ii**) Box whisker plots indicate range of the 50 % cell death end points for each experiment; * indicates a significant difference of $p < 0.05$, Mann-Whitney.

The optical density:dilution curves from the 3 different plates run in parallel within the same experiment are shown in figure 3F (i) and 3F (ii). The curves from different plates overlap each other and have a smaller range of 50 % end points in comparison to experiments A and B. In figure 3F (iii) the data is depicted in box-whisker format. The medians of the 50 % cell death end points of the two experiments were different (Figure 3E (ii)), whereas the medians of the 50 % cell death end points from different plates in the same experiment were similar (Figure 3F (iii)). To ascertain if samples run at the same time but on different plates could be analysed together, sample and population variance was determined by ANOVA. Although the distribution of the data is unknown, ANOVA is a strong statistical analysis and can withstand slight deviations from normal distribution. ANOVA assesses the likelihood of several samples being from the same population by determining whether the variance within samples is comparable to the variation within the population. The significance of ANOVA analysis is determined by calculating the F value and comparing this to the F distribution chart. All 3 plates assessed in the same experiment produced low F values, so they were not within the critical region of the F distribution and hence were not significantly different from each other. Consequentially, data obtained from different plates run at the same time can be analysed together without normalisation. However, serial dilutions of standard were assayed with each plate to further reduce the variation.

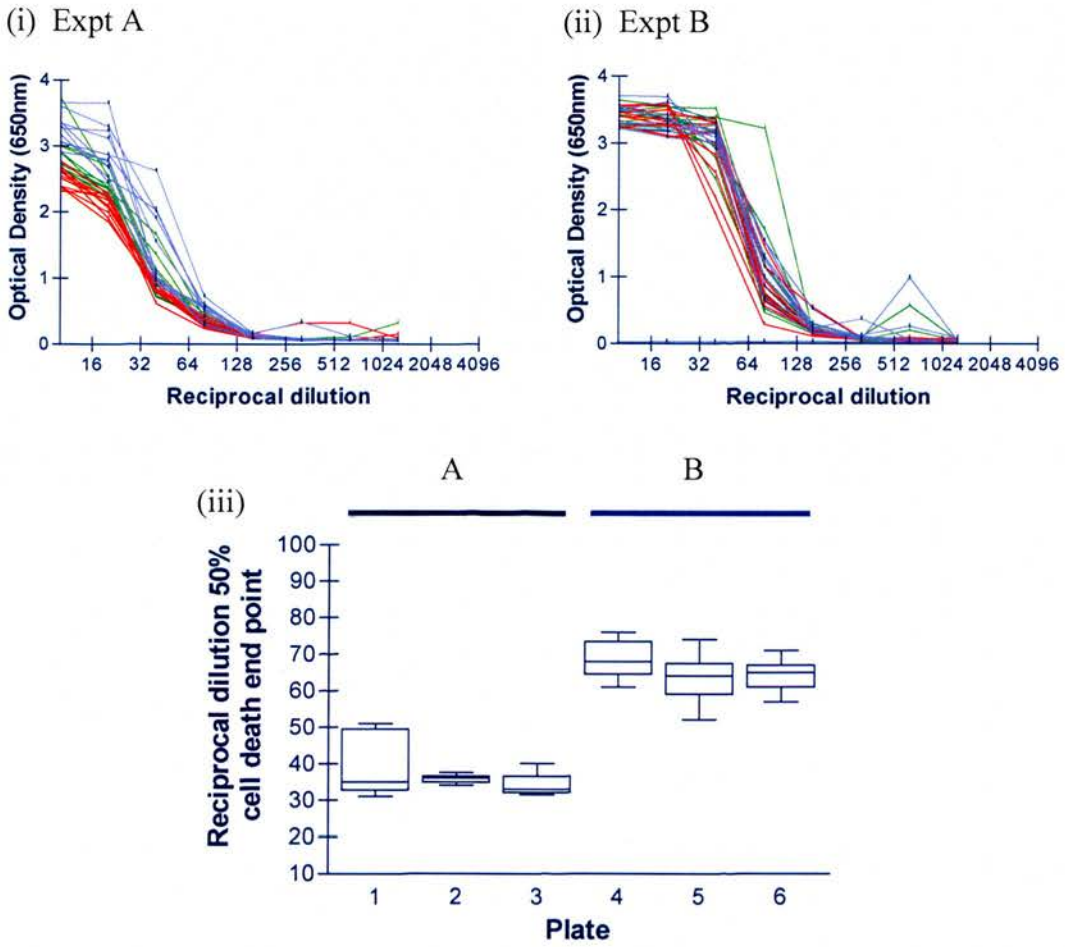

Figure 3F: Comparison of serial dilutions (i) and (ii) and median 50 % cell death end point values (iii) of the 3 plates assessed per experiment.
Laboratory IFN standard was run 11 times per plate and 3 plates were run per experiment. Samples run in a single plate, experiment A (**i**) and experiment B (**ii**) are represented by the same colour. Individual plate medians and data ranges (1 – 3, experiment A; 4 – 6, experiment B) are displayed as box whisker plots (**iii**). The central horizontal bar represents the median value of the 50 % cell death end point for each plate; data within the box equates to data within the inter-quartile range, the whiskers indicate the total range of the data.

The range of dilution curves within each plate is shown in figure 3G; the variation between the dilution curves in each plate is quite narrow. This demonstrates the reproducibility of the assay within a plate. From these figures the 50 % end point of each dilution curve was determined and is shown in table 3C. The range of the data from table 3C is shown in figure 3H (See also figure 3E (ii)).

Experiment A

(i) (a)

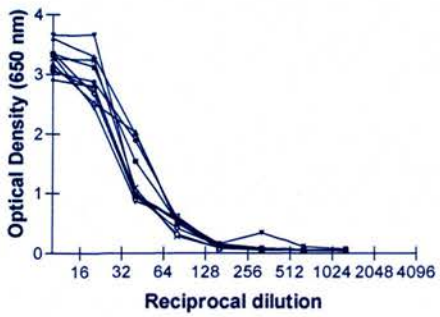

(i) (b)

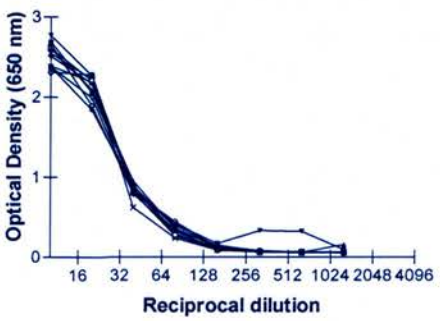

(i) (c)

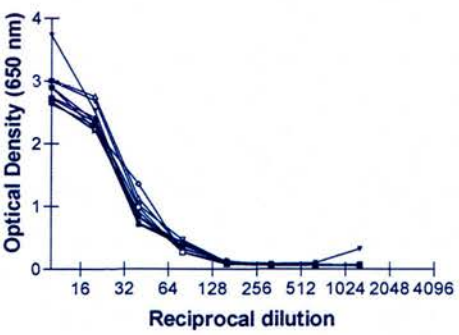

Experiment B

(ii) (a)

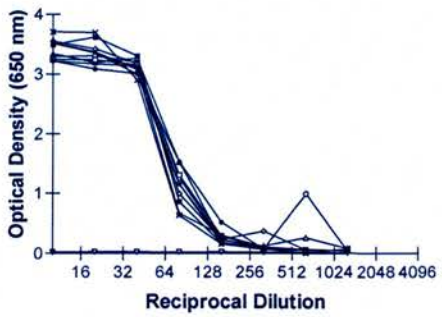

(ii) (b)

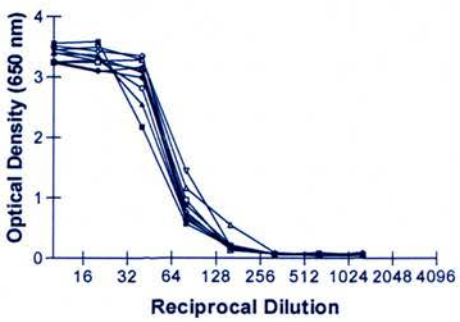

(ii) (c)

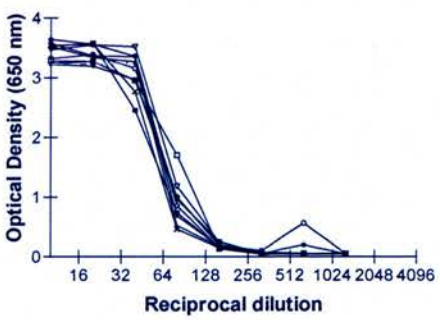

Figure 3G: Assessment of intra-plate variation of two-fold serial dilutions of laboratory standard IFN.

Two-fold serial dilutions of laboratory standard IFN were run 11 times in each plate. (**i**) - (a), (b) and (c) represent the 3 plates run in experiment A, (**ii**) - (a), (b) and (c) represent the 3 plates run in experiment B.

	50% End Point (Reciprocal Dilution)					
	Experiment A			Experiment B		
Plate	1	2	3	4	5	6
	31	34	32	61	46	57
	32	35	32	63	52	59
	34	35	32	66	58	63
	34	35	33	67	60	65
	35	35	33	68	63	65
	35	36	33	68	64	66
	39	36	34	71	64	67
	49	36	36	71	66	67
	50	36	37	76	66	71
	51	37	40	76	69	80
	62	38	49		74	

Table 3C: 50 % cell death end point values for laboratory standard IFN run on 6 plates.
Laboratory standard IFN was run 11 times per plate in a two-fold serial dilution, the 50 % cell death end points were determined for each run.

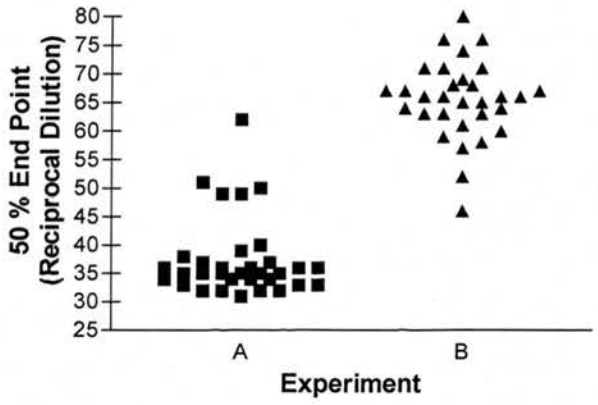

Figure 3H: Distribution of 50 % end points
The 50 % end points of experiment A and B were plotted to determine their distribution dynamics.

The 50 % end points generated during Experiment B demonstrate a normal distribution, however, the 50 % end points generated during Experiment A demonstrate a heavily skewed distribution pattern. As a consequence of the different

distributions of the two experiments no assumptions were made about the data and so it was decided to analyse results by the non-parametric Mann-Whitney test ($p < 0.05$).

Discussion

Two assays were developed to quantify type I IFN at the transcript and functional protein level. The variation within each assay was assessed. Assessment of standards suggested that both assays should be analysed with non-parametric assays i.e. Mann-Whitney analysis.

Quantitative PCR is a well-developed research tool; it has a huge dynamic range and the ability to rapidly analyse many samples and all mRNA species. However, normalisation needs to be established for each experimental model. The variability of qPCR is closely tied to the efficiency of polymerisation at both the RT step and the qPCR step. Several factors are known to affect amplification efficiency including low template copy numbers, RT-PCR primers and qPCR primers. Low template copy numbers adversely affect the efficiency of RT-PCR; all of the mRNA species investigated in this assay are likely to be relatively numerous in virus infected cells. Oligo-dT primers were used to prime the RT-PCR reaction. Oligo-dT is more specific for mRNA than random primers and generates a more reliable cDNA representation of the original mRNA population. However, good quality mRNA is a pre-requisite for oligo-dT priming as full length mRNA is required. All of the RNA samples used were assessed on the Agilent bioanalyser and any poor quality samples were discarded. Other considerations when using oligo-dT primers were the position of the upstream primers and the secondary structure of the transcript; the RT-PCR may fall short of the upstream qPCR primers, particularly if the transcript forms multiple secondary structures. These are clearly not major issues in this analysis as all of the transcripts investigated were reproducibly detected.

A primary consideration in qPCR primer design, with regard to amplification efficiency, was minimal annealing between primer pairs. Amplicons were detected by SYBR green fluorescence, which non-specifically binds to dsDNA; therefore specificity of the primers was paramount. Non-specific binding to template or to

other primers would have led to false positives and primer dimer formation would have severely diminished the amplification efficiency. These effects are indicated in the melt curve analysis for each primer pair; as only a single peak was observed in the melt curve for each primer pair, no primer dimer formed and only a single product size was amplified suggesting that the primers were specific to a single locus.

Normalisation is necessary to account for the variation of amplification efficiencies between reactions and differences between samples. However, given virus infection, target gene transcripts could not be normalised to housekeeping genes, as the expression of β-actin and GAPDH was significantly reduced compared to mock infected cells by 12 hours post-infection. Bustin et al., (2005) reviewed the most plausible methods for normalisation in any system and recommended normalising against total RNA mass, providing that the RNA sample was of high quality and accurately measured. This method of normalisation was applied to all of the qPCR experiments. It was also noted that for the assessment of cytokines, only when the data was normalised to rRNA were the results biologically relevant (Bas et al., 2004).

The CPERA was found to have a range of variation from 3 – 20 %. This variation could have arisen at any of the multiple stages; differences in the number of L-929 cells seeded per well, day-to-day differences in the incubator environment, differences in the volume aspirated by each tip of the multi-channel pipette whilst generating the two-fold dilution series, as well as differences in the number of challenge virions. Each of these aspects was controlled as tightly as possible; cells were counted and single cell suspensions produced to ensure an even distribution of cells within the seeding suspension, the same incubator was used for each experiment, the multi channel pipette was observed constantly to maintain comparable levels of aspirate and the titre of the challenge virus was checked regularly. When all of the standard curves were analysed for variation at each point of the dilution series, the variation increased down the plate. This was expected since the distance between two points doubles as the dilution series is extended, thereby increasing the potential error. This effect emphasizes the need for consideration of the practical limitations of the assay whilst interpreting the results.

For experimental analysis, ANOVA indicated that plates assessed on the same day could be directly compared; however, to further control variation between plates and to allow comparisons between experiments, duplicate runs of IFN standard were included on each plate to enable normalisation. This same method was used to normalise between experiments. However to ensure minimal variation, in this thesis experimental comparisons were always run in the same CPERA.

Summary

The objectives of this chapter were to develop assays which would allow quantification of IFN-β and IFN-α transcripts as well as functional IFN. Quantitative RT-PCR for virus and IFN transcripts and an IFN bioassay were established, validated and the level of variation determined.

Chapter 4: Does SFV4 infection induce IFN expression in vitro and in the brains of adult and neonatal mice?

Contents

Objectives....102
Introduction....102
Does SFV4 induce IFN in mouse fibroblasts?....103
Does SFV4 induce type I IFN transcripts in adult mouse brains?....107
Does SFV4 induce type I IFN transcripts in neonatal mouse brains?....110
Do neonatal and adult mouse brains produce functional IFN in response to an SFV4 infection?....113
Is human interferon protective against SFV encephalitis?....113
Does Multiferon© protect adult mice against SFV L10 infection?....114
Discussion....117
Is IFN protective against an SFV infection?....120
Summary....122

Does SFV4 infection induce IFN expression *in vitro* and in the brains of adult and neonatal mice?

Objectives

1) Determine whether SFV4 induces type I IFN transcripts in mouse L929 fibroblasts.
2) Quantify type I IFN transcripts and functional IFN in the brains of SFV infected adult and neonatal mice.
3) Determine whether passive administration of IFN can protect adult mice against virulent SFV infection.

Introduction

In vitro in cell cultures, the L10 and A7 strains of Semliki Forest virus (SFV) are well-known inducers of type I IFN responses. Anti-IFN antibodies increase the SFV plaque size in infected L-cells and exacerbate SFV pathogenicity in mice (Fauconnier et al., 1969). Blood IFN levels correlate with SFV viraemia levels (Bradish et al., 1975) and IFN can be detected in blood, muscle and spleen samples of SFV infected mice (Smillie et al., 1973). Recently, IFN-α mRNA transcripts have been detected in the brains of SFV4 infected adult mice (McKimmie et al., 2005). An interesting aspect of SFV encephalitis is the age-dependent outcome of infection. Avirulent strains, such as A7(74), induce fulminant encephalitis in neonates and suckling mice infected at up to 12 days of age whereas infection after 14 days of age results in a restricted CNS infection (Fleming et al., 1977; Oliver et al., 1997). Virulent strains induce pan-encephalitis following *ip* inoculation regardless of age (Fazakerley et al., 1993). One possible explanation of age-dependent virulence would be an impaired ability of immature (post-natal) CNS cells to produce or respond to IFN. The literature suggests that there may be age-related differences in type I IFN responses to RNA viruses. Adult human peripheral blood mononuclear cells and cord blood mononuclear cells were compared in their abilities to induce IFN-α in response to a viral infection. Infection with either Sendai virus or Newcastle Disease virus (NDV) resulted in production of lower levels of IFN-α from cord blood cells in comparison to adult blood cells; the most dramatic difference was observed in NDV infection. The

number of IFN producing cells was quantified for both adults and neonates and found to be comparable, 1 %, suggesting that neonate mononuclear cells are impaired in their ability to produce IFN- α (Neustock et al., 1993). Coxsackie B1 virus also induces differential IFN levels in the tissues of mice of different ages (Heinenberg et al., 1964).

To assess IFN production in neonatal and adult mice infected with SFV, groups of adult and neonatal mice were inoculated with SFV4. SFV4 is a cloned virulent virus, which is readily engineered, making it a powerful system for genetic analysis of SFV. Given this tool for genetic analysis of virus it was decided to use SFV4 over SFV L10 and SFV A7(74) to determine adult and neonate mouse IFN levels, despite the history of literature. Since the IFN response to SFV4 had not previously been studied, cultured cells were infected with SFV4 to determine, if like L10 and A7(74), SFV4 induced IFN.

Does SFV4 induce IFN in mouse fibroblasts?

Continually cultured mouse L-929 fibroblasts were infected with SFV4 and analysed for IFN-β transcripts. L-929 cells were used as these are known to be IFN competent. Other cell lines commonly used in virology, such as Vero cells and baby hamster kidney (BHK) cells, have impaired IFN systems which makes them useful for viral growth and replication studies, but not for assessing IFN responses (Diaz et al., 1988).

To determine the level of IFN induced during an SFV4 infection, L-929 cells were infected at a multiplicity of infection (moi) of 10. The moi represents the average number of virus plaque forming units per cell when infecting a culture. Using the Poisson distribution, the fraction of cells infected with 0, 1 or more virus particles can be calculated. The moi required to infect 99 % of cells in a culture can also be calculated and is 4.6 plaque-forming units (pfu) per cell. To study the kinetics of IFN gene induction and IFN protein production ideally requires a single step infection, in which all of the cells are infected synchronously, and therefore a relatively high (> 4.6) moi. Monolayers of L-929 cells were infected with SFV4 at a moi of 10 for 1 hour at room temperature and then incubated in 5 % CO_2 at 35°C for 2, 3, 4 or 6

hours. Low volumes of inoculate were used to increase the efficiency of infection. At each of the specified time points, cells from three infected and one mock-infected (PBS alone) culture were collected. RNA was extracted, quantified on an Agilent bioanalyser and 5 μg was reverse transcribed into cDNA. Each sample was assessed for levels of SFV RNA and IFN-β transcripts by qPCR. No viral RNA or IFN-β was detected in the mock-infected controls (data not shown). Figure 4A (i) shows the copies of SFV RNA at 2, 3, 4 and 6 hours post-infection. A steady rise in SFV RNA occurs over time, approximately a ten-fold rise per hour. The levels of IFN-β transcripts over the 6-hour time course are indicated in figure 4A (ii); IFN-β transcripts could only be detected at 4 and 6 hours post-infection. At both time points the levels of IFN-β transcripts were equivalent. No direct correlation was observed between the levels of SFV RNA and IFN-β transcripts (Figure 4B), suggesting that IFN-β gene transcription was either on or off. Although virus RNA levels continued to increase (10-fold) between 4 and 6 hours, IFN-β transcripts did not increase over this time. This is consistent with synchronous infection of the majority of cells in the culture and for each cell a maximum level of IFN gene transcription which cannot be exceeded (Figure 4B). However, Figure 4B(ii) may also indicate that IFN-β transcription has been abolished after 4 hours post-infection and that the maintenance of transcripts at the same level at 6 hours post-infection is indicative of the stability of IFN-β mRNA.

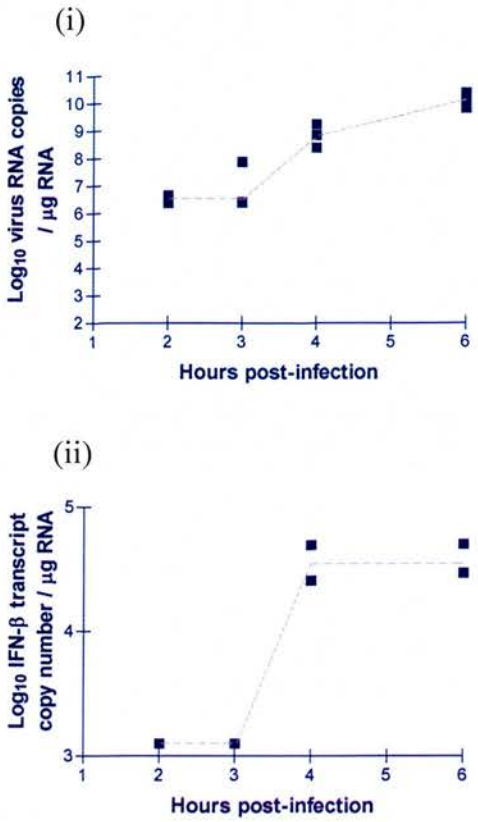

Figure 4A: Production of IFN-β transcripts in mouse L-cells following an SFV4 infection.

Mouse fibroblasts were infected with SFV4 at a moi of 10 and assayed for (**i**) SFV4 RNA and (**ii**) IFN-β transcripts at 2, 3, 4 and 6 hours post infection. The y-axis for each figure commences at each assay's limit of detection; each point represents an individual cell culture assayed in triplicate by qPCR.

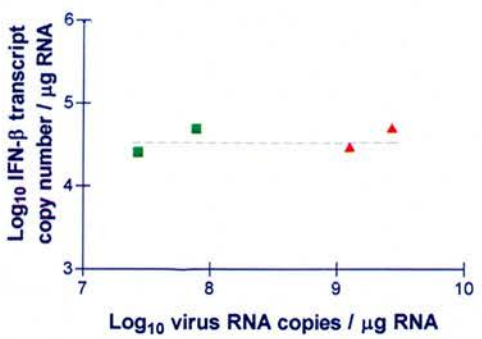

Figure 4B: IFN-β transcripts do not increase with increasing levels of virus RNA

L-929 cells were infected with SFV4 at a moi of 10 and assayed for SFV RNA species and IFN-β transcripts at 2, 3, 4 and 6 hours post-infection. Only cultures that produced detectable IFN-β transcripts are plotted; green symbols are cultures assayed at 4 hours post-infection and red symbols are cultures assayed at 6 hours post-infection.

To determine whether functional IFN could be detected in L-929 cells and to determine whether a moi of 10 was achieving maximum levels of infection, L-929 cells were seeded into chamberslides and at confluence infected with SFV4 at a moi 10 or 100 (in quadruplicate) or mock infected with PBS. Supernatant samples were taken at 24 hours to compare the amount of IFN and infectious virus in each sample (Figure 4C). The monolayers were then washed and stained with anti-nsP3 antibodies to ascertain the percentage of cells infected. Fifteen cell counts were carried out on different areas across the monolayer. No functional IFN or virus proteins were detected in the mock-infected cells. For both a moi of 10 and a moi of 100 the percentage infection was between 90 % and 100 % demonstrating that moi 10, as expected, achieved the maximum level of infection. All of the cultures produced similar amounts of infectious virus and functional IFN, indicating that once maximum infection had been achieved excess virus had no further effect. In conclusion, SFV4 infects L929 fibroblasts and establishes infection of > 90 % cells at moi 10; infected cells produce IFN-β transcripts starting at 4 hours and functional IFN is released into the media.

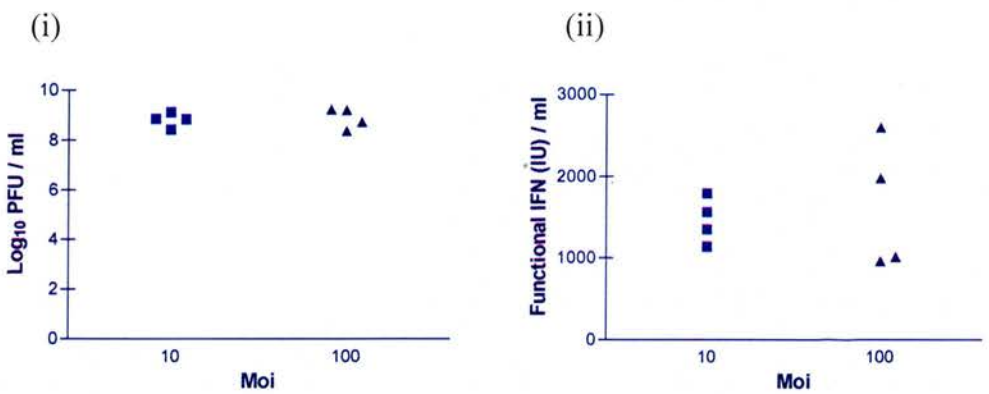

Figure 4C: Production of functional IFN by a mouse fibroblast cell line (L-929)
Chamberslides were seeded with L-929 cells and infected with SFV4 at a moi of 10 or 100. Supernatant samples were collected after 24 hours and assayed for levels of (**i**) infectious virus and (**ii**) functional IFN. Each point represents a single cell culture.

Does SFV4 induce type I IFN transcripts in adult mouse brains?

Adult 129/Sv/Ev mice were intracranially (*ic*) inoculated with 5 x 10^3 pfu SFV4 in 20 µl PBSA or mock infected with PBSA alone. *Ic* inoculation was used in preference to intraperitoneal (*ip*) since in pilot experiments SFV4 was found to be less neuroinvasive than other strains of SFV; *ip* inoculation of SFV4 resulted in encephalitis in only 1:3 cases (data not shown). Three mice were sampled for brain tissue at the following time points, 12, 24 and 40 hours post-inoculation. Before the brain was extracted, each mouse was perfused with PBS to remove blood from the cerebral blood vessels. This facilitated quantification of IFN produced within the brain by minimising any contribution from blood IFN. Half brains from each animal were stored in RNALater to prevent degradation of RNA. Forty mg of tissue was taken at random from each half brain and the RNA extracted. The RNA was reverse transcribed into cDNA and quantified for copies of SFV RNA, IFN-β, IFN-α and β-actin transcripts. In contrast to the high moi *in vitro* experiments, which resulted in synchronous infection of all cells and differentially downregulated cell housekeeping genes which are normally used for normalisation, *in vivo* infections are essentially low moi infections and therefore are not expected to affect global levels of cell housekeeping genes. Consequently, the levels of virus RNA and IFN transcripts can be normalised to housekeeping genes such as β-actin. All of the transcript data generated from *in vivo* studies was normalised to 100,000 β-actin copies. No viral RNA or IFN transcripts were detected in the mock-infected brains (data not shown). Figure 4D (i) indicates the level of SFV RNA in each mouse brain. No SFV RNA was detected for two of the mice at 12 hours post-inoculation. Levels were variable between mice but showed an increase between 12 and 24 hours. At 12 hours post-inoculation not all of the brain would have been infected; the negative samples at this time may have come from an uninfected area of the brain.

IFN- β transcripts were only detected at 24 and 40 hours post-infection, and only in two of the three mice sampled at each time point (Figure 4D (ii)). Only mice with greater than 1 x 10^6 copies SFV RNA / 100,000 β-actin copies produced detectable IFN-β transcripts. IFN-β gene transcript levels were similar at 24 hours and 40 hours

post-infection. A strong correlation ($R^2 = 0.91$) was observed between levels of SFV4 RNA and levels of IFN-β transcripts (Figure 4E); this suggests that IFN-β gene transcription in the brain was driven by virus RNA. IFN- α transcripts could only be detected in mice when IFN-β transcript levels were greater than 1.2×10^3 transcript copies / 100,000 β-actin copies (Figure 4D (iii)). Levels of IFN-α transcripts were similar at 24 and 40 hours post-infection. Levels of IFN-α transcripts were proportional to both levels of IFN- β transcripts and SFV RNA; linear regression analysis indicated R^2 values of 0.99 and 0.94, respectively.

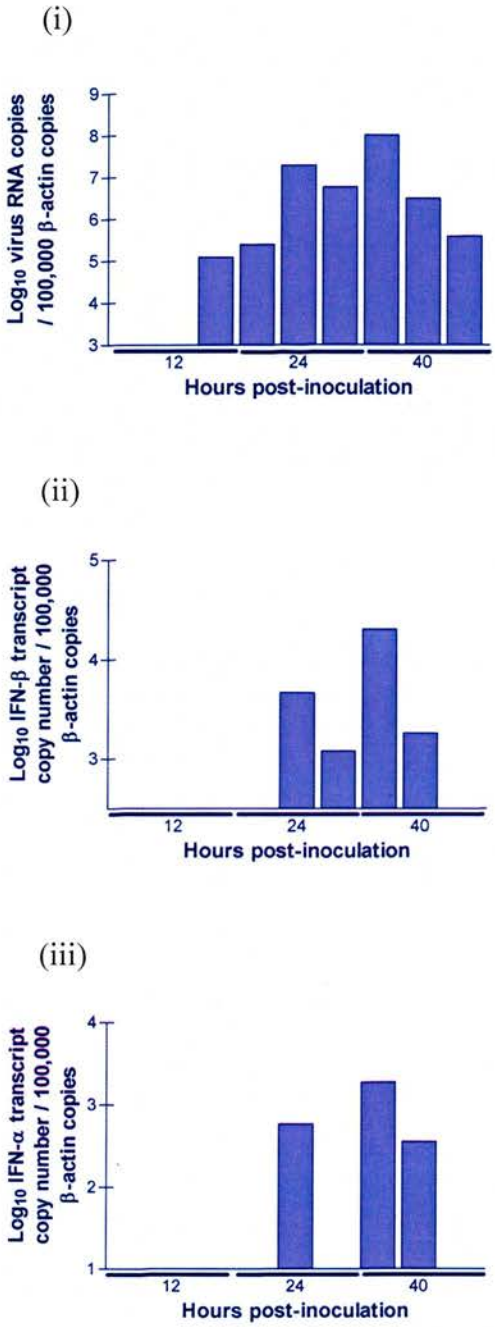

Figure 4D: Production of IFN-β transcripts in mouse brains following SFV4 infection

Adult 129/Sv/Ev wild type mice were inoculated *ic* with SFV4, after 12, 24 or 40 hours post-inoculation brains were sampled and assayed for (**i**) viral RNA species, (**ii**) IFN-β and (**iii**) IFN-α transcripts. All of the data was normalised to the level of 100,000 β-actin transcripts. Each bar represents one animal and the order of presentation is kept the same in each figure. The intersection of the x-axis and the y-axis is the limit of detection of the assay.

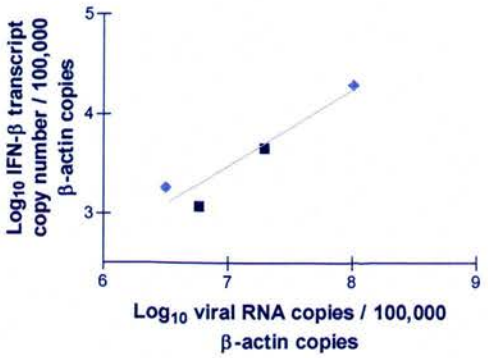

Figure 4E: Levels of IFN-β transcripts increase with increasing levels of virus RNA
Adult 129/Sv/Ev wild type mice were inoculated *ic* with SFV4, after 12, 24 or 40 hours post-inoculation brains were sampled and assayed for viral RNA species and IFN-β transcripts. Only brains that produced detectable amounts of IFN-β transcripts are plotted, dark blue symbols represent 24 hours post-infection and light blue symbols represent 40 hours post-infection, each point represents one mouse. Linear regression analysis produced an r^2 value of 0.91.

Does SFV4 induce type I IFN transcripts in neonatal mouse brains?

One hypothesis for the greater virulence of SFV in neonates versus adults is that immature CNS cells are impaired in their ability to produce type I IFNs in response to SFV infection. To test this, the levels of type I IFN transcripts induced by SFV4 infection in the neonate brain were determined. Neonatal mice (129/Sv/Ev) aged 4 days were intranasally (*in*) infected with approximately 50 µl of 1 x 10^5 pfu / ml SFV4 or mock infected with PBSA. Widespread neonatal brain infection is expected to occur between 24 and 40 hours post-infection (Oliver et al., 1997). At 30 hours post-inoculation mice were sampled and brains were removed and stored in RNALater until the RNA was extracted. The levels of SFV4 virus RNA detected in each neonate brain are shown in figure 4F (i). No virus RNA was detected in the negative controls (data not shown). All of the SFV4 infected mice had > 1 x 10^4 copies virus RNA / 100,000 β-actin copies. The level of virus RNA produced by each mouse varied by 2 Log_{10}. IFN-β transcripts were detected in all of the infected mice except one (Number 5), which showed the lowest level of SFV RNA (1 x 10^4 SFV4 RNA copies / 100,000 β-actin copies) (Figure 4F (ii)). All negative controls produced

low but detectable levels of IFN-β transcripts, consistent with very low level contamination of these samples. To allow for the possibility that the samples from the virus infected mice were also contaminated (although the negative result from mouse 5 suggests this was not the case) the limit of detection was raised to the highest negative control value. The levels of IFN-β transcripts were similar for all 5 animals in which they were detected. Only three of the neonates produced detectable IFN-α transcripts, these mice also produced the highest levels of IFN-β transcripts (approximately > 1 x 10^3 transcript copies / 100,000 β-actin copies) (Figure 4F (iii)). Linear regression analysis indicated that the levels of IFN-β and IFN-α did not correlate to the levels of virus RNA, however, the levels of IFN-α did correlate to the levels of IFN- β with an R^2 value of 0.99.

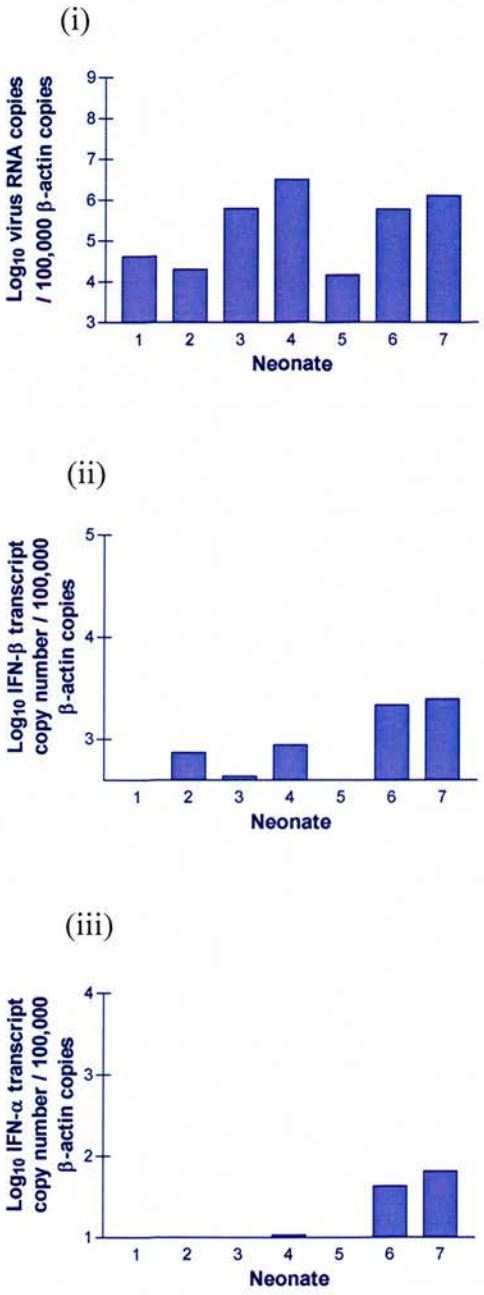

Figure 4F: Production of IFN-β transcripts in neonatal mouse brains following SFV4 infection.

Four-day-old neonates were infected *in* with SFV4; brain RNA was extracted at 30 hours post-inoculation and assayed for (**i**) SFV RNA, (**ii**) IFN-β transcripts and (**iii**) IFN-α transcripts. All of the data was normalised to 100,000 β-actin transcripts. Each bar represents one mouse and the x-axis crosses the y-axis at the limit of detection of the assay.

Do neonatal and adult mouse brains produce functional IFN in response to an SFV4 infection?

To determine if the IFN transcripts detected in both neonatal and adult mouse brains resulted in functional IFN, half brains were assessed in the bioassay (Figure 4G). IFN was detected at both 24 and 48 hours in neonates and levels increased over this time. Functional IFN was only assessed at 40 hours post-inoculation in adult brains; the amount detected was comparable to the amount detected in neonates at 24 hours.

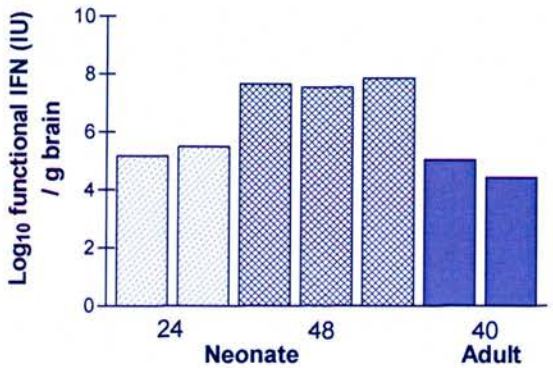

Figure 4G: Neonatal and adult mouse brains produce functional IFN.
129/Sv/Ev wt neonatal mice were inoculated *in* with SFV4 and half brains sampled at 24 and 48 hours. Wild type 129/Sv/Ev adult mice were inoculated *ic* with SFV4 and half brains were sampled at 40 hours post-inoculation. The amount of IFN present in each sample was quantified by CPERA. Each bar represents one mouse.

In conclusion, high levels of SFV4 RNA induce IFN-β and IFN-α gene expression in both adult and neonate mouse brains and functional IFN is produced in adult and neonate brains in response to SFV4 infection.

Is human interferon protective against SFV encephalitis?

SFV is a positive sense, single-stranded RNA virus, which targets the CNS and induces virus encephalitis. It belongs to the alphavirus family and is transmitted by mosquitoes (Weaver et al., 2000). Thirty-seven alphaviruses are known to cause human disease, including Eastern Equine Encephalitis virus (EEE), Venezuelan Equine Encephalitis virus (VEE), Ross River virus and Chikungunya virus. The

alphaviruses are endemic across the Americas, Africa and Australia (reviewed in Tsai et al., 2002) and the majority target the CNS. Other viruses, which commonly cause human encephalitis include Japanese encephalitis virus, rabies virus and measles virus. SFV can be used as a model to study the pathogenesis of neurotropic infections. For many viral encephalitides no vaccines are available and both vaccines and alternative prophylactics are desired. The SFV model system may have potential in evaluating human IFN preparations. This was determined by evaluating the ability of a new interferon product to affect the course of SFV encephalitis. The compound Multiferon© is being developed by Viragen Ltd (Edinburgh) and contains multiple types and sub-types of IFN. It was hypothesised that treatment with a broad range of IFNs would maximise the potential of an anti-viral effect and would be less likely to promote pathogen resistance.

This study investigated the protective effect of Multiferon© (Viragen), on SFV L10 infection. L10 is an extremely virulent strain of SFV; *ip* inoculation normally results in death (100 % of animals) within 3 – 4 days (Fazakerley, 2002).

Does Multiferon© protect adult mice against SFV L10 infection?

Six groups of six female Balb/c mice aged 4-6 weeks were inoculated *ip* with 1 x 10^3 pfu of SFV L10; each group was given a different Multiferon© treatment regime and assessed twice daily for survival. SFV L10 is extremely neurovirulent and is representative of a naturally acquired virulent arboviral encephalitis. Each treatment regime is described in table 4A. Where IFN was administered, 1 x 10^5 IU Muliferon© diluted in 0.1 ml PBS were inoculated *ip*.

	Time post virus inoculation							
Group	- 24 hr	0	5 hr	26 hr	Day 2	Day 3	Day 4	Day 5
A	-	L10	-	-	-	-	-	-
B	-	-	IFN	IFN	IFN	IFN	IFN	IFN
C	IFN	L10	IFN	IFN	IFN	IFN	IFN	IFN
D	-	L10	IFN	IFN	IFN	IFN	IFN	IFN
E	-	L10	-	IFN	IFN	IFN	IFN	IFN
F	-	L10	IFN	IFN	-	-	-	-

Table 4A: Multiferon treatment regime.
Six groups of Balb/c mice were inoculated with SFV L10 and treated with IFN where indicated. L10 represents *ip* inoculation of 1 x 10^3 pfu L10 / 0.1 ml PBSA; IFN indicates the *ip* administration of 1 x 10^5 IU Multiferon© / 0.1 ml PBS.

This experiment was carried out under the auspices of a UK Home Office licence. In accordance with these regulations, mice that had substantial clinical signs were euthanised. Mice first presented with clinical signs at day 3 when 4 of the mice in Group A became ill; 2 had signs of substantial disease (Figure 4H) and all mice in Group E appeared unwell with ruffled coats and slow, shaky movements. By day 4, 5 of the animals in Group A had died; the remaining mouse had a ruffled coat, an early sign of infection. Four of the animals in Group E were dead; another had hind limb paralysis and was consequently put down, the surviving animal showed the early signs of infection. By day 5 post-inoculation, one mouse was found dead in Group F, 2 more showed signs of poor grooming and 3 were asymptomatic. The infection in the surviving mice from Groups A and E had progressed; both mice had ruffled coats and displayed minimal movement, when stimulated their movements were shaky. At day 6, all of the mice in Groups A and E had succumbed to SFV encephalitis or had reached substantial clinically defined terminal end points and had been put down. A further 2 mice from Group F had died, but the 3 surviving mice were still asymptomatic. One mouse was found dead in Group C, the remaining 5 mice were asymptomatic. Another mouse was found dead in Group D and a further mouse was put down due to complete hind limb paralysis. Four remaining mice of Group D showed initial signs of infection. By day 7 another mouse from Group D was put down and the following day a mouse in Group C died. The experiment continued

until 12 days post-inoculation; however, after day 8 no more mice died. Healthy mice given Multiferon© survived without any clinical signs for the 12 days studied.

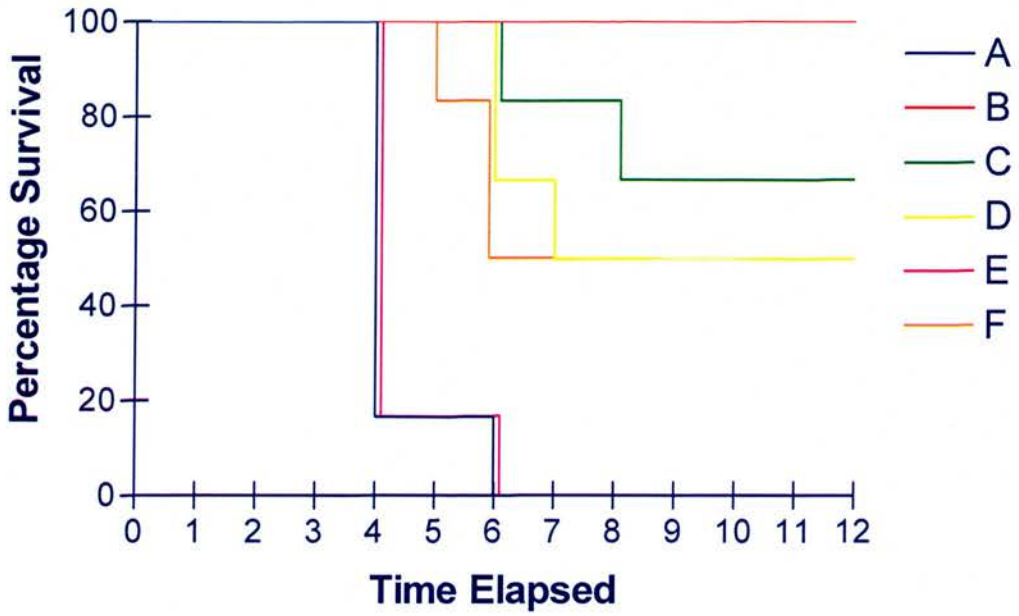

Figure 4H: Mouse survival (days) after SFV L10 inoculation and treatment with Multiferon©

Six female mice aged 4-6 weeks were assigned to each group. Each group received a different treatment regime: A - Inoculated with L10, B – Given Multiferon© at 5 and 26 hours post-inoculation and PID 2, 3, 4, 5, C – Inoculated with L10 and given Multiferon© at –24, 5, 26 hours post-inoculation and PID 2, 3, 4, 5, D – Inoculated with L10 and given Multiferon© at 5 and 26 hours post-inoculation and PID 2, 3, 4, 5, E – Inoculated with L10 and given Multiferon© at 26 hours post-inoculation and PID 2, 3, 4, 5, F – Inoculated with L10 and given Multiferon© at 5 and 26 hours post-inoculation only.

In conclusion, Multiferon© reduced the virulence of SFV L10 infection when administered 24 hours prior to virus or 5 hours after virus. However, Multiferon© administered 26 hours post-inoculation had no effect (GroupE had the same mortality rate as the positive controls, Group A). Following treatment 24 hours before or 5 hours after inoculation additional doses of Multiferon© did not have any additive value.

These results demonstrate the applicability of the SFV model system to study the anti-viral efficacy of human IFN preparations.

Discussion

Many virus infections are more severe in neonates than in adults; it has been postulated that this is related to an impaired ability of neonates to induce IFN responses. Neustock et al., (1993) demonstrated that cord blood mononuclear cells produced less IFN in comparison to adult blood cells following a virus infection. The experiments described in this thesis investigated the levels of IFN produced by neonatal and adult mouse brains in response to SFV4 infection. SFV4 induced IFN-β and IFN-α transcripts and functional IFN in both adult and neonates. Levels of IFN transcripts detected in neonatal mouse brains were approximately 10-fold lower than in adult brains; however, this corresponded to 10-fold lower virus RNA titres. This could be a consequence of the different inoculation sites (adults, *ic* and neonates, *in*). The ratio of IFN-β transcripts: 1 x 10^6 virus RNA is approximately the same for adults and neonates (3 and 3.25, respectively), demonstrating that adult and neonate brains produce equivalent levels of IFN-β in response to a certain virus RNA level. Given that neonates produce IFN and make a similar response to adult mice, indicates that lack of IFN in neonates is not the explanation for age-related virulence. This result is in agreement with those of Labrada et al., (2002) who demonstrated that high levels of Sindbis virus (SV) induce high levels of IFN and inflammation. Alternative explanations for the increased SFV virulence in neonates include 1) the stress hyporesponsive period, which is defined by the absence of a stress-induced adrenocortical response to mild stimuli between post-natal day 4 and 14 (Schapiro et al., 1962; Schoenfeld et al., 1980). It has since been shown that the developing CNS can produce a strong adrenocorticotrophin hormone (ACTH) response to multiple stimuli, for example, histamine (Kent et al., 1996), endotoxin (Witek-Janusek L, 1988), and IL-1 (Levine et al., 1994). 2) CNS maturation, neuronal maturation coincides with acquirement of resistance to SFV infection (Oliver et al., 1997; Oliver and Fazakerley, 1998). SFV replicates on smooth membranes. During CNS development high levels of smooth membrane production occur to support synaptogenesis. When smooth membrane production in adult mice was induced with aurothiolates, a normally avirulent SFV infection was able to spread throughout the brain (Mehta et al., 1990; Scallan and Fazakerley, 1999). Another factor that changes with CNS maturation is the propensity of CNS cells to undergo apoptosis. Neurons of the developing CNS are more susceptible to apoptosis (Levine et al., 1996; Havert et

al., 2000) and forced expression of anti-apoptotic proteins such as Bcl-2, Bax and CrmA, all reduce mortality of neonatal mice following infection with alphaviruses (Levine et al., 1996; Lewis et al., 1999; Nava et al., 1998). 3) Other differential immune responses, reduced NK cell activity in neonates has been observed (Nair et al., 1985). Adaptive immune responses are suppressed in neonates; however, SCID adult mice, which are deficient in their T and B cell responses, show a restricted infection with avirulent strains of SFV (Wesselingh et al., 1994; Fazakerley unpublished), suggesting that other factors play a role in SFV age-dependent pathology. Gene expression analysis revealed that during an SV infection only ISG-12 is expressed at greater levels in adult mice compared to neonates and enforced expression of ISG-12 in neonates delayed mortality (Labrada et al., 2002).

The adult and neonate *in vivo* data show that IFN-α transcript levels correlate to IFN-β transcript levels. This suggests that IFN-α transcript production is driven by IFN-β and is consistent with the two-phase IFN induction theory (Marie et al., 1998), which states that IFN-β is expressed initially and signals through the IFNAR to induce expression of anti-viral genes, including the transcription factor IRF-7. IRF-7 is required for the induction of many IFN-α subtypes. IFN-β expression is activated by virus and in the adult brain IFN-β levels correlate to SFV4 RNA levels. During a low moi infection such as this, as the virus spreads throughout the brain, increasing numbers of cells are infected. This enables greater levels of virus replication, which induces increasing numbers of cells to express IFN-β.

Interestingly when IFN-β transcripts were detected, the corresponding levels of SFV4 RNA were particularly high. When cultured cells were infected with SFV4, virus RNA was detected from 2 hours post-infection and virus levels continued to increase until 6 hours post-infection. However, IFN-β transcripts were not detected until 4 hours post-infection when virus RNA levels were > 1 x 10^8 RNA copies / μg total RNA. IFN is one of the first anti-viral responses, but virus RNA levels were high before this crucial primary response was detected. Possible explanations are that (i) IFN-β transcripts are induced earlier but at levels below the limit of detection of the assay (< 1000 copies); (ii) a certain level of virus replication needs to be present per cell to induce IFN gene expression; (iii) SFV4 is able to suppress, or at least delay,

induction of IFN gene expression. To address each in turn, qPCR is a very sensitive assay, but for IFN-β transcript detection the limit of detection is 1000 copies per μg total RNA. However, given that the levels of IFN-β increase 50-fold from below the limit of detection (< 1000 copies) within an hour, it is unlikely that transcripts have not been detected. The high moi *in vitro* experiment indicates that approximately 10^9 SFV4 RNA copies / μg total RNA were detected at 4 hours post-infection. Approximately 30 μg RNA were extracted from 2 x 10^6 cells, therefore 3 x 10^{10} SFV4 RNA molecules were produced by 2 x 10^6 cells, equating roughly to 10,000 SFV4 RNA molecules per cell at 4 hours, the time when IFN-β is first detected. The 4-hour delay between infection and IFN-β transcript detection could represent the minimal delay between virus detection and initiation of gene transcription. However, crg-2, the murine equivalent of IP-10, which is an immediate early expressed gene (like IFN-β) and is induced by IFN-γ, poly I:C and viruses, can be detected within 2 hours following IFN- γ induction and within 3 hours following NDV infection (Vanguri and Farber, 1994). Poly I:C treatment of primary tamarin hepatocytes induces a 12-fold increase in IFN-β transcripts within 2 hours (Lanford et al., 2003). In addition to virus replication, IFN expression is induced by non-replicating SFV as a result of virus entry into the cell, which might be expected to result in rapid IFN gene expression (Hidmark et al., 2005). Alternatively, the 4 hour delay before detectable IFN gene transcription could represent SFV4 suppression of IFN-β expression. Many viruses have developed mechanisms to antagonise the IFN response so this is a plausible concept.

SFV4 infection of mouse fibroblasts resulted in a continual increase in SFV RNA copies / μg total RNA over 6 hours; however after induction at 4 hours, even though the levels of virus RNA increased 100-fold, IFN-β transcript levels maintained a constant level until 6 hours. As this was a high moi infection, IFN-β expression should have been induced in all cells synchronously but whereas virus RNA levels would be expected to increase as the number of potential transcription templates increased with time there are only two copies of the IFN-β gene and so transcript levels reach a plateau. However, this may also suggest that IFN-β transcription has been abolished after 4 hours post-infection and that the maintenance of transcripts at the same level at 6 hours post-infection is indicative of the stability of IFN-β mRNA.

The sensitivity of SFV to IFN is examined in the second section of this chapter; however, in figure 4A (i) there is a decline in the rate of virus RNA accumulation between 4 and 6 hours post-infection and this correlates to the time of IFN-β expression suggesting that SFV is sensitive to the effects of IFN.

Mice inoculated *ic* displayed considerable variation in the levels of virus RNA. SFV is known to infect neurons, oligodendrocytes, meningal, ependymal and choroid plexus cells but infection of astrocytes has not been observed (Balluz et al., 1993; Pathak et al., 1983). Inoculation into a particularly brain area may result in predominant infection of a certain cell type for example, oligodendrocytes in the corpus callosum or neurons in the thalamus, and different cells may be better at supporting SFV infection and may respond to SFV infection by producing different levels of IFN. To date, IFN production in the CNS has been mostly attributed to astrocytes (Ogata et al., 2004), however neurons have recently been identified as major IFN producers and IFN has been detected in resident macrophages and brain epithelial cells (Delhaye et al., in press; Barber et al., 2004). The variability between animals inoculated *ic* in the levels of both virus RNA and IFN transcripts is likely to reflect the variability in cell types and brain regions infected in different animals. Mice inoculated *in* also demonstrated variability in the levels of virus RNA detected in the brain. Following *in* inoculation, neurotropic viruses can invade the brain by infecting vomeronasal chemosensory neurons e.g. HSV-1 and HSV-2 (Mori et al. 2005). These viruses do not induce apoptosis in the infected neurons; it is believed that this may facilitate viral transmission to the CNS. H5N1 influenza A virus induces CNS pathology by travel from the nasal cavity along the cranial nerves (Iwasaki et al., 2004). *In* inoculation of SFV results in SFV spread along neurites in a circuit-specific manner throughout the olfactory bulb (Oliver and Fazakerley, 1998). By *in* inoculation the virus is not directly inoculated into the brain, and must traverse one of several nerves to enter the CNS. The time at which it infects the CNS may vary between animals.

Is IFN protective against an SFV infection?

The L10 strain of SFV, which is highly virulent in adult mice was shown to be sensitive to a human IFN preparation (Multiferon©). This effect was conditional upon

the time prior / post infection that IFN was administered. Only mice treated with IFN 5 hours post-infection (ip) had an improved survival rate. By 5 hours virus would have started to spread from the originally infected cells of the peritoneal cavity. Administration of IFN at this time should have stimulated an antiviral state in uninfected cells and greatly reduced the second and subsequent waves of virus production. IFN administered at or after 26 hours post-infection was ineffective. By this time the virus would have established infection in many tissues. This is consistent with the observation that in the mouse, IFN levels are high by 24 hours post-infection, but this fails to prevent virulence of L10 virus (Bradish and Titmuss, 1981). Mice given IFN treatment 24 hours in advance of the L10 infection demonstrated the highest percentage of survival. Advance IFN treatment would have established an anti-viral state in all cells prior to infection. In the clinical setting, the use of IFN as preventative treatment for virus infections would be of little value as the induced anti-viral state is downregulated within a few days if an infection is not detected. Finter, (1966) observed that the antiviral state can only be stimulated 1-2 days in advance of infection to still be protective against SFV.

These studies demonstrate that the mouse:SFV L10 system can be used to screen human IFN preparations. However, the results also demonstrate the potential problems of IFN as an anti-viral therapy for an acute infection. In this study the time window for effectiveness was very small (hours before and after the infection). In a clinical setting, this would be of little value as most patients would not realise they had been infected until they presented symptoms by which time IFN treatment could be of no value. However, IFN treatment could be useful as a post-exposure therapy following for example laboratory infection with a dangerous virus. Venezuelan equine encephalitis virus (VEE), an alphavirus related to SFV has been associated with over 20 laboratory infections resulting in clinical illness (Koprouski and Cox, 1947).

Summary

The objectives of this chapter were to determine whether SFV4 induced type I IFN gene expression in mouse fibroblasts; to quantify type I IFN responses in the brains of SFV4 infected adult and neonatal mice and to assess the efficacy of passive IFN administration to treat a neurovirulent infection. As with other strains of SFV and as expected, SFV4 induced type I IFNs in cultured mouse (L-929) fibroblasts. Similar levels of type I IFN transcripts and functional IFN were induced in both adult and neonatal mouse brains following SFV4 infection. It is therefore unlikely that differences in the generation of IFN contribute to SFV induced age-dependent virulence. Type I IFN is a potent anti-viral response, however the ability of the Multiferon© preparation to protect against lethal SFV encephalitis was very dependent upon the time at which the IFN was administered. Mice had an increased chance of survival if IFN was given prior to, or at 5 hours post-infection, but not if given 26 hours post-infection. However, these results do demonstrate the applicability of this mouse model for the testing of human IFN preparations.

Chapter 5: Does Protein Kinase R (PKR) have a role in IFN induction during SFV infection?

Contents

Objectives:.....124
Introduction.....124
Is PKR required for the mouse brain IFN response to SFV?.....126
Does PKR affect IFN-β transcription in the mouse brain in response to SFV?.....129
Does PKR affect IFN-β transcript production *in vitro* in response to SFV infection?.....134
Are the levels of IFN-α influenced by PKR?.....136
What accounts for the observed reduction in IFN transcription?.....138
Does PKR affect functional IFN production *in vitro* in response to SFV infection?.....140
Summary of findings.....142
Discussion.....143
Summary.....146

Does Protein Kinase R (PKR) have a role in IFN induction during SFV infection

Objectives:

1) Does PKR affect IFN-β transcript production in the mouse brain in response to SFV infection?
2) Does PKR affect functional IFN production in the mouse brain in response to SFV infection?
3) Does PKR affect IFN-β transcript production *in vitro* in response to SFV infection?
4) Does PKR affect functional IFN production *in vitro* in response to SFV infection?

Introduction

PKR (Clemens et al., 1993) is an IFN induced antiviral protein, with two domains, the N-terminal regulatory domain, composed of two dsRNA binding motifs (dsRBM), and the C-terminal catalytic domain, which encompasses the protein kinase function (Meurs et al., 1990). Attachment of dsRNA to the dsRBM induces a conformational change resulting in autophosphorylation and activation of PKR. The dsRBM may also be responsible for PKR ribosomal targeting (Zhu et al., 1996). Following autophosphorylation, PKR forms a homodimer and this active PKR targets several proteins for phosphorylation. The best known target is eIF-2α, although other roles in growth factor (platelet derived growth factor) and calcium-mediated signal transduction as well as in transcription regulation have been defined (Mundschau and Faller, 1995; Srivastava et al., 1995; Kumar et al., 1994). PKR is expressed constitutively in all cell types (Baier et al., 1993) and its antiviral effect can be activated immediately following virus infection; other antiviral proteins (e.g. Mx) are induced following IFN expression and therefore act less rapidly. PKR phosphorylation of eIF-2α locks eIF2 in a complex with GDP; this prevents guanine

nucleotide exchange factor cycling of GDP and GTP which is required for continued initiation of translation (Merrick, 1992). The inability of a cell to initiate translation effectively culminates in protein translation shut-off. The role of PKR in transcription regulation is linked to the phosphorylation of inhibitory kappa B kinase (IκK); phosphorylation and activation of IκK results in IκK phosphorylation of IκB and ultimately targets IκB for proteosome degradation. Under non-inflammatory conditions, IκB maintains NF-κB within the cytoplasm in an inactive form. Degradation of IκB releases NF-κB, which forms a homodimer and enters the nucleus. Within the nucleus NF-κB associates with several promoters including the IFN-β promoter.

The previously assumed pivotal role for PKR in IFN-β expression is now questioned by the recent discovery of several other cytoplasmic dsRNA-activated, IFN inducing proteins such as RIG-I and mda-5 and experimental evidence which has indicated that PKR mutant mice do not display increased sensitivity to certain viral infections e.g. vaccinia virus and EMCV (Yang et al., 1995; Zhou et al., 1999). Yang et al. demonstrated that MEFs without functional PKR ($PKR^{o/o}$) stimulated with poly I:C did not express IFN-β or IFN-α mRNA, where as wt cells expressed both. However, when $PKR^{o/o}$ and wt cells were infected with Newcastle Disease virus (NDV), comparable levels of both IFN-β and IFN-α transcripts were detected. This implies that cells contain a multitude of sensors which can stimulate the IFN response and possibly that viruses differ in their requirement for PKR to activate the IFN response.

The mechanism of IFN induction in an SFV infection has not been investigated. Dendritic cell (DC) cultures with defective PKR and RNase L proteins were infected with Sindbis virus, an alphavirus related to SFV; these demonstrated a dependence upon PKR for early but not late suppression of viral protein synthesis (Ryman et al., 2002). In Sindbis virus infection, both PKR-dependent and PKR-independent pathways participate in host cell translational shut-off; the most likely major pathway was the independent pathway (Gorchakov et al., 2004), leaving open the question, is PKR required for IFN-β gene expression in alphaviruses infections? Early in infection the main role of PKR is probably to enhance IFN-β expression. It has also been suggested that PKR is required for the induction of interferon regulatory factor

(IRF) -1 expression (Kirchhoff et al., 1995), allowing IFN-α induction or expression of other antiviral genes.

In the following experiments, the importance of PKR for IFN-β and IFN-α induction in SFV infection of murine brain tissue and MEFs was studied.

Is PKR required for the mouse brain IFN response to SFV?

To determine whether PKR has a role in IFN induction during SFV infection, 129/Sv/Ev mice carrying a mutated PKR gene, $PKR^{o/o}$ (Yang et al., 1995), control 129/Sv/Ev mice, and mouse embryo fibroblasts (MEFs) derived from these, were assessed for their ability to induce IFN-β transcripts and functional IFN following SFV infection. The $PKR^{o/o}$ mice were created by insertion of a neomycin resistance gene in an antisense orientation with an upstream transcription termination sequence, between and partially overlapping exons 2 and 3 of the PKR gene. The mutated PKR gene was inserted into 129/Sv/Ev embryonic stem cells by homologous recombination and then injected into C57BL/6 blastocysts. The transcription termination sequence was not effective but the mRNA expressed by the mutant mice lacked exons 2 and 3 resulting in a frame shift and deletion of the first 17 amino acids including the initiation codon (Yang et al., 1995). A C-terminal fragment of PKR mRNA can be expressed but is not functional. To confirm the PKR gene status, all cells and animals investigated were characterised by PCR; RNA was extracted from ear clippings or cell cultures and transcribed into cDNA from oligo dT primers. cDNA was assessed for the presence of the deleted section of the PKR gene by PCR. The primers and conditions are described in the Materials and Methods, Table 2D; figure 5A demonstrates the presence or absence of the sequence overlapping exons 2 and 3 of the PKR gene.

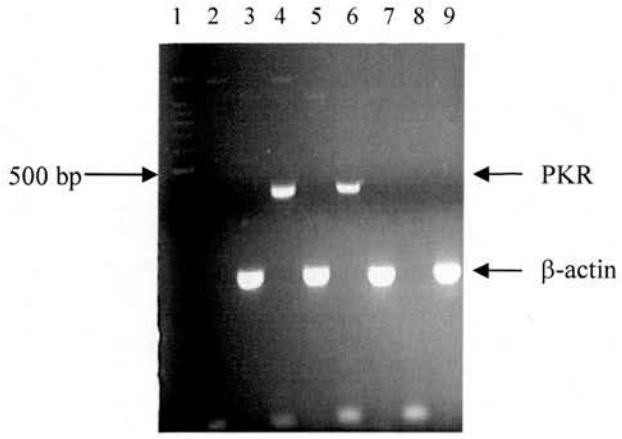

Lane	Primers	Strain	Sample
1	-	-	100 bp ladder
2	PKR	$PKR^{o/o}$	Brain
3	β-actin	$PKR^{o/o}$	Brain
4	PKR	WT	Brain
5	β-actin	WT	Brain
6	PKR	WT	MEFs
7	β-actin	WT	MEFs
8	PKR	$PKR^{o/o}$	MEFs
9	β-actin	$PKR^{o/o}$	MEFs

Figure 5A: Genetic confirmation of $PKR^{o/o}$ or wild type mouse strains and MEFs.

RNA was extracted from $PKR^{o/o}$ or wt strains and reverse transcribed into cDNA; the cDNA was assessed for a sequence partially overlapping exons 2 and 3 of the PKR gene (PCR product = 369 bp). This was absent in $PKR^{o/o}$ and present in wt mice and cells. Each sample was also assessed for β-actin (PCR product = 202 bp) to ensure that the PCR was valid. Annealing was carried out at 55°C. The lane order is indicated in the table.

To determine whether PKR has a role in IFN induction in the mouse brain, three strains of mice were compared for their ability to induce functional IFN in response to SFV infection - Balb/c, 129/Sv/Ev and $PKR^{o/o}$. Balb/c and 129/Sv/Ev mice both possess a functional PKR gene. Groups of four adult mice aged 4 – 6 weeks were inoculated *ic* with $5x10^3$ pfu SFV4 in 0.02 ml PBSA or with PBSA alone. After 24 hours the mice were sampled; half brains were snap frozen in dry ice and assessed for infectious virus and functional IFN by plaque assay and CPERA, respectively (Figure 5B).

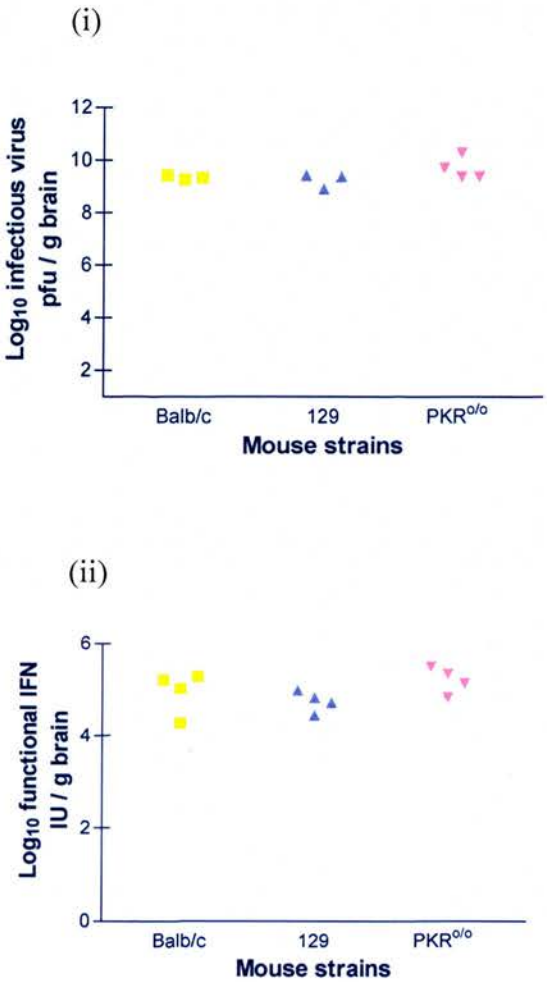

Figure 5B: Functional IFN in the brains of SFV4 infected (*ic*) wild type and PKR$^{o/o}$ mice at 24 hours.
Balb/c, 129/Sv/Ev and PKR$^{o/o}$ mice were *ic* inoculated with SFV4 and their brains sampled and assessed for levels of (**i**) infectious virus and (**ii**) functional IFN at 24 hours post-inoculation. Each point represents a single mouse brain.

Levels of infectious virus and functional IFN were not significantly different ($p > 0.05$, Kruskal Wallis test or Mann-Whitney) between the three strains of mice. No infectious virus or functional IFN was detected in the brains of control mice inoculated with PBSA alone (data not shown). This data clearly demonstrates that PKR is not required for functional IFN induction in the brain. Furthermore, the equivalent brain virus titres in the PKR$^{o/o}$ and wt mice suggest that PKR has no effect on brain virus, at least at 24 hours post-infection. However, the functional IFN assay detects all subtypes of IFN and most studies suggest that PKR is involved in IFN-β induction.

Does PKR affect IFN-β transcription in the mouse brain in response to SFV?

To determine IFN-β gene expression and relate this to levels of virus and functional IFN in the brain, 129/Sv/Ev wt and $PKR^{o/o}$ mice were inoculated *ic* with $5x10^3$ pfu SFV4 in 20 µl of PBSA or with PBSA alone. Brains were sampled at 12, 24 or 40 hours post-inoculation; animals were perfused with sPBS to remove contaminating blood prior to dissection. Half brains were stored in RNALater to prevent RNA degradation. RNA was extracted, transcribed into cDNA and assessed by qPCR for levels of IFN transcripts and SFV RNA species (Figure 5C). The other half of each brain was assayed for functional IFN and infectious virus (Figure 5F).

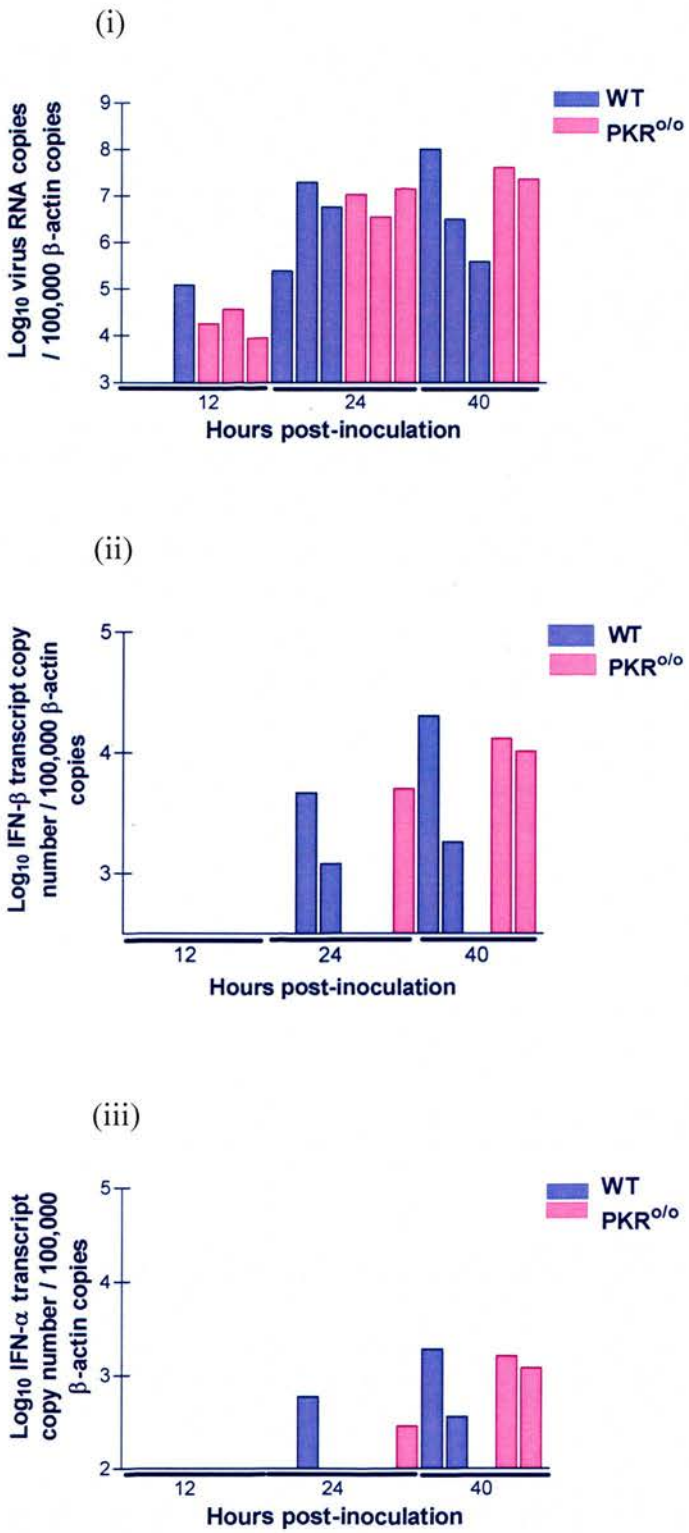

Figure 5C: IFN-β and IFN-α transcripts in wt and PKR$^{o/o}$ mouse brains after SFV4 infection.

129/Sv/Ev wt and PKR$^{o/o}$ mice were infected with SFV4. At 12, 24 or 40 hours post-inoculation brains were sampled and assessed for (**i**) SFV RNA, (**ii**) IFN-β transcripts, and (**iii**) IFN-α transcripts. The data was normalised to 100,000 β-actin copies. A single bar represents an individual mouse brain and the sample order is maintained in each panel so the data can be compared; mean values were not determined due to the variation between mice. The x-axes intersect the y-axes at the limit of detection of the assay.

No SFV RNA or IFN transcripts were detected in any of the mouse brains inoculated with PBSA alone (data not shown). SFV RNA was detected in all virus inoculated mouse brains except for two of the wt mice sampled at 12 hours post-inoculation. At this early time point it is likely that large areas of the brain would still be uninfected. Only approximately ¼ of the brain is used for virus titration so the negative samples at this time may have come from an uninfected area of the brain. Virus RNA levels increased approximately 100-fold between 12 and 24 hours post-infection. At 24 and 40 hours post-infection there was no significant difference in the levels of virus RNA in the brain between the two strains of mice ($p > 0.05$, Kruskal Wallis test). IFN-β transcripts were not detected in the brains of either wt or $PKR^{o/o}$ mice until 24 hours post-infection. There was no significant difference in the levels of IFN-β transcripts detected in the two mouse strains at 40 hours post-infection ($p > 0.05$, Kruskal Wallis test). In conclusion, absence of functional PKR did not affect the levels of virus RNA or the levels of induced IFN-β transcripts.

For both mouse strains, IFN-β transcripts were only detected in brains when levels of viral RNA > 1 x 10^6 copies / 100,000 β-actin copies. Where IFN-β transcripts were detected, levels strongly correlated with virus RNA copies (wt cells $R^2 = 0.91$, $PKR^{o/o}$ $R^2 = 0.9$, Figure 5D), suggesting that virus RNA levels drive IFN-β gene expression in both wt and $PKR^{o/o}$ mouse brains. IFN-α transcript levels were also investigated. PKR has been suggested to be required for IRF-1 induction (Kirchhoff et al., 1995). Presence or absence of PKR did not affect the level of IFN-α expression. At 40 hours there was no significant difference in the levels of IFN-α transcripts between wt and $PKR^{o/o}$ mice ($p > 0.05$, Kruskal Wallis test). IFN-α transcripts were only detected in mouse brains when SFV4 RNA levels were > 1 x 10^6 copies / 100,000 β-actin copies and IFN-β transcript levels were > 2 x 10^3 copies / 100,000 β-actin copies. The level of IFN-α transcripts in wt mice strongly correlated with the levels of SFV RNA and IFN-β transcripts with R^2 values of 0.94 and 0.99, respectively. The level of IFN-α transcripts also correlated with the levels of SFV RNA and IFN-β transcripts, with R^2 values of 0.845 and 0.99, respectively, in $PKR^{o/o}$ mice (Figure 5E). This suggests that for both strains of mice virus and IFN-β expression drive IFN-α transcription.

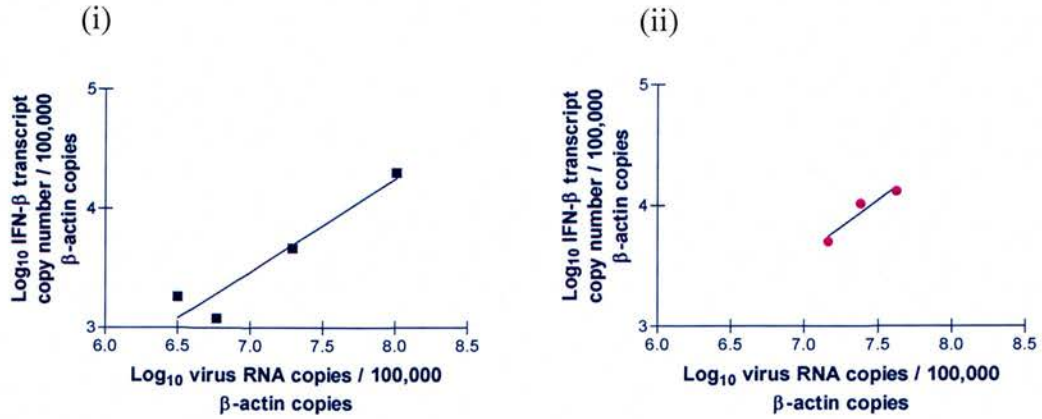

Figure 5D: Levels of IFN-β transcripts correlated with levels of SFV RNA.
(**i**) 129/Sv/Ev wt and (**ii**) $PKR^{o/o}$ mice were infected with SFV4. At 12, 24 and 40 hours post-inoculation brains were sampled and assessed for SFV RNA and IFN-β transcripts. Each point represents an individual mouse brain. The linear regression co-efficient produced by plotting the levels of IFN-β against virus RNA levels was $R^2 = 0.91$ and 0.9, wt and $PKR^{o/o}$, respectively.

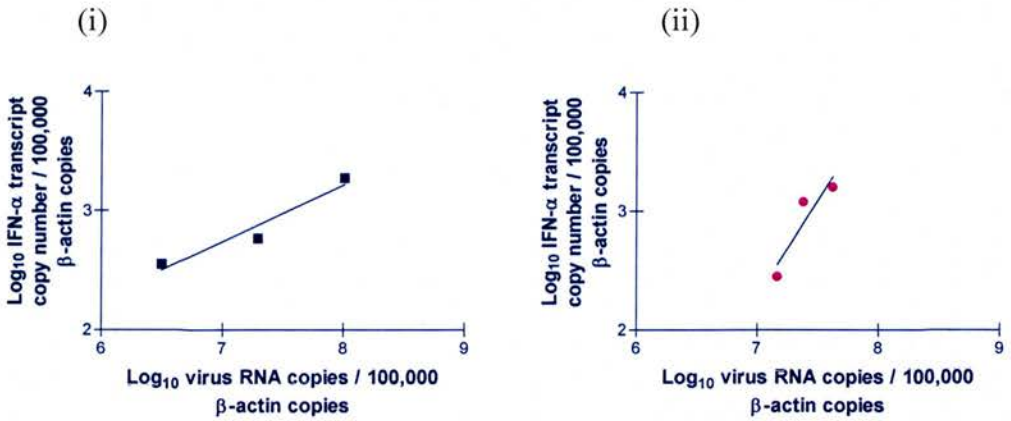

Figure 5E: Levels of IFN-α transcripts correlated with levels of SFV RNA.
(**i**) 129/Sv/Ev wt and (**ii**) $PKR^{o/o}$ mice were infected with SFV4. At 12, 24 and 40 hours post-inoculation brains were sampled and assessed for SFV RNA and IFN-α transcripts. Each point represents an individual mouse brain. The linear regression co-efficient produced by plotting the levels of IFN-α against virus RNA levels was $R^2 = 0.94$ and 0.845, wt and $PKR^{o/o}$, respectively.

The other half brain from each of the mice sampled at 40 hours was assayed for infectious virus and functional IFN (Figure 5F).

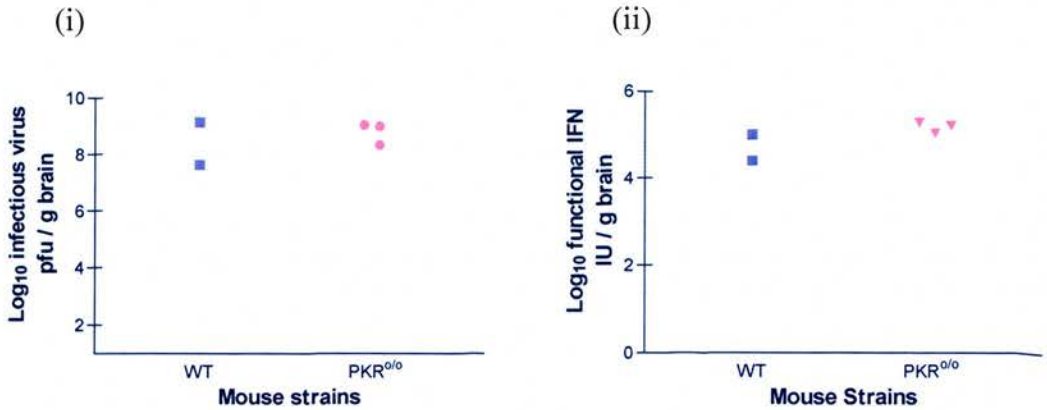

Figure 5F: Functional IFN and infectious virus levels in 129/Sv/Ev and PKR$^{o/o}$ mice infected with SFV4.

129/Sv/Ev wt and PKR$^{o/o}$ mice were inoculated *ic* with $5x10^3$ pfu SFV4 in 20 µl of PBSA. At 40 hours post-inoculation mice were perfused with sPBS and the brains removed. Brains were assayed for (**i**) infectious virus and (**ii**) functional IFN. Each point represents an individual mouse brain.

There was no significant difference in the levels of either infectious virus or functional IFN between wt and PKR$^{o/o}$ mouse brains ($p > 0.05$, Kruskal Wallis test). This supports the previous data (Figure 5B) and again demonstrates that PKR is not required for IFN expression and does not enhance or suppress viral replication, at least within 40 hours post-infection (Table 5A).

	wt			PKR$^{o/o}$		
	1	2	3	1	2	3
Log_{10} infectious virus (pfu / g brain)	9.09	-	-	8.98	9.02	8.32
Log_{10} virus RNA copies	8.01	6.50	5.59	7.63	7.38	-
Log_{10} IFN-β transcripts	4.31	3.26	0.00	4.12	4.02	-
Log_{10} IFN-α transcripts	3.28	2.55	0.00	3.21	3.08	-
Log_{10} functional IFN (IU / g brain)	5.03	-	-	5.08	5.32	5.24
Ratio PFU : virus RNA	1.14	-	-	1.18	1.22	-
Ratio virus RNA : IFN-β	0.31	0.33	-	0.31	0.31	-
Ratio virus RNA : IFN-α	0.41	0.42	-	0.40	0.40	-
Ratio virus RNA : functional IFN	0.27	-	-	0.25	0.23	-

Table 5A: A comparison of virus and IFN levels between wt and PKR$^{o/o}$ mouse brains.

The levels of infectious virus, virus RNA, IFN-β and IFN-α transcripts and functional IFN detected in wt and PKR$^{o/o}$ mouse brains at 40 hours post-infection. Each mouse brain assayed from each strain is indicated numerically. The ratios were determined per 10^6 pfu infectious virus or 10^6 virus RNA copies. – indicates no data available.

Does PKR affect IFN-β transcript production *in vitro* in response to SFV infection?

Given the surprising result that PKR had no detectable affect on SFV replication, IFN gene transcription or IFN functional activity in the brain, at least at 24 and 40 hours post-infection, it was decided to investigate the role of PKR at earlier time points and in a less complex *in vitro* system. Wild type and PKR$^{o/o}$ MEFs were grown to confluence and infected at a moi of 10 with SFV4 or mock infected with sPBS. At 4, 8 and 12 hours post-infection, 3 cultures each of wt and PKR$^{o/o}$ cells were collected, RNA extracted and reverse transcribed into cDNA. The cDNA was assessed for SFV RNA species and IFN-β transcripts (Figure 5G).

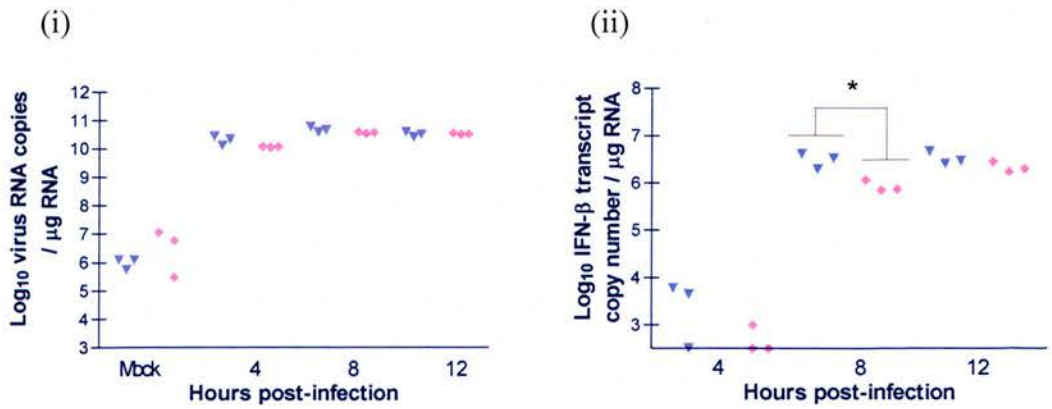

Figure 5G: IFN-β transcripts in wt and PKR$^{o/o}$ MEFs after SFV4 infection. 129/Sv/Ev wt (blue) and PKR$^{o/o}$ (pink) MEFs were grown to confluence in T20 flasks and infected with SFV4 at moi 10 or mock-infected with sPBS. At 4, 8 and 12 hours post-infection cells were harvested, RNA extracted and reverse transcribed into cDNA to determine levels of (**i**) SFV RNA species and (**ii**) IFN-β transcripts. Each point represents an individual cell culture assayed in triplicate by qPCR; the limit of detection of each assay is at the intersection of the axes. * indicates a significant difference ($p < 0.05$, Kruskal Wallis test) between 129/Sv/Ev wt and PKR$^{o/o}$ groups.

No IFN-β transcripts were detected in the negative controls; however, low levels of virus RNA (10^6 copies / µg RNA) were detected, suggesting that contamination had occurred. This was most likely due to SFV4 plasmid contamination of the PCR assay. SFV4 RNA levels remained relatively constant over the 12 hour period for both cell types. A high moi (10) was used, which should have resulted in complete monolayer infection and an early high and thereafter constant level of virus replication as is

shown by the data. There was no difference observed between the two cell types in their ability to support virus replication. In both cell types, the levels of IFN-β transcripts increased approximately 100-fold between 4 and 8 hours post-infection and then remained at a constant level up until 12 hours post-infection. There was no significant difference in the levels of IFN-β transcripts between cell types at 4 or 12 hours post-infection ($p > 0.05$, Kruskal Wallis). However, at all of the time points investigated, $PKR^{o/o}$ cells appeared to produce slightly lower amounts of IFN-β transcripts. At 8 hours post-infection $PKR^{o/o}$ cells produced slightly but significantly lower levels of IFN-β transcripts than wt cells ($p < 0.05$, Kruskal Wallis).

The experiment was repeated twice (II, III) and similar results were obtained (Figure 5H). In these experiments, no SFV RNA or IFN-β transcripts were detected from MEFs mock-infected with sPBS (data not shown). In experiment II, levels of virus RNA species increased slightly from 4 to 8 hours post-infection, perhaps suggesting that not all cells were initially infected (Figure 5H (i)). No significant difference was observed in either repeat experiment between the two cell types in their ability to support virus replication ($p > 0.05$, Kruskal Wallis). In experiment II, IFN-β transcripts steadily increased over the 12 hours post-infection for both cell types. At all three time points, $PKR^{o/o}$ cells induced significantly lower levels of IFN-β transcripts ($p < 0.05$, Kruskal Wallis) than wt cells (Figure 5H (ii)). To determine significance, data from all three time points were grouped into wt and $PKR^{o/o}$ cells to allow Kruskal Wallis analysis. In experiment III the $PKR^{o/o}$ cells also appeared to produce less IFN-β transcripts than wt cells, but this difference was not significant ($p > 0.05$, Kruskal Wallis, data not shown). In conclusion, SFV4 infection in the absence of PKR induces lower levels of IFN-β transcripts, at least during the first 12 hours of infection.

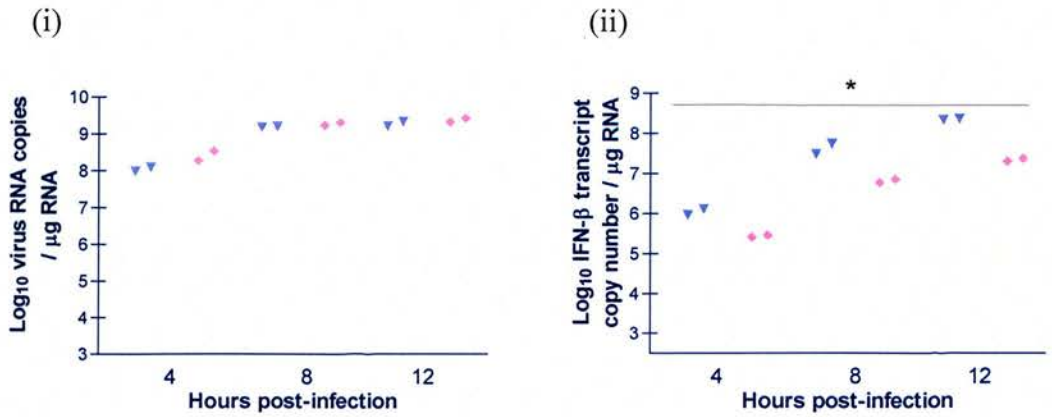

Figure 5H: Experiment II: IFN-β transcripts in wt and PKR$^{o/o}$ MEFs after SFV4 infection.
129/Sv/Ev wt (blue) and PKR$^{o/o}$ (pink) MEFs were grown to confluence in T20 flasks and infected with SFV4 at moi 10 or mock-infected with sPBS. At 4, 8 and 12 hours post-infection cells were harvested, RNA extracted and reverse transcribed into cDNA to determine the levels of (**i**) SFV RNA and (**ii**) IFN-β transcripts. Each point represents an individual cell culture assayed in triplicate by qPCR; the limit of detection of each assay is at the intersection of the axes and * indicates a significant difference ($p < 0.05$, Kruskal Wallis) between groups.

Are the levels of IFN-α influenced by PKR?

It has been suggested that PKR may be required for IRF-1 expression. IFN-α transcript induction does not need the multitude of transcription factors required for IFN-β transcription. IRFs are sufficient to induce IFN-α expression. To assess the levels of IFN-α induced, the cDNA samples generated to determine the levels of SFV RNA and IFN-β transcripts (Figure 5G; Figure 5H) were assayed for IFN-α transcripts with redundant primers based on IFN-α_4 (Figure 5I).

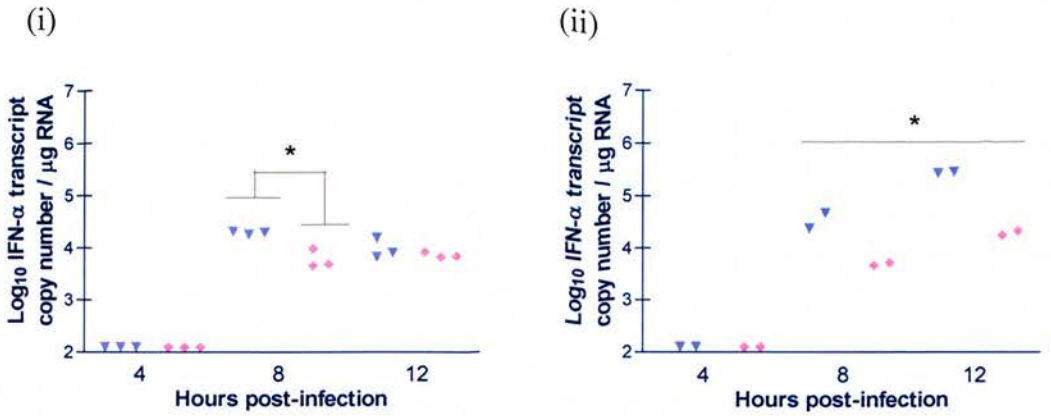

Figure 5I: IFN-α transcripts in wt and PKR$^{o/o}$ MEFs after SFV4 infection.
129/Sv/Ev wt (blue) and PKR$^{o/o}$ (pink) MEFs were grown to confluence in T20 flasks and infected with SFV4 at moi 10 or mock-infected with sPBS. At 4, 8 and 12 hours post-infection cells were harvested, RNA extracted and reverse transcribed into cDNA to determine the levels of IFN-α transcripts. IFN-α transcripts were detected in (**i**) experiment I and (**ii**) experiment II. Each point represents an individual cell culture assayed in triplicate by qPCR; the limit of detection of each assay is at the intersection of the axes. * indicates a significant difference ($p < 0.05$, Kruskal Wallis) between 129 wt and PKR$^{o/o}$ groups.

No IFN-α transcripts were detected in the mock-infected controls (data not shown) or in either experiment at 4 hours post-infection. In experiment I, IFN-α transcripts were detected in both wt and PKR$^{o/o}$ cells at 8 and 12 hours post-infection (Figure 5I (i)). The level of IFN-α transcripts detected in PKR$^{o/o}$ cells was significantly lower than wt cells at 8 hours post-infection ($p < 0.05$, Kruskal Wallis). This correlates with the level of IFN-β transcripts, which was also significantly lower in PKR$^{o/o}$ cells than wt cells at 8 hours post-infection (Figure 5G (ii)). In experiment II, the levels of IFN-α transcripts detected appeared lower in PKR$^{o/o}$ cells than wt cells at both 8 and 12 hours post-infection and pooling both time points, this difference was significant ($p < 0.05$, Kruskal Wallis, Figure 5I (ii)). Again this correlated with the IFN-β transcripts (Figure 5H (ii). Experiment III also demonstrated that IFN-α transcript levels were significantly lower in PKR$^{o/o}$ cells than wt cells at both 8 and 12 hours post-infection ($p < 0.05$, Kruskal Wallis, data not shown).

To determine whether there was any correlation between IFN-α and IFN-β transcripts, samples from 8 and 12 hours post-infection were compared (Experiment I). For each cell type there was no correlation between IFN-α and IFN-β transcript

levels; R^2 values were < 0.3. This was supported by experiment III, which also produced very low R^2 values; however, experiment II contradicted both of these sets of data and demonstrated a strong correlation between IFN-α and IFN-β transcripts for both cell types with R^2 values of 0.99. Experiments which demonstrated no correlation between IFN-α and IFN-β expression also showed constant levels of IFN-α and IFN-β transcripts at 8 and 12 hours post-infection; this implies that IFN gene expression had reached a maximum level. Where IFN-β levels increased between 8 and 12 hours post-infection (Experiment II), the levels of IFN-α transcripts also increased. In conclusion, these results suggest that PKR does not affect the level of IFN-α transcripts independently of an affect on IFN-β gene expression.

What accounts for the observed reduction in IFN transcription?

The reduced levels of IFN-α and IFN-β transcripts in SFV4 infected $PKR^{o/o}$ MEFs (Figure 5G; Figure 5H; Figure 5I) relative to wt MEFs are not associated with differences in virus replication (Figure 5G (i); Figure 5H (i)) and most likely result from a specific reduction in IFN gene activation. However, this difference could also result from a general decrease in gene transcription, increased transcript degradation or increased cell death. PKR is associated with regulation of the cell cycle through interactions with NF-κB. Reduced activation of NF-κB, a transcription factor involved in prolonging cell viability, could for example, cause increased cell death in $PKR^{o/o}$ MEFs resulting in lower levels of IFN transcripts. To assess cellular transcription, the cDNA generated to determine the levels of SFV RNA, IFN-β and IFN-α transcripts, was assayed for levels of β-actin transcripts (Figure 5J). β-actin transcription decreased after infection in both wt and $PKR^{o/o}$ cells. In experiment I, wt cells produced significantly lower levels of β-actin transcripts than mock-infected controls at 4, 8 and 12 hours post-infection ($p < 0.05$, Kruskal Wallis); in $PKR^{o/o}$ cells, β-actin levels were only significantly lower than mock-infected cells at 12 hours post-infection ($p < 0.05$, Kruskal Wallis) (Figure 5J (i)). Levels of β-actin in $PKR^{o/o}$ cells, but not wt cells, were also significantly lower than mock-infected cells at 12 hours post-infection in experiment II ($p < 0.05$, Kruskal Wallis) (Figure 5J (ii)). This

demonstrates that virus infection does result in degradation or shut-off of host gene transcription or cell death.

In experiment I, wt cells produced significantly lower levels of β-actin transcripts than PKR$^{o/o}$ cells at 8 and 12 hours post-infection ($p < 0.05$, Kruskal Wallis) and in experiment II, PKR$^{o/o}$ cells produced lower levels of β-actin transcripts at 12 hours post-infection than wt cells. Overall the data suggests neither cell type has a greater likelihood to induce transcriptional shut off or transcript degradation.

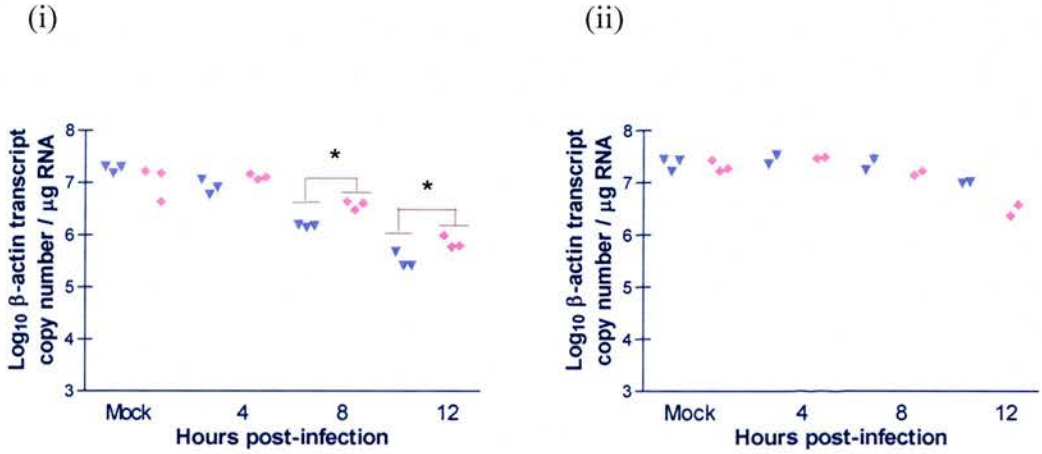

Figure 5J: β-actin transcripts in wt and PKR$^{o/o}$ MEFs after SFV4 infection.
129/Sv/Ev wt (blue) and PKR$^{o/o}$ (pink) MEFs were grown to confluence in T20 flasks and infected with SFV4 at a moi of 10 or mock-infected with sPBS. At 4, 8 and 12 hours post-infection cells were harvested, RNA extracted and reverse transcribed into cDNA to determine the levels of β-actin transcripts. β-actin transcripts were detected in (**i**) experiment I and (**ii**) experiment II. Each point represents an individual cell culture assayed in triplicate by qPCR; the limit of detection of each assay is at the intersection of the axes. * indicates a significant difference ($p < 0.05$, Kruskal Wallis) between 129 wt and PKR$^{o/o}$ groups.

To determine whether the decline in cellular transcription observed by 12 hours was related to cell death, MEFs grown to 90 % confluence in 96 well plates were infected (moi = 10) with SFV4, in replicates of 12 and at 6, 8, 10 and 12 hours post-infection were incubated with WST-1 reagent for 3 hours to determine viability (Figure 5K). No difference in cell viability was detected with time or between the cell types. The decrease with time in β-actin transcripts cannot be attributed to cell death.

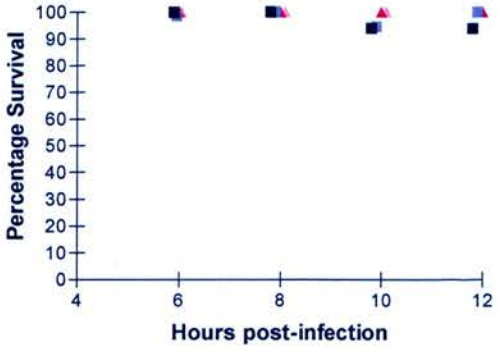

Figure 5K: MEF percentage survival after SFV4 infection
Wild type (Blue square) and PKR$^{o/o}$ (Pink triangle) MEFs were infected, in replicates of 12, with SFV4 (dark blue or dark pink) at a moi of 10 or mock-infected with PBS (light blue or light pink). At 6, 8, 10 or 12 hours post-infection cells were assayed for viability. Each point represents the mean of 12 replicates.

Does PKR affect functional IFN production *in vitro* in response to SFV infection?

Differences in the levels of transcripts for IFN-β and IFN-α observed between wt and PKR$^{o/o}$ MEFs should translate to differences in the levels of functional IFN. To investigate this, wt and PKR$^{o/o}$ MEFs were seeded at 2 x 10^5 cells per well in chamberslides, grown to confluence and infected (moi 10) with SFV4 or mock-infected with sPBS. Supernatant samples were collected at 24 hours post-infection to assess levels of infectious virus and functional IFN (Figure 5L). No infectious virus or functional IFN was detected for the mock-infected controls (data not shown). Equivalent levels of infectious virus were detected in supernatant samples taken from wt and PKR$^{o/o}$ MEFs (Figure 5L, i-a). However, the level of functional IFN in the infected PKR$^{o/o}$ cells was significantly reduced ($p < 0.05$, Mann-Whitney) in comparison to infected wt cells (Figure 5L, i-b). In a repeat experiment, (Figure 5L, (ii)), supernatant samples were taken at 18 and 24 hours post-infection and assayed for infectious virus (Figure 5L, ii-a) and functional IFN (Figure 5L, ii-b). Levels of infectious virus were similar in both cell types at 18 and 24 hours post-infection; however, no functional IFN could be detected from PKR$^{o/o}$ cells at either time point. Levels of functional IFN produced in wt cells were similar at both 18 and 24 hours.

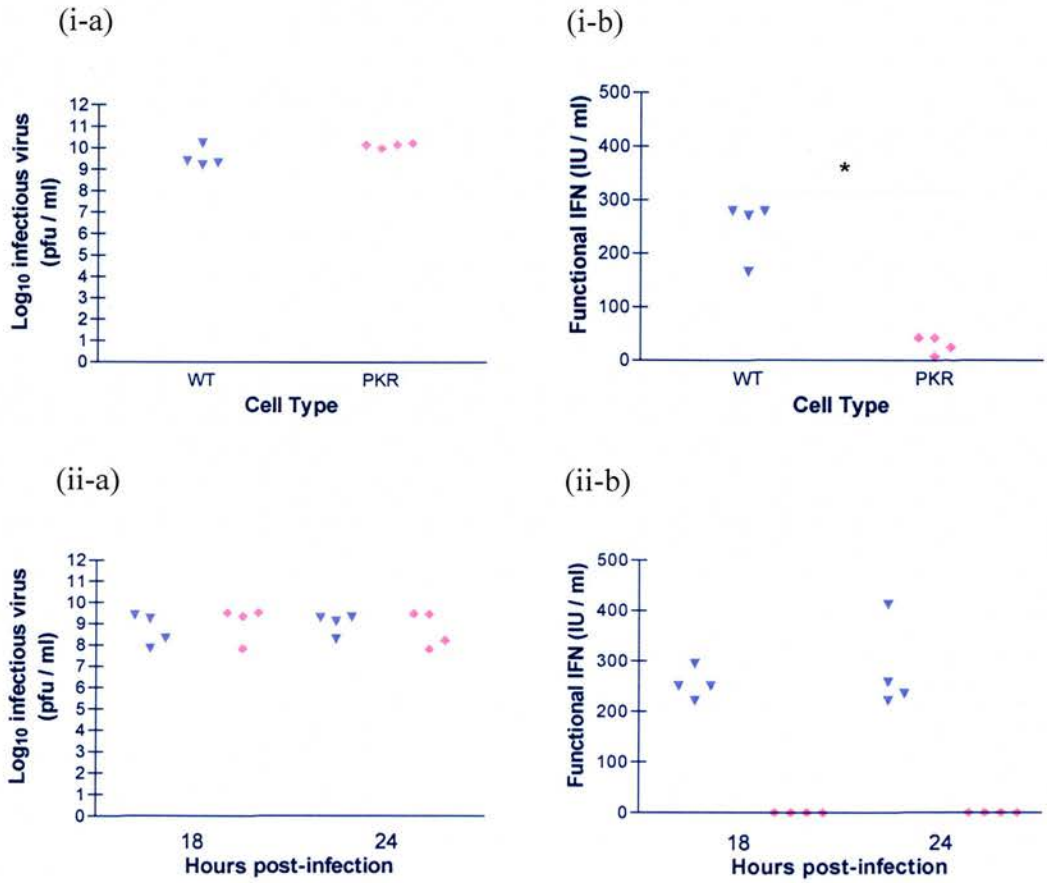

Figure 5L: Functional IFN levels in wt and PKR$^{o/o}$ cells after SFV infection.
129/Sv/Ev wt (blue) and PKR$^{o/o}$ (pink) MEFs were grown to 90 % confluence in chamberslide wells and then infected at a moi of 10 with SFV4. At (**i**) 24 hours and (**ii**) 18 and 24 hours post-infection supernatants were sampled and assayed for (a) infectious virus and (b) functional IFN. Each point represents an individual cell culture mean and * indicates a significant difference ($p < 0.05$, Mann-Whitney) between 129 wt and PKR$^{o/o}$ groups.

.

Summary of findings

In vivo,

- There were no significant differences in SFV4 infectious virus titres at 24 hours post-infection or virus at 12, 24 or 40 hours post-infection in the brains of wt and $PKR^{o/o}$ mice.
- At 24 and 40 hours post-infection there were no significant differences in levels of functional IFN between 129/Sv/Ev wt and $PKR^{o/o}$ mouse brains.
- IFN-β transcripts were detected in both mouse strains by 24 hours. At 24 and 40 hours transcript levels were similar. IFN-β transcripts were only detected in mouse brains with viral RNA titres of $> 1 \times 10^6$ copies / 100,000 β-actin copies. IFN-β transcripts strongly correlated with SFV4 RNA levels in wt and $PKR^{o/o}$ cells ($R^2 = 0.91$ and 0.9, respectively).
- IFN-α transcripts were detected in both wt and $PKR^{o/o}$ mice after 24 hours, but only when IFN-β transcript levels $> 2 \times 10^3$ copies / 100,000 β-actin copies. In both cell types, IFN-α transcripts were proportional to SFV4 RNA ($R^2 = 0.94$ and 0.85, wt and $PKR^{o/o}$ respectively) and IFN-β transcripts ($R^2 = 0.99$ and 0.99, wt and $PKR^{o/o}$ respectively).

In vitro,

- SFV4 infectious virus titres and virus RNA copies demonstrated no significant difference between 129/Sv/Ev wt and $PKR^{o/o}$ MEFs.
- IFN-β transcripts were consistently lower in $PKR^{o/o}$ cells than 129 wt cells at 4, 8, and 12 hours post-infection and were significantly lower at 8 hours ($p < 0.05$, Kruskal Wallis test).
- IFN-α transcripts were detected by 8 hours post-infection in both wt and $PKR^{o/o}$ cells. IFN-α transcripts were significantly lower in $PKR^{o/o}$ cells than in 129 wt cells ($p < 0.05$, Kruskal Wallis test).
- Reduced IFN transcript levels in $PKR^{o/o}$ cells was not associated with greater cell death, increased transcript degradation or greater transcription shut-off.
- At 24 hours post-infection, functional IFN levels in the supernatants of cultured $PKR^{o/o}$ MEFs were 10-fold lower than in 129 wt MEF supernatants ($p < 0.05$, Mann-Whitney test).

Discussion

The role of PKR in IFN induction has not been defined in alphavirus infections. Investigations into the role of PKR in SFV4 infected mouse brains demonstrated that there was no significant difference in the levels of IFN-α transcripts, IFN-β transcripts or functional IFN between wt and $PKR^{o/o}$ strains at 24 or 40 hours post-inoculation and that the virulence of SFV4 infection did not alter between the strains. However, comparisons between SFV4 infected wt and $PKR^{o/o}$ MEFs at 4, 8 and 12 hours post-infection demonstrated that relative to wt, $PKR^{o/o}$ cells produced consistently lower levels of IFN-α transcripts, IFN-β transcripts and functional IFN. This decrease in IFN expression was not related to differences in virus replication, transcript degradation, transcription shut-off or cell death.

In vivo infections showed considerable variation between mice, due to the variability of the site of inoculation, the resulting cell types infected and a low moi of infection. Small differences resulting from the ablation of PKR function would be unlikely to be observed in this *in vivo* system. In contrast, *in vitro* experiments used cultured primary cell lines infected at a high moi to allow for a synchronous infection of most cells; this resulted in synchronous induction of IFN-β gene expression and allowed detection of small differences resulting from the presence or absence of PKR.

Previous experiments, which compared the same wt and $PKR^{o/o}$ mice, showed that NDV infection induced similar levels of IFN-α and IFN-β transcripts in the spleen, lung and liver of both wt and $PKR^{o/o}$ mice and that EMCV infection induced similar IFN serum levels in both strains of mice (Yang et al., 1995). In contrast to the results found in this chapter, NDV also induced similar levels of IFN-α and IFN-β transcripts in wt and $PKR^{o/o}$ MEFs. However, the northern blot technique described in Yang et al. (1995) would have been unlikely to have detected subtle differences in the level of IFN-β or IFN-α transcripts, whereas the qPCR used here is a very sensitive assay and so can distinguish small differences. The *in vitro* data described here suggests that PKR contributed to IFN-β gene expression during the early stages of SFV4 infection. PKR is continuously and constitutively expressed in cells (Baier et al., 1993) and as such it is likely that it is a first-line sentinel of infection. Loss of PKR would therefore be expected to reduce the rate of virus detection resulting in a delay in the

induction of IFN. PKR is an upstream inducer of IFN-β gene expression during reovirus infection of primary myocyte cardiac cultures (Stewart et al., 2003) and during EMCV infection of U-937 cells (Der and Lau, 1995). U-937 cells over-expressing PKR antisense RNA or dominant negative PKR and then infected with EMCV did not produce IFN-β transcripts by 6 hours post-infection and only produced variable levels of IFN after 16 hours. Additionally, PKR inhibitors ablate poly I:C gene induction in intestinal epithelial cells. Localisation of this inhibition is identical to that of pharmacological inhibition of gene expression responses to rotavirus, suggesting that PKR has a role in activating gene expression in response to rotavirus infection (Vijay-Kumar et al., 2005). It has also been suggested that RNase-L and PKR induced transcriptional and/or translational shut off may be required to prevent the expression of inhibitors of MKK4 and c-jun N-terminal kinase (JNK) (Iordanov et al., 2001). JNK phosphorylates and activates the transcription factor c-jun, a component of AP-1, one of the transcription factors required to induce IFN-β expression. Consequently, the loss of PKR may enable continued expression of these kinase inhibitors, reducing the amount of IFN-β expressed.

PKR is an intracellular dsRNA activated protein kinase. Recently several other intracellular dsRNA activated proteins have been described, e.g. RIG-I and mda-5, which induce IFN-β gene expression. This complementarity in the detection of dsRNA may provide an explanation for the partial but not complete reduction of IFN-β expression observed in $PKR^{o/o}$ cells.

Mice lacking PKR do not have a defective immune response (Yang et al., 1995), but many viruses show increased virulence in $PKR^{o/o}$ cells (Streitenfeld et al., 2003; Balachandran et al., 2000). Only IFN-γ responses are reduced in $PKR^{o/o}$ mice (Abraham et al., 1999; Yang et al., 1995). This is possibly associated with PKR interactions with STAT-1. The IFN- γ receptor signals through STAT-1 homodimers. PKR modulates the ability of STAT-1 to induce transcription (Wong et al., 1997); $PKR^{o/o}$ cells demonstrate reduced STAT-1 serine 727 phosphorylation and transactivation (Koromilas et al., 1992; Ramana et al., 2000). Despite several viruses demonstrating increased virulence in $PKR^{o/o}$ cells (Bunyamwera virus (Streitenfeld et al., 2003), VSV and influenza virus (Balachandran et al., 2000)), SFV produced

similar levels of virus RNA at 4, 8 and 12 hours post-infection and of infectious virus at 24 hours post-infection in wt and $PKR^{o/o}$ cells. SFV4 was able to establish an infection more rapidly in $PKR^{o/o}$ cells than in wt cells (unpublished data provided by Gerald Barry). 129 wt and $PKR^{o/o}$ cells were infected with SFV4-eGFP, an SFV4 vector encoding enhanced green fluorescent protein (eGFP). At 3 hours post-infection eGFP was observed in the $PKR^{o/o}$ cells whereas eGFP was only observed in the wt cells at 7 hours post-infection. These results suggest that $PKR^{o/o}$ cells replicate SFV4 more rapidly than do wt cells. In $PKR^{o/o}$ cells virus may not be detected as early as in the presence of PKR, allowing replication to progress further before IFN-β gene expression is initiated. In the presence of PKR, host translation is shut off by the phosphorylation of eIF-2α. eIF-2α phosphorylation induces the formation of stress granules which sequester mRNA and pre-initiation complexes (Kedersha et al., 1999; 2002; Gilks et al., 2004). Maintaining components of translation in the stress granules inhibits virus access to translation initiation complexes and may account for the delay in eGFP detection. Alternatively, SFV has some resistance to PKR and so the lack of functional PKR does not promote virus replication. Recently a highly stable hairpin loop, downstream of the translation start site of Sindbis virus 26 S mRNA has been implicated in resistance to eIF-2α phosphorylation (Ventoso et al., 2006). This structure stalls the ribosome at the correct start site enabling translation to bypass the requirement of an initiation complex. Bovine viral diarrhoea virus (BVDV) modulates PKR activity; the non-cytopathic strain (ncpBVDV) does not induce PKR and challenge with a poliovirus does not initiate PKR phosphorylation (Gil et al., 2005); infection with poliovirus alone would normally result in PKR phosphorylation, therefore ncpBVDV prevents PKR activation.

Interestingly, the increased virulence of some virus infections of $PKR^{o/o}$ mice is associated with the site of inoculation. VSV and WSN strain of influenza virus infections following *in* inoculations of $PKR^{o/o}$ mice are much more virulent than *iv* inoculations (Balachandran et al., 2000). It is possible that this form of inoculation allows these viruses access to the CNS through the olfactory nerves, although PKR may be important in respiratory immune responses. Basal PKR levels are higher in pulmonary tissues (Krust et al., 1982); this supports the role of PKR as a sentinel for infection, as respiratory epithelia are directly exposed to invading pathogens.

Summary

This chapter determined whether there was a role for PKR in IFN-β induction and functional IFN expression in mouse brains and primary cell lines during an SFV4 infection. No significant differences were observed in the levels of IFN transcripts or functional IFN between wt and $PKR^{o/o}$ mouse brains. However, $PKR^{o/o}$ mouse embryo fibroblasts consistently produced significantly lower levels of type I IFN transcripts and functional IFN in comparison to wt cells. This was not explained by changes in cell death or RNA degradation.

Chapter 6: Differential dynamics of IFN induction by different strains of SFV

Contents

Objectives....148
Introduction....148
Comparison of IFN induction by SFV4, SFV4nsP2RDR and SFV4nsP3Δ50....149
Comparison of growth of SFV4 and SFV4nsP2RDR in BHK cells and MEFs....152
Comparison of virus RNA and IFN-β transcript levels in SFV4, SFV4nsP2RDR and SFV A7(74) infected L-929 cells and MEFs....153
Comparison of β-actin and GAPDH transcript levels in SFV4, SFV4nsP2RDR and SFV A7(74) infected L-929 cells and MEFs....155
Comparison of IFN levels in SFV4 and SFV4nsP2RDR infected L-929 cells....159
Comparison of translation shut off kinetics between SFV4 and SFV4nsP2RDR infected BHKs....161
Comparison of NF-κB and IRF-3 nuclear translocation between SFV4 and SFV4nsP2RDR infected MEFs....163
Comparison of NF-κB IFN-β promoter binding in SFV4 and SFV4nsP2RDR infected MEFs....165
Summary of Findings....168
Discussion....169
Summary....172

Differential dynamics of IFN induction by different strains of SFV

Objectives

1) To determine whether virulent (SFV4) and avirulent (SFV A7(74), SFV4nsP2RDR and SFV4nsP3Δ50) strains of SFV induce different levels of IFN-β transcripts.
2) To determine whether virulent (SFV4) and avirulent (SFV4nsP2RDR) strains of SFV induce different amounts of functional IFN.
3) To determine whether SFV antagonises the IFN response and if so, by what mechanism.

Introduction

There are several strains of SFV, which can pathologically be divided into two groups, those that cause panencephalitis in adult mice and those that have a restricted CNS infection. Following virulent infection, virus antigen can be detected throughout the brain; following an avirulent infection, virus can only be detected in small foci of cells around blood vessels (Fazakerley et al., 1993). A possible explanation for the differential pathology could be that the virulent SFV strains induce less IFN or delay IFN expression. This would allow greater virus replication and spread. To study the affect of SFV infection on IFN induction, several different SFV strains, virulent and avirulent, were investigated, SFV4, SFV4nsP3Δ50, SFV4nsP2RDR and SFV A7(74). The 'prototype' strain of SFV was derived from SFV L10 and like L10 is virulent in adult mice. SFV4 is an infectious molecular clone of the prototype virus (Liljestrom et al., 1991). SFV4nsP3Δ50 and SFV4nsP2RDR are engineered mutants of SFV4; SFV4nsP3Δ50 has a 50 amino acid deletion at the C-terminal end, which includes a hyperphosphorylated region. NsP3 has yet to be assigned any particular roles; it is part of the replicase complex and other mutational studies have implicated it to be important in virulence (Tuitilla et al., 2001); no function has been determined for the hyperphosphorylation. SFV4nsP2RDR possesses a single amino acid mutation (RDR) in the nuclear localisation signal (RRR) of the non-structural protein (nsP) 2

(Rikkonen et al., 1992). There are several defined functions for nsP2; these include helicase activity, papain-like protease activity and triphosphatase activity (Rikkonen et al., 1994). In addition, 50 % of nsP2 enters the nucleus during an infection (Rikkonen, 1996), although currently there is no known function for nuclear nsP2. The SFV4nsP2RDR mutation completely disrupts the ability of nsP2 to translocate into the nucleus (Rikkonen, 1996). SFV A7(74) is an avirulent strain of SFV.

In vivo investigations comparing SFV4nsP2RDR and SFV4 inoculated *ip* into wildtype 129 mice show that SFV4nsP2RDR only establishes a restricted infection whereas, SFV4 establishes a panencephalitis; however, when inoculated into $IFNAR^{-/-}$ mice, SFV4nsP2RDR also produces a panencephalitis (Fazakerley et al., 2002). Disruption of the type I IFN receptor renders $IFNAR^{-/-}$ mice unresponsive to type I IFN. This result suggests that whereas type I IFN controls the CNS spread of SFV4nsP2RDR preventing panencephalitis, it does not effectively limit the spread of SFV4. Possible explanations for this result and the differential pathology between the two strains could be: 1) that the SFV4nsP2RDR mutation reduces the rate of virus replication enabling the establishment of the IFN anti-viral response and control of the infection. This could also be a factor in other avirulent infections (SFV A7(74) and SFV4nsP3Δ50); 2) that avirulent strains of SFV are more sensitive to the effect of IFN and 3) that SFV4 but not SFV4nsP2RDR or SFV A7(74) is able to evade the IFN response. These possibilities were investigated by characterising and comparing the level of IFN induction between SFV4, and avirulent SFV4nsP2RDR, SFV A7(74) and SFV4nsP3Δ50.

Comparison of IFN induction by SFV4, SFV4nsP2RDR and SFV4nsP3Δ50

To investigate IFN induction between molecularly defined virulent and avirulent viruses, IFN levels induced by SFV4, SFV4nsP2RDR and SFV4nsP3Δ50 were compared. Stocks of SFV4nsP2RDR and SFV4nsP3Δ50 were analysed to confirm the phenotype and genotype prior to use. In SFV4 infected cells, nsP2 was located both in the cytoplasm and the nucleus. Cells infected with SFV4nsP2RDR, as

expected, showed no nuclear staining for nsP2 (Figure 6A). Both viruses were sequenced to confirm their mutations; T80 flasks of BHK cells were infected at a moi of 10 with SFV4, SFV4nsP2RDR or SFV4 nsP3Δ50 and incubated for 11 hours. RNA was extracted from the infected cell cultures and quantified on an Agilent bioanalyser. Five μg of RNA were transcribed into cDNA using a specific primer outside the mutated region (Table 2D, Materials & Methods). A high fidelity PCR reaction was performed and the product size confirmed on a gel. Each of the PCR products were cloned into TOPO vectors, which were then transformed into *E.coli* and grown overnight on LB- Kanamycin plates. Three colonies from each plate were selected and grown as cultures. DNA was extracted by mini-prep and sent for sequencing (VBS, University of Edinburgh). All sequences were as expected.

Several studies with SFV4nsP3Δ50 demonstrated that, regardless of the moi, only 50 - 60 % infection of cell monolayers was ever observed. This effect was observed in two separate laboratories. To study the affects of IFN induction, a high level of infection of the cell monolayers is necessary for uncomplicated data interpretation. Consequently, further studies of SFV4nsP3Δ50 interactions with the IFN response were terminated.

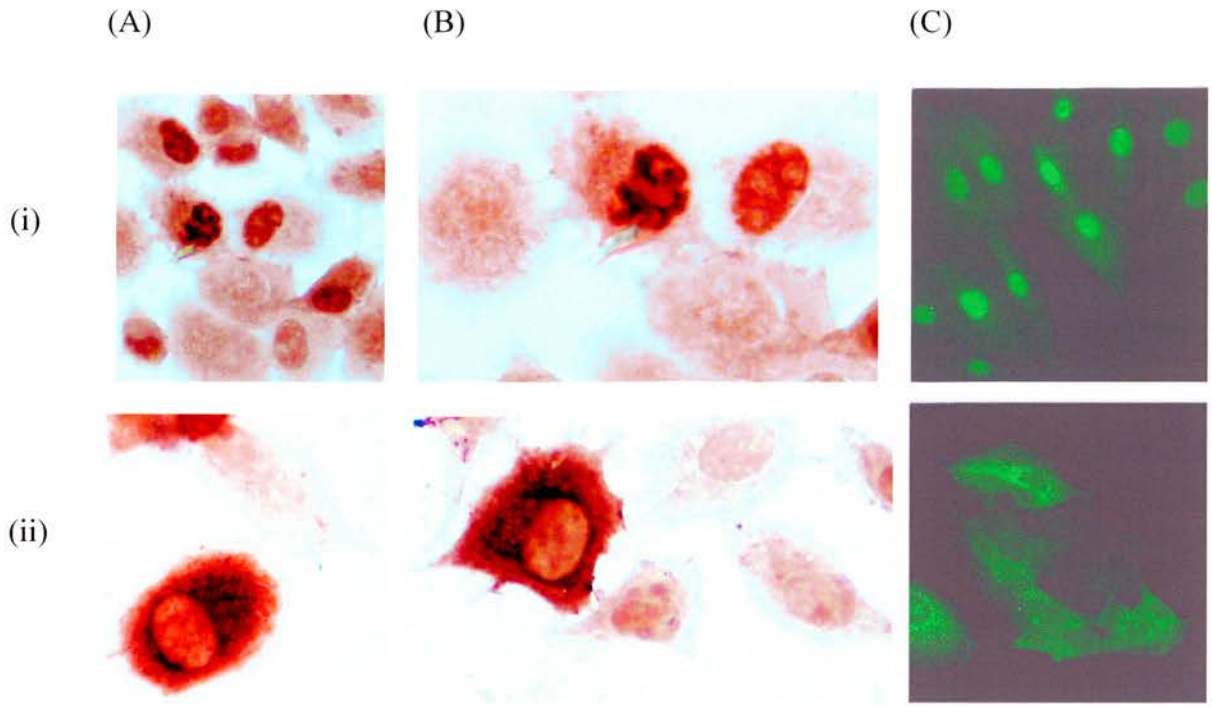

Figure 6A: Localisation of nsP2 during an SFV4 or SFV4nsP2RDR infection
MEFs were infected with (**i**) SFV4 or (**ii**) SFV4nsP2RDR virus (A, B) or non-replicating vectors (C). MEFs were infected at a moi of 1 with either strain and stained for nsP2 with Novared chromogen (A, B) or immunofluoresence (C). (C) was kindly donated by Gerald McInerney (Karolinska Institutet, Sweden).

Comparison of growth of SFV4 and SFV4nsP2RDR in BHK cells and MEFs

The growth of these two viruses was compared in BHK cells and in MEFs in multi-step growth curves. This data was generated in collaboration with Pia Dosenovic (Karolinska Institutet, Sweden). BHK cells have impaired IFN responses, whereas MEFs are IFN competent. For each cell type, in duplicate, T25 flasks were infected with either SFV4 or SFV4nsP2RDR at a moi of 0.05. Cells were infected at a low moi (0.05) to produce a multi-step growth curve; this infection should reveal any differences in the ability of the viruses to replicate and spread across the cell monolayer. In contrast, high moi infections (> 10) enable investigations into cellular responses or virus protein function, independent of virus replication and spread. Supernatant samples were taken at 4, 8, 12, 24 and 48 hours post-infection and the levels of infectious virus were determined by plaque assay (Figure 6B). Similar titres of infectious virus were present at each time point in BHK cell supernatants. This was also observed in infected MEFs up until 12 hours post-infection. After 12 hours the levels of RDR infectious virus remained approximately 0.5 $\log_{10}$ lower than the levels of SFV4 infectious virus.

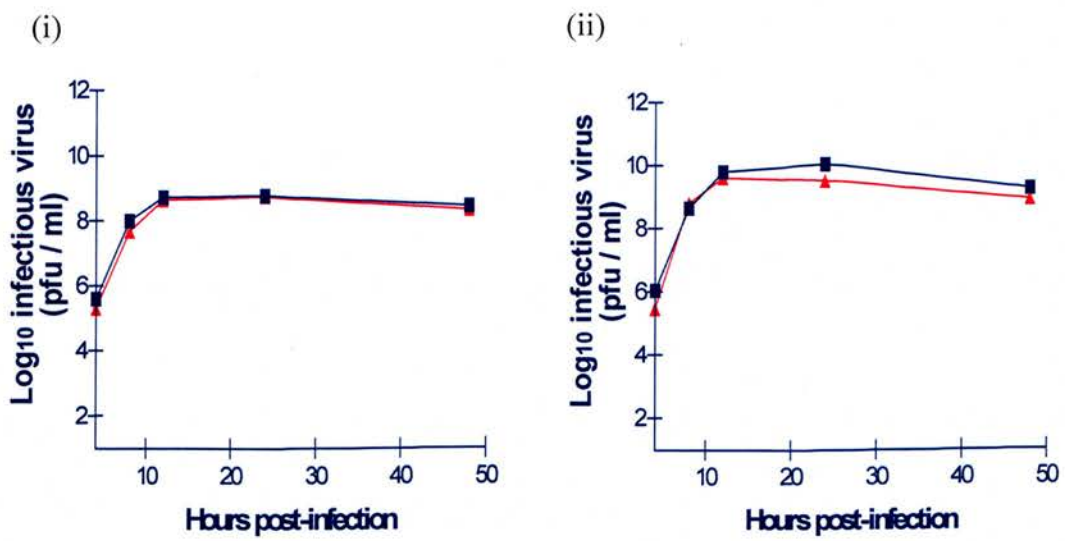

Figure 6B: Growth curves of SFV4 and SFV4nsP2RDR in BHK cells and MEFs. Cultures of (**i**) BHK cells or (**ii**) MEFs were infected with SFV4 (Blue) or SFV4nsP2RDR (Red) at a moi of 0.05. Supernatant samples were collected at 4, 8, 12, 24 and 48 hours post-infection and assayed for infectious virus. Each point represents the mean of two supernatant samples. Data provided in collaboration with Pia Dosenovic (Karolinska Institutet, Sweden).

Comparison of virus RNA and IFN-β transcript levels in SFV4, SFV4nsP2RDR and SFV A7(74) infected L-929 cells and MEFs

To determine whether levels of IFN induction varied between SFV4, SFV4nsP2RDR and SFV A7(74) infections, levels of virus RNA and IFN-β transcripts were measured. T20 flasks were seeded with either L-929 cells or MEFs and incubated until confluent. At confluence, triplicate cultures of cells were infected with either SFV4, SFV4nsP2RDR or SFV A7(74) at a moi of 50 or mock infected with PBS. Initially, SFV4nsP3Δ50 was included in these experiments, but was only observed to infect 50 – 60 % of the monolayer at a moi of 10, consequently the moi was raised to 50. Despite increasing the moi, SFV4nsP3Δ50 still only infected approximately 50 % of cells and so was removed from the experiment. To maintain consistency with the preliminary experiments the moi was kept at 50. At 12 hours post-infection, cells were harvested and the RNA extracted and reverse transcribed into cDNA. The levels of virus RNA and IFN-β transcripts were quantified from the cDNA by qPCR (Figure 6C). No virus RNA or IFN-β transcripts were detected in the mock infected cell cultures (data not shown). Similar levels of virus RNA were produced by all three virus strains in both cell types (Figure 6C (a)). SFV4 and SFV A7(74) induced similar levels of IFN-β transcripts in both L-929 cells and MEFs (Figure 6C (b)); however, SFV4nsP2RDR induced significantly higher levels of IFN-β transcripts compared to SFV4 in both cell types ($p < 0.05$, Kruskal Wallis test). This correlated to a 50 – 200 fold increase in the duplicate experiments in L-929 cells (Figure 6C (c)) and a 5-fold increase in MEFs. The two cell types both demonstrated that SFV4nsP2RDR induces more IFN-β gene expression than SFV4.

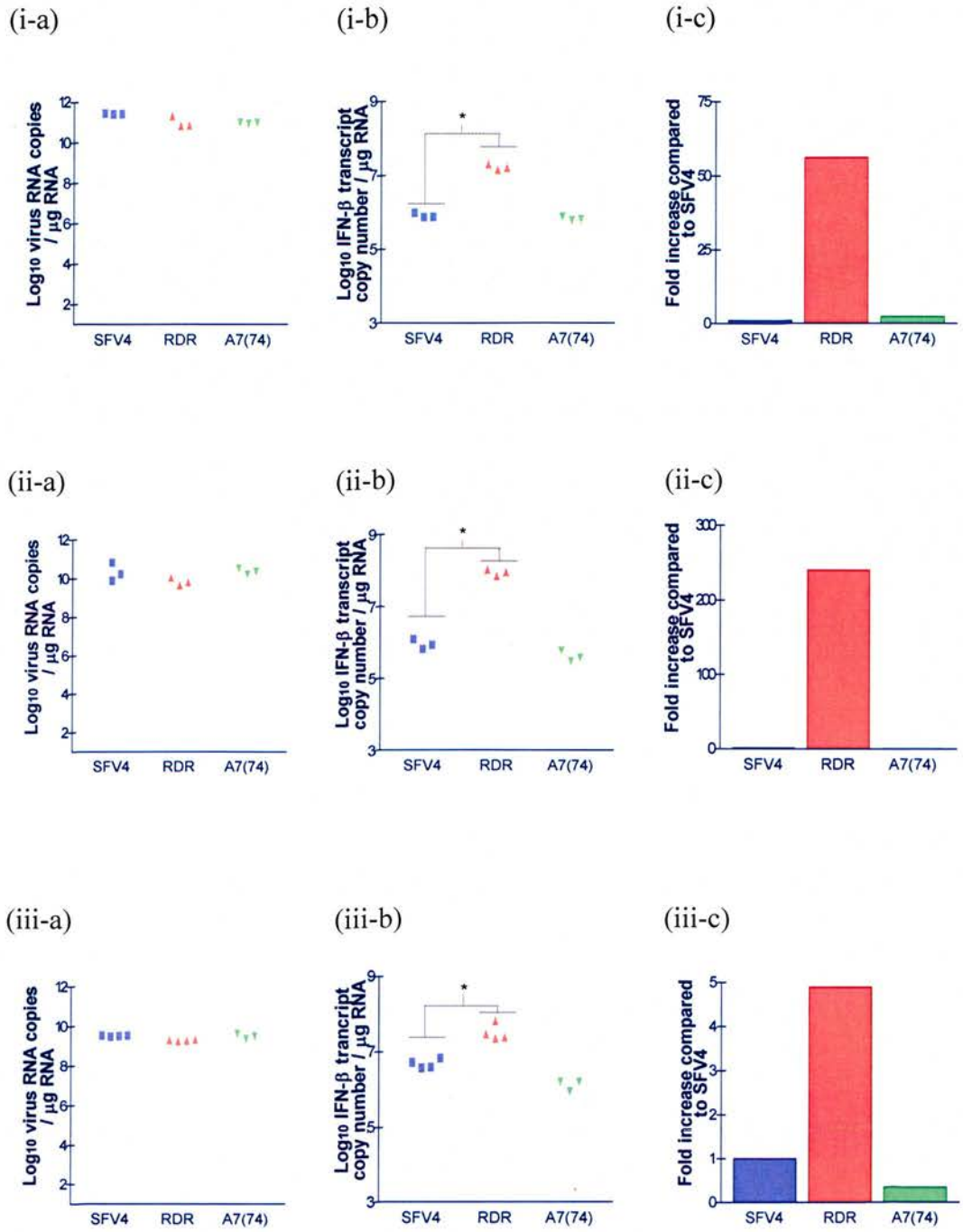

Figure 6C: IFN-β transcript induction by SFV4, SFV4nsP2RDR and SFV A7(74). Cultures of (**i; ii**) L-929 cells or (**iii**) MEFs were infected at a moi of 50 with SFV4, SFV4nsP2RDR or SFV A7(74). At 12 hours post-infection, RNA extracted from the cultures was assayed for (a) virus RNA and (b) IFN-β transcripts. Each point represents the mean value from a cell culture assayed in triplicate by qPCR; * indicates that the IFN-β transcript levels induced were significantly different to IFN-β transcripts induced by SFV4 ($p < 0.05$, Kruskal Wallis test). Bars represent the fold increase in the levels of IFN-β transcripts per 10^6 SFV4nsPRDR virus RNA copies compared to the levels of IFN-β transcripts per 10^6 SFV4 RNA copies.

In conclusion, SFV4nsP2RDR induces more IFN-β transcripts per 1 x 10^6 virus RNA copies than SFV4 or SFV A7(74). The observed increase of IFN-β transcripts during an SFV4nsP2RDR infection could be specific to IFN-β or could reflect lack of downregulation of all cellular transcripts.

Comparison of β-actin and GAPDH transcript levels in SFV4, SFV4nsP2RDR and SFV A7(74) infected L-929 cells and MEFs

To determine whether the effect of increased transcript expression was specific to IFN-β in an SFV4nsP2RDR infection, two housekeeping genes β-actin and GAPDH were also investigated. Confluent T20 flasks of L-929 cells and MEFs were infected at a moi of 50 with SFV4, SFV4nsP2RDR, SFV A7(74) or mock infected with PBS. At 12 hours post-infection the cell cultures were harvested and RNA extracted and reverse transcribed into cDNA. The level of β-actin and GAPDH transcripts in the cDNA was determined by qPCR (Figure 6D). For both β-actin and GAPDH, transcript levels were similar between the two cell types for mock infection, with GAPDH transcript levels approximately 10-fold lower than β-actin transcript levels (Figure 6D (a; b). Both L-929 cells and MEFs infected with all three viruses expressed similar levels of β-actin transcripts, approximately 10^6 / μg total RNA (Figure 6D (a)). This was a 10-fold decrease in the levels of β-actin transcripts from the duplicate experiments in L-929 cells and a 3-fold decrease in the levels of β-actin transcripts in MEFs (Figure 6D (c)). These levels were all significantly lower than mock infected cultures ($p < 0.05$, Kruskal Wallis test). The levels of GAPDH transcripts were similar between cultures infected with all three viruses in 2 out of 3 experiments. This correlated to a 5-fold decrease in the levels of GAPDH transcripts in both cell types (Figure 6D (c)). In all three experiments the levels of GAPDH transcripts were significantly lower in virus infected cells than in mock infected cells ($p < 0.05$, Kruskal Wallis test) (Figure 6D (b).

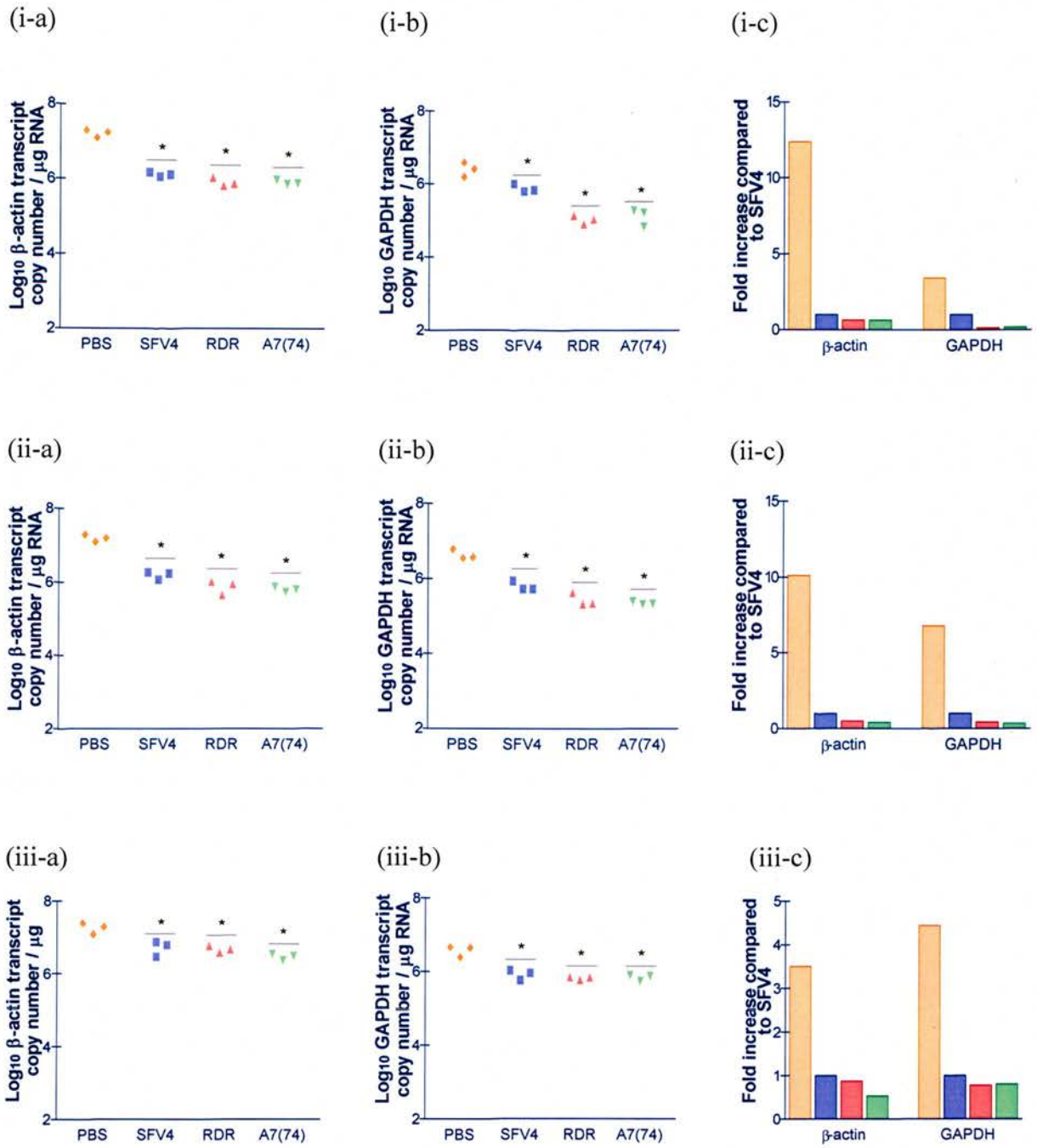

Figure 6D: β-actin and GAPDH transcript levels in PBS, SFV4, SFV4nsP2RDR and SFV A7(74) infected cell cultures.

Cell cultures of (**i; ii**) L-929 cells and (**iii**) MEFs were infected at a moi of 50 with SFV4, SFV4nsP2RDR, SFV A7(74) or mock infected. At 12 hours post-infection the cultures were assayed for levels of (a) β-actin and (b) GAPDH transcripts. Each point represents the mean value from a cell culture assayed in triplicate by qPCR; * represents transcript levels were significantly lower than mock infected cells ($p < 0.05$, Kruskal Wallis test). Bars represent the fold-increase in the levels of transcripts compared to SFV4 infected cell cultures.

To summarise, at 12 hours post-infection the levels of β-actin and GAPDH transcripts in virus infected cells were significantly less than in mock infected cells. This reduction in cellular mRNA could result from virus induced cellular transcription shut-off and mRNA degradation. There was no difference between the reduced levels of cellular transcripts between the three virus strains. This suggests that the higher levels of IFN-β transcripts observed in SFV4nsP2RDR infected cells relative to SFV4 infected cells was specific to IFN-β gene expression. However, it could be argued that only two cellular transcripts were investigated. As another test, MEFs were seeded onto a 6 well plate and infected in triplicate at a moi of 50 with SFV4, SFV4nsP2RDR or mock infected with PBS, (this experiment was carried out by Pia Dosenovic, Karolinska Institutet, Sweden). Two of the three wells were used to assess RNA replication; the remaining well was used to ascertain the level of infection. To determine the level of infection, the infected monolayer was stained for SFV envelope 2 antigen and 15 separate areas from the monolayer were counted for infected cells. For both viruses the level of infection was approximately 95 – 100 %. To assess RNA replication, actinomycin D was added to one of the infected wells at 4.5 hours post-infection and incubated for 30 minutes prior to the addition of [^{14}C]Uridine. After a further 3 hours, at 8 hours post-infection, the cells were lysed and RNA extracted. 1.8 μg of each RNA sample was run on a gel and exposed on film (Figure 6E). Actinomycin D prevents cellular transcription; therefore all actinomycin D positive wells only showed virus RNA species. These include the 42 S genomic RNA and the 26 S sub-genomic RNA. Actinomycin D positive, mock infected cells showed no detectable bands (Figure 6E - column 1); however, SFV4 and SFV4nsP2RDR infected cells showed the two virus RNA species and no cellular RNA transcripts (Figure 6E – columns 2 and 3). In contrast, actinomycin D negative wells showed both cellular and virus RNA species. Several bands of cellular transcripts are observed in mock infected cells (Figure 6E – column 4); however, SFV4 and SFV4nsP2RDR infected cells show the two virus RNA species and dramatically reduced levels of cellular RNA transcripts compared to mock infected cells (Figure 6E – column 5 and 6). Together with the qPCR data (Figure 6D), this suggests that during an SFV infection cellular transcription is reduced and that this is not obviously different for these two viruses.

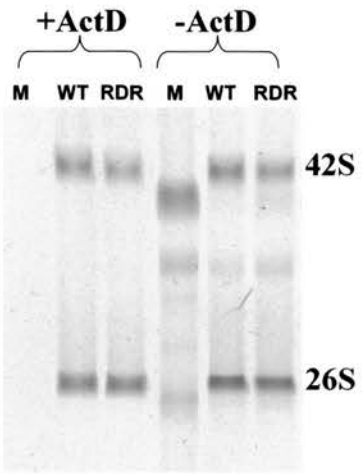

Figure 6E: Reduction of cellular transcripts in SFV infected cells.
MEFs were infected at a moi of 50 with SFV4 (WT), SFV4nsP2RDR (RDR) or mock infected with PBS (M). MEFs were incubated with or without actinomycin D (Act D) and then cultured in media containing [^{14}C]Uridine. At 8 hours post-infection the cells were harvested and RNA extracted. Bands labelled as 42 S and 26 S correspond to virus genomic and sub-genomic RNA species; unlabelled bands represent cellular RNA transcripts. Kindly provided by Pia Dosenovic (Karolinska Institutet, Sweden).

Comparison of IFN levels in SFV4 and SFV4nsP2RDR infected L-929 cells

Functional IFN levels were determined, as virus induced host translation shut-off could alter the IFN protein levels so that they did not correlate with the IFN transcript levels. SFV4 and SFV4nsP2RDR were compared for their ability to induce functional IFN in L-929 cells. SFV4nsP2RDR induced higher levels of IFN-β transcripts than SFV4 in L-929 cells, and should induce higher levels of functional IFN in comparison to SFV4. To assess the levels of functional IFN induced by these two viruses, chamber slides were seeded with L-929 cells and at confluence were infected at a moi of 50 with SFV4, SFV4nsP2RDR or mock infected with PBS. After 24 hours, supernatant samples were taken and assayed for infectious virus and functional IFN by plaque assay and the IFN bioassay, respectively. No infectious virus or IFN was detected in mock infected cells (data not shown). The titres of infectious virus were similar between the two strains (Figure 6F (i)). However, the levels of functional IFN induced by SFV4 were consistently lower than the levels of IFN induced by SFV4nsP2RDR (Figure 6F (ii)). This 3-fold difference in the levels of functional IFN induced by SFV4 and SFV4nsP2RDR was also observed in a repeat experiment (data not shown).

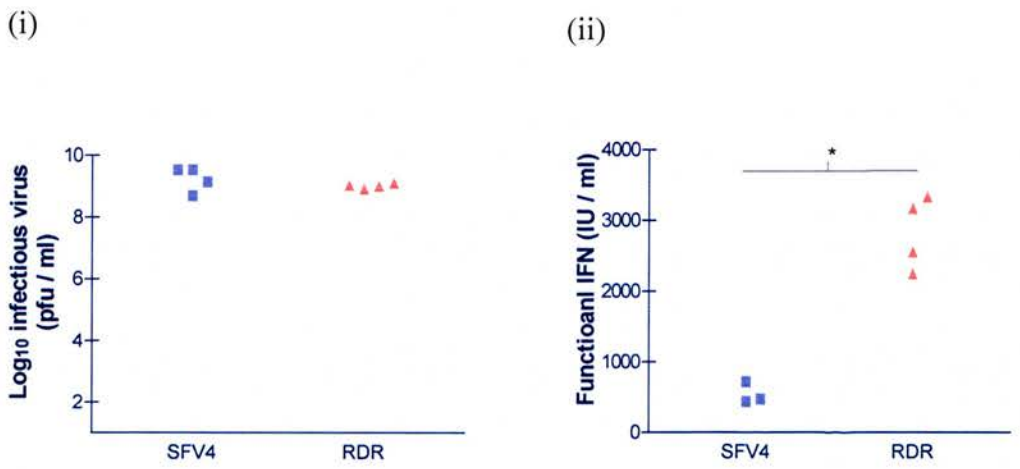

Figure 6F: Functional IFN induced by SFV4 and SFV4nsP2RDR in L-929 cells. Chamber slides were infected at a moi of 50 with SFV4 or SFV4nsP2RDR (RDR); supernatant samples were taken at 24 hours post-infection and assayed for levels of (**i**) infectious virus and (**ii**) functional IFN. Each point represents an individual cell culture.

SFV4nsP2RDR induced more functional IFN in L-929 cells than SFV4; to determine whether the same effect would be observed in a different cell type, MEFs were infected at a moi of 50 with SFV4, SFV4nsP2RDR or mock infected with PBS. Supernatant samples were collected at 4, 8, 12 and 24 hours post-infection and assayed for functional IFN by the Swedish IFN bioassay.

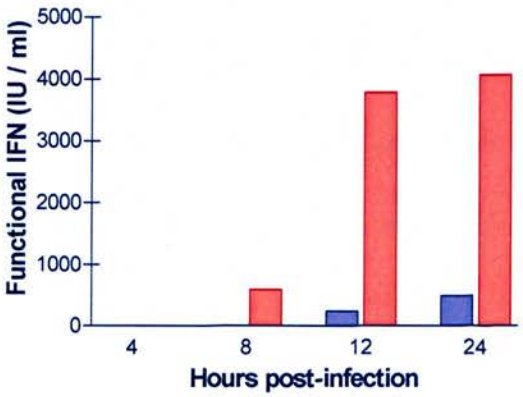

Figure 6G: Functional IFN induced by SFV4 or SFV4nsP2RDR infected MEFs over 24 hours.
MEFs were infected at a moi of 50 with SFV4 (Blue) or SFV4nsP2RDR (Red); supernatants were collected at 4, 8, 12, and 24 hours post-infection and assayed in duplicate for functional IFN by the Swedish IFN bioassay. Each bar represents the mean of the duplicate tests.

No functional IFN was detected in the negative controls (data not shown). The extent of infection in the MEFs was the same between the two viruses, as determined by immuno-fluorescence detection of virus envelope antigen. IFN was detected from 8 hours post-infection in SFV4nsP2RDR infected cell cultures and the levels of IFN continued to rise until 24 hours post-infection (Figure 6G). In contrast, IFN was initially detected at 12 hours post-infection in SFV4 infected cells. At all time points the level of IFN induced by SFV4nsP2RDR was higher than the level of IFN induced by SFV4. A repeat experiment, supported the data in figure 6G. IFN was detected at 12 hours post-infection in SFV4 infected MEFs and at 8 hours post-infection in SFV4nsP2RDR infected MEFs. IFN levels induced by SFV4nsP2RDR virus were between 5-10 times higher at 24 hours post-infection than those induced by SFV4 (data not shown).

Comparison of translation shut off kinetics between SFV4 and SFV4nsP2RDR infected BHKs

Cellular transcription was shut-off in both SFV4 and SFV4nsP2RDR infected cells (Figure 6E). To determine whether cellular translation was shut off similarly by both strains, BHKs were seeded into 24 well plates and at confluence were infected at a moi of 10 with SFV4 or SFV4nsP2RDR non-replicating vectors, (This experiment was carried out by Pia Dosenovic, Karolinska Institutet, Sweden). Non-replicating vectors do not encode the virus structural proteins; they infect similarly to replicating viruses, but are unable to produce progeny. In this experiment the structural proteins were replaced with influenza nucleoprotein (NP) attached to the SFV enhancer element. The enhancer element is fused with foot and mouth disease virus (FMDV) 2A cleavage peptide, which is cloned in frame with NP. This cleavage peptide is approximately 90 % effective; consequently, two proteins are expressed – influenza NP and enhancer-FMDV 2A tagged influenza NP (b1-2A-NP). At 2, 2.5, 3, 3.5, 4, 4.5 and 5 hrs post-infection cells were starved and then incubated with media containing [^{35}S]Methionine. After this incubation, the cells were lysed and the lysate run on an SDS-PAGE gel (Figure 6H). In both infections the majority of cellular translation was shut-off after 3.5 hours post-infection, only influenza NP and enhancer FMDV 2A tagged NP under the control of the SFV sub-genomic promoter and low levels of β-actin were observed after 3.5 hours (Figure 6H). In conclusion, both viruses induce cellular translation shut-off at a similar time post-infection.

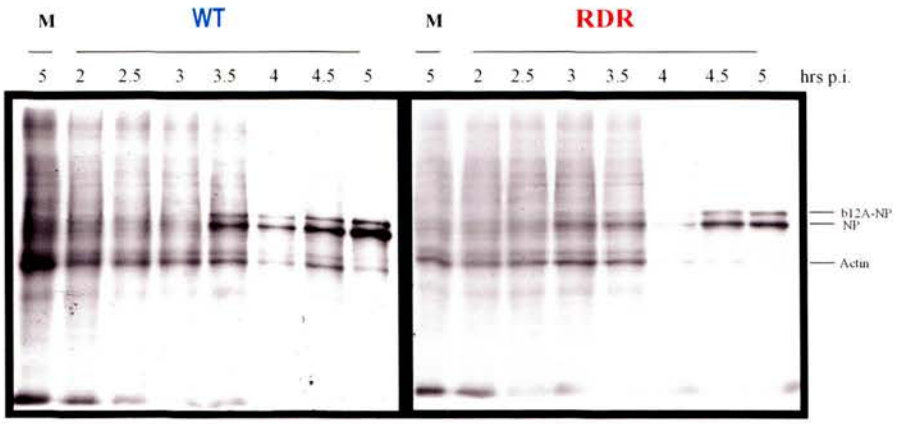

Figure 6H: Cellular translation shut-off in SFV4 and SFV4nsP2RDR infected MEFs.

BHKs were infected at a moi of 10 with non-replicating vectors of SFV4 (WT), SFV4nsP2RDR (RDR) or mock infected with PBS (M); at 2, 2.5, 3, 3.5, 4, 4.5 and 5 hours post-infection the cells were starved and then incubated with [^{35}S]Methionine. Each column represents the proteins translated at that particular time point. NP-nucleoprotein, b1-2A-NP – enhancer-FMDV 2A tagged nucleoprotein. Kindly provided by Pia Dosenovic, (Karolinska Institutet, Sweden).

Comparison of NF-κB and IRF-3 nuclear translocation between SFV4 and SFV4nsP2RDR infected MEFs

Cell cultures infected with SFV4nsP2RDR produced higher levels of IFN-β transcripts and functional IFN in comparison to SFV4 infected cells (Figure 6C; Figure 6F; Figure 6G). This increase in gene expression was specific to IFN-β as both viruses reduced cellular transcription (Figure 6D; Figure 6E) and translation (Figure 6H) equally. A combination of transcription factors is required to induce IFN-β expression, NF-κB, IRF-3 and AP-1. NF-κB is maintained in the cytoplasm in association with IκB; cellular detection of virus infection activates a cascade of kinases which ultimately ubiquitinate IκB, targeting it for proteosome degradation. Release of NF-κB enables its translocation into the nucleus and binding to the IFN-β promoter. IRF-3 shuttles in and out of the nucleus, but once a virus infection is detected in the cell, IRF-3 is phosphorylated and is maintained within the nucleus where it associates as a dimer with the IFN-β promoter. To determine whether NF-κB and IRF-3 translocate into the nucleus during SFV4 and SFV4nsP2RDR infections, MEFs were infected at a moi of 1; a low moi was used so that infected and uninfected cells could be observed and compared under the microscope. MEFs were infected with SFV4, SFV4nsP2RDR, SFV4nsP3Δ50 (a mutant with a functional nsP2) or mock infected with PBS. At 6 hours post-infection, monolayers were fixed and stained for NF-κB p65 subunit, IRF-3 and SFV envelope protein 2 (E2) (Figure 6I). No virus antigen was detected in the mock infected cells; virus infected cells were detected in all virus infections. For all three virus strains, virus infection resulted in nuclear translocation of NF-κB and IRF-3. Interestingly, cultures infected with SFV4nsP3Δ50 demonstrated NF-κB translocation in cells where E2 protein could not be detected. In conclusion, both NF-κB and IRF-3 entered the nucleus in SFV4, SFV4nsP2RDR and SFV4nsP3Δ50 infected MEFs, demonstrating that these cells detected the presence of all three viruses and initiated signalling events.

(i)

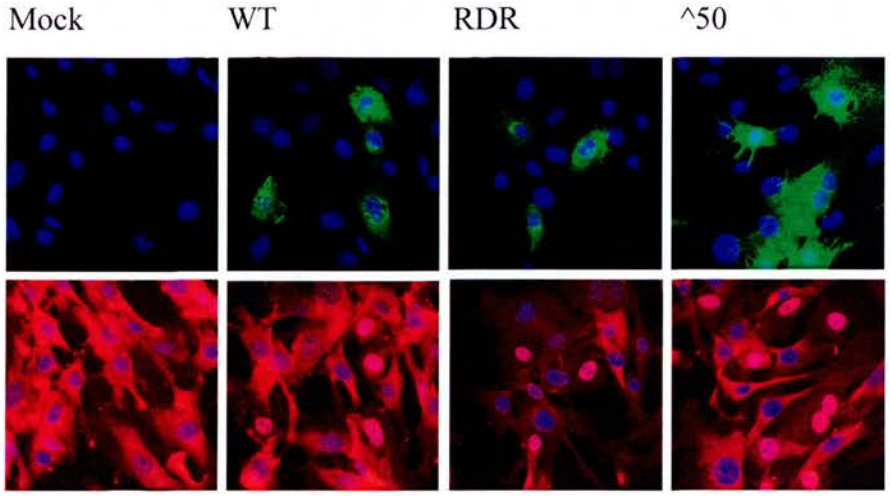

(ii)

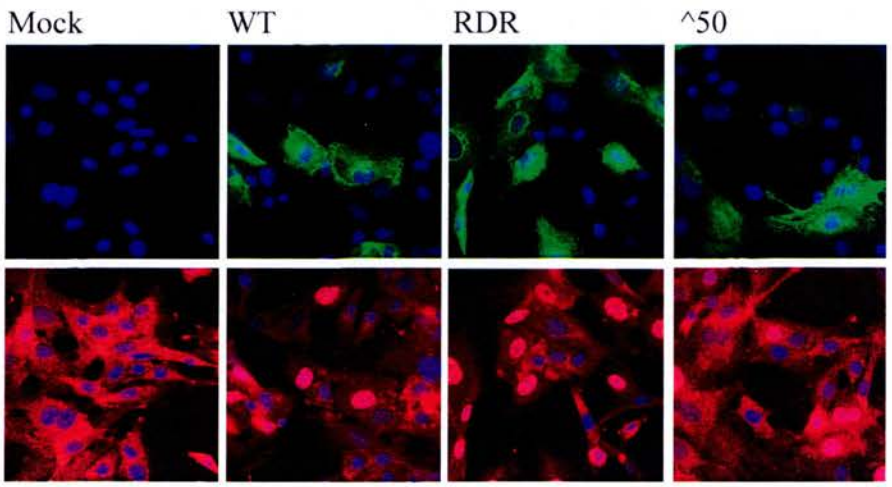

Figure 6I: Nuclear translocation of NF-κB and IRF-3 in SFV infected MEFs. MEFs were infected at a moi of 1 with SFV4 (WT), SFV4nsP2RDR (RDR), SFV4nsP3Δ50 (^50) or mock infected with PBS (Mock). At 6 hours post-infection cells were fixed and stained for virus envelope protein (green), (**i**) NF-κB p65 subunit (red) or (**ii**) IRF-3 (red).

Comparison of NF-κB IFN-β promoter binding in SFV4 and SFV4nsP2RDR infected MEFs

Following activation and nuclear translocation, NF-κB and IRF-3 associate with the IFN-β promoter. As both accumulated in the nucleus in both SFV4 and SFV4nsP2RDR infected cells, any virus interference with IFN gene activation is most probably down stream of this event. To establish whether the ability of NF-κB and IRF-3 to bind to the IFN-β promoter differed in cells infected with the two virus strains an electromobility shift assay (EMSA) was set up to measure binding. EMSA probes representing the regions of the IFN-β promoter that bind to NF-κB or IRF-3 were designed. A 5' overhang containing a guanine residue was incorporated into each of the probes so that [^{32}P]CTP would be present after probe labelling, enabling visualisation on film. MEFs were infected at a moi of 50 with SFV4, SFV4nsP2RDR or mock infected with PBS. At 5 and 7 hours post-infection, cells were harvested and nuclei extracted. Equal amounts of nuclear protein were incubated with [^{32}P]CTP labelled probes for 10 minutes and then run on an acrylamide gel. At completion, the gel was dried and exposed to film (Figure 6J). No bound IRF-3 could be detected, suggesting that the assay conditions were sub-optimal (data not shown). There was no probe bound to NF-κB in nuclear extracts from mock infected cells (Figure 6J (i) – column 5). At 5 hours post-infection, levels of probe bound to NF-κB were similar in both SFV4 and SFV4nsP2RDR infected cells; by 7 hours post-infection very little probe bound to NF-κB was detected in SFV4 infected nuclear extracts whereas, SFV4nsP2RDR infected nuclear extracts showed higher levels of probe bound to this transcription factor, although this was reduced in comparison to the levels observed at 5 hours post-infection (Figure 6J (i)). To clarify that the band presumed to be probe bound to NF-κB did indeed contain NF-κB, another probe known to bind NF-κB was incubated with the same nuclear extracts and produced a band at an equivalent position to the IFN-β promoter probe (data not shown). In addition, the nuclear extracts were incubated with NF-κB p65 antibody or a negative control antibody, (an antibody for another transcription factor PAX), prior to incubation with the labelled probes. When run on the gel, the specific NF-κB antibody caused a band shift indicating the specificity of the original band presumed to contain NF-κB. This was associated with p65 antibody binding to NF-κB, which slows probe:transcription

factor complex movement through the gel (Figure 6J (ii)). Although promising, this experiment was only performed once due to time constraints and so must be interpreted as preliminary data. Subsequent repeat experiments carried out by Pia Dosenovic, Gerald McInerney and Mauro D'Amato in the Karolinska Institut have generated more evidence to support the theory that SFV4 interferes with NF-κB association with the IFN-β promoter.

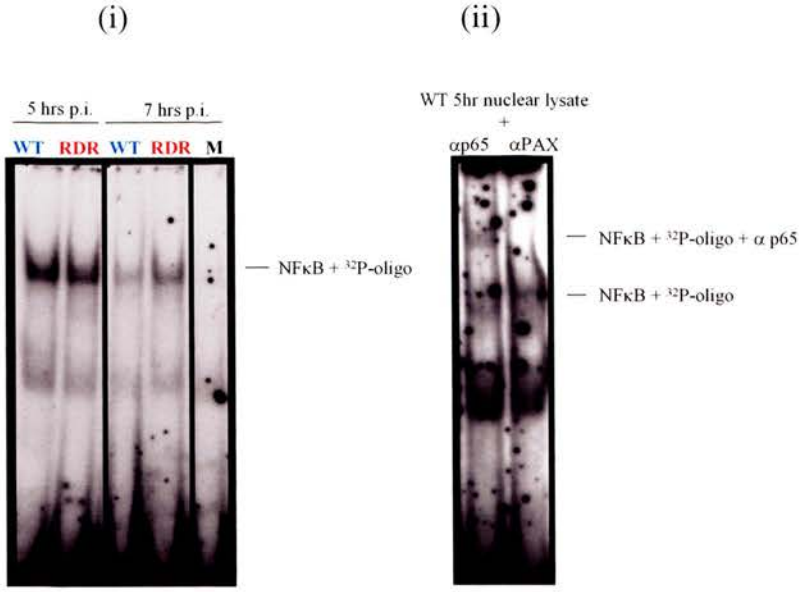

Figure 6J: IFN-β promoter bound NF-κB during an SFV4 or SFV4nsP2RDR infection.

(**i**) Nuclear extracts from MEFs infected at a moi of 50 with SFV4 (WT), SFV4nsP2RDR (RDR) or mock infected with PBS (M) were collected at 5 and 7 hours post-infection. The samples were incubated with [^{32}P]CTP labelled probes specific for NF-κB. (**ii**) Nuclear extracts from MEFs infected with SFV4 at 5 hours post-infection were incubated with NF-κB p65 antibody or PAX antibody and then incubated with labelled probes prior to the gel run.

Summary of Findings

- SFV4 and SFV4nsP2RDR had similar replication rates in BHK cells and MEFs.
- SFV4nsP2RDR induced significantly more IFN-β transcripts than SFV4 in two cell types ($p < 0.05$, Kruskal Wallis test) and more functional IFN.
- At 12 hours post-infection SFV A7(74) RNA levels were similar to SFV4 RNA levels and both strains of virus induced similar levels of IFN-β transcripts.
- At 12 hours post-infection β-actin and GAPDH transcripts were significantly reduced in virally infected cells compared to mock infected cells ($p < 0.05$, Kruskal Wallis test).
- Both β-actin and GAPDH transcripts were down regulated to similar levels in SFV4 and SFV4nsP2RDR infected cells.
- Global cellular transcription and translation was shut-off in both infections.
- IRF-3 and NF-κB translocated to the nucleus in SFV4 and SFV4nsP2RDR infections.
- Possibly less NF-κB was bound to the IFN-β promoter at 7 hours post-infection during an SFV4 infection than during an SFV4nsP2RDR infection.

Discussion

In adult mice, virulent strains of SFV including SFV4 induce panencephalitis whereas avirulent strains of SFV e.g. A7(74) induce a restricted CNS infection. One possible explanation for the different pathologies is that virulent strains induce less IFN. However, *in vivo* data has suggested that both V13 (virulent) and A7 (avirulent) strains induce similar amounts of IFN in mouse blood, muscle and spleen samples (Smillie et al., 1973). In the present study, comparisons of SFV4 and A7(74) in two cultured cell lines, L-929 and MEFs, indicated that both SFV4 and A7(74) replicated to similar levels and induced similar levels of IFN-β gene expression. This indicates that *in vitro*, SFV A7(74) is not impaired in its ability to induce IFN gene expression compared to SFV4.

In both L-929 cells and MEFs, SFV4nsP2RDR induced significantly higher levels of IFN-β transcripts per copy of viral RNA than SFV4 ($p < 0.05$, Kruskal Wallis test). The levels of IFN-β induced by SFV4nsP3Δ50 were similar to SFV4; however, SFV4nsP3Δ50 could only infect 50 – 60 % of the cell monolayer, as determined by immuno-fluorescence using antibodies specific for nsP3 or E2 (data not shown). All of the other strains investigated infected 95 – 100 % of the cell monolayer. SFV4nsP3Δ50 has a deletion in the 3' end of nsP3; this is a highly phosphorylated region. The importance of this hyperphosphorylation of nsP3 has yet to be elucidated. To date, deletions in the C-terminal region of nsP3 are associated with significantly reduced viral RNA synthesis (Vihinen et al., 2001). In figure 6I, several MEFs infected with SFV4nsP3Δ50 showed NF-κB nuclear translocation but no SFV E2 antigen. One explanation would be that virus entered the cell but could not replicate, at least to the level of structural protein production. The hyperphosphorylated region of nsP3 could be involved in the formation of the replicase complex or in transcription of the genomic or sub-genomic RNA. However in 50 % of cells, nsP3 (replicase polyprotein) and E2 (structural polyprotein) were detected and so the hyperphosphorylated region of nsP3 is not critical for replication in all cells but its deletion is severely detrimental to replication in the up to 50 % of cells. Another possible explanation is that the ability of the SFV4nsP3Δ50 to replicate within a cell is dependent upon the cell cycle stage and that at a certain stage of the cycle cell the

hyperphosphorylated region is essential for virus replication. Alternatively, cytokines expressed by the infected cells, such as TNF-α, could induce NF-κB nuclear translocation.

In comparison to SFV4, SFV4nsP2RDR reproducibly induced higher levels of IFN-β transcripts and functional IFN per copy of virus RNA or per unit of infectious virus. Transcription and translation shut-off experiments indicate that this increase in gene expression was specific to IFN-β. SFV4nsP2 contains a nuclear translocation signal consisting of three sequential arginine residues. In SFV4nsP2RDR the second arginine residue is replaced with an aspartic acid residue (Rikkonen et al., 1996). Disruption of this signal prevents nsP2 nuclear translocation. Theoretically, the nsP2 RDR nuclear localisation signal mutation could be functioning in the cytosol or in the nucleus and in either case wt nsP2 could be suppressing IFN responses or the mutant nsP2 could be augmenting them. To induce expression of IFN-β, several transcription factors need to be activated; NF-κB, IRF-3 and AP-1 are activated in the cytoplasm and translocate into the nucleus where they associate with chromatin remodelling elements e.g. CREB binding protein (CBP) prior to binding the IFN-β promoter. Cells in culture most likely detect virus infection by cytoplasmic dsRNA binding proteins, such as RIG-I and mda-5. Both of these proteins signal through CARD domains to induce a kinase cascade, ultimately activating TBK-1, IKK-ε and TAK-1 (Andrejeva et al., 2004; Yoneyama et al., 2004). TBK-1 and IKK-ε phosphorylate IRF-3, enabling it to form homodimers and enter the nucleus (Fitzgerald et al., 2003; Sharma et al., 2003); TAK-1 activates IKK, which phosphorylates IκB targeting it for ubquitination and degradation (Kawai et al., 2005). This releases NF-κB enabling it to enter the nucleus. Immuno-staining specific for each of these transcription factors showed that both accumulated in the nucleus in SFV4 and SFV4nsP2RDR infections, although the proportion of NF-κB or IRF-3 in the nucleus of either infection was not established. The preliminary EMSA data suggests that nsP2 may reduce NF-κB binding to its positive regulatory domain within the IFN-β promoter. Modulation of IFN expression has been observed in one other alphavirus, Sindbis virus (Frolova et al., 2002). All alphaviruses encode a conserved proline residue at position 726 in nsP2. When this is mutated, higher levels of IFN are induced in comparison to another Sindbis virus mutant with comparable replication kinetics (Frolova et al.,

2002). However, the Sindbis virus nsP2 mutants cannot induce host cell transcription or translation shut-off similarly to the wt virus, therefore the conserved proline residue of nsP2 may not specifically downregulate IFN induction (Gorchakov et al., 2004).

There are few examples of alphaviruses that interact with IFN-β induction; however, many other viruses target IRF-3 and NF-κB. For example, the VP35 protein of Ebola virus (Basler et al., 2003), NS3/4A of Hepatitis C virus (Foy et al., 2003) and the NS1/NS2 complex of respiratory syncytial virus (Bossert et al., 2003) prevent IRF-3 phosphorylation and hence dimerisation, reducing IRF-3 nuclear accumulation. Herpes simplex virus 1 also prevents nuclear accumulation of IRF-3 through its ICP0 protein (Melroe et al., 2004). More relevant to the postulated SFV4 nuclear mechanism, the ML protein of Thogoto virus does not affect nuclear accumulation, but interferes with IRF-3 dimerisation and IRF-3 recruitment of CBP (Hagmaier et al., 2003; Jennings et al., 2005). Several other viruses bind to and inactivate or inhibit activation of IRF-3; these include rotavirus (Graff et al., 2002), human papilloma virus (Ronco et al., 1998), simian virus 5 (Poole et al., 2002) and Sendai virus (Komatsu et al., 2004). NF-κB, unlike IRF-3, is not specific to IFN induction. It additionally promotes the expression of inflammatory genes, therefore viruses that interfere with NF-κB suppress inflammation as well as the IFN response (Karin and Greten, 2005). NF-κB is downregulated by human herpes virus 8, vIRF-3 protein inhibits the activation of IκB kinase β (Lubyova and Pitha, 2000; Seo et al., 2004). Vaccinia virus N1L protein suppresses the expression of NF-κB by interacting with IKK and TBK-1 to prevent NF-κB release from IκB in the cytoplasm (DiPerna et al., 2004). Adenovirus E3 10.4k and 14.5 k proteins suppress assembly of the TNF receptor signalling complex at the plasma membrane, which also signals through NF-κB, and decreases the surface levels of TNFR1 (Fessler et al., 2004). Of particular interest is the picornavirus mechanism to suppress NF-κB activation. Picornaviruses intercept NF-κB post-activation; poliovirus, ECHO virus and rhinovirus 3C proteins cleave the p65-RelA subunit of NF-κB (Neznanov et al., 2005). SFV4 nsP2 is also a protease (Merits et al., 2001) so it is plausible to suggest that nuclear SFV4nsP2 inhibits NF-κB IFN-β promoter binding by cleaving NF-κB.

SFV has been detected in astrocytes and oligodendrocytes at 183 days post-infection (Khalili-Shirazi et al., 1988), indicating viral persistence in the brain. The brain is an immuno-privileged site and therefore ideal for establishing a persistent infection. Partial suppression of IFN during the early stages of infection would enable SFV to establish a viraemia in the periphery, which would consequentially lead to neuronal infections. Other alphaviruses produce persistent infections; Ross River virus (RRV) induces epidemic polyarthritis, which is a relapsing disease. RRV is known to enhance macrophage activity, a potential cause of the associated pathology, and dysregulate CD80, IFN-γ and TNF-α signalling, which may facilitate persistence of RRV infection (Way et al., 2002). The Sindbis virus genome can be detected up until 17 months post-infection in Balb/c mice (Levine and Griffin, 1992), although the route to persistence and the immune mechanism responsible for infectious virus clearance has yet to be completely defined.

Summary

Different CNS pathology is observed between virulent and avirulent strains of SFV. The objectives of this chapter were to determine whether this pathology could be related to differential expression of IFN. Similar levels of IFN-β transcripts were induced by both SFV A7(74) and SFV4. However, an SFV4 mutant that had a defective nuclear localisation signal in the nsP2 protein reproducibly induced higher levels of IFN-β transcripts and functional IFN than SFV4. Cellular transcriptional and translational shut-off experiments indicated that the increased gene induction during an SFV4nsP2RDR infection was specific to IFN-β. This suggests that nsP2 is an antagonist of IFN-β induction. Preliminary data implied that the underlying mechanism might involve prevention of NF-κB binding to the IFN-β promoter.

Chapter 7: Final Discussion

The Role of Type I Interferon in SFV encephalitis

IFN is a powerful component of the anti-viral innate immune response (Issacs and Lindenmann, 1957). Mice lacking the IFNAR are unable to respond to IFN and are highly susceptible to a variety of infections such as vaccinia virus, lymphocytic choriomeningitis virus, vesicular stomatitis virus, Sindbis virus and SFV (Muller et al., 1994; Van den Broek et al., 1995; Hwang et al., 1995; Ryman et al., 2000; Fazakerley et al., 2002). In the case of SFV, IFNAR$^{-/-}$ mice infected *ip* with SFV4 succumb to a morbid infection within two days whereas wt mice infected with the same virus survive the infection (Fazakerley et al., 2002), demonstrating the importance of IFN in controlling SFV infection.

Recently, research has been heavily focused on delineating the signalling pathways responsible for IFN gene expression. Several receptors, which detect virus and ultimately induce IFN-β expression have been described and include TLR-3, PKR, RIG-I and mda-5 (Yoneyama et al., 2004; Clemens et al., 1993; Andrejeva et al., 2004). TLR-3 detects dsRNA (Alexopoulou et al., 2001) and is located both within the endosome and on the surface of some cells. The endosomal and surface location of this receptor suggests that it may be capable of detecting virus within the surrounding environment of the cell. The other receptors, PKR, RIG-I and mda-5 also bind dsRNA but are cytoplasmic and are therefore well placed to detect virus infection of the cell. The importance of PKR as a sentinel of infection that induces IFN-β gene expression is disputed and is dependent upon the infecting virus. Newcastle disease virus (NDV) induces similar levels of IFN-α and IFN-β transcripts in both the absence and presence of PKR, *in vivo* and *in vitro* (Yang et al., 1995). In contrast, PKR is required for IFN-β gene expression in reovirus infection of primary myocyte cardiac cultures (Stewart et al., 2003), EMCV infection of U-937 cells (Der and Lau, 1995) and rotavirus infection of intestinal epithelial cells (Vijay-Kumar et al., 2005). This thesis examined the importance of PKR for IFN-β gene induction following an SFV4 infection. The study indicated that PKR is required, but not critical for IFN-β expression during the early stages of infection (up to 12 hours post-

infection). Continued IFN-β expression in the absence of PKR demonstrated that other cellular proteins exist that can detect SFV replication intermediates or virions. The recently discovered RIG-I or mda-5 CARD-domain containing proteins which detect dsRNA (Andrejeva et al., 2004) may be responsible for this gene expression. RIG-I$^{-/-}$ cells infected with vesicular stomatitis virus (VSV) have severely impaired IFN-β responses compared to wt cells (Kato et al., 2005). Further evidence to support the importance of RIG-I for IFN expression was found during HCV infection. HCV antagonises RIG-I signalling, the HCV NS3-4A protease cleaves the RIG-I adaptor protein IPS-1 (Foy et al., 2005). In contrast to RIG-I, mda-5 and TLR-3, PKR has not been associated with IRF-3 activation, a transcription factor required for IFN-β expression. This may further suggest that PKR only plays a minor role in IFN-β expression. It would be of interest to investigate the importance of RIG-I for IFN-β induction in SFV infection and hence determine which cellular protein is responsible for IFN-β induction in SFV infection. This may also provide further insight into SFV biology with regards to the location of the dsRNA binding protein.

Intriguingly, despite the requirement of PKR for complete IFN-β expression, the absence of PKR had no effect upon the level of SFV4 replication. In both wt and PKR$^{o/o}$ cells the levels of virus RNA detected were similar at all three time points (4, 8 and 12 hours post-infection). In other virus infections, for example Bunyamwera virus (Streitenfeld et al., 2003), VSV and influenza virus (Balachandran et al., 2000) virulence is increased and where measured, virus titres are slightly higher in the absence of PKR. It would be expected that since PKR enhances IFN-β gene expression, absence of PKR could allow greater virus replication. Additionally, PKR induces host cell translation shut-off; continued cellular translation should also enable more virus replication. However, in SFV4 infection the levels of virus transcripts remain constant in the two cell types, implying that SFV4 replication is not affected by PKR at early time points. PKR$^{o/o}$ mice infected with SFV or Sindbis virus, a close relative of SFV, do not demonstrate an increase in morbidity or mortality in comparison to wt mice (Fazakerley, unpublished; Ryman et al., 2002). Although, at around 6 days post infection virus titres are higher in PKR $^{o/o}$ mice implying that the anti-viral effects of PKR are most effective during the later stages of infection

(Fazakerley, unpublished; Ryman et al., 2002). Further evidence implying that PKR does not affect SFV is found during Sindbis virus infection, where only a minor role is attributed to PKR for the induction of host translation shut-off (Gorchakov et al., 2004). A possible explanation for the minor affects of PKR on SFV and Sindbis virus infections is that SFV and Sindbis virus may possess resistance to PKR. Recently, a highly stable hairpin loop downstream of the translation start site of Sindbis virus 26 S mRNA has been implicated in resistance to PKR phosphorylation of eIF-2α (Ventoso et al., 2006). This structure stalls the ribosome at the correct start site enabling translation to bypass the requirement of an initiation complex. In other virus infections resistance to PKR is a common feature of virus antagonism of the IFN response. For example, HSV ICPγ34.5 gene product recruits a cellular phosphatase to dephosphorylate and hence inactivate PKR (He et al., 1997); adenovirus VA RNAs associate with the dsRBM of PKR and prevent its activation (Kitajewski et al., 1986); influenza virus NS1 protein antagonises dsRNA binding to PKR by sequestering dsRNA within the nucleus (Lu et al., 1995); HCV NS5A protein binds to and inactivates PKR (Gale et al., 1997) and the HIV transactivator protein (Tat) is an inhibitor of PKR expression (Roy et al., 1990; Agy et al., 1990). In conclusion, whilst PKR is an important cellular defence mechanism against viral infections, through the induction of IFN-β and activation of host translation shut-off, as demonstrated by the multitude of viruses that encoded PKR antagonists, it does not affect SFV replication. Possible strategies of SFV resistance to PKR are not known and further investigations into this area would be an interesting extension of this study.

SFV strains can be divided into two types, virulent and avirulent. Virulent strains induce a panencephalitis in both neonatal and adult mice, whereas an interesting consequence of avirulent strains is age-dependent pathology. Avirulent strains only induce panencephalitis in neonates infected up until 12 days of age. Adult mice infected with an avirulent strain of SFV develop a restricted CNS infection (Fazakerley et al., 1993). One possible explanation for this age-dependent pathology is that immature CNS cells have an impaired ability to induce IFN. IFN is one of the first responses to virus infection; if immature CNS cells were impaired in their ability to produce IFN, this could contribute to a more extensive infection that leads to increased pathology that is observed in neonates. Some evidence exists to support

this theory, differential levels of IFN expression have been demonstrated in NDV or Sendai virus infected neonatal umbilical cord blood mononuclear cells and human adult mononuclear cells (Neustock et al., 1993). However, gene array analysis of Sindbis virus infected adult and neonatal mouse brains demonstrates that neonates produce high levels of inflammatory genes transcripts, including IFN transcripts. This study also showed that a single gene product was found to be upregulated in adult mice compared to neonatal mice, ISG 12, and over expression of this protein extended the survival of Sindbis virus infected neonates (Labrada et al., 2002). As both young and older mice induce high levels of IFN transcripts, this suggests that ISG 12 may be controlled by another factor which is not expressed in neonates.
In the present study, SFV4 infection of neonate and adult mouse brains demonstrated that functional IFN in addition to IFN-β and IFN-α transcripts could be detected and that the main driving force in the production of IFN was the level of virus RNA. This demonstrates that the neonate brain is not impaired in its ability to induce IFN.

IFN is unlikely to be the major determinant of age-dependent pathology of avirulent SFV infections and therefore other factors must contribute to this pathology. Possible explanations include: i) that avirulent virus is unable to spread in the adult mouse brain due to structural differences between the adult and neonatal mouse brains, ii) that neonate neurones are more susceptible to apoptosis than adult neurones, iii) that the adult immune system can control the avirulent infection whereas the neonatal immune response is impaired. Taking each point in turn, up until 12 days post partum, neonates are still developing their synaptic connections (reviewed by Fazakerley JK, 2001), this includes neuronal synaptogenesis and differentiation, which involves a significant amount of smooth membrane vesicle production (reviewed by Fazakerley, 2001). Evidence suggests that increased smooth membrance production is important for SFV replication as SFV A7(74) infection of mice pre-treated with aurothiolates (gold containing compounds) results in wide spread infection and high virus titres (Scallan and Fazakerley, 1999). These observations were not due to toxic effects of the aurothiolates resulting in neuronal death. It seems that the aurothiolates alter neuronal physiology to increase smooth membrane proliferation which allows virus replication (Mehta et al., 1990). Additionally, in the adult brain, the rostral migratory stream, which is an area of the

brain where neurones are constantly being replaced and differentiating is permissive to infection with avirulent strains (Sammin et al., 1999). This suggests that CNS metabolic differences play a role in the age-dependent pathology of avirulent SFV strains. Immature neurones are highly susceptible to apoptosis; a mechanism used to remove incorrect or weak synapses in the developing CNS. As the brain matures around the age of 12 days, neurones become more resistant to apoptosis (Scallan et al., 1997). Potentially avirulent strains can spread throughout the neonatal mouse brain by inducing neuronal apoptosis. Programmed cell death is normally associated with preventing virus spread; however, there are examples of viruses that exploit this mechanism, such as influenza virus. Influenza virus triggers apoptosis through induction of Fas ligand. Blocking Fas expression reduces the spread of the infection (Wurzer et al., 2004). At present nothing is known about the relationship between the spread of SFV infection and apoptosis, demonstrating that further investigations into this area are required. An alternative explanation is that the adult CNS immune response can control the avirulent infection whereas the neonate CNS immune response is impaired. The maturity of the adaptive immune response has a significant role in protection against virus infections. For example, respiratory syncytial virus (RSV) causes more severe infections in animals less than 6 months old. A comparison of infections between young and older calves demonstrated that the older calves express higher numbers of mononuclear cells, B cells and bovine RSV-specific IgA and IgG responses (Grell et al., 2005). HSV infected neonates are impaired in their ability to activate CD8 T cells and demonstrate reduced CTL effector functions in comparison to adults (Evans and Jones, 2005). A similar pathology was observed in Hantavirus infected neonates; 3-day-old mice infected with Hantavirus have reduced numbers of IFN-γ producing CD8 T cells compared to adults (Araki et al., 2004). In CMV infection of young children, it was the levels of IFN-γ producing CD4 T cells that were reduced in comparison to adults (Tu et al., 2004). However, during SFV infection adult SCID mice, lacking functional B and T cell responses, show a similar restricted infection to wt adults (Amor et al., 1996) indicating that viral spread is not controlled by the adaptive immune response.

In the adult mouse brain it is possible that virulent strains are able to overcome the CNS immune responses whereas the avirulent strains are not. To date, none of the SFV proteins have been assigned a role for interference of the host immune responses.

However, several pieces of data imply that the nsP2 of SFV and Sindbis virus can interfere with IFN expression (Frolova et al., 2002; Fazakerley et al, 2002). NsP2 possesses ATPase, GTPase, RNA triphosphatase and RNA helicase activities (Rikkonen et al., 1994a; Gomez de Cedron et al., 1999). It is involved in terminating negative strand production, controlling subgenomic RNA synthesis and cleaving the non-structural polyprotein (Suopanki et al., 1998; Merits et al., 2001). Approximately 50 % of nsP2 is targeted to the nucleus (Rikkonen et al., 1992; 1994b). An nsP2 mutant, SFV4nsP2RDR demonstrated that the nuclear localisation signal (NLS) of nsP2 was not essential for viral replication but was a determinant of neurovirulence (Fazakerley et al., 2002; Rikkonen, 1996). Mice inoculated *ic* with SFV4nsP2RDR survived whereas those infected with SFV4 died and demonstrated higher brain virus titres than those infected with the mutant virus. To determine the role of the IFN response in this pathology, both viruses were inoculated into $IFNAR^{-/-}$ mice; all mice succumbed to infection regardless of the inoculating strain and produced similar virus titres (Fazakerley et al., 2002). Potentially, the ability of SFV4nsP2RDR to replicate *in vivo* is reduced and this slower replication allows time for control by the IFN response. Alternatively, SFV4 downregulates the IFN response, or is not susceptible to it, whereas SFV4nsP2RDR cannot suppress the response or is susceptible to it. Research with Sindbis virus (SV) indicates that mutating the nsP2 P_{726} residue, conserved throughout the alphaviruses, suppresses cytopathic effect and increases IFN production (Frolova et al., 2002). In the present study, SFV4 was compared to SFV4nsP2RDR to determine the ability of either strain to induce IFN-β transcripts and functional IFN *in vitro*, where they are known to replicate at similar rates (Fazakerley et al., 2002). In comparison to SFV4, SFV4nsP2RDR reproducibly induced higher levels of IFN-β transcripts and functional IFN per copy of virus RNA or per unit of infectious virus. Transcription and translation shut-off experiments indicated that this increase in gene expression was specific to IFN-β. IFN-β gene expression is regulated by several transcription factors, including NF-κB and IRF-3. Both are maintained in an inactive state within the cytoplasm and can only translocate to the nucleus when activated upon cell detection of virus infection. Many viruses prevent IRF-3 and NF-κB nuclear accumulation. For example, the VP35 protein of Ebola virus (Basler et al., 2003), NS3/4A of Hepatitis C virus (Foy et al., 2003) and the NS1/NS2 complex of respiratory syncytial virus (Bossert et al., 2003) all prevent

IRF-3 phosphorylation and hence dimerisation, reducing IRF-3 nuclear accumulation. Herpes simplex virus 1 also prevents nuclear accumulation of IRF-3 through its ICP0 protein (Melroe et al., 2004). NF-κB is downregulated by human herpes virus 8 vIRF-3 protein, which inhibits the activation of IκB kinase β subunit (Lubyova and Pitha, 2000; Seo et al., 2004). Vaccinia virus N1L protein suppresses the expression of NF-κB by interacting with IKK and TBK-1 to prevent NF-κB release from IκB in the cytoplasm (DiPerna et al., 2004). The A238L gene product of African swine fever virus acts as an IκB homologue and prevents NF-κB activation after virus infection (Powell at al., 1996; Revilla et al., 1998). During SFV4 and SFV4nsP2RDR infection both NF-κB and IRF-3 were observed to accumulate in the nucleus. The proportion of NF-κB or IRF-3 in the nucleus following infection was not established for either virus; however, this data implies that SFV4 suppression of IFN-β gene expression acts after the transcription factors have entered the nucleus. Other viruses also interfere with IFN-β gene expression after transcription factor nuclear translocation. For example, the ML protein of Thogoto virus interferes with IRF-3 dimerisation and IRF-3 recruitment of CBP (Hagmaier et al., 2003; Jennings et al., 2004) and picornavirus (poliovirus, ECHO virus and rhinovirus) 3C proteins cleave the p65-RelA subunit of NF-κB post-activation (Neznanov et al., 2005). In the present study, preliminary EMSA data suggested that nsP2 reduced NF-κB binding to its positive regulatory domain within the IFN-β promoter. SFV4 nsP2 is a protease (Merits et al., 2001) so it is plausible to suggest that like the picornaviruses, nuclear SFV4 nsP2 inhibits NF-κB IFN-β promoter binding by cleaving NF-κB. However, further investigations are required to clarify the mechanism of SFV4 nsP2 NF-κB interference.

Recent investigations have provided further data to support the role of SFV4 nsP2 in NF-κB antagonism. TNF-α is a cytokine whose expression is regulated by NF-κB (reviewed in Ware, 2005). SFV4nsP2RDR was shown to induce higher levels of TNF-α in comparison to SFV4, suggesting that nuclear nsP2 is required to downregulate TNF-α expression (Pia Dosenovic, Karolinska Institutet, unpublished data). This result provides another link between nsP2 and NF-κB. There is some evidence that another alphavirus, Ross River virus (RRV), also reduces the mRNA levels of TNF-α, alongside other pro-inflammatory cytokines in RRV antibody

dependent enhanced (ADE) infection of macrophages stimulated with LPS. The suppression of transcript levels correlated with a reduction in the nuclear levels of several transcription factors including NF-κB (Mahalingam and Lidbury, 2002). However, in this study due to the complexities of the infection model, the authors could not distinguish between the affects of RRV and ADE infection upon NF-κB. A side issue of this study demonstrated that high levels of IL-10 are expressed by macrophages during a RRV infection (Mahalingam and Lidbury, 2002). IL-10 is an immuno-suppressive cytokine that can inhibit the production of IFN-γ, TNF-α and IL-12 and importantly suppresses NF-κB activation (Moore et al., 2001). In an SFV infection the role of IL-10 is not yet known. One way by which NF-κB is repressed during an SFV infection could be by IL-10, although, IL-10 is not produced immediately and is more associated with the adaptive immune response.

This thesis has discovered intriguing features of the relationship between IFN and SFV. The studies described, showed that both neonatal and adult mouse brains express IFN during an SFV infection, that PKR is required but is not critical for IFN-β induction and that a virulent strain of SFV suppresses IFN-β expression putatively through regulation of NF-κB gene induction. These results have opened up further questions such as, during an SFV infection which cellular proteins are responsible for IFN-β induction if not PKR and how SFV4 regulates NF-κB gene induction, which need to be addressed to fully appreciate the relationship between SFV and IFN.

Reference List

1. **Abate, D. A., S. Watanabe, and E. S. Mocarski**. 2004. Major human cytomegalovirus structural protein pp65 (ppUL83) prevents interferon response factor 3 activation in the interferon response. J Virol. **78**:10995-11006.

2. **Abraham, N., D. F. Stojdl, P. I. Duncan, N. Methot, T. Ishii, M. Dube, B. C. Vanderhyden, H. L. Atkins, D. A. Gray, M. W. McBurney, A. E. Koromilas, E. G. Brown, N. Sonenberg, and J. C. Bell**. 1999. Characterization of transgenic mice with targeted disruption of the catalytic domain of the double-stranded RNA-dependent protein kinase, PKR. J Biol Chem **274**:5953-5962.

3. **Adler, B., H. Adler, H. Pfister, T. W. Jungi, and E. Peterhans**. 1997. Macrophages infected with cytopathic bovine viral diarrhea virus release a factor(s) capable of priming uninfected macrophages for activation-induced apoptosis. J Virol. **71**:3255-3258.

4. **Agy, M. B., M. Wambach, K. Foy, and M. G. Katze**. 1990. Expression of cellular genes in CD4 positive lymphoid cells infected by the human immunodeficiency virus, HIV-1: evidence for a host protein synthesis shut-off induced by cellular mRNA degradation. Virology **177**:251-258.

5. **Ahmad, S., Y. M. Alsayed, B. J. Druker, and L. C. Platanias**. 1997. The type I interferon receptor mediates tyrosine phosphorylation of the CrkL adaptor protein. J Biol Chem **272**:29991-29994.

6. **Ahmed, M., M. O. McKenzie, S. Puckett, M. Hojnacki, L. Poliquin, and D. S. Lyles**. 2003. Ability of the matrix protein of vesicular stomatitis virus to suppress beta interferon gene expression is genetically correlated with the inhibition of host RNA and protein synthesis. J Virol. **77**:4646-4657.

7. **Ahola, T., P. Laakkonen, H. Vihinen, and L. Kaariainen**. 1997. Critical residues of Semliki Forest virus RNA capping enzyme involved in methyltransferase and guanylyltransferase-like activities. J Virol **71**:392-397.

8. **Alberts B, Bray D Lewis J Raff M Roberts K Watson JD**. 1994 Molecular biology of the cell 3rd edition. Garland Publishing NY.

9. **Alcami, A., J. A. Symons, and G. L. Smith**. 2000. The vaccinia virus soluble alpha/beta interferon (IFN) receptor binds to the cell surface and protects cells from the antiviral effects of IFN. J Virol. **74**:11230-11239.

10. **Alexopoulou, L., A. C. Holt, R. Medzhitov, and R. A. Flavell**. 2001. Recognition of double-stranded RNA and activation of NF-kappaB by Toll-like receptor 3. Nature **413**:732-738.

11. **Allsopp, T. E., M. F. Scallan, A. Williams, and J. K. Fazakerley**. 1998. Virus infection induces neuronal apoptosis: A comparison with trophic factor withdrawal. Cell Death. Differ. **5**:50-59.

12. **Allsopp, T. E. and J. K. Fazakerley**. 2000. Altruistic cell suicide and the specialized case of the virus-infected nervous system. Trends Neurosci. **23**:284-290.

13. **Amor, S., M. F. Scallan, M. M. Morris, H. Dyson, and J. K. Fazakerley**. 1996. Role of immune responses in protection and pathogenesis during Semliki Forest virus encephalitis. J Gen. Virol **77 (Pt 2)**:281-291.

14. **Andrejeva, J., K. S. Childs, D. F. Young, T. S. Carlos, N. Stock, S. Goodbourn, and R. E. Randall**. 2004. The V proteins of paramyxoviruses bind the IFN-inducible RNA helicase, mda-5, and inhibit its activation of the IFN-beta promoter. Proc Natl Acad Sci U S A **101**:17264-17269.

15. **Araki, K., K. Yoshimatsu, B. H. Lee, M. Okumura, H. Kariwa, I. Takashima, and J. Arikawa.** 2004. Age-dependent hantavirus-specific CD8(+) T-cell responses in mice infected with Hantaan virus. Arch. Virol **149**:1373-1382.

16. **Arnheiter, H. and O. Haller.** 1983. Mx gene control of interferon action: different kinetics of the antiviral state against influenza virus and vesicular stomatitis virus. J. Virol. **47**:626-630.

17. **Ashkenazi, A. and V. M. Dixit.** 1999. Apoptosis control by death and decoy receptors. Curr. Opin. Cell Biol **11**:255-260.

18. **Atkins, G. J., B. J. Sheahan, and P. Liljestrom.** 1999. The molecular pathogenesis of Semliki Forest virus: a model virus made useful? J Gen. Virol **80 (Pt 9)**:2287-2297.

19. **Bach EA, Aguet M Schreiber RD.** The IFN gamma receptor: a paradigm for cytokine receptor signaling. Annu Rev Immunol. 15, 563-591. 1997.

20. **Baier, L. J., T. Shors, S. T. Shors, and B. L. Jacobs.** 1993. The mouse antiphosphotyrosine immunoreactive kinase, TIK, is indistinguishable from the double-stranded RNA-dependent, interferon-induced protein kinase, PKR. Nucleic Acids Res **21**:4830-4835.

21. **Baigent, S. J., G. Zhang, M. D. Fray, H. Flick-Smith, S. Goodbourn, and J. W. McCauley.** 2002. Inhibition of beta interferon transcription by noncytopathogenic bovine viral diarrhea virus is through an interferon regulatory factor 3-dependent mechanism. J Virol. **76**:8979-8988.

22. **Balachandran, S., C. N. Kim, W. C. Yeh, T. W. Mak, K. Bhalla, and G. N. Barber.** 1998. Activation of the dsRNA-dependent protein kinase, PKR, induces apoptosis through FADD-mediated death signaling. EMBO J **17**:6888-6902.

23. **Balachandran, S., P. C. Roberts, L. E. Brown, H. Truong, A. K. Pattnaik, D. R. Archer, and G. N. Barber.** 2000. Essential role for the dsRNA-dependent protein kinase PKR in innate immunity to viral infection. Immunity **13**:129-141.

24. **Baldwin, A. S., Jr.** 1996. The NF-kappa B and I kappa B proteins: new discoveries and insights. Annu Rev Immunol. **14**:649-683.

25. **Balluz, I. M., G. M. Glasgow, H. M. Killen, M. J. Mabruk, B. J. Sheahan, and G. J. Atkins.** 1993. Virulent and avirulent strains of Semliki Forest virus show similar cell tropism for the murine central nervous system but differ in the severity and rate of induction of cytolytic damage. Neuropathol. Appl. Neurobiol. **19**:233-239.

26. **Barber, S. A., D. S. Herbst, B. T. Bullock, L. Gama, and J. E. Clements.** 2004. Innate immune responses and control of acute simian immunodeficiency virus replication in the central nervous system. J Neurovirol. **10 Suppl 1**:15-20.

27. **Barnes BJ, Moore PA Pitha PM.** Virus-specific activation of a novel interferon regulatory factor, IRF-5, results in the induction of distinct interferon alpha genes. J Biol Chem **276**(26), 23382-23390. 2001

28. **Barnes, B. J., J. Richards, M. Mancl, S. Hanash, L. Beretta, and P. M. Pitha.** 2004. Global and distinct targets of IRF-5 and IRF-7 during innate response to viral infection. J Biol Chem **279**:45194-45207.

29. **Bas, A., G. Forsberg, S. Hammarstrom, and M. L. Hammarstrom.** 2004. Utility of the housekeeping genes 18S rRNA, beta-actin and glyceraldehyde-3-phosphate-dehydrogenase for

normalization in real-time quantitative reverse transcriptase-polymerase chain reaction analysis of gene expression in human T lymphocytes. Scand. J Immunol. **59**:566-573.

30. **Basler, C. F., A. Mikulasova, L. Martinez-Sobrido, J. Paragas, E. Muhlberger, M. Bray, H. D. Klenk, P. Palese, and A. Garcia-Sastre**. 2003. The Ebola virus VP35 protein inhibits activation of interferon regulatory factor 3. J Virol. **77**:7945-7956.

31. **Bass BL, Weintraub H.** An unwinding activity that covalently modifies its double-stranded RNA substrate. Cell 55(6), 1089-1098. 1988.

32. **Bass, B. L.** 1997. RNA editing and hypermutation by adenosine deamination. Trends Biochem Sci **22**:157-162.

33. **Bass, B. L.** 2002. RNA editing by adenosine deaminases that act on RNA. Annu Rev Biochem **71**:817-846.

34. **Bekisz, J., H. Schmeisser, J. Hernandez, N. D. Goldman, and K. C. Zoon**. 2004. Human interferons alpha, beta and omega. Growth Factors **22**:243-251.

35. **Benedict, C. A., P. S. Norris, and C. F. Ware**. 2002. To kill or be killed: viral evasion of apoptosis. Nat Immunol. **3**:1013-1018.

36. **Berkowitz B, Huang DB Chen-Park FE Sigler PB Ghosh G.** The x-ray crystal structure of the NF-kappa B p50.p65 heterodimer bound to the interferon beta -kappa B site. J Biol Chem. 277(27), 24694-24700. 2002.

37. **Bertin, J., R. C. Armstrong, S. Ottilie, D. A. Martin, Y. Wang, S. Banks, G. H. Wang, T. G. Senkevich, E. S. Alnemri, B. Moss, M. J. Lenardo, K. J. Tomaselli, and J. I. Cohen**. 1997. Death effector domain-containing herpesvirus and poxvirus proteins inhibit both Fas- and TNFR1-induced apoptosis. Proc Natl Acad Sci U S A **94**:1172-1176.

38. **Bieback, K., E. Lien, I. M. Klagge, E. Avota, J. Schneider-Schaulies, W. P. Duprex, H. Wagner, C. J. Kirschning, M. Ter, V, and S. Schneider-Schaulies**. 2002. Hemagglutinin protein of wild-type measles virus activates toll-like receptor 2 signaling. J Virol. **76**:8729-8736.

39. **Biron, C. A., L. P. Cousens, M. C. Ruzek, H. C. Su, and T. P. Salazar-Mather**. 1998. Early cytokine responses to viral infections and their roles in shaping endogenous cellular immunity. Adv. Exp. Med. Biol **452**:143-149.

40. **Biron, C. A.** 1999. Initial and innate responses to viral infections--pattern setting in immunity or disease. Curr. Opin. Microbiol. **2**:374-381.

41. **Biron, C. A.** 2001. Interferons alpha and beta as immune regulators--a new look. Immunity **14**:661-664.

42. **Black, T. L., G. N. Barber, and M. G. Katze**. 1993. Degradation of the interferon-induced 68,000-M(r) protein kinase by poliovirus requires RNA. J Virol **67**:791-800.

43. **Bode, J. G., S. Ludwig, C. Ehrhardt, U. Albrecht, A. Erhardt, F. Schaper, P. C. Heinrich, and D. Haussinger**. 2003. IFN-alpha antagonistic activity of HCV core protein involves induction of suppressor of cytokine signaling-3. FASEB J **17**:488-490.

44. **Boehm, U., T. Klamp, M. Groot, and J. C. Howard**. 1997. Cellular responses to interferon-gamma. Annu Rev Immunol. **15**:749-795.

45. **Bohn, W., F. Ciampor, R. Rutter, and K. Mannweiler**. 1990. Localization of nucleocapsid associated polypeptides in measles virus-infected cells by immunogold labelling after resin embedding. Arch. Virol. **114**:53-64.

46. **Bos, J. L., J. de Rooij, and K. A. Reedquist**. 2001. Rap1 signalling: adhering to new models. Nat Rev Mol Cell Biol **2**:369-377.

47. **Bossert, B., S. Marozin, and K. K. Conzelmann**. 2003. Nonstructural proteins NS1 and NS2 of bovine respiratory syncytial virus block activation of interferon regulatory factor 3. J Virol. **77**:8661-8668.

48. **Boutell C, Canning M Orr A Everett RD**. Reciprocal activities between herpes simplex virus type 1 regulatory protein ICP0, a ubiquitin E3 ligase, and ubiquitin-specific protease USP7. J Virol. 79(19), 12342-12354. 2005.

49. **Bowie, A., E. Kiss-Toth, J. A. Symons, G. L. Smith, S. K. Dower, and L. A. O'Neill**. 2000. A46R and A52R from vaccinia virus are antagonists of host IL-1 and toll-like receptor signaling. Proc Natl Acad Sci U S A **97**:10162-10167.

50. **Brack, K., I. Berk, T. Magulski, J. Lederer, A. Dotzauer, and A. Vallbracht**. 2002. Hepatitis A virus inhibits cellular antiviral defense mechanisms induced by double-stranded RNA. J Virol **76**:11920-11930.

51. **Bradish, C. J., K. Allner, and R. Fitzgeorge**. 1975. Immunomodification and the expression of virulence in mice by defined strains of Semliki Forest virus: the effects of cyclophosphamide. J Gen. Virol **28**:225-237.

52. **Bradish, C. J. and D. Titmuss**. 1981. The effects of interferon and double-stranded RNA upon the virus-host interaction: studies with togavirus strains in mice. J Gen. Virol **53**:21-30.

53. **Brennan, C. A. and K. V. Anderson**. 2004. Drosophila: the genetics of innate immune recognition and response. Annu Rev Immunol. **22**:457-483.

54. **Brierley, M. M. and E. N. Fish** . 2002. Review: IFN-alpha/beta receptor interactions to biologic outcomes: understanding the circuitry. J. Interferon Cytokine Res. **22** :835-845.

55. **Browne, E. P. and T. Shenk**. 2003. Human cytomegalovirus UL83-coded pp65 virion protein inhibits antiviral gene expression in infected cells. Proc Natl Acad Sci U S A **100**:11439-11444.

56. **Brownlie, J., M. C. Clarke, and C. J. Howard**. 1989. Experimental infection of cattle in early pregnancy with a cytopathic strain of bovine virus diarrhoea virus. Res. Vet. Sci **46**:307-311.

57. **Brzozka, K., S. Finke, and K. K. Conzelmann**. 2005. Identification of the rabies virus alpha/beta interferon antagonist: phosphoprotein P interferes with phosphorylation of interferon regulatory factor 3. J Virol. **79**:7673-7681.

58. **Burns, K., J. Clatworthy, L. Martin, F. Martinon, C. Plumpton, B. Maschera, A. Lewis, K. Ray, J. Tschopp, and F. Volpe**. 2000. Tollip, a new component of the IL-1RI pathway, links IRAK to the IL-1 receptor. Nat Cell Biol **2**:346-351.

59. **Burysek, L., W. S. Yeow, B. Lubyova, M. Kellum, S. L. Schafer, Y. Q. Huang, and P. M. Pitha**. 1999. Functional analysis of human herpesvirus 8-encoded viral interferon regulatory factor 1 and its association with cellular interferon regulatory factors and p300. J Virol. **73**:7334-7342.

60. **Burysek, L. and P. M. Pitha**. 2001. Latently expressed human herpesvirus 8-encoded interferon regulatory factor 2 inhibits double-stranded RNA-activated protein kinase. J Virol. **75**:2345-2352.

61. **Bustin, S. A., V. Benes, T. Nolan, and M. W. Pfaffl**. 2005. Quantitative real-time RT-PCR--a perspective. J Mol Endocrinol. **34**:597-601.

62. **Casey, J. L.** 2002. RNA editing in hepatitis delta virus genotype III requires a branched double-hairpin RNA structure. J Virol **76**:7385-7397.

63. **Cassady, K. A., M. Gross, and B. Roizman**. 1998. The herpes simplex virus US11 protein effectively compensates for the gamma1(34.5) gene if present before activation of protein kinase R by precluding its phosphorylation and that of the alpha subunit of eukaryotic translation initiation factor 2. J Virol. **72**:8620-8626.

64. **Cassady, K. A. and M. Gross**. 2002. The herpes simplex virus type 1 U(S)11 protein interacts with protein kinase R in infected cells and requires a 30-amino-acid sequence adjacent to a kinase substrate domain. J Virol. **76**:2029-2035.

65. **Castelli, J. C., B. A. Hassel, K. A. Wood, X. L. Li, K. Amemiya, M. C. Dalakas, P. F. Torrence, and R. J. Youle**. 1997. A study of the interferon antiviral mechanism: apoptosis activation by the 2-5A system. J. Exp. Med. **186**:967-972.

66. **Charleston, B., M. D. Fray, S. Baigent, B. V. Carr, and W. I. Morrison**. 2001. Establishment of persistent infection with non-cytopathic bovine viral diarrhoea virus in cattle is associated with a failure to induce type I interferon. J Gen. Virol. **82**:1893-1897.

67. **Chelbi-Alix, M. K., F. Quignon, L. Pelicano, M. H. Koken, and H. de The**. 1998. Resistance to virus infection conferred by the interferon-induced promyelocytic leukemia protein. J Virol. **72**:1043-1051.

68. **Chen, F., V. Castranova, X. Shi, and L. M. Demers**. 1999. New insights into the role of nuclear factor-kappaB, a ubiquitous transcription factor in the initiation of diseases. Clin. Chem **45**:7-17.

69. **Cheshire, J. L., B. R. Williams, and A. S. Baldwin, Jr.** 1999. Involvement of double-stranded RNA-activated protein kinase in the synergistic activation of nuclear factor-kappaB by tumor necrosis factor-alpha and gamma-interferon in preneuronal cells. J Biol Chem **274**:4801-4806.

70. **Chesler, D. A. and C. S. Reiss** . 2002. The role of IFN-gamma in immune responses to viral infections of the central nervous system. Cytokine Growth Factor Rev **13**:441-454.

71. **Child SJ, Jarrahian S Harper VM Geballe AP**. Complementation of vaccinia virus lacking the double-stranded RNA-binding protein gene E3L by human cytomegalovirus. J Virol. 76(10), 4912-4918. 2002.

72. **Chin, K. C. and P. Cresswell**. 2001. Viperin (cig5), an IFN-inducible antiviral protein directly induced by human cytomegalovirus. Proc Natl Acad Sci U S A **98**:15125-15130.

73. **Chinsangaram, J., M. E. Piccone, and M. J. Grubman**. 1999. Ability of foot-and-mouth disease virus to form plaques in cell culture is associated with suppression of alpha/beta interferon. J Virol. **73**:9891-9898.

74. **Chu WM, Ostertag D Li ZW Chang L Chen Y Hu Y Williams B Perrault J Karin M**. JNK2 and IKKbeta are required for activating the innate response to viral infection. Immunity 11(6), 721-731. 1999.

75. **Clarke, P., R. L. Debiasi, R. Goody, C. C. Hoyt, S. Richardson-Burns, and K. L. Tyler**. 2005. Mechanisms of reovirus-induced cell death and tissue injury: role of apoptosis and virus-induced perturbation of host-cell signaling and transcription factor activation. Viral Immunol. **18**:89-115.

76. **Clemens, M. J., J. W. Hershey, A. C. Hovanessian, B. C. Jacobs, M. G. Katze, R. J. Kaufman, P. Lengyel, C. E. Samuel, G. C. Sen, and B. R. Williams**. 1993. PKR: proposed nomenclature for the RNA-dependent protein kinase induced by interferon. J Interferon Res. **13**:241.

77. **Clemens, M. J. and A. Elia**. 1997. The double-stranded RNA-dependent protein kinase PKR: structure and function. J. Interferon Cytokine Res. **17**:503-524.

78. **Coccia, E. M., E. Stellacci, G. Marziali, G. Weiss, and A. Battistini**. 2000. IFN-gamma and IL-4 differently regulate inducible NO synthase gene expression through IRF-1 modulation. Int. Immunol. **12**:977-985.

79. **Colamonici, O., H. Yan, P. Domanski, R. Handa, D. Smalley, J. Mullersman, M. Witte, K. Krishnan, and J. Krolewski**. 1994. Direct binding to and tyrosine phosphorylation of the alpha subunit of the type I interferon receptor by p135tyk2 tyrosine kinase. Mol Cell Biol **14**:8133-8142.

80. **Colasanti, M., T. Persichini, E. Cavalieri, C. Fabrizi, S. Mariotto, M. Menegazzi, G. M. Lauro, and H. Suzuki**. 1999. Rapid inactivation of NOS-I by lipopolysaccharide plus interferon-gamma-induced tyrosine phosphorylation. J. Biol. Chem. **274**:9915-9917.

81. **Cremer, I., J. Ghysdael, and V. Vieillard**. 2002. A non-classical ISRE/ISGF3 pathway mediates induction of RANTES gene transcription by type I IFNs. FEBS Lett. **511**:41-45.

82. **Crespo, P., X. R. Bustelo, D. S. Aaronson, O. A. Coso, M. Lopez-Barahona, M. Barbacid, and J. S. Gutkind**. 1996. Rac-1 dependent stimulation of the JNK/SAPK signaling pathway by Vav. Oncogene **13**:455-460.

83. **Cunningham, C., S. Barnard, D. J. Blackbourn, and A. J. Davison**. 2003. Transcription mapping of human herpesvirus 8 genes encoding viral interferon regulatory factors. J Gen. Virol. **84**:1471-1483.

84. **Cusson-Hermance, N., S. Khurana, T. H. Lee, K. A. Fitzgerald, and M. A. Kelliher**. 2005. Rip1 mediates the Trif-dependent toll-like receptor 3- and 4-induced NF-{kappa}B activation but does not contribute to interferon regulatory factor 3 activation. J Biol Chem **280**:36560-36566.

85. **Darnell, J. E., Jr.** 1997. STATs and gene regulation. Science **277**:1630-1635.

86. **David, M., H. E. Chen, S. Goelz, A. C. Larner, and B. G. Neel**. 1995. Differential regulation of the alpha/beta interferon-stimulated Jak/Stat pathway by the SH2 domain-containing tyrosine phosphatase SHPTP1. Mol Cell Biol **15**:7050-7058.

87. **Davies, M. V., H. W. Chang, B. L. Jacobs, and R. J. Kaufman**. 1993. The E3L and K3L vaccinia virus gene products stimulate translation through inhibition of the double-stranded RNA-dependent protein kinase by different mechanisms. J Virol. **67**:1688-1692.

88. **Deb, A., S. J. Haque, T. Mogensen, R. H. Silverman, and B. R. Williams**. 2001. RNA-dependent protein kinase PKR is required for activation of NF-kappa B by IFN-gamma in a STAT1-independent pathway. J Immunol. **166**:6170-6180.

89. **Deng, L., C. Wang, E. Spencer, L. Yang, A. Braun, J. You, C. Slaughter, C. Pickart, and Z. J. Chen**. 2000. Activation of the IkappaB kinase complex by TRAF6 requires a dimeric ubiquitin-conjugating enzyme complex and a unique polyubiquitin chain. Cell **103**:351-361.

90. **Denzler, K. L. and B. L. Jacobs**. 1994. Site-directed mutagenic analysis of reovirus sigma 3 protein binding to dsRNA. Virology **204**:190-199.

91. **Der, S. D. and A. S. Lau**. 1995. Involvement of the double-stranded-RNA-dependent kinase PKR in interferon expression and interferon-mediated antiviral activity. Proc Natl Acad Sci U S A **92**:8841-8845.

92. **Devaney, M. A., V. N. Vakharia, R. E. Lloyd, E. Ehrenfeld, and M. J. Grubman**. 1988. Leader protein of foot-and-mouth disease virus is required for cleavage of the p220 component of the cap-binding protein complex. J Virol. **62**:4407-4409.

93. **Deveraux, Q. L. and J. C. Reed** . 1999. IAP family proteins--suppressors of apoptosis. Genes Dev **13**:239-252.

94. Diao L, Zhang B Fan J Gao X Sun S Yang K Xin D Jin N Geng Y Wang C. **Herpes virus proteins ICP0 and BICP0 can activate NF-kappaB by catalyzing IkappaBalpha ubiquitination.** Cell Signal. 17(2), 217-229. 2005.
Ref Type: Generic

95. **Diaz, M. O., S. Ziemin, M. M. Le Beau, P. Pitha, S. D. Smith, R. R. Chilcote, and J. D. Rowley**. 1988. Homozygous deletion of the alpha- and beta 1-interferon genes in human leukemia and derived cell lines. Proc Natl Acad Sci U S A **85**:5259-5263.

96. **DiPerna, G., J. Stack, A. G. Bowie, A. Boyd, G. Kotwal, Z. Zhang, S. Arvikar, E. Latz, K. A. Fitzgerald, and W. L. Marshall**. 2004. Poxvirus protein N1L targets the I-kappaB kinase complex, inhibits signaling to NF-kappaB by the tumor necrosis factor superfamily of receptors, and inhibits NF-kappaB and IRF3 signaling by toll-like receptors. J Biol Chem **279**:36570-36578.

97. **Dong, B., D. S. Horowitz, R. Kobayashi, and A. R. Krainer**. 1993. Purification and cDNA cloning of HeLa cell p54nrb, a nuclear protein with two RNA recognition motifs and extensive homology to human splicing factor PSF and Drosophila NONA/BJ6. Nucleic Acids Res. **21**:4085-4092.

98. **Dong, B. and R. H. Silverman**. 1995. 2-5A-dependent RNase molecules dimerize during activation by 2-5A. J Biol Chem **270**:4133-4137.

99. **Donze, O., R. Jagus, A. E. Koromilas, J. W. Hershey, and N. Sonenberg**. 1995. Abrogation of translation initiation factor eIF-2 phosphorylation causes malignant transformation of NIH 3T3 cells. EMBO J **14**:3828-3834.

100. **Doyle, S. E., R. O'Connell, S. A. Vaidya, E. K. Chow, K. Yee, and G. Cheng**. 2003. Toll-like receptor 3 mediates a more potent antiviral response than Toll-like receptor 4. J Immunol. **170**:3565-3571.

101. **Duong FH, Filipowicz M Tripodi M La Monica N Heim MH.** Hepatitis C virus inhibits interferon signaling through up-regulation of protein phosphatase 2A. Gastroenterology. 126(1), 263-277. 2004.

102. **Eisenbeis, C. F., H. Singh, and U. Storb**. 1995. Pip, a novel IRF family member, is a lymphoid-specific, PU.1-dependent transcriptional activator. Genes Dev. **9**:1377-1387.

103. **Elia, A., K. G. Laing, A. Schofield, V. J. Tilleray, and M. J. Clemens**. 1996. Regulation of the double-stranded RNA-dependent protein kinase PKR by RNAs encoded by a repeated sequence in the Epstein-Barr virus genome. Nucleic Acids Res. **24**:4471-4478.

104. **Ellenberger, T. E., C. J. Brandl, K. Struhl, and S. C. Harrison**. 1992. The GCN4 basic region leucine zipper binds DNA as a dimer of uninterrupted alpha helices: crystal structure of the protein-DNA complex. Cell **71**:1223-1237.

105. **Elser, B., M. Lohoff, S. Kock, M. Giaisi, S. Kirchhoff, P. H. Krammer, and M. Li-Weber**. 2002. IFN-gamma represses IL-4 expression via IRF-1 and IRF-2. Immunity **17**:703-712.

106. **Espert, L., G. Degols, C. Gongora, D. Blondel, B. R. Williams, R. H. Silverman, and N. Mechti**. 2003. ISG20, a new interferon-induced RNase specific for single-stranded RNA, defines an alternative antiviral pathway against RNA genomic viruses. J Biol Chem **278**:16151-16158.

107. **Esteban, M., M. A. Garcia, E. Domingo-Gil, J. Arroyo, C. Nombela, and C. Rivas**. 2003. The latency protein LANA2 from Kaposi's sarcoma-associated herpesvirus inhibits apoptosis induced by dsRNA-activated protein kinase but not RNase L activation. J Gen. Virol. **84**:1463-1470.

108. **Evans, I. A. and C. A. Jones**. 2005. HSV induces an early primary Th1 CD4 T cell response in neonatal mice, but reduced CTL activity at the time of the peak adult response. Eur. J Immunol **35**:1454-1462.

109. **Falvo, J. V., B. S. Parekh, C. H. Lin, E. Fraenkel, and T. Maniatis**. 2000. Assembly of a functional beta interferon enhanceosome is dependent on ATF-2-c-jun heterodimer orientation. Mol Cell Biol **20**:4814-4825.

110. **Fantuzzi, G., D. Reed, M. Qi, S. Scully, C. A. Dinarello, and G. Senaldi**. 2001. Role of interferon regulatory factor-1 in the regulation of IL-18 production and activity. Eur. J Immunol. **31**:369-375.

111. **Farrar, M. A. and R. D. Schreiber**. 1993. The molecular cell biology of interferon-gamma and its receptor. Annu Rev Immunol. **11**:571-611.

112. **Fauconnier, B.** 1969. Enhancing effect of interferon antiserum on viral growth. Nature **222**:185-186.

113. **Fazakerley, J. K. and H. E. Webb**. 1987. Semliki Forest virus-induced, immune-mediated demyelination: adoptive transfer studies and viral persistence in nude mice. J Gen. Virol **68 (Pt 2)**:377-385.

114. **Fazakerley, J. K., S. Pathak, M. Scallan, S. Amor, and H. Dyson**. 1993. Replication of the A7(74) strain of Semliki Forest virus is restricted in neurons. Virology **195**:627-637.

115. **Fazakerley, J. K.** 2001. Neurovirology and developmental neurobiology. Adv. Virus Res **56**:73-124.

116. **Fazakerley, J. K.** 2002. Pathogenesis of Semliki Forest virus encephalitis. J Neurovirol. **8 Suppl 2**:66-74.

117. **Fazakerley, J. K., A. Boyd, M. L. Mikkola, and L. Kaariainen**. 2002. A single amino acid change in the nuclear localization sequence of the nsP2 protein affects the neurovirulence of Semliki Forest virus. J Virol **76**:392-396.

118. **Feller, S. M.** 2001. Crk family adaptors-signalling complex formation and biological roles. Oncogene **20**:6348-6371.

119. **Ferreon, J. C., A. C. Ferreon, K. Li, and S. M. Lemon**. 2005. Molecular determinants of TRIF proteolysis mediated by the hepatitis C virus NS3/4A protease. J Biol Chem **280**:20483-20492.

120. **Fessler, S. P., Y. R. Chin, and M. S. Horwitz**. 2004. Inhibition of tumor necrosis factor (TNF) signal transduction by the adenovirus group C RID complex involves downregulation of surface levels of TNF receptor 1. J Virol **78**:13113-13121.

121. **Finter, N. B.** 1966. Interferon as an antiviral agent in vivo: quantitative and temporal aspects of the protection of mice against Semliki Forest virus. Br. J Exp. Pathol. **47**:361-371.

122. **Fish, E. N., S. Uddin, M. Korkmaz, B. Majchrzak, B. J. Druker, and L. C. Platanias**. 1999. Activation of a CrkL-stat5 signaling complex by type I interferons. J Biol Chem **274**:571-573.

123. **Fitzgerald, K. A., E. M. Palsson-McDermott, A. G. Bowie, C. A. Jefferies, A. S. Mansell, G. Brady, E. Brint, A. Dunne, P. Gray, M. T. Harte, D. McMurray, D. E. Smith, J. E. Sims, T. A. Bird, and L. A. O'Neill**. 2001. Mal (MyD88-adapter-like) is required for Toll-like receptor-4 signal transduction. Nature **413**:78-83.

124. **Fitzgerald, K. A., S. M. McWhirter, K. L. Faia, D. C. Rowe, E. Latz, D. T. Golenbock, A. J. Coyle, S. M. Liao, and T. Maniatis**. 2003. IKKepsilon and TBK1 are essential components of the IRF3 signaling pathway. Nat Immunol. **4**:491-496.

125. **Fleming, P.** 1977. Age-dependent and strain-related differences of virulence of Semliki Forest virus in mice. J Gen. Virol **37**:93-105.

126. **Floyd-Smith, G., E. Slattery, and P. Lengyel**. 1981. Interferon action: RNA cleavage pattern of a (2'-5')oligoadenylate--dependent endonuclease. Science **212**:1030-1032.

127. **Foster, G. R. and N. B. Finter**. 1998. Are all type I human interferons equivalent? J. Viral Hepat. **5**:143-152.

128. **Foy, E., K. Li, C. Wang, R. Sumpter, Jr., M. Ikeda, S. M. Lemon, and M. Gale, Jr.** 2003. Regulation of interferon regulatory factor-3 by the hepatitis C virus serine protease. Science **300**:1145-1148.

129. **Foy, E., K. Li, R. Sumpter, Jr., Y. M. Loo, C. L. Johnson, C. Wang, P. M. Fish, M. Yoneyama, T. Fujita, S. M. Lemon, and M. Gale, Jr.** 2005. Control of antiviral defenses through hepatitis C virus disruption of retinoic acid-inducible gene-I signaling. Proc Natl Acad Sci U S A **102**:2986-2991.

130. **Frolova, E. I., R. Z. Fayzulin, S. H. Cook, D. E. Griffin, C. M. Rice, and I. Frolov**. 2002. Roles of nonstructural protein nsP2 and Alpha/Beta interferons in determining the outcome of Sindbis virus infection. J Virol **76**:11254-11264.

131. **Fukui T, S Yumura and T. K. Yumura**. Agar-overlay Immunofluorescence: High resolution studies of cytoskeletal components and their changes during chemotaxis. Methods in Cell Biol. 28, 347-356. 1987.

132. **Gale, M. J., Jr., M. J. Korth, N. M. Tang, S. L. Tan, D. A. Hopkins, T. E. Dever, S. J. Polyak, D. R. Gretch, and M. G. Katze**. 1997. Evidence that hepatitis C virus resistance to interferon is mediated through repression of the PKR protein kinase by the nonstructural 5A protein. Virology **230**:217-227.

133. **Galon, J., C. Sudarshan, S. Ito, D. Finbloom, and J. J. O'Shea**. 1999. IL-12 induces IFN regulating factor-1 (IRF-1) gene expression in human NK and T cells. J Immunol. **162**:7256-7262.

134. **Garcia-Sastre, A., R. K. Durbin, H. Zheng, P. Palese, R. Gertner, D. E. Levy, and J. E. Durbin**. 1998. The role of interferon in influenza virus tissue tropism. J Virol. **72**:8550-8558.

135. **Garcia-Sastre, A.** 2002. Mechanisms of inhibition of the host interferon alpha/beta-mediated antiviral responses by viruses. Microbes. Infect. **4**:647-655.

136. **Garcia-Sastre, A.** 2004. Identification and characterization of viral antagonists of type I interferon in negative-strand RNA viruses. Curr. Top. Microbiol. Immunol. **283**:249-280.

137. **Gates, M. C., B. J. Sheahan, M. A. O'Sullivan, and G. J. Atkins**. 1985. The pathogenicity of the A7, M9 and L10 strains of Semliki Forest virus for weanling mice and primary mouse brain cell cultures. J Gen. Virol **66 (Pt 11)**:2365-2373.

138. **Geiss, G. K., V. S. Carter, Y. He, B. K. Kwieciszewski, T. Holzman, M. J. Korth, C. A. Lazaro, N. Fausto, R. E. Bumgarner, and M. G. Katze**. 2003. Gene expression profiling of the cellular transcriptional network regulated by alpha/beta interferon and its partial attenuation by the hepatitis C virus nonstructural 5A protein. J Virol. **77**:6367-6375.

139. **Gil, J., J. Alcami, and M. Esteban**. 2000. Activation of NF-kappa B by the dsRNA-dependent protein kinase, PKR involves the I kappa B kinase complex. Oncogene **19**:1369-1378.

140. **Gil, L. H., A. L. van Olphen, S. K. Mittal, and R. O. Donis**. 2005. Modulation of PKR activity in cells infected by bovine viral diarrhea virus. Virus Res.

141. **Gilks, N., N. Kedersha, M. Ayodele, L. Shen, G. Stoecklin, L. M. Dember, and P. Anderson**. 2004. Stress granule assembly is mediated by prion-like aggregation of TIA-1. Mol Biol Cell **15**:5383-5398.

142. **Gimenez-Barcons, M., C. Wang, M. Chen, J. M. Sanchez-Tapias, J. C. Saiz, and M. Gale, Jr.** 2005. The oncogenic potential of hepatitis C virus NS5A sequence variants is associated with PKR regulation. J Interferon Cytokine Res. **25**:152-164.

143. **Gohda, J., T. Matsumura, and J. Inoue**. 2004. Cutting edge: TNFR-associated factor (TRAF) 6 is essential for MyD88-dependent pathway but not toll/IL-1 receptor domain-containing adaptor-inducing IFN-beta (TRIF)-dependent pathway in TLR signaling. J Immunol. **173**:2913-2917.

144. **Gomez, d. C., N. Ehsani, M. L. Mikkola, J. A. Garcia, and L. Kaariainen**. 1999. RNA helicase activity of Semliki Forest virus replicase protein NSP2. FEBS Lett. **448** :19-22.

145. **Goodbourn, S., L. Didcock, and R. E. Randall**. 2000. Interferons: cell signalling, immune modulation, antiviral response and virus countermeasures. J Gen. Virol. **81** :2341-2364.

146. **Gorchakov, R., E. Frolova, B. R. Williams, C. M. Rice, and I. Frolov**. 2004. PKR-dependent and -independent mechanisms are involved in translational shutoff during Sindbis virus infection. J Virol **78**:8455-8467.

147. **Graff, J. W., D. N. Mitzel, C. M. Weisend, M. L. Flenniken, and M. E. Hardy**. 2002. Interferon regulatory factor 3 is a cellular partner of rotavirus NSP1. J Virol **76**:9545-9550.

148. **Grandvaux, N., M. J. Servant, B. tenOever, G. C. Sen, S. Balachandran, G. N. Barber, R. Lin, and J. Hiscott**. 2002. Transcriptional profiling of interferon regulatory factor 3 target genes: direct involvement in the regulation of interferon-stimulated genes. J Virol. **76**:5532-5539.

149. **Grell, S. N., U. Riber, K. Tjornehoj, L. E. Larsen, and P. M. Heegaard**. 2005. Age-dependent differences in cytokine and antibody responses after experimental RSV infection in a bovine model. Vaccine **23**:3412-3423.

150. **Grieder, F. B. and S. N. Vogel**. 1999. Role of interferon and interferon regulatory factors in early protection against Venezuelan equine encephalitis virus infection. Virology **257**:106-118.

151. **Grimley, P. M., I. K. Berezesky, and R. M. Friedman**. 1968. Cytoplasmic structures associated with an arbovirus infection: loci of viral ribonucleic acid synthesis. J Virol **2**:1326-1338.

152. **Grimley, P. M. and R. M. Friedman**. 1970. Development of Semliki forest virus in mouse brain: an electron microscopic study. Exp. Mol Pathol. **12**:1-13.

153. **Gross, M., B. Liu, J. Tan, F. S. French, M. Carey, and K. Shuai**. 2001. Distinct effects of PIAS proteins on androgen-mediated gene activation in prostate cancer cells. Oncogene **20**:3880-3887.

154. **Grubman MJ and Chinsangaram J**. Foot and mouth disease virus: the role of the leader protein in viral pathogenesis. Recent Res Dev Virol 2, 123-134. 2000.

155. **Grumbach, I. M., I. A. Mayer, S. Uddin, F. Lekmine, B. Majchrzak, H. Yamauchi, S. Fujita, B. Druker, E. N. Fish, and L. C. Platanias**. 2001. Engagement of the CrkL adaptor in interferon alpha signalling in BCR-ABL-expressing cells. Br. J Haematol. **112**:327-336.

156. **Guarne, A., J. Tormo, R. Kirchweger, D. Pfistermueller, I. Fita, and T. Skern**. 1998. Structure of the foot-and-mouth disease virus leader protease: a papain-like fold adapted for self-processing and eIF4G recognition. EMBO J **17**:7469-7479.

157. **Guidotti, L. G. and F. V. Chisari**. 2001. Noncytolytic control of viral infections by the innate and adaptive immune response. Annu Rev Immunol. **19**:65-91.

158. **Hagmaier, K., S. Jennings, J. Buse, F. Weber, and G. Kochs**. 2003. Novel gene product of Thogoto virus segment 6 codes for an interferon antagonist. J Virol **77**:2747-2752.

159. **Hahn, Y. S., E. G. Strauss, and J. H. Strauss**. 1989. Mapping of RNA- temperature-sensitive mutants of Sindbis virus: assignment of complementation groups A, B, and G to nonstructural proteins. J Virol **63**:3142-3150.

160. **Haller, O. and G. Kochs**. 2002. Interferon-induced mx proteins: dynamin-like GTPases with antiviral activity. Traffic. **3**:710-717.

161. **Han JQ, Wroblewski G Xu Z Silverman RH Barton DJ.** Sensitivity of hepatitis C virus RNA to the antiviral enzyme ribonuclease L is determined by a subset of efficient cleavage sites. J Interferon Cytokine Res. 24(11), 664-676. 2004.

162. **Harte, M. T., I. R. Haga, G. Maloney, P. Gray, P. C. Reading, N. W. Bartlett, G. L. Smith, A. Bowie, and L. A. O'Neill**. 2003. The poxvirus protein A52R targets Toll-like receptor signaling complexes to suppress host defense. J Exp. Med. **197**:343-351.

163. **Hassel, B. A., A. Zhou, C. Sotomayor, A. Maran, and R. H. Silverman**. 1993. A dominant negative mutant of 2-5A-dependent RNase suppresses antiproliferative and antiviral effects of interferon. EMBO J **12**:3297-3304.

164. **Hattori, M. and N. Minato**. 2003. Rap1 GTPase: functions, regulation, and malignancy. J Biochem (Tokyo) **134**:479-484.

165. **Havert, M. B., B. Schofield, D. E. Griffin, and D. N. Irani**. 2000. Activation of divergent neuronal cell death pathways in different target cell populations during neuroadapted sindbis virus infection of mice. J Virol **74**:5352-5356.

166. **He, B., M. Gross, and B. Roizman**. 1997. The gamma(1)34.5 protein of herpes simplex virus 1 complexes with protein phosphatase 1alpha to dephosphorylate the alpha subunit of the eukaryotic translation initiation factor 2 and preclude the shutoff of protein synthesis by double-stranded RNA-activated protein kinase. Proc Natl Acad Sci U S A **94**:843-848.

167. **Heil, F., H. Hemmi, H. Hochrein, F. Ampenberger, C. Kirschning, S. Akira, G. Lipford, H. Wagner, and S. Bauer** . 2004. Species-specific recognition of single-stranded RNA via toll-like receptor 7 and 8. Science **303**:1526-1529.

168. **Heim, M. H., D. Moradpour, and H. E. Blum**. 1999. Expression of hepatitis C virus proteins inhibits signal transduction through the Jak-STAT pathway. J Virol. **73**:8469-8475.

169. **Heineberg H, Gold E, Robbins FC.** Differences in interferon content in tissues of mice of various ages infected with Coxsackie B1 virus. Proc Soc Exp Biol Med 115, 947-953.

170. **Heise, M. T., L. J. White, D. A. Simpson, C. Leonard, K. A. Bernard, R. B. Meeker, and R. E. Johnston**. 2003. An attenuating mutation in nsP1 of the Sindbis-group virus S.A.AR86 accelerates nonstructural protein processing and up-regulates viral 26S RNA synthesis. J Virol **77**:1149-1156.

171. **Helbig, K. J., D. T. Lau, L. Semendric, H. A. Harley, and M. R. Beard**. 2005. Analysis of ISG expression in chronic hepatitis C identifies viperin as a potential antiviral effector. Hepatology **42**:702-710.

172. **Hemmi, H., O. Takeuchi, S. Sato, M. Yamamoto, T. Kaisho, H. Sanjo, T. Kawai, K. Hoshino, K. Takeda, and S. Akira**. 2004. The roles of two IkappaB kinase-related kinases in lipopolysaccharide and double stranded RNA signaling and viral infection. J Exp. Med. **199**:1641-1650.

173. **Henderson, S., D. Huen, M. Rowe, C. Dawson, G. Johnson, and A. Rickinson**. 1993. Epstein-Barr virus-coded BHRF1 protein, a viral homologue of Bcl-2, protects human B cells from programmed cell death. Proc Natl Acad Sci U S A **90**:8479-8483.

174. **Her, L. S., E. Lund, and J. E. Dahlberg**. 1997. Inhibition of Ran guanosine triphosphatase-dependent nuclear transport by the matrix protein of vesicular stomatitis virus. Science **276**:1845-1848.

175. **Hidmark, A. S., G. M. McInerney, E. K. Nordstrom, I. Douagi, K. M. Werner, P. Liljestrom, and G. B. Karlsson Hedestam**. 2005. Early alpha/beta interferon production by myeloid dendritic cells in response to UV-inactivated virus requires viral entry and interferon regulatory factor 3 but not MyD88. J Virol. **79**:10376-10385.

176. **Hirschfeld, M., Y. Ma, J. H. Weis, S. N. Vogel, and J. J. Weis**. 2000. Cutting edge: repurification of lipopolysaccharide eliminates signaling through both human and murine toll-like receptor 2. J Immunol. **165**:618-622.

177. **Hoff, H. S. and R. O. Donis**. 1997. Induction of apoptosis and cleavage of poly(ADP-ribose) polymerase by cytopathic bovine viral diarrhea virus infection. Virus Res. **49**:101-113.

178. **Hofmann, K.** 1999. The modular nature of apoptotic signaling proteins. Cell Mol Life Sci **55**:1113-1128.

179. **Honda, K., H. Yanai, T. Mizutani, H. Negishi, N. Shimada, N. Suzuki, Y. Ohba, A. Takaoka, W. C. Yeh, and T. Taniguchi**. 2004. Role of a transductional-transcriptional processor complex involving MyD88 and IRF-7 in Toll-like receptor signaling. Proc. Natl. Acad. Sci U. S. A **101**:15416-15421.

180. **Honda, K., H. Yanai, A. Takaoka, and T. Taniguchi**. 2005. Regulation of the type I IFN induction: a current view. Int. Immunol. **17**:1367-1378.

181. **Hu, C. M., S. Y. Jang, J. C. Fanzo, and A. B. Pernis**. 2002. Modulation of T cell cytokine production by interferon regulatory factor-4. J Biol Chem **277**:49238-49246.

182. **Huismans, H. and W. K. Joklik** . 1976. Reovirus-coded polypeptides in infected cells: isolation of two native monomeric polypeptides with affinity for single-stranded and double-stranded RNA, respectively. Virology **70**:411-424.

183. **Hwang, S. Y., P. J. Hertzog, K. A. Holland, S. H. Sumarsono, M. J. Tymms, J. A. Hamilton, G. Whitty, I. Bertoncello, and I. Kola**. 1995. A null mutation in the gene encoding a type I interferon receptor component eliminates antiproliferative and antiviral responses to interferons alpha and beta and alters macrophage responses. Proc Natl Acad Sci U S A **92**:11284-11288.

184. **Imani, F. and B. L. Jacobs**. 1988. Inhibitory activity for the interferon-induced protein kinase is associated with the reovirus serotype 1 sigma 3 protein. Proc Natl Acad Sci U S A **85**:7887-7891.

185. **Iordanov MS, Paranjape JM Zhou A Wong J Williams BR Meurs EF Silverman RH Magun BE.** Activation of p38 mitogen-activated protein kinase and c-Jun NH(2)-terminal kinase by double-stranded RNA and encephalomyocarditis virus: involvement of RNase L, protein kinase R, and alternative pathways. Mol Cell Biol. 20(2), 617-627. 2000.

186. **Iordanov, M. S., J. Wong, J. C. Bell, and B. E. Magun**. 2001. Activation of NF-kappaB by double-stranded RNA (dsRNA) in the absence of protein kinase R and RNase L demonstrates the existence of two separate dsRNA-triggered antiviral programs. Mol Cell Biol **21**:61-72.

187. **Isaacs, A and Lindenmann J**. 1957. Virus interference. I. The interferon. Proc. R. Soc. Lond B Biol. Sci. **147**:258-267.

188. **Iwasaki, T., S. Itamura, H. Nishimura, Y. Sato, M. Tashiro, T. Hashikawa, and T. Kurata**. 2004. Productive infection in the murine central nervous system with avian influenza virus A (H5N1) after intranasal inoculation. Acta Neuropathol. (Berl) **108**:485-492.

189. **Izaguirre, A., B. J. Barnes, S. Amrute, W. S. Yeow, N. Megjugorac, J. Dai, D. Feng, E. Chung, P. M. Pitha, and P. Fitzgerald-Bocarsly**. 2003. Comparative analysis of IRF and IFN-alpha expression in human plasmacytoid and monocyte-derived dendritic cells. J Leukoc. Biol **74**:1125-1138.

190. **Jennings S, Martinez-Sobrido L Garcia-Sastre A Weber F Kochs G**. Thogoto virus ML protein suppresses IRF3 function. Virology 331(1), 63-72. 2005.

191. **Juang, Y. T., W. Lowther, M. Kellum, W. C. Au, R. Lin, J. Hiscott, and P. M. Pitha**. 1998. Primary activation of interferon A and interferon B gene transcription by interferon regulatory factor 3. Proc Natl Acad Sci U S A **95**:9837-9842.

192. **Kallman, A. M., M. Sahlin, and M. Ohman**. 2003. ADAR2 A-->I editing: site selectivity and editing efficiency are separate events. Nucleic Acids Res. **31**:4874-4881.

193. **Kameoka, S., P. Duque, and M. M. Konarska**. 2004. p54(nrb) associates with the 5' splice site within large transcription/splicing complexes. EMBO J **23**:1782-1791.

194. **Kamijo, R., H. Harada, T. Matsuyama, M. Bosland, J. Gerecitano, D. Shapiro, J. Le, S. I. Koh, T. Kimura, S. J. Green, and .** 1994. Requirement for transcription factor IRF-1 in NO synthase induction in macrophages. Science **263**:1612-1615.

195. **Karin, M. and F. R. Greten**. 2005. NF-kappaB: linking inflammation and immunity to cancer development and progression. Nat Rev Immunol. **5**:749-759.

196. **Kato, H., S. Sato, M. Yoneyama, M. Yamamoto, S. Uematsu, K. Matsui, T. Tsujimura, K. Takeda, T. Fujita, O. Takeuchi, and S. Akira**. 2005. Cell type-specific involvement of RIG-I in antiviral response. Immunity. **23**:19-28.

197. **Katze, M. G., M. Wambach, M. L. Wong, M. Garfinkel, E. Meurs, K. Chong, B. R. Williams, A. G. Hovanessian, and G. N. Barber**. 1991. Functional expression and RNA binding analysis of the interferon-induced, double-stranded RNA-activated, 68,000-Mr protein kinase in a cell-free system. Mol Cell Biol **11**:5497-5505.

198. **Kawai, T., O. Takeuchi, T. Fujita, J. Inoue, P. F. Muhlradt, S. Sato, K. Hoshino, and S. Akira**. 2001. Lipopolysaccharide stimulates the MyD88-independent pathway and results in activation of IFN-regulatory factor 3 and the expression of a subset of lipopolysaccharide-inducible genes. J Immunol. **167**:5887-5894.

199. **Kawai, T., K. Takahashi, S. Sato, C. Coban, H. Kumar, H. Kato, K. J. Ishii, O. Takeuchi, and S. Akira**. 2005. IPS-1, an adaptor triggering RIG-I- and Mda5-mediated type I interferon induction. Nat Immunol. **6**:981-988.

200. **Kawamoto, S., K. Oritani, H. Asada, I. Takahashi, J. Ishikawa, H. Yoshida, M. Yamada, N. Ishida, H. Ujiie, H. Masaie, Y. Tomiyama, and Y. Matsuzawa**. 2003. Antiviral activity of limitin against encephalomyocarditis virus, herpes simplex virus, and mouse hepatitis virus: diverse requirements by limitin and alpha interferon for interferon regulatory factor 1. J. Virol. 77:9622-9631.

201. **Kedersha, N. L., M. Gupta, W. Li, I. Miller, and P. Anderson**. 1999. RNA-binding proteins TIA-1 and TIAR link the phosphorylation of eIF-2 alpha to the assembly of mammalian stress granules. J Cell Biol **147**:1431-1442.

202. **Kedersha, N. L., M. Gupta, W. Li, I. Miller, and P. Anderson**. 1999. RNA-binding proteins TIA-1 and TIAR link the phosphorylation of eIF-2 alpha to the assembly of mammalian stress granules. J Cell Biol **147**:1431-1442.

203. **Kent, S., S. D. Kernahan, and S. Levine**. 1996. Effects of excitatory amino acids on the hypothalamic-pituitary-adrenal axis of the neonatal rat. Brain Res Dev Brain Res **94**:1-13.

204. **Keogh, B., G. J. Atkins, K. H. Mills, and B. J. Sheahan**. 2003. Role of interferon-gamma and nitric oxide in the neuropathogenesis of avirulent Semliki Forest virus infection. Neuropathol. Appl. Neurobiol. **29**:553-562.

205. **Keranen, S. and L. Kaariainen** . 1979. Functional defects of RNA-negative temperature-sensitive mutants of Sindbis and Semliki Forest viruses. J Virol **32**:19-29.

206. **Kerr, I. M. and R. E. Brown**. 1978. pppA2'p5'A2'p5'A: an inhibitor of protein synthesis synthesized with an enzyme fraction from interferon-treated cells. Proc Natl Acad Sci U S A **75**:256-260.

207. **Khabar, K. S., F. Al Zoghaibi, M. N. Al Ahdal, T. Murayama, M. Dhalla, N. Mukaida, M. Taha, S. T. Al Sedairy, Y. Siddiqui, G. Kessie, and K. Matsushima**. 1997. The alpha chemokine, interleukin 8, inhibits the antiviral action of interferon alpha. J Exp. Med. **186**:1077-1085.

208. **Khalili-Shirazi, A., N. Gregson, and H. E. Webb**. 1988. Immunocytochemical evidence for Semliki Forest virus antigen persistence in mouse brain. J Neurol. Sci **85**:17-26.

209. **Kielian, M. and S. Jungerwirth**. 1990. Mechanisms of enveloped virus entry into cells. Mol Biol Med 7:17-31.

210. **Kirchhoff, S., A. E. Koromilas, F. Schaper, M. Grashoff, N. Sonenberg, and H. Hauser**. 1995. IRF-1 induced cell growth inhibition and interferon induction requires the activity of the protein kinase PKR. Oncogene **11**:439-445.

211. **Kirchhoff, S., D. Wilhelm, P. Angel, and H. Hauser**. 1999. NFkappaB activation is required for interferon regulatory factor-1-mediated interferon beta induction. Eur. J Biochem **261**:546-554.

212. **Kitajewski, J., R. J. Schneider, B. Safer, S. M. Munemitsu, C. E. Samuel, B. Thimmappaya, and T. Shenk**. 1986. Adenovirus VAI RNA antagonizes the antiviral action of interferon by preventing activation of the interferon-induced eIF-2 alpha kinase. Cell **45**:195-200.

213. **Knipe DM, Samuel CE Palese P.** Virus-host cell interactions. Fields virology 4th edition , 133-170. 2001. Lippincott-Raven, Philadelphia.

214. **Kochs, G. and O. Haller**. 1999. Interferon-induced human MxA GTPase blocks nuclear import of Thogoto virus nucleocapsids. Proc Natl Acad Sci U S A **96**:2082-2086.

215. **Kochs, G., C. Janzen, H. Hohenberg, and O. Haller**. 2002. Antivirally active MxA protein sequesters La Crosse virus nucleocapsid protein into perinuclear complexes. Proc Natl Acad Sci U S A **99**:3153-3158.

216. **Komatsu, T., K. Takeuchi, J. Yokoo, and B. Gotoh**. 2004. C and V proteins of Sendai virus target signaling pathways leading to IRF-3 activation for the negative regulation of interferon-beta production. Virology **325**:137-148.

217. **Koprouski H and Cox HR**. New England J Med 236, 647. 1947.

218. **Koromilas, A. E., S. Roy, G. N. Barber, M. G. Katze, and N. Sonenberg**. 1992. Malignant transformation by a mutant of the IFN-inducible dsRNA-dependent protein kinase. Science **257**:1685-1689.

219. **Kotenko SV, Gallagher G Baurin VV Lewis-Antes A Shen M Shah NK Langer JA Sheikh F Dickensheets H Donnelly RP.** IFN-lambdas mediate antiviral protection through a distinct class II cytokine receptor complex. Nat Immunol. 4(1), 69-77. 2003.

220. **Krug A, Luker GD Barchet W Leib DA Akira S Colonna M**. Herpes simplex virus type 1 activates murine natural interferon-producing cells through toll-like receptor 9. Blood. 103(4), 1433-1437. 2004.

221. **Krust, B., Y. Riviere, and A. G. Hovanessian**. 1982. p67K kinase in different tissues and plasma of control and interferon-treated mice. Virology **120**:240-246.

222. **Kuhen, K. L. and C. E. Samuel** . 1997. Isolation of the interferon-inducible RNA-dependent protein kinase Pkr promoter and identification of a novel DNA element within the 5'-flanking region of human and mouse Pkr genes. Virology **227**:119-130.

223. **Kujala, P., A. Ikaheimonen, N. Ehsani, H. Vihinen, P. Auvinen, and L. Kaariainen**. 2001. Biogenesis of the Semliki Forest virus RNA replication complex. J Virol **75**:3873-3884.

224. **Kumar, A., J. Haque, J. Lacoste, J. Hiscott, and B. R. Williams**. 1994. Double-stranded RNA-dependent protein kinase activates transcription factor NF-kappa B by phosphorylating I kappa B. Proc Natl Acad Sci U S A **91**:6288-6292.

225. **Kumar, A., Y. L. Yang, V. Flati, S. Der, S. Kadereit, A. Deb, J. Haque, L. Reis, C. Weissmann, and B. R. Williams**. 1997. Deficient cytokine signaling in mouse embryo fibroblasts with a targeted deletion in the PKR gene: role of IRF-1 and NF-kappaB. EMBO J **16**:406-416.

226. **Kumar, M. and G. G. Carmichael**. 1997. Nuclear antisense RNA induces extensive adenosine modifications and nuclear retention of target transcripts. Proc Natl Acad Sci U S A **94**:3542-3547.

227. **Kurt-Jones EA, Popova L Kwinn L Haynes LM Jones LP Tripp RA Walsh EE Freeman MW Golenbock DT Anderson LJ Finberg RW.** Pattern recognition receptors TLR4 and CD14 mediate response to respiratory syncytial virus. Nat Immunol. 1(5), 398-401. 2000.

228. **Kurt-Jones, E. A., M. Chan, S. Zhou, J. Wang, G. Reed, R. Bronson, M. M. Arnold, D. M. Knipe, and R. W. Finberg**. 2004. Herpes simplex virus 1 interaction with Toll-like receptor 2 contributes to lethal encephalitis. Proc Natl Acad Sci U S A **101**:1315-1320.

229. **Laakkonen, P., T. Ahola, and L. Kaariainen**. 1996. The effects of palmitoylation on membrane association of Semliki forest virus RNA capping enzyme. J Biol Chem **271** :28567-28571.

230. **Labrada, L., X. H. Liang, W. Zheng, C. Johnston, and B. Levine**. 2002. Age-dependent resistance to lethal alphavirus encephalitis in mice: analysis of gene expression in the central nervous system and identification of a novel interferon-inducible protective gene, mouse ISG12. J Virol **76**:11688-11703.

231. **LaFleur, D. W., B. Nardelli, T. Tsareva, D. Mather, P. Feng, M. Semenuk, K. Taylor, M. Buergin, D. Chinchilla, V. Roshke, G. Chen, S. M. Ruben, P. M. Pitha, T. A. Coleman, and P. A. Moore**. 2001. Interferon-kappa, a novel type I interferon expressed in human keratinocytes. J. Biol. Chem. **276**:39765-39771.

232. **Lanford RE, Guerra B Lee H Averett DR Pfeiffer B Chavez D Notvall L Bigger C.** Antiviral effect and virus-host interactions in response to alpha interferon, gamma interferon, poly(i)-poly(c), tumor necrosis factor alpha, and ribavirin in hepatitis C virus subgenomic replicons. J Virol 77, 1092-1104. 2003.

233. **Langland, J. O., P. N. Kao, and B. L. Jacobs**. 1999. Nuclear factor-90 of activated T-cells: A double-stranded RNA-binding protein and substrate for the double-stranded RNA-dependent protein kinase, PKR. Biochemistry **38**:6361-6368.

234. **Le May, N., S. Dubaele, D. S. Proietti, A. Billecocq, M. Bouloy, and J. M. Egly**. 2004. TFIIH transcription factor, a target for the Rift Valley hemorrhagic fever virus. Cell **116**:541-550.

235. **Lee, S. B., D. Rodriguez, J. R. Rodriguez, and M. Esteban**. 1997. The apoptosis pathway triggered by the interferon-induced protein kinase PKR requires the third basic domain, initiates upstream of Bcl-2, and involves ICE-like proteases. Virology **231**:81-88.

236. **Lee, T. G., J. Tomita, A. G. Hovanessian, and M. G. Katze**. 1990. Purification and partial characterization of a cellular inhibitor of the interferon-induced protein kinase of Mr 68,000 from influenza virus-infected cells. Proc Natl Acad Sci U S A **87**:6208-6212.

237. **Lefevre, F., M. Guillomot, S. D'Andrea, S. Battegay, and C. La Bonnardiere**. 1998. Interferon-delta: the first member of a novel type I interferon family. Biochimie **80**:779-788.

238. **Lekmine, F., S. Uddin, A. Sassano, S. Parmar, S. M. Brachmann, B. Majchrzak, N. Sonenberg, N. Hay, E. N. Fish, and L. C. Platanias**. 2003. Activation of the p70 S6 kinase and phosphorylation of the 4E-BP1 repressor of mRNA translation by type I interferons. J Biol Chem **278**:27772-27780.

239. **Lemm, J. A. and C. M. Rice**. 1993. Roles of nonstructural polyproteins and cleavage products in regulating Sindbis virus RNA replication and transcription. J Virol **67**:1916-1926.

240. **Lemm, J. A. and C. M. Rice**. 1993. Assembly of functional Sindbis virus RNA replication complexes: requirement for coexpression of P123 and P34. J Virol **67**:1905-1915.

241. **Lenschow, D. J., N. V. Giannakopoulos, L. J. Gunn, C. Johnston, A. K. O'Guin, R. E. Schmidt, B. Levine, and H. W. Virgin**. 2005. Identification of interferon-stimulated gene 15 as an antiviral molecule during Sindbis virus infection in vivo. J Virol. **79**:13974-13983.

242. **Levine, B. and D. E. Griffin**. 1992. Persistence of viral RNA in mouse brains after recovery from acute alphavirus encephalitis. J Virol **66**:6429-6435.

243. **Levine, B., J. E. Goldman, H. H. Jiang, D. E. Griffin, and J. M. Hardwick**. 1996. Bcl-2 protects mice against fatal alphavirus encephalitis. Proc Natl Acad Sci U S A **93**:4810-4815.

244. **Levine, S., F. Berkenbosch, D. Suchecki, and F. J. Tilders**. 1994. Pituitary-adrenal and interleukin-6 responses to recombinant interleukin-1 in neonatal rats. Psychoneuroendocrinology **19**:143-153.

245. **Levy, D. E. and C. K. Lee**. 2002. What does Stat3 do? J Clin. Invest **109**:1143-1148.

246. **Lewis, J., G. A. Oyler, K. Ueno, Y. R. Fannjiang, B. N. Chau, J. Vornov, S. J. Korsmeyer, S. Zou, and J. M. Hardwick**. 1999. Inhibition of virus-induced neuronal apoptosis by Bax. Nat Med **5**:832-835.

247. **Li G, Xiang Y Sabapathy K Silverman RH.** An apoptotic signaling pathway in the interferon antiviral response mediated by RNase L and c-Jun NH2-terminal kinase. J Biol Chem 279(2), 1123-1131. 2004.

248. **Li Y, Sassano A Majchrzak B Deb DK Levy DE Gaestel M Nebreda AR Fish EN Platanias LC.** Role of p38alpha Map kinase in Type I interferon signaling. J Biol Chem. 279(2), 970-979. 2004.

249. **Li, C. C., R. M. Dai, and D. L. Longo**. 1995. Inactivation of NF-kappa B inhibitor I kappa B alpha: ubiquitin-dependent proteolysis and its degradation product. Biochem Biophys. Res. Commun. **215**:292-301.

250. **Li, K., E. Foy, J. C. Ferreon, M. Nakamura, A. C. Ferreon, M. Ikeda, S. C. Ray, M. Gale, Jr., and S. M. Lemon** . 2005. Immune evasion by hepatitis C virus NS3/4A protease-mediated cleavage of the Toll-like receptor 3 adaptor protein TRIF. Proc Natl Acad Sci U S A **102**:2992-2997.

251. **Li, S., A. Strelow, E. J. Fontana, and H. Wesche**. 2002. IRAK-4: a novel member of the IRAK family with the properties of an IRAK-kinase. Proc. Natl. Acad. Sci U. S. A **99**:5567-5572.

252. **Liao, J., Y. Fu, and K. Shuai** . 2000. Distinct roles of the NH2- and COOH-terminal domains of the protein inhibitor of activated signal transducer and activator of transcription (STAT) 1 (PIAS1) in cytokine-induced PIAS1-Stat1 interaction. Proc Natl Acad Sci U S A **97**:5267-5272.

253. **Liljestrom, P., S. Lusa, D. Huylebroeck, and H. Garoff**. 1991. In vitro mutagenesis of a full-length cDNA clone of Semliki Forest virus: the small 6,000-molecular-weight membrane protein modulates virus release. J Virol **65**:4107-4113.

254. **Lin, H. W., Y. Y. Chang, M. L. Wong, J. W. Lin, and T. J. Chang**. 2004. Functional analysis of virion host shutoff protein of pseudorabies virus. Virology **324**:412-418.

255. **Lin, R., C. Heylbroeck, P. Genin, P. M. Pitha, and J. Hiscott**. 1999. Essential role of interferon regulatory factor 3 in direct activation of RANTES chemokine transcription. Mol Cell Biol **19**:959-966.

256. **Lin, R., P. Genin, Y. Mamane, M. Sgarbanti, A. Battistini, W. J. Harrington, Jr., G. N. Barber, and J. Hiscott**. 2001. HHV-8 encoded vIRF-1 represses the interferon antiviral response by blocking IRF-3 recruitment of the CBP/p300 coactivators. Oncogene **20**:800-811.

257. **Lin, R., R. S. Noyce, S. E. Collins, R. D. Everett, and K. L. Mossman**. 2004. The herpes simplex virus ICP0 RING finger domain inhibits IRF-3 and IRF-7-mediated activation of interferon-stimulated genes. J Virol. **78**:1675-1684.

258. **Liu, B., J. Liao, X. Rao, S. A. Kushner, C. D. Chung, D. D. Chang, and K. Shuai**. 1998. Inhibition of Stat1-mediated gene activation by PIAS1. Proc Natl Acad Sci U S A **95**:10626-10631.

259. **Lohoff, M., D. Ferrick, H. W. Mittrucker, G. S. Duncan, S. Bischof, M. Rollinghoff, and T. W. Mak**. 1997. Interferon regulatory factor-1 is required for a T helper 1 immune response in vivo. Immunity **6**:681-689.

260. **Lohoff, M., H. W. Mittrucker, S. Prechtl, S. Bischof, F. Sommer, S. Kock, D. A. Ferrick, G. S. Duncan, A. Gessner, and T. W. Mak**. 2002. Dysregulated T helper cell differentiation in the absence of interferon regulatory factor 4. Proc Natl Acad Sci U S A **99**:11808-11812.

261. **Lohoff, M. and T. W. Mak**. 2005. Roles of interferon-regulatory factors in T-helper-cell differentiation. Nat Rev Immunol. **5**:125-135.

262. **Lu, Y., M. Wambach, M. G. Katze, and R. M. Krug**. 1995. Binding of the influenza virus NS1 protein to double-stranded RNA inhibits the activation of the protein kinase that phosphorylates the eIF-2 translation initiation factor. Virology **214**:222-228.

263. **Lubyova B, Kellum MJ Frisancho AJ Pitha PM.** Kaposi's sarcoma-associated herpesvirus-encoded vIRF-3 stimulates the transcriptional activity of cellular IRF-3 and IRF-7. J Biol Chem. 279(9), 7643-7654. 2004.

264. **Lubyova, B. and P. M. Pitha**. 2000. Characterization of a novel human herpesvirus 8-encoded protein, vIRF-3, that shows homology to viral and cellular interferon regulatory factors. J Virol **74**:8194-8201.

265. **Luft, T., K. C. Pang, E. Thomas, P. Hertzog, D. N. Hart, J. Trapani, and J. Cebon**. 1998. Type I IFNs enhance the terminal differentiation of dendritic cells. J Immunol. **161**:1947-1953.

266. **Lund, J., A. Sato, S. Akira, R. Medzhitov, and A. Iwasaki**. 2003. Toll-like receptor 9-mediated recognition of Herpes simplex virus-2 by plasmacytoid dendritic cells. J Exp. Med. **198**:513-520.

267. **Mabruk, M. J., G. M. Glasglow, A. M. Flack, J. C. Folan, J. G. Bannigan, J. M. Smyth, M. A. O'Sullivan, B. J. Sheahan, and G. J. Atkins**. 1989. Effect of infection with the ts22 mutant of Semliki Forest virus on development of the central nervous system in the fetal mouse. J Virol **63**:4027-4033.

268. **Mahalingam, S. and B. A. Lidbury**. 2002. Suppression of lipopolysaccharide-induced antiviral transcription factor (STAT-1 and NF-kappa B) complexes by antibody-dependent enhancement of macrophage infection by Ross River virus. Proc Natl Acad Sci U S A **99**:13819-13824.

269. **Manche, L., S. R. Green, C. Schmedt, and M. B. Mathews**. 1992. Interactions between double-stranded RNA regulators and the protein kinase DAI. Mol Cell Biol **12**:5238-5248.

270. **Maniatis T, Falvo JV Kim TH Kim TK Lin CH Parekh BS Wathelet MG.** Structure and function of the interferon-beta enhanceosome. Cold Spring Harb Symp Quant Biol. 63, 609-620. 1998.

271. **Mansell, A., E. Brint, J. A. Gould, L. A. O'Neill, and P. J. Hertzog**. 2004. Mal interacts with tumor necrosis factor receptor-associated factor (TRAF)-6 to mediate NF-kappaB activation by toll-like receptor (TLR)-2 and TLR4. J Biol Chem **279**:37227-37230.

272. **Marie, I., J. E. Durbin, and D. E. Levy**. 1998. Differential viral induction of distinct interferon-alpha genes by positive feedback through interferon regulatory factor-7. EMBO J **17**:6660-6669.

273. **Marletta, M. A.** 1993. Nitric oxide synthase structure and mechanism. J. Biol. Chem. **268**:12231-12234.

274. **Marletta, M. A.** 1993. Nitric oxide synthase: function and mechanism. Adv. Exp. Med. Biol. **338**:281-284.

275. **Marletta, M. A.** 1994. Nitric oxide synthase: aspects concerning structure and catalysis. Cell **78**:927-930.

276. **Marshall, W. L., R. Datta, K. Hanify, E. Teng, and R. W. Finberg**. 1999. U937 cells overexpressing bcl-xl are resistant to human immunodeficiency virus-1-induced apoptosis and human immunodeficiency virus-1 replication. Virology **256**:1-7.

277. **Martal, J. L., N. M. Chene, L. P. Huynh, R. M. L'Haridon, P. B. Reinaud, M. W. Guillomot, M. A. Charlier, and S. Y. Charpigny**. 1998. IFN-tau: a novel subtype I IFN1. Structural characteristics, non-ubiquitous expression, structure-function relationships, a pregnancy hormonal embryonic signal and cross-species therapeutic potentialities. Biochimie **80**:755-777.

278. **Martin, M. U. and H. Wesche**. 2002. Summary and comparison of the signaling mechanisms of the Toll/interleukin-1 receptor family. Biochim. Biophys. Acta **1592**:265-280.

279. **Martinand, C., T. Salehzada, M. Silhol, B. Lebleu, and C. Bisbal**. 1998. RNase L inhibitor (RLI) antisense constructions block partially the down regulation of the 2-5A/RNase L pathway in encephalomyocarditis-virus-(EMCV)-infected cells. Eur. J Biochem **254**:248-255.

280. **Mashimo, T., M. Lucas, D. Simon-Chazottes, M. P. Frenkiel, X. Montagutelli, P. E. Ceccaldi, V. Deubel, J. L. Guenet, and P. Despres**. 2002. A nonsense mutation in the gene encoding 2'-5'-oligoadenylate synthetase/L1 isoform is associated with West Nile virus susceptibility in laboratory mice. Proc Natl Acad Sci U S A **99**:11311-11316.

281. **Mashimo, T., P. Glaser, M. Lucas, D. Simon-Chazottes, P. E. Ceccaldi, X. Montagutelli, P. Despres, and J. L. Guenet**. 2003. Structural and functional genomics and evolutionary relationships in the cluster of genes encoding murine 2',5'-oligoadenylate synthetases. Genomics **82**:537-552.

282. **Mathews, M. B. and T. Shenk**. 1991. Adenovirus virus-associated RNA and translation control. J Virol. **65**:5657-5662.

283. **Matikainen, S., T. Sareneva, T. Ronni, A. Lehtonen, P. J. Koskinen, and I. Julkunen**. 1999. Interferon-alpha activates multiple STAT proteins and upregulates proliferation-associated IL-2Ralpha, c-myc, and pim-1 genes in human T cells. Blood **93** :1980-1991.

284. **Matsumoto, M., S. Kikkawa, M. Kohase, K. Miyake, and T. Seya**. 2002. Establishment of a monoclonal antibody against human Toll-like receptor 3 that blocks double-stranded RNA-mediated signaling. Biochem. Biophys. Res. Commun. **293**:1364-1369.

285. **Mayer, B. J., M. Hamaguchi, and H. Hanafusa**. 1988. A novel viral oncogene with structural similarity to phospholipase C. Nature **332**:272-275.

286. **Mayer, I. A., A. Verma, I. M. Grumbach, S. Uddin, F. Lekmine, F. Ravandi, B. Majchrzak, S. Fujita, E. N. Fish, and L. C. Platanias**. 2001. The p38 MAPK pathway mediates the growth inhibitory effects of interferon-alpha in BCR-ABL-expressing cells. J Biol Chem **276**:28570-28577.

287. **McIntosh, B. M., Worth, C. B. and R. H. Kokernot**. 1961. Isolation of Semliki Forest virus from Aedes (Aedimorphus) argenteopunctatus (Theobald) collected in Portuguese East Africa. Transfusion (Paris) **55**:192-198.

288. **McKimmie, C. S., N. Johnson, A. R. Fooks, and J. K. Fazakerley**. 2005. Viruses selectively upregulate Toll-like receptors in the central nervous system. Biochem Biophys. Res Commun. **336**:925-933.

289. **McWhirter SM, Fitzgerald KA Rosains J Rowe DC Golenbock DT Maniatis T**. IFN-regulatory factor 3-dependent gene expression is defective in Tbk1-deficient mouse embryonic fibroblasts. Proc Natl Acad Sci U S A. 101(1), 233-238. 2004.

290. **Medina, M., E. Domingo, J. K. Brangwyn, and G. J. Belsham**. 1993. The two species of the foot-and-mouth disease virus leader protein, expressed individually, exhibit the same activities. Virology **194**:355-359.

291. **Medzhitov, R., P. Preston-Hurlburt, E. Kopp, A. Stadlen, C. Chen, S. Ghosh, and C. A. Janeway, Jr.** 1998. MyD88 is an adaptor protein in the hToll/IL-1 receptor family signaling pathways. Mol. Cell **2**:253-258.

292. **Mehta, S., S. Pathak, and H. E. Webb**. 1990. Induction of membrane proliferation in mouse CNS by gold sodium thiomalate with reference to increased virulence of the avirulent Semliki Forest virus. Biosci. Rep. **10**:271-279.

293. **Meier, J. L. and J. A. Pruessner**. 2000. The human cytomegalovirus major immediate-early distal enhancer region is required for efficient viral replication and immediate-early gene expression. J Virol. **74**:1602-1613.

294. **Melroe, G. T., N. A. DeLuca, and D. M. Knipe**. 2004. Herpes simplex virus 1 has multiple mechanisms for blocking virus-induced interferon production. J Virol **78**:8411-8420.

295. **Melville, M. W., W. J. Hansen, B. C. Freeman, W. J. Welch, and M. G. Katze**. 1997. The molecular chaperone hsp40 regulates the activity of P58IPK, the cellular inhibitor of PKR. Proc Natl Acad Sci U S A **94**:97-102.

296. **Melville, M. W., S. L. Tan, M. Wambach, J. Song, R. I. Morimoto, and M. G. Katze**. 1999. The cellular inhibitor of the PKR protein kinase, P58(IPK), is an influenza virus-activated co-chaperone that modulates heat shock protein 70 activity. J Biol Chem **274**:3797-3803.

297. **Merits, A., L. Vasiljeva, T. Ahola, L. Kaariainen, and P. Auvinen**. 2001. Proteolytic processing of Semliki Forest virus-specific non-structural polyprotein by nsP2 protease. J Gen. Virol **82**:765-773.

298. **Merrick, W. C.** 1992. Mechanism and regulation of eukaryotic protein synthesis. Microbiol Rev **56**:291-315.

299. **Meurs, E., K. Chong, J. Galabru, N. S. Thomas, I. M. Kerr, B. R. Williams, and A. G. Hovanessian**. 1990. Molecular cloning and characterization of the human double-stranded RNA-activated protein kinase induced by interferon. Cell **62**:379-390.

300. **Meurs, E. F., Y. Watanabe, S. Kadereit, G. N. Barber, M. G. Katze, K. Chong, B. R. Williams, and A. G. Hovanessian**. 1992. Constitutive expression of human double-stranded RNA-activated p68 kinase in murine cells mediates phosphorylation of eukaryotic initiation factor 2 and partial resistance to encephalomyocarditis virus growth. J Virol. **66**:5805-5814.

301. **Meylan, E., K. Burns, K. Hofmann, V. Blancheteau, F. Martinon, M. Kelliher, and J. Tschopp**. 2004. RIP1 is an essential mediator of Toll-like receptor 3-induced NF-kappa B activation. Nat Immunol. **5**:503-507.

302. **Meylan, E., J. Curran, K. Hofmann, D. Moradpour, M. Binder, R. Bartenschlager, and J. Tschopp**. 2005. Cardif is an adaptor protein in the RIG-I antiviral pathway and is targeted by hepatitis C virus. Nature **437**:1167-1172.

303. **Miller, D. M., B. M. Rahill, J. M. Boss, M. D. Lairmore, J. E. Durbin, J. W. Waldman, and D. D. Sedmak**. 1998. Human cytomegalovirus inhibits major histocompatibility complex class II expression by disruption of the Jak/Stat pathway. J Exp. Med. **187**:675-683.

304. **Miller, D. M., Y. Zhang, B. M. Rahill, W. J. Waldman, and D. D. Sedmak**. 1999. Human cytomegalovirus inhibits IFN-alpha-stimulated antiviral and immunoregulatory responses by blocking multiple levels of IFN-alpha signal transduction. J Immunol. **162**:6107-6113.

305. **Mizel, S. B. and J. A. Snipes** . 2002. Gram-negative flagellin-induced self-tolerance is associated with a block in interleukin-1 receptor-associated kinase release from toll-like receptor 5. J Biol Chem **277**:22414-22420.

306. **Mogensen, K. E., M. Lewerenz, J. Reboul, G. Lutfalla, and G. Uze**. 1999. The type I interferon receptor: structure, function, and evolution of a family business. J Interferon Cytokine Res. **19**:1069-1098.

307. **Mokhtarian, F., C. M. Huan, C. Roman, and C. S. Raine**. 2003. Semliki Forest virus-induced demyelination and remyelination--involvement of B cells and anti-myelin antibodies. J Neuroimmunol. **137**:19-31.

308. **Moller, A. and M. L. Schmitz**. 2003. Viruses as hijackers of PML nuclear bodies. Arch. Immunol. Ther. Exp. (Warsz.) **51**:295-300.

309. **Moore DL, S Reddy FM Akinkugbe VH Lee TS David-West OR Causey and DE Carey.** An epidemic of Chikungunya fever at Ibandan, Nigeria, 1969. Ann Trop Med Parasitol 68, 59-68. 1974.

310. **Moore, K. W., M. R. de Waal, R. L. Coffman, and A. O'Garra**. 2001. Interleukin-10 and the interleukin-10 receptor. Annu Rev Immunol **19**:683-765.

311. **Mori, I., F. Goshima, H. Ito, N. Koide, T. Yoshida, T. Yokochi, Y. Kimura, and Y. Nishiyama**. 2005. The vomeronasal chemosensory system as a route of neuroinvasion by herpes simplex virus. Virology **334**:51-58.

312. **Morris, A., M. Cooley, and M. Blackman**. 1986. The interaction of interferon with the immune response. J Hepatol. **3 Suppl 2**:S161-S169.

313. **Morris, M. M., H. Dyson, D. Baker, L. S. Harbige, J. K. Fazakerley, and S. Amor**. 1997. Characterization of the cellular and cytokine response in the central nervous system following Semliki Forest virus infection. J Neuroimmunol. **74**:185-197.

314. **Moss, W. J., M. O. Ota, and D. E. Griffin**. 2004. Measles: immune suppression and immune responses. Int. J Biochem Cell Biol **36**:1380-1385.

315. **Mossman, K. L. and A. A. Ashkar**. 2005. Herpesviruses and the innate immune response. Viral Immunol. **18**:267-281.

316. **Moynagh, P. N.** 2005. TLR signalling and activation of IRFs: revisiting old friends from the NF-kappaB pathway. Trends Immunol. **26**:469-476.

317. **Muller, R.** 1995. Transcriptional regulation during the mammalian cell cycle. Trends Genet. **11**:173-178.

318. **Muller, U., U. Steinhoff, L. F. Reis, S. Hemmi, J. Pavlovic, R. M. Zinkernagel, and M. Aguet**. 1994. Functional role of type I and type II interferons in antiviral defense. Science **264**:1918-1921.

319. **Mundschau, L. J. and D. V. Faller**. 1995. Platelet-derived growth factor signal transduction through the interferon-inducible kinase PKR. Immediate early gene induction. J Biol Chem **270**:3100-3106.

320. **Nair, M. P., S. A. Schwartz, and M. Menon**. 1985. Association of decreased natural and antibody-dependent cellular cytotoxicity and production of natural killer cytotoxic factor and interferon in neonates. Cell Immunol. **94**:159-171.

321. **Nava, V. E., A. Rosen, M. A. Veliuona, R. J. Clem, B. Levine, and J. M. Hardwick**. 1998. Sindbis virus induces apoptosis through a caspase-dependent, CrmA-sensitive pathway. J Virol **72**:452-459.

322. **Neilan, J. G., Z. Lu, C. L. Afonso, G. F. Kutish, M. D. Sussman, and D. L. Rock**. 1993. An African swine fever virus gene with similarity to the proto-oncogene bcl-2 and the Epstein-Barr virus gene BHRF1. J Virol **67**:4391-4394.

323. **Neustock, P., J. M. Brand, A. Kruse, and H. Kirchner**. 1993. Cytokine production of the human monocytic cell line Mono Mac 6 in comparison to mature monocytes in peripheral blood mononuclear cells. Immunobiology **188**:293-302.

324. **Neznanov, N., K. M. Chumakov, L. Neznanova, A. Almasan, A. K. Banerjee, and A. V. Gudkov**. 2005. Proteolytic cleavage of the p65-RelA subunit of NF-kappaB during poliovirus infection. J Biol Chem **280**:24153-24158.

325. **Nguyen, H. J. Hiscott & P. M. Pitha**. The growing family of interferon regulatory factors. Cytokine Growth Factor Rev 8, 293-312. 1997.

326. **Nimmannitya, S., S. B. Halstead, S. N. Cohen, and M. R. Margiotta**. 1969. Dengue and chikungunya virus infection in man in Thailand, 1962-1964. I. Observations on hospitalized patients with hemorrhagic fever. Am. J Trop Med Hyg. **18**:954-971.

327. **Ninomiya-Tsuji J, Kishimoto K Hiyama A Inoue J Cao Z Matsumoto K.** The kinase TAK1 can activate the NIK-I kappaB as well as the MAP kinase cascade in the IL-1 signalling pathway. Nature. 398(6724), 252-256. 1999.

328. **Nolan T.** Getting started - the basics of setting up a qPCR assay. edited by Bustin SA. A-Z of quantitative PCR , 529-543. 2004.

329. **Novick, D., B. Cohen, and M. Rubinstein**. 1994. The human interferon alpha/beta receptor: characterization and molecular cloning. Cell **77**:391-400.

330. **Ogata, S., A. Ogata, S. Schneider-Schaulies, and J. Schneider-Schaulies**. 2004. Expression of the interferon-alpha/beta-inducible MxA protein in brain lesions of subacute sclerosing panencephalitis. J Neurol. Sci **223**:113-119.

331. **Oliver KR.** Consequences of neurotropic virus infections of developing and adult mice. Thesis . 1995.

332. **Oliver, K. R., M. F. Scallan, H. Dyson, and J. K. Fazakerley**. 1997. Susceptibility to a neurotropic virus and its changing distribution in the developing brain is a function of CNS maturity. J Neurovirol. **3**:38-48.

333. **Oliver, K. R. and J. K. Fazakerley**. 1998. Transneuronal spread of Semliki Forest virus in the developing mouse olfactory system is determined by neuronal maturity. Neuroscience **82**:867-877.

334. **Oritani, K. and Y. Kanakura**. 2005. IFN-zeta/ limitin: a member of type I IFN with mild lympho-myelosuppression. J. Cell Mol. Med. **9**:244-254.

335. **Oshiumi, H., M. Sasai, K. Shida, T. Fujita, M. Matsumoto, and T. Seya**. 2003. TIR-containing adapter molecule (TICAM)-2, a bridging adapter recruiting to toll-like receptor 4 TICAM-1 that induces interferon-beta. J Biol Chem **278**:49751-49762.

336. **Overton, H., D. McMillan, L. Hope, and P. Wong-Kai-In**. 1994. Production of host shutoff-defective mutants of herpes simplex virus type 1 by inactivation of the UL13 gene. Virology **202**:97-106.

337. **Palosaari, H., J. P. Parisien, J. J. Rodriguez, C. M. Ulane, and C. M. Horvath**. 2003. STAT protein interference and suppression of cytokine signal transduction by measles virus V protein. J Virol. 77:7635-7644.

338. **Panne, D., T. Maniatis, and S. C. Harrison**. 2004. Crystal structure of ATF-2/c-Jun and IRF-3 bound to the interferon-beta enhancer. EMBO J **23**:4384-4393.

339. **Parisien, J. P., J. F. Lau, J. J. Rodriguez, B. M. Sullivan, A. Moscona, G. D. Parks, R. A. Lamb, and C. M. Horvath**. 2001. The V protein of human parainfluenza virus 2 antagonizes type I interferon responses by destabilizing signal transducer and activator of transcription 2. Virology **283**:230-239.

340. **Patel, C. V., I. Handy, T. Goldsmith, and R. C. Patel**. 2000. PACT, a stress-modulated cellular activator of interferon-induced double-stranded RNA-activated protein kinase, PKR. J Biol Chem **275**:37993-37998.

341. **Pathak, S., H. E. Webb, S. W. Oaten, and S. Bateman**. 1976. An electron-microscopic study of the development of virulent and avirulent strains of Semliki forest virus in mouse brain. J Neurol. Sci **28**:289-300.

342. **Pathak, S., S. J. Illavia, and H. E. Webb**. 1983. The identification and role of cells involved in CNS demyelination in mice after Semliki Forest virus infection: an ultrastructural study. Prog. Brain Res **59**:237-254.

343. **Pellegrini S, Schindler C**. Early events in signalling by interferons. Trends Biochem Sci 18(9), 338-342. 1993.

344. **Peranen, J., K. Takkinen, N. Kalkkinen, and L. Kaariainen**. 1988. Semliki Forest virus-specific non-structural protein nsP3 is a phosphoprotein. J Gen. Virol **69 (Pt 9)**:2165-2178.

345. **Peranen, J. and L. Kaariainen** . 1991. Biogenesis of type I cytopathic vacuoles in Semliki Forest virus-infected BHK cells. J Virol **65**:1623-1627.

346. **Perry, A. K., E. K. Chow, J. B. Goodnough, W. C. Yeh, and G. Cheng**. 2004. Differential requirement for TANK-binding kinase-1 in type I interferon responses to toll-like receptor activation and viral infection. J Exp. Med. **199**:1651-1658.

347. **Platanias, L. C.** 2005. Mechanisms of type-I- and type-II-interferon-mediated signalling. Nat Rev Immunol. **5**:375-386.

348. **Plougastel, B. F. and W. M. Yokoyama**. 2006. Extending missing-self? Functional interactions between lectin-like NKrp1 receptors on NK cells with lectin-like ligands. Curr. Top. Microbiol. Immunol. **298**:77-89.

349. **Polson, A. G., P. F. Crain, S. C. Pomerantz, J. A. McCloskey, and B. L. Bass**. 1991. The mechanism of adenosine to inosine conversion by the double-stranded RNA unwinding/modifying activity: a high-performance liquid chromatography-mass spectrometry analysis. Biochemistry **30**:11507-11514.

350. **Polson, A. G., B. L. Bass, and J. L. Casey**. 1996. RNA editing of hepatitis delta virus antigenome by dsRNA-adenosine deaminase. Nature **380**:454-456.

351. **Poltorak, A., I. Smirnova, X. He, M. Y. Liu, C. Van Huffel, O. McNally, D. Birdwell, E. Alejos, M. Silva, X. Du, P. Thompson, E. K. Chan, J. Ledesma, B. Roe, S. Clifton, S. N. Vogel, and B. Beutler**. 1998. Genetic and physical mapping of the Lps locus: identification of the toll-4 receptor as a candidate gene in the critical region. Blood Cells Mol. Dis. **24**:340-355.

352. **Poole, E., B. He, R. A. Lamb, R. E. Randall, and S. Goodbourn**. 2002. The V proteins of simian virus 5 and other paramyxoviruses inhibit induction of interferon-beta. Virology **303**:33-46.

353. **Powell, P. P., L. K. Dixon, and R. M. Parkhouse**. 1996. An IkappaB homolog encoded by African swine fever virus provides a novel mechanism for downregulation of proinflammatory cytokine responses in host macrophages. J Virol **70**:8527-8533.

354. **Prietzsch, H., J. Brock, H. D. Kleine, S. Liebe, and R. Jaster**. 2002. Interferon-alpha inhibits cell cycle progression by Ba/F3 cells through the antagonisation of interleukin-3 effects on key regulators of G(1)/S transition. Cell Signal. **14**:751-759.

355. **Ramaiah, K. V., M. V. Davies, J. J. Chen, and R. J. Kaufman**. 1994. Expression of mutant eukaryotic initiation factor 2 alpha subunit (eIF-2 alpha) reduces inhibition of guanine nucleotide exchange activity of eIF-2B mediated by eIF-2 alpha phosphorylation. Mol Cell Biol **14**:4546-4553.

356. **Ramana, C. V., M. Chatterjee-Kishore, H. Nguyen, and G. R. Stark**. 2000. Complex roles of Stat1 in regulating gene expression. Oncogene **19**:2619-2627.

357. **Rani, M. R., G. R. Foster, S. Leung, D. Leaman, G. R. Stark, and R. M. Ransohoff**. 1996. Characterization of beta-R1, a gene that is selectively induced by interferon beta (IFN-beta) compared with IFN-alpha. J. Biol. Chem. **271**:22878-22884.

358. **Rani, M. R., L. Hibbert, N. Sizemore, G. R. Stark, and R. M. Ransohoff**. 2002. Requirement of phosphoinositide 3-kinase and Akt for interferon-beta-mediated induction of the beta-R1 (SCYB11) gene. J Biol Chem **277**:38456-38461.

359. **Reading, P. C., A. Khanna, and G. L. Smith**. 2002. Vaccinia virus CrmE encodes a soluble and cell surface tumor necrosis factor receptor that contributes to virus virulence. Virology **292**:285-298.

360. **Rebouillat, D. and A. G. Hovanessian**. 1999. The human 2',5'-oligoadenylate synthetase family: interferon-induced proteins with unique enzymatic properties. J Interferon Cytokine Res. **19**:295-308.

361. **Regad, T. and M. K. Chelbi-Alix**. 2001. Role and fate of PML nuclear bodies in response to interferon and viral infections. Oncogene **20**:7274-7286.

362. **Revilla, Y., M. Callejo, J. M. Rodriguez, E. Culebras, M. L. Nogal, M. L. Salas, E. Vinuela, and M. Fresno**. 1998. Inhibition of nuclear factor kappaB activation by a virus-encoded IkappaB-like protein. J Biol Chem **273**:5405-5411.

363. **Rikkonen, M., J. Peranen, and L. Kaariainen**. 1992. Nuclear and nucleolar targeting signals of Semliki Forest virus nonstructural protein nsP2. Virology **189**:462-473.

364. **Rikkonen, M., J. Peranen, and L. Kaariainen**. 1994. ATPase and GTPase activities associated with Semliki Forest virus nonstructural protein nsP2. J Virol **68**:5804-5810.

365. **Rikkonen, M., J. Peranen, and L. Kaariainen**. 1994. Nuclear targeting of Semliki Forest virus nsP2. Arch. Virol Suppl **9**:369-377.

366. **Rikkonen, M.** 1996. Functional significance of the nuclear-targeting and NTP-binding motifs of Semliki Forest virus nonstructural protein nsP2. Virology **218**:352-361.

367. **Roberts, R. M., L. Liu, Q. Guo, D. Leaman, and J. Bixby**. 1998. The evolution of the type I interferons. J. Interferon Cytokine Res. **18**:805-816.

368. **Robertson, B., G. Kong, Z. Peng, M. Bentivoglio, and K. Kristensson**. 2000. Interferon-gamma-responsive neuronal sites in the normal rat brain: receptor protein distribution and cell activation revealed by Fos induction. Brain Res. Bull. **52**:61-74.

369. **Rodriguez, J. J., J. P. Parisien, and C. M. Horvath**. 2002. Nipah virus V protein evades alpha and gamma interferons by preventing STAT1 and STAT2 activation and nuclear accumulation. J Virol. **76**:11476-11483.

370. **Rodriguez, J. J., L. F. Wang, and C. M. Horvath**. 2003. Hendra virus V protein inhibits interferon signaling by preventing STAT1 and STAT2 nuclear accumulation. J Virol. 77:11842-11845.

371. **Ronco, L. V., A. Y. Karpova, M. Vidal, and P. M. Howley**. 1998. Human papillomavirus 16 E6 oncoprotein binds to interferon regulatory factor-3 and inhibits its transcriptional activity. Genes Dev **12**:2061-2072.

372. **Roos, G., T. Leanderson, and E. Lundgren**. 1984. Interferon-induced cell cycle changes in human hematopoietic cell lines and fresh leukemic cells. Cancer Res. **44**:2358-2362.

373. **Rottenberg, M. and K. Kristensson**. 2002. Effects of interferon-gamma on neuronal infections. Viral Immunol. **15**:247-260.

374. **Roy, S., M. G. Katze, N. T. Parkin, I. Edery, A. G. Hovanessian, and N. Sonenberg**. 1990. Control of the interferon-induced 68-kilodalton protein kinase by the HIV-1 tat gene product. Science **247**:1216-1219.

375. **Ruekert RR**. Picornaviridae:the viruses and their replication. In BN Fields, DM Knipe and PH Howley (ed) Virology , 609-654. 1996. Philadelphia Pa, Lippincott-Raven Publishers.

376. **Ryman, K. D., W. B. Klimstra, K. B. Nguyen, C. A. Biron, and R. E. Johnston**. 2000. Alpha/beta interferon protects adult mice from fatal Sindbis virus infection and is an important determinant of cell and tissue tropism. J Virol **74**:3366-3378.

377. **Ryman, K. D., L. J. White, R. E. Johnston, and W. B. Klimstra**. 2002. Effects of PKR/RNase L-dependent and alternative antiviral pathways on alphavirus replication and pathogenesis. Viral Immunol. **15**:53-76.

378. **Sakatsume, M., L. F. Stancato, M. David, O. Silvennoinen, P. Saharinen, J. Pierce, A. C. Larner, and D. S. Finbloom**. 1998. Interferon gamma activation of Raf-1 is Jak1-dependent and p21ras-independent. J. Biol. Chem. **273**:3021-3026.

379. **Salonen A, Ahola T Kaariainen L**. Viral RNA replication in association with cellular membranes. Curr Top Microbiol Immunol. 285, 139-173. 2005.

380. **Sambucetti, L. C., J. M. Cherrington, G. W. Wilkinson, and E. S. Mocarski**. 1989. NF-kappa B activation of the cytomegalovirus enhancer is mediated by a viral transactivator and by T cell stimulation. EMBO J **8**:4251-4258.

381. **Sammin, D. J., D. Butler, G. J. Atkins, and B. J. Sheahan**. 1999. Cell death mechanisms in the olfactory bulb of rats infected intranasally with Semliki forest virus. Neuropathol. Appl. Neurobiol. **25**:236-243.

382. **Samuel, C. E.** 2001. Antiviral actions of interferons. Clin. Microbiol. Rev. **14**:778-809, table.

383. **Sarid, R., T. Sato, R. A. Bohenzky, J. J. Russo, and Y. Chang**. 1997. Kaposi's sarcoma-associated herpesvirus encodes a functional bcl-2 homologue. Nat Med. **3**:293-298.

384. **Sarkar, S. N., K. L. Peters, C. P. Elco, S. Sakamoto, S. Pal, and G. C. Sen**. 2004. Novel roles of TLR3 tyrosine phosphorylation and PI3 kinase in double-stranded RNA signaling. Nat Struct. Mol. Biol **11**:1060-1067.

385. **Sasai M, Oshiumi H Matsumoto M Inoue N Fujita F Nakanishi M Seya T.** Cutting Edge: NF-kappaB-activating kinase-associated protein 1 participates in TLR3/Toll-IL-1 homology domain-containing adapter molecule-1-mediated IFN regulatory factor 3 activation. J Immunol. 174(1), 27-30. 2005.

386. **Sato, S., M. Sugiyama, M. Yamamoto, Y. Watanabe, T. Kawai, K. Takeda, and S. Akira**. 2003. Toll/IL-1 receptor domain-containing adaptor inducing IFN-beta (TRIF) associates with TNF receptor-associated factor 6 and TANK-binding kinase 1, and activates two distinct transcription factors, NF-kappa B and IFN-regulatory factor-3, in the Toll-like receptor signaling. J Immunol. **171**:4304-4310.

387. **Scadden, A. D. and C. W. Smith**. 2001. Specific cleavage of hyper-edited dsRNAs. EMBO J **20**:4243-4252.

388. **Scallan, M. F., T. E. Allsopp, and J. K. Fazakerley**. 1997. bcl-2 acts early to restrict Semliki Forest virus replication and delays virus-induced programmed cell death. J Virol **71**:1583-1590.

389. **Scallan, M. F. and J. K. Fazakerley**. 1999. Aurothiolates enhance the replication of Semliki Forest virus in the CNS and the exocrine pancreas. J Neurovirol. **5**:392-400.

390. **Schafer, S. L., R. Lin, P. A. Moore, J. Hiscott, and P. M. Pitha**. 1998. Regulation of type I interferon gene expression by interferon regulatory factor-3. J. Biol. Chem. **273**:2714-2720.

391. **SCHAPIRO, S., E. GELLER, and S. EIDUSON**. 1962. Neonatal adrenal cortical response to stress and vasopressin. Proc Soc Exp Biol Med **109**:937-941.

392. **Scherer, D. C., J. A. Brockman, Z. Chen, T. Maniatis, and D. W. Ballard**. 1995. Signal-induced degradation of I kappa B alpha requires site-specific ubiquitination. Proc. Natl. Acad. Sci U. S. A **92**:11259-11263.

393. **Schiff, L. A., M. L. Nibert, M. S. Co, E. G. Brown, and B. N. Fields**. 1988. Distinct binding sites for zinc and double-stranded RNA in the reovirus outer capsid protein sigma 3. Mol Cell Biol **8**:273-283.

394. **Schlender, J., V. Hornung, S. Finke, M. Gunthner-Biller, S. Marozin, K. Brzozka, S. Moghim, S. Endres, G. Hartmann, and K. K. Conzelmann**. 2005. Inhibition of toll-like receptor 7- and 9-mediated alpha/beta interferon production in human plasmacytoid dendritic cells by respiratory syncytial virus and measles virus. J Virol. **79**:5507-5515.

395. **Schneider-Schaulies, S., I. M. Klagge, and M. Ter, V**. 2003. Dendritic cells and measles virus infection. Curr. Top. Microbiol. Immunol. **276**:77-101.

396. **Schoenemeyer, A., B. J. Barnes, M. E. Mancl, E. Latz, N. Goutagny, P. M. Pitha, K. A. Fitzgerald, and D. T. Golenbock**. 2005. The interferon regulatory factor, IRF5, is a central mediator of toll-like receptor 7 signaling. J Biol Chem **280**:17005-17012.

397. **Schoenfeld, N. M., J. H. Leathem, and J. Rabii**. 1980. Maturation of adrenal stress responsiveness in the rat. Neuroendocrinology **31**:101-105.

398. **Seo, T., D. Lee, B. Lee, J. H. Chung, and J. Choe**. 2000. Viral interferon regulatory factor 1 of Kaposi's sarcoma-associated herpesvirus (human herpesvirus 8) binds to, and inhibits transactivation of, CREB-binding protein. Biochem Biophys. Res. Commun. **270**:23-27.

399. **Seo, T., J. Park, C. Lim, and J. Choe**. 2004. Inhibition of nuclear factor kappaB activity by viral interferon regulatory factor 3 of Kaposi's sarcoma-associated herpesvirus. Oncogene **23**:6146-6155.

400. **Servant, M. J., N. Grandvaux, and J. Hiscott**. 2002. Multiple signaling pathways leading to the activation of interferon regulatory factor 3. Biochem Pharmacol. **64**:985-992.

401. **Seth, R. B., L. Sun, C. K. Ea, and Z. J. Chen**. 2005. Identification and characterization of MAVS, a mitochondrial antiviral signaling protein that activates NF-kappaB and IRF 3. Cell **122**:669-682.

402. **Sharma, S., B. R. tenOever, N. Grandvaux, G. P. Zhou, R. Lin, and J. Hiscott**. 2003. Triggering the interferon antiviral response through an IKK-related pathway. Science **300**:1148-1151.

403. **Shi, Y.** 2002. Mechanisms of caspase activation and inhibition during apoptosis. Mol Cell **9**:459-470.

404. **Shirako, Y. and J. H. Strauss** . 1990. Cleavage between nsP1 and nsP2 initiates the processing pathway of Sindbis virus nonstructural polyprotein P123. Virology **177**:54-64.

405. **Shirako, Y. and J. H. Strauss** . 1994. Regulation of Sindbis virus RNA replication: uncleaved P123 and nsP4 function in minus-strand RNA synthesis, whereas cleaved products from P123 are required for efficient plus-strand RNA synthesis. J Virol **68**:1874-1885.

406. **Shisler, J., C. Yang, B. Walter, C. F. Ware, and L. R. Gooding**. 1997. The adenovirus E3-10.4K/14.5K complex mediates loss of cell surface Fas (CD95) and resistance to Fas-induced apoptosis. J Virol **71**:8299-8306.

407. **Shuai, K.** 1999. The STAT family of proteins in cytokine signaling. Prog. Biophys. Mol Biol **71**:405-422.

408. **Siegal, F. P., N. Kadowaki, M. Shodell, P. A. Fitzgerald-Bocarsly, K. Shah, S. Ho, S. Antonenko, and Y. J. Liu**. 1999. The nature of the principal type 1 interferon-producing cells in human blood. Science **284**:1835-1837.

409. **Smiley, J. R.** 2004. Herpes simplex virus virion host shutoff protein: immune evasion mediated by a viral RNase? J Virol. **78**:1063-1068.

410. **Smillie, J., R. Pusztai, and H. Smith**. 1973. Studies of the influence of host deference mechanisms on infection of mice with an avirulent or virulent strain of Semliki Forest virus. Br. J Exp. Pathol. **54**:260-266.

411. **Smith, C. A., T. Davis, D. Anderson, L. Solam, M. P. Beckmann, R. Jerzy, S. K. Dower, D. Cosman, and R. G. Goodwin**. 1990. A receptor for tumor necrosis factor defines an unusual family of cellular and viral proteins. Science **248**:1019-1023.

412. **Smithburn KC and Harrow WJ.** Semliki Forest virus I. Isolation and pathogenic properties. J Immunol. 49, 141-145. 1944.

413. **Solanas, M., R. Moral, and E. Escrich**. 2001. Unsuitability of using ribosomal RNA as loading control for Northern blot analyses related to the imbalance between messenger and ribosomal RNA content in rat mammary tumors. Anal. Biochem **288**:99-102.

414. **Spann, K. M., K. C. Tran, B. Chi, R. L. Rabin, and P. L. Collins**. 2004. Suppression of the induction of alpha, beta, and lambda interferons by the NS1 and NS2 proteins of human respiratory syncytial virus in human epithelial cells and macrophages [corrected]. J Virol. **78**:4363-4369.

415. **Srivastava, S. P., M. V. Davies, and R. J. Kaufman**. 1995. Calcium depletion from the endoplasmic reticulum activates the double-stranded RNA-dependent protein kinase (PKR) to inhibit protein synthesis. J Biol Chem **270**:16619-16624.

416. **Stack, J., I. R. Haga, M. Schroder, N. W. Bartlett, G. Maloney, P. C. Reading, K. A. Fitzgerald, G. L. Smith, and A. G. Bowie**. 2005. Vaccinia virus protein A46R targets multiple Toll-like-interleukin-1 receptor adaptors and contributes to virulence. J Exp. Med. **201**:1007-1018.

417. **Stewart, M. J., M. A. Blum, and B. Sherry**. 2003. PKR's protective role in viral myocarditis. Virology **314**:92-100.

418. **Strauss, E. G., C. M. Rice, and J. H. Strauss**. 1983. Sequence coding for the alphavirus nonstructural proteins is interrupted by an opal termination codon. Proc Natl Acad Sci U S A **80**:5271-5275.

419. **Strebel, K. and E. Beck**. 1986. A second protease of foot-and-mouth disease virus. J Virol. **58**:893-899.

420. **Streitenfeld, H., A. Boyd, J. K. Fazakerley, A. Bridgen, R. M. Elliott, and F. Weber**. 2003. Activation of PKR by Bunyamwera virus is independent of the viral interferon antagonist NSs. J Virol **77**:5507-5511.

421. **Suckling, A. J., S. Pathak, S. Jagelman, and H. E. Webb**. 1978. Virus-associated demyelination. A model using avirulent Semliki Forest virus infection of mice. J Neurol. Sci **39**:147-154.

422. **Suhara, W., M. Yoneyama, I. Kitabayashi, and T. Fujita**. 2002. Direct involvement of CREB-binding protein/p300 in sequence-specific DNA binding of virus-activated interferon regulatory factor-3 holocomplex. J Biol Chem **277**:22304-22313.

423. **Sumpter, R., Jr., C. Wang, E. Foy, Y. M. Loo, and M. Gale, Jr.** 2004. Viral evolution and interferon resistance of hepatitis C virus RNA replication in a cell culture model. J Virol. **78**:11591-11604.

424. **Sundararajan, R. and E. White** . 2001. E1B 19K blocks Bax oligomerization and tumor necrosis factor alpha-mediated apoptosis. J Virol **75**:7506-7516.

425. **Suomalainen, M., P. Liljestrom, and H. Garoff**. 1992. Spike protein-nucleocapsid interactions drive the budding of alphaviruses. J Virol **66**:4737-4747.

426. **Suopanki, J., D. L. Sawicki, S. G. Sawicki, and L. Kaariainen**. 1998. Regulation of alphavirus 26S mRNA transcription by replicase component nsP2. J Gen. Virol **79 (Pt 2)**:309-319.

427. **Taguchi, T., M. Nagano-Fujii, M. Akutsu, H. Kadoya, S. Ohgimoto, S. Ishido, and H. Hotta**. 2004. Hepatitis C virus NS5A protein interacts with 2',5'-oligoadenylate synthetase and inhibits antiviral activity of IFN in an IFN sensitivity-determining region-independent manner. J Gen. Virol. **85**:959-969.

428. **Takaoka, A., H. Yanai, S. Kondo, G. Duncan, H. Negishi, T. Mizutani, S. Kano, K. Honda, Y. Ohba, T. W. Mak, and T. Taniguchi**. 2005. Integral role of IRF-5 in the gene induction programme activated by Toll-like receptors. Nature **434**:243-249.

429. **Takeda, K.** 2005. Evolution and integration of innate immune recognition systems: the Toll-like receptors. J Endotoxin. Res. **11**:51-55.

430. **Takkinen, K.** 1986. Complete nucleotide sequence of the nonstructural protein genes of Semliki Forest virus. Nucleic Acids Res **14**:5667-5682.

431. **Tanaka, N., M. Sato, M. S. Lamphier, H. Nozawa, E. Oda, S. Noguchi, R. D. Schreiber, Y. Tsujimoto, and T. Taniguchi**. 1998. Type I interferons are essential mediators of apoptotic death in virally infected cells. Genes Cells **3**:29-37.

432. **Tang, N. M., M. J. Korth, M. Gale, Jr., M. Wambach, S. D. Der, S. K. Bandyopadhyay, B. R. Williams, and M. G. Katze**. 1999. Inhibition of double-stranded RNA- and tumor necrosis factor alpha-mediated apoptosis by tetratricopeptide repeat protein and cochaperone P58(IPK). Mol Cell Biol **19**:4757-4765.

433. **Taniguchi T, Takaoka A.** A weak signal for strong responses: interferon-alpha/beta revisited. Nat Rev Mol Cell Biol. 2, 378-386. 2001.

434. **Taylor, D. R., S. T. Shi, P. R. Romano, G. N. Barber, and M. M. Lai**. 1999. Inhibition of the interferon-inducible protein kinase PKR by HCV E2 protein. Science **285** :107-110.

435. **tenOever, B. R., M. J. Servant, N. Grandvaux, R. Lin, and J. Hiscott**. 2002. Recognition of the measles virus nucleocapsid as a mechanism of IRF-3 activation. J Virol **76**:3659-3669.

436. **Tewari, M. and V. M. Dixit**. 1995. Fas- and tumor necrosis factor-induced apoptosis is inhibited by the poxvirus crmA gene product. J Biol Chem **270**:3255-3260.

437. **Thanos, D. and T. Maniatis**. 1995. Virus induction of human IFN beta gene expression requires the assembly of an enhanceosome. Cell **83**:1091-1100.

438. **Thomas, D., G. Blakqori, V. Wagner, M. Banholzer, N. Kessler, R. M. Elliott, O. Haller, and F. Weber**. 2004. Inhibition of RNA polymerase II phosphorylation by a viral interferon antagonist. J Biol Chem **279**:31471-31477.

439. **Thomas, S. M., R. A. Lamb, and R. G. Paterson**. 1988. Two mRNAs that differ by two nontemplated nucleotides encode the amino coterminal proteins P and V of the paramyxovirus SV5. Cell **54**:891-902.

440. **Thome M, Tschopp J.** Regulation of lymphocyte proliferation and death by FLIP. Nat Rev Immunol. 1(1), 50-58. 2001.

441. **Tojima, Y., A. Fujimoto, M. Delhase, Y. Chen, S. Hatakeyama, K. Nakayama, Y. Kaneko, Y. Nimura, N. Motoyama, K. Ikeda, M. Karin, and M. Nakanishi**. 2000. NAK is an IkappaB kinase-activating kinase. Nature **404**:778-782.

442. **Tollefson, A. E., T. W. Hermiston, D. L. Lichtenstein, C. F. Colle, R. A. Tripp, T. Dimitrov, K. Toth, C. E. Wells, P. C. Doherty, and W. S. Wold**. 1998. Forced degradation of Fas inhibits apoptosis in adenovirus-infected cells. Nature **392**:726-730.

443. **Tonks, N. K. and B. G. Neel**. 2001. Combinatorial control of the specificity of protein tyrosine phosphatases. Curr. Opin. Cell Biol **13**:182-195.

444. **Torpey, N., S. E. Maher, A. L. Bothwell, and J. S. Pober**. 2004. Interferon alpha but not interleukin 12 activates STAT4 signaling in human vascular endothelial cells. J Biol Chem **279**:26789-26796.

445. **Tsai TF, Weaver S and Monath TP**. Alphaviruses. In Clinical Virology, DD Rickman, RJ Whitley and FG Hayden eds. 2002. Washington DC, ASM press.

446. **Tsukahara, T., M. Kannagi, T. Ohashi, H. Kato, M. Arai, G. Nunez, Y. Iwanaga, N. Yamamoto, K. Ohtani, M. Nakamura, and M. Fujii**. 1999. Induction of Bcl-x(L) expression by human T-cell leukemia virus type 1 Tax through NF-kappaB in apoptosis-resistant T-cell transfectants with Tax. J Virol **73**:7981-7987.

447. **Tu, W., S. Chen, M. Sharp, C. Dekker, A. M. Manganello, E. C. Tongson, H. T. Maecker, T. H. Holmes, Z. Wang, G. Kemble, S. Adler, A. Arvin, and D. B. Lewis**. 2004. Persistent and selective deficiency of CD4+ T cell immunity to cytomegalovirus in immunocompetent young children. J Immunol **172**:3260-3267.

448. **Tuittila, M. T., M. G. Santagati, M. Roytta, J. A. Maatta, and A. E. Hinkkanen**. 2000. Replicase complex genes of Semliki Forest virus confer lethal neurovirulence. J Virol **74**:4579-4589.

449. **Uddin, S., L. Yenush, X. J. Sun, M. E. Sweet, M. F. White, and L. C. Platanias**. 1995. Interferon-alpha engages the insulin receptor substrate-1 to associate with the phosphatidylinositol 3'-kinase. J Biol Chem **270**:15938-15941.

450. **Uddin, S., E. N. Fish, D. Sher, C. Gardziola, O. R. Colamonici, M. Kellum, P. M. Pitha, M. F. White, and L. C. Platanias**. 1997. The IRS-pathway operates distinctively from the Stat-pathway in hematopoietic cells and transduces common and distinct signals during engagement of the insulin or interferon-alpha receptors. Blood **90**:2574-2582.

451. **Uddin, S., B. Majchrzak, J. Woodson, P. Arunkumar, Y. Alsayed, R. Pine, P. R. Young, E. N. Fish, and L. C. Platanias**. 1999. Activation of the p38 mitogen-activated protein kinase by type I interferons. J Biol Chem **274**:30127-30131.

452. **Uddin, S., F. Lekmine, N. Sharma, B. Majchrzak, I. Mayer, P. R. Young, G. M. Bokoch, E. N. Fish, and L. C. Platanias**. 2000. The Rac1/p38 mitogen-activated protein kinase pathway is required for interferon alpha-dependent transcriptional activation but not serine phosphorylation of Stat proteins. J Biol Chem **275**:27634-27640.

453. **Uematsu, S., S. Sato, M. Yamamoto, T. Hirotani, H. Kato, F. Takeshita, M. Matsuda, C. Coban, K. J. Ishii, T. Kawai, O. Takeuchi, and S. Akira**. 2005. Interleukin-1 receptor-associated kinase-1 plays an essential role for Toll-like receptor (TLR)7- and TLR9-mediated interferon-{alpha} induction. J Exp. Med. **201**:915-923.

454. **Ulane, C. M. and C. M. Horvath**. 2002. Paramyxoviruses SV5 and HPIV2 assemble STAT protein ubiquitin ligase complexes from cellular components. Virology **304**:160-166.

455. **Ulane, C. M., J. J. Rodriguez, J. P. Parisien, and C. M. Horvath**. 2003. STAT3 ubiquitylation and degradation by mumps virus suppress cytokine and oncogene signaling. J Virol. **77**:6385-6393.

456. **Upton, C., J. L. Macen, M. Schreiber, and G. McFadden**. 1991. Myxoma virus expresses a secreted protein with homology to the tumor necrosis factor receptor gene family that contributes to viral virulence. Virology **184**:370-382.

457. **van den Broek MF, Muller U Huang S Zinkernagel RM Aguet M**. Immune defence in mice lacking type I and/or type II interferon receptors. Immunol Rev. 148, 5-18. 1995.

458. **Vanguri, P. and J. M. Farber**. 1994. IFN and virus-inducible expression of an immediate early gene, crg-2/IP-10, and a delayed gene, I-A alpha in astrocytes and microglia. J Immunol. **152**:1411-1418.

459. **Veals, S. A., C. Schindler, D. Leonard, X. Y. Fu, R. Aebersold, J. E. Darnell, Jr., and D. E. Levy**. 1992. Subunit of an alpha-interferon-responsive transcription factor is related to interferon regulatory factor and Myb families of DNA-binding proteins. Mol Cell Biol **12**:3315-3324.

460. **Ventoso, I., M. A. Sanz, S. Molina, J. J. Berlanga, L. Carrasco, and M. Esteban**. 2006. Translational resistance of late alphavirus mRNA to eIF2{alpha} phosphorylation: a strategy to overcome the antiviral effect of protein kinase PKR. Genes Dev **20**:87-100.

461. **Vidy, A., M. Chelbi-Alix, and D. Blondel**. 2005. Rabies virus P protein interacts with STAT1 and inhibits interferon signal transduction pathways. J Virol. **79**:14411-14420.

462. **Vihinen, H., T. Ahola, M. Tuittila, A. Merits, and L. Kaariainen**. 2001. Elimination of phosphorylation sites of Semliki Forest virus replicase protein nsP3. J Biol Chem **276**:5745-5752.

463. **Vijay-Kumar, M., J. R. Gentsch, W. J. Kaiser, N. Borregaard, M. K. Offermann, A. S. Neish, and A. T. Gewirtz**. 2005. Protein kinase R mediates intestinal epithelial gene remodeling in response to double-stranded RNA and live rotavirus. J Immunol **174**:6322-6331.

464. **Vivanco, I. and C. L. Sawyers** . 2002. The phosphatidylinositol 3-Kinase AKT pathway in human cancer. Nat Rev Cancer **2**:489-501.

465. **Wahlberg, J. M. and H. Garoff** . 1992. Membrane fusion process of Semliki Forest virus. I: Low pH-induced rearrangement in spike protein quaternary structure precedes virus penetration into cells. J Cell Biol **116**:339-348.

466. **Wang, Q., Z. Zhang, K. Blackwell, and G. G. Carmichael**. 2005. Vigilins bind to promiscuously A-to-I-edited RNAs and are involved in the formation of heterochromatin. Curr. Biol **15**:384-391.

467. **Ware, C. F.** 2005. Network communications: lymphotoxins, LIGHT, and TNF. Annu Rev Immunol. **23**:787-819.

468. **Way, S. J., B. A. Lidbury, and J. L. Banyer**. 2002. Persistent Ross River virus infection of murine macrophages: an in vitro model for the study of viral relapse and immune modulation during long-term infection. Virology **301**:281-292.

469. **Weaver SC, Dalgarno L Frey TK Huang HV Kinney RM Rice CM Roehri JT Shope RE and Strauss EG.** Family Togaviridae. In MHV van Regenmortel, CM Fauquet, DHL Bishop, Carstens EB, Estes MK, SM Lemon, J Maniloff, M A Mayo, DJ McGeogh, CR Pringle and RB Wicker (ed), Viral Taxonomy.Classification and Nomenclature of Viruses. 879-889. 2000. San Diego, California, Academic Press Inc.

470. **Weber F, Kochs G Haller O.** Inverse interference: how viruses fight the interferon system. Viral Immunol. 17(4), 498-515. 2004.

471. **Weber, F., A. Bridgen, J. K. Fazakerley, H. Streitenfeld, N. Kessler, R. E. Randall, and R. M. Elliott**. 2002. Bunyamwera bunyavirus nonstructural protein NSs counteracts the induction of alpha/beta interferon. J Virol. **76**:7949-7955.

472. **Weinberg, R. A.** 1995. The retinoblastoma protein and cell cycle control. Cell **81**:323-330.

473. **Wenger, F.** 1977. Venezuelan equine encephalitis. Teratology **16**:359-362.

474. **Wesselingh, S. L., B. Levine, R. J. Fox, S. Choi, and D. E. Griffin**. 1994. Intracerebral cytokine mRNA expression during fatal and nonfatal alphavirus encephalitis suggests a predominant type 2 T cell response. J Immunol. **152**:1289-1297.

475. **Williams, B. R.** 1999. PKR; a sentinel kinase for cellular stress. Oncogene **18**:6112-6120.

476. **Witek-Janusek, L.** 1988. Pituitary-adrenal response to bacterial endotoxin in developing rats. Am. J Physiol **255**:E525-E530.

477. **Wolf, D., V. Witte, B. Laffert, K. Blume, E. Stromer, S. Trapp, P. d'Aloja, A. Schurmann, and A. S. Baur**. 2001. HIV-1 Nef associated PAK and PI3-kinases stimulate Akt-independent Bad-phosphorylation to induce anti-apoptotic signals. Nat Med. 7 :1217-1224.

478. **Wong, A. H., N. W. Tam, Y. L. Yang, A. R. Cuddihy, S. Li, S. Kirchhoff, H. Hauser, T. Decker, and A. E. Koromilas**. 1997. Physical association between STAT1 and the interferon-inducible protein kinase PKR and implications for interferon and double-stranded RNA signaling pathways. EMBO J **16**:1291-1304.

479. **Wong, S. K., S. Sato, and D. W. Lazinski**. 2001. Substrate recognition by ADAR1 and ADAR2. RNA. 7:846-858.

480. **Wurzer, W. J., C. Ehrhardt, S. Pleschka, F. Berberich-Siebelt, T. Wolff, H. Walczak, O. Planz, and S. Ludwig**. 2004. NF-kappaB-dependent induction of tumor necrosis factor-related apoptosis-inducing ligand (TRAIL) and Fas/FasL is crucial for efficient influenza virus propagation. J Biol Chem **279**:30931-30937.

481. **Xiang, Y., R. C. Condit, S. Vijaysri, B. Jacobs, B. R. Williams, and R. H. Silverman**. 2002. Blockade of interferon induction and action by the E3L double-stranded RNA binding proteins of vaccinia virus. J Virol. **76**:5251-5259.

482. **Yamamoto, M., S. Sato, H. Hemmi, K. Hoshino, T. Kaisho, H. Sanjo, O. Takeuchi, M. Sugiyama, M. Okabe, K. Takeda, and S. Akira**. 2003. Role of adaptor TRIF in the MyD88-independent toll-like receptor signaling pathway. Science **301**:640-643.

483. **Yang, Y. L., L. F. Reis, J. Pavlovic, A. Aguzzi, R. Schafer, A. Kumar, B. R. Williams, M. Aguet, and C. Weissmann**. 1995. Deficient signaling in mice devoid of double-stranded RNA-dependent protein kinase. EMBO J **14**:6095-6106.

484. **Yasukawa, H., H. Misawa, H. Sakamoto, M. Masuhara, A. Sasaki, T. Wakioka, S. Ohtsuka, T. Imaizumi, T. Matsuda, J. N. Ihle, and A. Yoshimura**. 1999. The JAK-binding protein JAB inhibits Janus tyrosine kinase activity through binding in the activation loop. EMBO J **18**:1309-1320.

485. **Yi, A. K. and A. M. Krieg**. 1998. CpG DNA rescue from anti-IgM-induced WEHI-231 B lymphoma apoptosis via modulation of I kappa B alpha and I kappa B beta and sustained activation of nuclear factor-kappa B/c-Rel. J Immunol. **160**:1240-1245.

486. **Yie, J., M. Merika, N. Munshi, G. Chen, and D. Thanos**. 1999. The role of HMG I(Y) in the assembly and function of the IFN-beta enhanceosome. EMBO J **18**:3074-3089.

487. **Yokota, S., N. Yokosawa, T. Kubota, T. Suzutani, I. Yoshida, S. Miura, K. Jimbow, and N. Fujii**. 2001. Herpes simplex virus type 1 suppresses the interferon signaling pathway by inhibiting phosphorylation of STATs and janus kinases during an early infection stage. Virology **286**:119-124.

488. **Yokota, S., N. Yokosawa, T. Okabayashi, T. Suzutani, S. Miura, K. Jimbow, and N. Fujii**. 2004. Induction of suppressor of cytokine signaling-3 by herpes simplex virus type 1 contributes to inhibition of the interferon signaling pathway. J Virol. **78**:6282-6286.

489. **Yoneyama, M., M. Kikuchi, T. Natsukawa, N. Shinobu, T. Imaizumi, M. Miyagishi, K. Taira, S. Akira, and T. Fujita**. 2004. The RNA helicase RIG-I has an essential function in double-stranded RNA-induced innate antiviral responses. Nat. Immunol. **5**:730-737.

490. **Yuan, H., B. K. Yoza, and D. S. Lyles**. 1998. Inhibition of host RNA polymerase II-dependent transcription by vesicular stomatitis virus results from inactivation of TFIID. Virology **251**:383-392.

491. **Zamanian-Daryoush, M., S. D. Der, and B. R. Williams**. 1999. Cell cycle regulation of the double stranded RNA activated protein kinase, PKR. Oncogene **18**:315-326.

492. **Zamanian-Daryoush, M., T. H. Mogensen, J. A. DiDonato, and B. R. Williams**. 2000. NF-kappaB activation by double-stranded-RNA-activated protein kinase (PKR) is mediated through NF-kappaB-inducing kinase and IkappaB kinase. Mol Cell Biol **20**:1278-1290.

493. **Zang YC, Halder JB Samanta AK Hong J Rivera VM Zhang JZ**. Regulation of chemokine receptor CCR5 and production of RANTES and MIP-1alpha by interferon-beta. J Neuroimmunol. 112(1-2), 174-180. 2001.

494. **Zhang, Z. and G. G. Carmichael**. 2001. The fate of dsRNA in the nucleus: a p54(nrb)-containing complex mediates the nuclear retention of promiscuously A-to-I edited RNAs. Cell **106**:465-475.

495. **Zhou, A., J. M. Paranjape, S. D. Der, B. R. Williams, and R. H. Silverman**. 1999. Interferon action in triply deficient mice reveals the existence of alternative antiviral pathways. Virology **258**:435-440.

496. **Zhu, F. X., S. M. King, E. J. Smith, D. E. Levy, and Y. Yuan**. 2002. A Kaposi's sarcoma-associated herpesviral protein inhibits virus-mediated induction of type I interferon by blocking IRF-7 phosphorylation and nuclear accumulation. Proc Natl Acad Sci U S A **99**:5573-5578.

497. **Zhu, S., A. Y. Sobolev, and R. C. Wek**. 1996. Histidyl-tRNA synthetase-related sequences in GCN2 protein kinase regulate in vitro phosphorylation of eIF-2. J Biol Chem **271**:24989-24994.

498. **Zimmermann, A., M. Trilling, M. Wagner, M. Wilborn, I. Bubic, S. Jonjic, U. Koszinowski, and H. Hengel**. 2005. A cytomegaloviral protein reveals a dual role for STAT2 in IFN-{gamma} signaling and antiviral responses. J Exp. Med. **201**:1543-1553.

499. **Zimmermann, K. C., C. Bonzon, and D. R. Green**. 2001. The machinery of programmed cell death. Pharmacol. Ther. **92**:57-70.

500. **Zlotnik, I., D. P. Grant, and D. Batter-Hatton**. 1972. Encephalopathy in mice following inapparent Semliki Forest Virus (S.F.V.) infection. Br. J Exp. Pathol. **53**:125-129.